2010

ARSENITE OXIDATION BY PURE CULTURES OF *THIOMONAS ARSENIVORANS* STRAIN B6 IN BIOREACTOR SYSTEMS

Aniruddha Dastidar
University of Kentucky, anir.dast@gmail.com

ABSTRACT OF DISSERTATION

Aniruddha Dastidar

ARSENITE OXIDATION BY PURE CULTURES OF *THIOMONAS ARSENIVORANS*
STRAIN B6 IN BIOREACTOR SYSTEMS

_____

ABSTRACT OF DISSERTATION
_____

A dissertation submitted in partial fulfillment of the
requirements for the degree of Doctor of Philosophy in the
College of Engineering
at the University of Kentucky

By
Aniruddha Dastidar

Lexington, Kentucky

Director: Dr. Y.T. (Ed) Wang, Professor of Civil Engineering

Lexington, Kentucky

2010

ABSTRACT OF DISSERTATION

ARSENITE OXIDATION BY PURE CULTURES OF *THIOMONAS ARSENIVORANS*
STRAIN B6 IN BIOREACTOR SYSTEMS

The removal of arsenic toxicity from water is accomplished by a preliminary pre-oxidative step transforming the most toxic form, arsenite (As (III)), to the least toxic form, arsenate (As (V)). The potential of As (III) oxidation to As (V) was initially investigated in batch reactors using the chemoautotrophic *Thiomonas arsenivorans* strain b6 under varying initial As (III) and cell concentrations and at optimal pH and temperature conditions (pH 6.0 and temperature 30°C). The strain b6 completely oxidized As (III) to As (V) during exponential growth phase for lower levels of As (III) concentrations ($\leq$ 100 mg/L) but continued into stationary phase of growth for higher levels ($\geq$ 500 mg/L). Other important factors such as oxygen and carbon limitations during biological As (III) oxidation were also evaluated. The biokinetic parameters of the strain b6 were estimated using a Haldane-substrate inhibition model with the aid of a non-linear estimation technique.

Microbial As (III) oxidation was further investigated in continuous-flow bioreactors (CSTR and biofilm reactor) under varying As (III) loading rates. Both the reactors achieved As (III) oxidation efficiency exceeding 99% during the steady-state conditions. The reactors were also able to recover from an As (III) overloading phase establishing the resilient nature of the microorganism. The basic mass balance expressions on As (III) and biomass along with the Monod model were used to linearly estimate the biokinetic parameters in the CSTR study. However, in the biofilm study, a steady-state flux model was used to estimate the same parameters. The performance of the model was very good in simulating the transient and steady-state conditions.

Finally, the potential application of one-stage and two-stage reactor systems was investigated for the near complete removal of arsenic. Activated alumina was used as the adsorbent for the As (V) produced by the biological oxidation of As (III). The two-stage reactor process performed better than the one-stage reactor system in lowering the arsenic level below the detection limit (1 mg/L) for at least eight days of operation. However, pH

fluctuations and probable competition from ions such as PO_4^{3-}, SO_4^{2-}, and Cl^- severely impacted the performance of the reactors. Further study is needed to improve the overall efficiency of the reactor systems for achieving complete removal of arsenic for a longer operating time.

KEYWORDS: Arsenite, Arsenate, CSTR, Biofilm reactor, Two-stage reactor system

Aniruddha Dastidar
Student's Signature

October 17, 2010
Date

ARSENITE OXIDATION BY PURE CULTURES OF *THIOMONAS ARSENIVORANS*
STRAIN B6 IN BIOREACTOR SYSTEMS

By

Aniruddha Dastidar

<u>Dr.Y.T. (Ed) Wang</u>
Director of Dissertation

<u>Dr.Kamyar C. Mahboub</u>
Director of Graduate Studies

<u>Date: October 17, 2010</u>

RULES FOR THE USE OF DISSERTATIONS

Unpublished dissertations submitted for the Doctor's degree and deposited in the University of Kentucky Library are as a rule open for inspection, but are to be used only with due regard to the rights of the authors. Bibliographical references may be noted, but quotations or summaries of parts may be published only with the permission of the author, and with the usual scholarly acknowledgments.

Extensive copying or publication of the dissertation in whole or in part also requires the consent of the Dean of the Graduate School of the University of Kentucky.

A library that borrows this dissertation for use by its patrons is expected to secure the signature of each user.

Name

                                   Date

_____

_____

_____

_____

_____

_____

_____

DISSERTATION

Aniruddha Dastidar

The Graduate School

University of Kentucky

2010

ARSENITE OXIDATION BY PURE CULTURES OF *THIOMONAS ARSENIVORANS*
STRAIN B6 IN BIOREACTOR SYSTEMS

_____

DISSERTATION

_____

A dissertation submitted in partial fulfillment of the
requirements for the degree of Doctor of Philosophy in the
College of Engineering
at the University of Kentucky

By
Aniruddha Dastidar

Lexington, Kentucky

Director: Dr. Y.T. (Ed) Wang, Professor of Civil Engineering

Lexington, Kentucky

2010

DEDICATION

I dedicate this dissertation work to my ever-loving family.

ACKNOWLEDGEMENTS

during the entire period of my education. Finally, I would like to thank my brother, Mr. Anirban Dastidar, my sister-in-law, Mrs. Moumita Dastidar, my uncle, Mr. Amol Kumar Dastidar, my aunt, Ms. Lucy Clarke, and all my other family members for all their support, love, and encouragement.

Last, but not least, I am really thankful to Dr. Samantha Freitas, Prince Kowsuvon, Dr. Lauren E. Black, Mike Snyder, Abheetha Peiris, Dr. Balasubramanian Datchanamourty, and Dr. Arthon Suttigarn, their support throughout my Ph.D work.

TABLE OF CONTENTS

LIST OF TABLES

LIST OF FIGURES

Chapter 1: Introduction

Arsenic is a toxic metalloid in the environment obtained from both natural and anthropogenic sources. Prolonged exposure to the metalloid can have carcinogenic effects not only in humans but in most other forms of life (Lloyd and Oremland 2006). It is mostly detected in environments such as groundwater, soils and sediments (Simeonova et al. 2005). USEPA (2001) has recently lowered the MCL (maximum contaminant level) of arsenic from 50 to 10 µg /L in drinking water. High levels ($\geq$ 500 mg/L) of arsenic concentration have been detected in several metalliferous manufacturing industries such as copper and gold smelter (Basha et al. 2008).

Arsenic has four oxidation states, 0 (elemental), -3 (arsine), +3 (arsenite) and +5 (arsenate), with the predominant soluble forms being As (III) and As (V) (Suttigarn and Wang 2005; Hoven and Santini 2004; Rhine et al. 2006). The speciation of the arsenic in water is controlled by redox potential (Eh), pH and the presence of other chemical compounds such as sulfate, birnessite (δ-MnO$_2$), and ferric hydroxide (Fe(OH)$_3$) (Manning et al. 2002; Nikolaidis et al. 2000). As (III) is generally present in anoxic environments, whereas As (V) is present in aerobic conditions, with the former being more toxic and mobile than the latter (Oremland and Stolz 2003; Lievremont et al. 2003; Clifford 1990).

Studies have shown that a pre-oxidation step transforming As (III) to As (V) is very useful for the total removal of arsenic from water. Conventional chemical oxidation methods may release harmful by-products as a result of the oxidation process. Biological oxidation of As (III) to As (V) may be considered as an alternative to the conventional chemical oxidation strategies. Microbial oxidation of As (III) to As (V) was first noted in

1918 in cattle-dipping tanks (Green 1918). Heterotrophic microorganisms oxidize As (III) to As (V) by means of a detoxification mechanism, whereas, autotrophic bacteria utilize the energy released during the oxidation process for cellular growth. Cell synthesis in autotrophic microorganisms is generally achieved either by using HCO_3^- or by fixing CO_2 via the Calvin-Benson-Bassham cycle as a source of carbon (Anderson et al. 1992; Ilyaletdinov and Abdrashitova 1981; Santini et al. 2000).

In this study, the chemoautotrophic *Thiomonas arsenivorans* strain b6 was used to assess As (III) oxidation in various bioreactor systems. In order to achieve the maximum transformation rate of As (III) to As (V), As (III) oxidation studies in the bioreactor systems were investigated at the optimal conditions (pH and temperature) of growth of the strain b6. The potential application of biological As (III) oxidation in continuous flow bioreactors by the autotrophic *T.arsenivorans* strain b6 is quite interesting and insightful from the standpoint of a bioremediation strategy. The removal of As (V) ions by activated alumina (AA) under different As (III) loading conditions for achieving complete removal of arsenic was also investigated in column reactor processes.

The specific objectives of the research were as follows:

1. To investigate As (III) oxidation in batch systems and also evaluate the potential application of the determined parameters in simulating the As (III) oxidation patterns.

2. To assess As (III) oxidation in continuous flow bioreactor systems (CSTR and biofilm reactor) under varying As (III) loading rates. The usage of an appropriate biokinetic model in predicting the transient and steady-state conditions was also evaluated.

3. To investigate the potential combination of a biological and chemical process for the complete removal of arsenic in bench-scale column reactors.

Chapter 2: Literature Review

2.1 Arsenic (As)

Arsenic (As) (atomic number: 33 and atomic weight: 74.9216) is a group V member of the periodic table of elements and is classified as a heavy metal (Wackett et al. 2004). Arsenic is the twentieth most abundant element in the earth's crust with concentrations greater than Hg, Cd, Au, Ag, Sb, and Se respectively (Bhumbla and Keefer 1994). The toxic metalloid arsenic is known to cause serious environmental and health problems to humans and other living organisms (Jang et al. 2006; Singh et al. 2008). Ingestion of potable water contaminated with arsenic and inhalation of inorganic arsenic have shown to cause skin, liver, lung, bladder and kidney cancers in humans and animals (Smith et al. 1992). WHO (2006) estimated that 70 million people alone in regions such as Bangladesh and Eastern India have been poisoned by elevated levels of arsenic in drinking water. Currently, the maximum contaminant level of arsenic in drinking water is set by USEPA (2001) at 10 μg/L. Both anthropogenic and natural means are responsible for the release of arsenic to the environment.

2.2 Sources of Arsenic in the Environment

2.2.1 Natural Arsenic Sources

The most natural occurrence of arsenic in terrestrial and aquatic environment under both oxic and anoxic conditions is due to the weathering of As minerals and volcanic activity (Rhine et al. 2006). Oxidation and dissolution of the most common arsenic bearing minerals such as arsenian pyrite ($Fe(AsS)_2$), arsenopyrite (FeAsS), realgar (AsS), and orpiment (As_2S_3), are the major natural sources of arsenic release in ground water (Nordstrom 2002; Wang and Mulligan 2006). Table 2.1 shows the most

common arsenic bearing minerals in the environment and the place of occurrences. Studies also indicated the concentrations of these minerals to be extremely high in the presence of transition metals such as Cd, Pb, Ag, Au, Sb, P, W, and Mo respectively (Smedley and Kinniburgh 2002). Even though arsenopyrite, realgar, and orpiment are formed at very high temperature in the earth's crust, Rittle et al. (1995) detected the presence of authigenic arsenopyrite in sediments. Newman et al. (1998) detected orpiment formed as a result of microbial precipitation. The concentration of arsenopyrite is generally less compared to arsenian pyrite (Fe (SAs) $_2$) in the ore zone (Nordstrom 2000).

Aquifers of strongly reducing nature comprised of alluvial sediments and closed basins in volcanogenic provinces are the two other natural sources of arsenic contamination in ground water. Aquifers composed of ordinary sediments may be sources of high dissolved arsenic (> 50 µg/L) in water supplies (Nordstrom 2002).

Arsenic concentration is most igneous rock types averages at 1.5 mg kg^{-1}, whereas, in volcanic gases, arsenic level is around 5 mg kg^{-1} (Ure and Berrow 1982; Smedley and Kinniburgh 2002). In metamorphic rocks, arsenic concentration is generally 5 mg kg^{-1} with Pelitic rocks exhibiting the highest concentration of 18 mg Kg^{-1} (Boyle and Jonasson 1973). Arsenic typically ranges between 5-10 mg kg^{-1} (Webster 1999) in sedimentary rocks. Coal and bituminous deposits generally have very high arsenic concentration with Belkin et al. (2000) reporting 35,000 mg Kg^{-1} in some collected coal samples.

Table 2.1 Major arsenic minerals occurring in nature (Smidley and Kinniburgh 2002)

Mineral	Composition	Occurrence
Native arsenic	As	Hydrothermal veins
Niccolite	NiAs	Vein deposits and norites
Realgar	AsS	Vein deposits, clays and limestones, deposits from hot spring
Orpiment	As_2S_3	Hydrothermal veins, hot springs, volcanic sublimation products
Cobaltite	CoAsS	High temperature deposits, metamorphic rocks
Arsenopyrite	FeAsS	Mineral veins
Tennantite	$(Cu, Fe)_{12} As_4 S_{13}$	Hydrothermal veins
Enargite	Cu_3AsS_4	Hydrothermal veins
Arsenolite	As_2O_3	Secondary mineral formed by oxidation of arsenopyrite, native arsenic, and other As minerals
Claudetite	As_2O_3	Secondary mineral formed by oxidation of realgar, arsenopyrite, and other As minerals
Scorodite	$FeAsO_4. 2H_2O$	Secondary mineral
Annabergite	$(Ni, Co)_3(AsO_4)_2.8H_2 0$	Secondary mineral
Hoernesite	$Mg_3 (AsO_4)_2.8H_2O$	Secondary mineral, smelter waters
Haematolite	$(Mn, Mg)_4Al (AsO_4)(OH)_8$	------
Conichalcite	$CaCu (AsO_4)(OH)$	Secondary mineral
Pharmacosiderite	$Fe_3(AsO_4)_2(OH)_3.5H_2 0$	Oxidation product of arsenopyrite and other As minerals

The baseline arsenic concentration in soils generally ranges between 5-10 mg kg^{-1}. Boyle and Jonasson (1973) estimated the average baseline arsenic concentration to be at 7.2 mg kg^{-1}, whereas, Ure and Berrow (1982) quoted a higher average value at 11.3 mg kg^{-1}. The arsenic content in soils is generally governed by principal factors such as climate, organic and inorganic component of the soil, and redox potential respectively. Arsenic generally appears in the inorganic forms (As (III), As (V)) in soil. However, under oxidizing conditions, certain microorganisms can methylate inorganic arsenic species leading to the formation of monomethylarsonic acid (MMA), dimethylarsinic acid (DMA), and trimethyl arsine oxide (TMAsO) respectively (Mandal and Suzuki 2002). The inorganic arsenic ions also possess the ability to bind to other organic materials in the soil.

Arsenic is generally present at very low concentration in natural waters. However, Smedley et al. (1996) reported arsenic concentration in the range of 100 – 5,000 μg l^{-1} in unpolluted fresh waters located in areas of sulfide mineralization and mining. The concentration of arsenic in seawater generally varies between 0.09 to 24 μg L^{-1}, whereas, in fresh water, the concentration can vary between 0.15 – 0.45 μg L^{-1} respectively (Leonard 1991). Laboratory studies also indicate the release of arsenic from soils into water bodies following flooding and the development of anaerobic conditions (Hess and Blanchar 1977; McGeehan and Naylor 1994).

2.2.2 Anthropogenic Sources

Anthropogenic sources such as smelter slag, coal combustion, run-off from mine tailings, hide tanning waste, pigment production for paints and dyes, and the application of arsenic based pesticides are the major causes of arsenic contamination (Oremland and

Stolz 2003). Arsenic concentration as high as 1,628 mg/L have been reported in the effluent of industrial discharges from metallurgical industries involved in smelting operations for mining metals (Basha et al. 2008). The smelting operations of Cu, Ni, Pb, and Zn have emitted 62, 000 tons of arsenic with 80% generated alone through copper smelters (Bissen and Frimmel 2003). Sadler et al. (1994) reported arsenic level in soil near a lead smelter was 2g /Kg, whereas, near a copper smelter, the concentration was 0.55 g/Kg respectively. Table 2.2 lists arsenic concentrations in natural waters and effluent wastes of some manufacturing industries.

The volatilization of arsenic hexoxide (As_4O_6) during coal combustion leads to the emission of arsenic in the environment which eventually condenses in the flue system (Bhumbla 1994). Fly ash from the thermal power plants may also contribute to arsenic contamination of the soil. Another anthropogenic source of arsenic release is its use in coloring agents such as Scheele's green ($CuHAsO_3$) or Paris green (Cu (AsO_2)$_2$Cu ($C_2H_3O_2$)$_2$) (Azcue and Nriagu 1994).

Arsenic contamination of the environment can also occur through the use of arsenical fungicides, herbicides, and insecticides in the agriculture and wood industry (Bissen and Frimmel 2003). The most common wood preservatives used in the industry are chromated copper arsenate (CCA) and ammonical copper arsenate (ACA) in conjunction with 99% of the arsenical wood preservatives (Perker 1981). Currently, arsenic is being used in the production of glass and semiconductor industry (Azcue and Nriagu 1994), adding to the anthropogenic sources of arsenic contamination. Nriagu and Pacyna (1988) reported 82,000 metric tons/year of arsenic generation worldwide trough anthropogenic sources.

Table 2.2 Arsenic concentration in water and wastewater (Smedley and Kinniburgh 2002; Peterson 1985)

Water Body and Location / Source	Arsenic Concentration (mg/L)
Gold Ore Extraction	1012
Sulfuric Acid manufacture	20-500
Ammonia manufacture	430
Copper smelting operation	1628
Mining-contaminated groundwater	0.01-5
Geothermal Water	0.01-5
Mine drainage (Iron mountain)	85
Mine drainage (Ural mountain)	400
Arsenic Herbicide Plant, Texas	408
Searles lake brine, California (Oilfield and related brine)	243
Ground water in arsenic rich provinces	0.01-5
Stream electric plant cleaning	0.0 -310
Arsenic trioxide plant	310

2.3 Aqueous Speciation of Arsenic

The speciation of arsenic in the aquatic system is controlled by both the redox potential (Eh) and pH. Arsenic has four oxidation states, 0 (elemental), -3 (arsine), +3 (arsenite), and +5 (arsenate), with the predominant soluble forms being As (III) ($H_3AsO_4^{2-}$ or $H_2AsO_3^{-}$), and As (V) ($H_2AsO_4^{-}$ or $HAsO_4^{2-}$) (Suttigarn and Wang 2005; Hoven and Santini 2004; Rhine et al. 2006). Studies have shown that As (III) is more mobile and toxic than As (V) and is difficult to remove from water (Rhine et al. 2006; Clifford 1990). The high mobility of As (III) is due to its neutral charge at most pH ranges in natural water. The binding of As (V) to minerals occur at wide pH range, whereas, As (III) may bind to certain compounds such Fe-(III)-oxyhydroxides and metal sulfides at a very narrow pH range (Belzile and Tessier 1990; Welch et al. 2000).

The aqueous form of inorganic arsenic in anoxic environments is dominated by As (III), whereas As (V) is mostly prevalent in aerobic environments (Oremland and Stolz 2003; Lievremont et al. 2003). However, As (III) and As (V) have been simultaneously detected in both oxic and anoxic conditions in the environment (Oremland and Stolz 2003; Smedley and Kinniburgh 2002).

The speciation of arsenic in water can be explained by Eh-pH diagram as shown in Figure 2.1. Under oxidizing conditions, the hydrolysis of arsenate can result in the formation of two major thermodynamically stable ionic species ($H_2AsO_4^{-}$, $HAsO_4^{2-}$) (Table 2.3; Table 2.4a). However, under extreme acidic (pH ≤ 2.2) and alkaline (pH ≥ 11.5) conditions other stable arsenate species may exist such as $H_3AsO_4^{0}$, and AsO_4^{3-}, respectively (Table 2.4a). At pH ≤ 9.2, neutral and stable $H_3AsO_3^{0}$ will be the predominant arsenic specie in the aqueous solution under reducing conditions, before

10

losing a proton to become $H_2AsO_3^-$ at pH $\geq$ 9.2, or $HAsO_3^{2-}$ at pH $\geq$ 12.3, respectively (Table 2.3; Table 2.4b). Thus reducing environment does contribute to high arsenic concentrations in ground water. Realgar (AsS) and orpiment (As_2S_3) have very low solubilities and occur in their corresponding stable form at pH values less than 5.5 and Eh values of 0 volts (Ferguson and Gavis 1972). $HAsS_2$ (aq) predominates at low pH values ($\leq$ 4), whereas, AsS_2^- predominates at pH values greater than 3.7, respectively. At extremely low Eh values arsine (AsH_3) gas may be formed.

The percentage distribution of arsenic species based on pH (ionic strength) values is shown in Figure 2.2 (Smedley and Kinniburgh 2002). The three dissociation constant for arsenate ions ($pKa_{1, 2, 3}$ = 2.2, 6.9, 11.5), and two dissociation constants for As (III) ions ($pKa_{1, 2}$ = 9.22, 12.3) govern the percentage distribution of each species under both oxidizing and reducing conditions, respectively.

Apart from As (III), and As (V), methylated forms of arsenic specie have been also detected in the natural environment. These methylated compounds are produced as a result of biomethylation by certain group of microorganisms. Biomethylation is generally considered a detoxification mechanism for most bacteria (Stolz et al. 2006). The methylated arsenic compounds formed as result of a series of biomethylation chain reactions are monomethylarsonic acid (MMA (V)), monomethyarsonous acid (MMA(III)), dimethylarsinic acid (DMA (V)), dimethylarsinous acid (DMA (III)), trimethylarsine oxide (TMA (V)), and trimethylarsine (TMA (III)) respectively (Dombrowski et al. 2005).
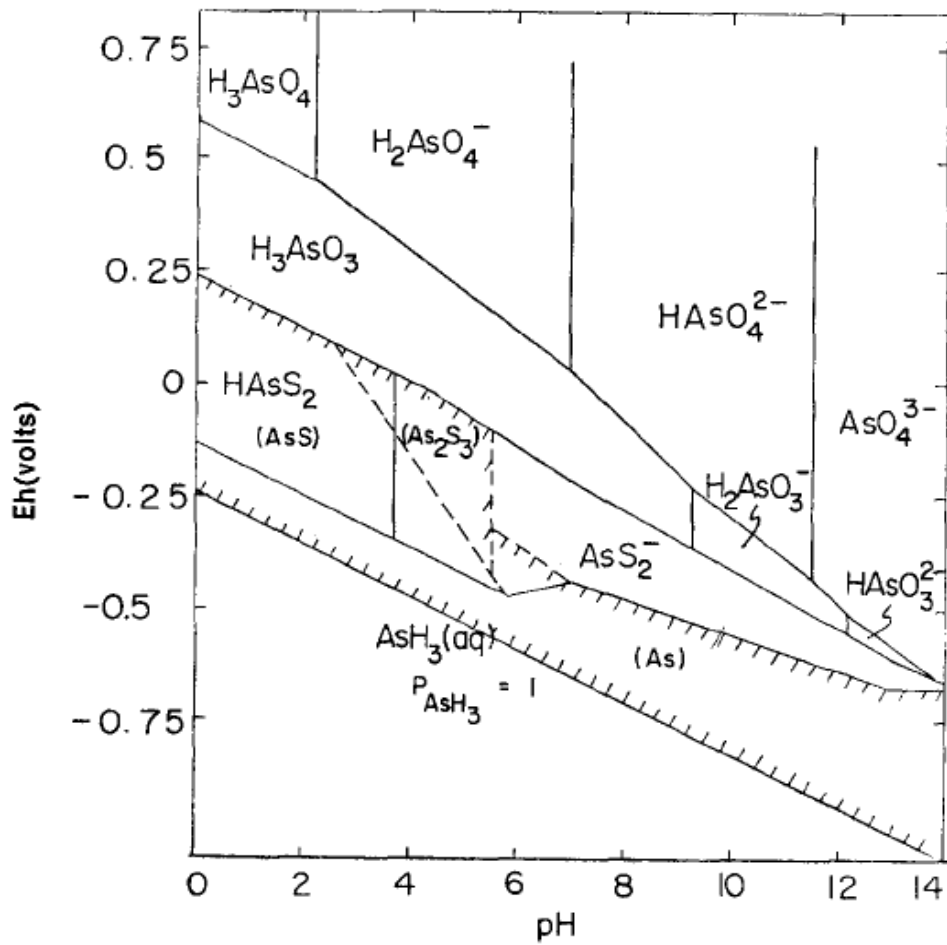
Figure2.1 The Eh-pH diagram for As at 25°C and 1 atm with total As of 10^{-5} mol^{-1} and total sulfur of 10^{-3} mol^{-1}. Solid species enclosed in parentheses and cross-hatched area indicates solubility of less than $10^{-5.3}$ mol l^{-1} (Ferguson and Gavis 1972)
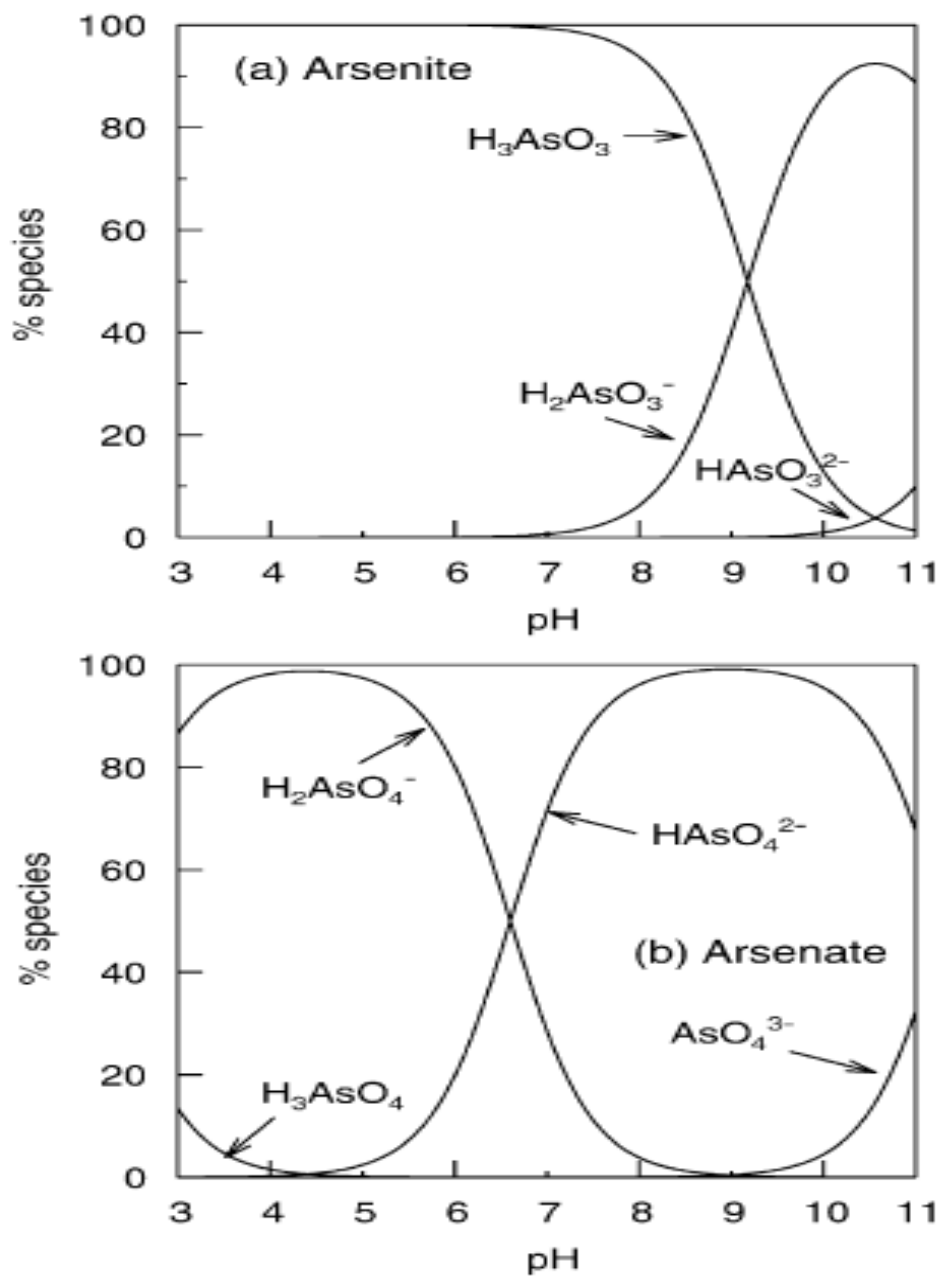
Figure2.2 Speciation of (a) arsenite, and (b) arsenate as a function of pH (ionic strength of 0.01 M) (Smedley and Kinniburgh 2002)

Table 2.3 Gibb's free energies of formation of arsenic species at 25 °C and 1 atm (ΔGf °, kcal mole^{-1}) (Ferguson and Gavis 1972)

Species	State	ΔG_f °
H_3AsO_4	aqueous	-184
$H_2AsO_4^-$	aqueous	-181
$HAsO_4^{2-}$	aqueous	-171.5
AsO_4^{3-}	aqueous	-155.8
H_3AsO_3	aqueous	-154.4
$H_2AsO_3^-$	aqueous	-141.8
$HAsO_3^{2-}$	aqueous	-125.3
$HAsS_2$	aqueous	-11.61
AsS_2^-	aqueous	-6.56
AsS	solid	-16.81
As_2S_3	solid	-40.25
As	solid	0
AsH_3	aqueous	23.8
AsH_3	gaseous	16.5
As_2O_3	solid	-140.8
As_2O_5	solid	-186.9

Table 2.4a Equations representing arsenate speciation (Baes and Mesmer 1976)

$$H_3AsO_4 \rightleftharpoons H_2AsO_4^- + H^+ \ , \ pK_1 = 2.19$$

$$H_2AsO_4^- \rightleftharpoons H_2AsO_4^{2-} + H^+ \ , \ pK_2 = 6.94$$

$$H_2AsO_4^{2-} \rightleftharpoons H_2AsO_4^{3-} + H^+ \ , \ pK_3 = 11.50$$
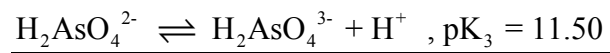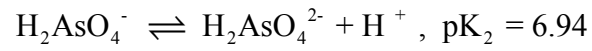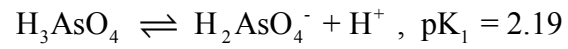
Table 2.4b Equations representing arsenite speciation (Wagman et al. 1968)

$$H_3AsO_3 \rightleftharpoons H_2AsO_3^- + H^+ \ , \ pK_1 = 9.22$$

$$H_2AsO_3^- \rightleftharpoons HAsO_3^{2-} + H^+ \ , \ pK_2 = 12.3$$
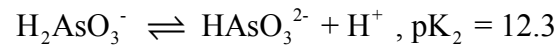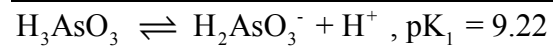
2.4 Arsenic Geocycle in the Environment

The four most primary elemental oxidation states of arsenic are As (III), As (V), As (O), and As (-III), respectively. As mentioned earlier, As (III) is more mobile and toxic than the predominant As (V) ions under aerobic/oxic conditions. Burning of coal, smelting operations, semiconductor industries, and mining including bio-mining, are some of the potential anthropogenic sources of arsenic in the environment. Microbes play a very important role in the arsenic geocycle in the environment as shown in Figure 2.3 (Mukhopadhyay et al. 2002).

As (III) can be released from arsenate laden sediments by arsenate respiring bacteria leading to arsenic contamination of the ground water (Oremland and Stolz 2006). These microbes generally use As (V) as a terminal electron acceptor in the anaerobic respiration process (Oremland and Stolz 2003). The released As (III) can be further oxidized to As (V) by certain bacteria via detoxification mechanism or utilize the energy released during the oxidation process for cellular growth (Stolz et al. 2006; Santini et al. 2000). The As (V) as a result of the oxidation process may be converted to water or lipid-soluble organic compounds such as methylarsonic acid or dimethylarsinic acid (DMA), trimethylated arsenic derivatives (TMA), arsenocholine, arsenobetaine, arsenosugars, and arsenolipids by marine organisms such as phytoplankton, algae, crustaceans, mollusks, and fish (Knowles and Benson 1983; Frankenberger W.T). The arsenosugars and arsenolipids are converted to arsenobetaine by animals in the marine environment (Mukhopadhyay et al. 2002). The arsenic geocycle is completed with the conversion of arsenobetaine back into inorganic arsenic species as a result of microbial metabolism (Dembitsky and Levitsky 2004).
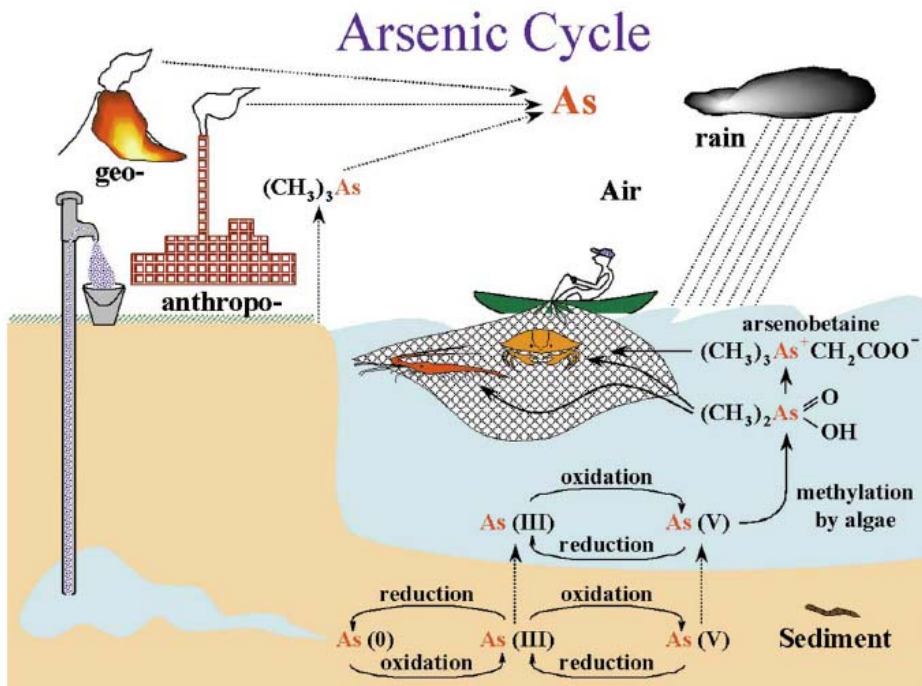
Figure2.3 The global geocycle of arsenic (Mukhopadhyay et al. 2002)

2.5 Arsenic Removal Techniques from Water and Wastewater

The effective removal of arsenic from water requires a preliminary pre-oxidation step to transform As (III) to As (V). The step becomes critical due to the extreme mobility and toxicity of As (III) compared to As (V) ions (Clifford 1990). Arsenic removal by water and wastewater treatment plants is generally accomplished with the application of some conventional treatment techniques. The efficiency of these arsenic removal techniques is greatly enhanced with the application of this pre-oxidation step because of the ease of removal of As (V) compared to As (III).

2.5.1 Coagulation and Filtration

Coagulation and Filtration are the most widely used techniques for the removal of arsenic from water using metal salts such as alum, ferric chloride, and ferric sulfate respectively (Johnston and Heijnen 2001). Laboratory study conducted by Cheng et al. (1994) showed arsenic removal efficiency of 99% using ferric or alum salts, with residual arsenic of less than 1 µg/L in the water. Edwards (1994) and Jekel (1994) explained the three simple mechanisms of the coagulation and filtration process for remediation of arsenic contaminated water. Precipitation reactions leading to the conversion of arsenic to insoluble forms such as Al (AsO_4) or Fe (AsO_4), co-precipitation onto the metal-hydroxide phase, and adsorption of arsenic onto the external surface of the insoluble metal hydroxides, are the principal components of the coagulation and filtration process. The arsenic removal efficiencies with chemical precipitation or co-precipitation using the following chemical reagents are as follows: 94-96% (Fe $(OH)_3$, Legault et al. 1993), 81-100% ($FeCl_3$, Edwards 1994, Legault et al. 1993), 80-99% ($Fe_2(SO4)_3$, Legault et al. 1993), and 85-98% ($Al_2(SO4)_3$, Hering et al. 1997; Legault 1993), respectively. After the

completion of coagulation, filtration using micro filters improves the overall removal efficiency of arsenic removal from water. It is also worth mentioning that several key factors such as coagulant type, coagulant pH, initial As (III) /As (V) concentration, and co-occurring inorganic solutes can greatly influence the coagulation process (USEPA 2000).

2.5.2 Ion Exchange

Ion exchange is a physico-chemical process by which an ion in the liquid medium is exchanged for saturated ion on the solid phase. Synthetic resin saturated with the preferred anion is most widely used for exchanging arsenic anions in contaminated water (USEPA 2000; Johnston and Heijnen 2001). The synthetic resin can be regenerated or replaced with a solution of the exchangeable anion prior to breakthrough of the arsenic in the effluent medium (Clifford 1999; Clifford et al. 2003). Generally strong-base resins (SBA) and sulfate-selective resins are found to be most efficient in arsenic removal over a broader pH range (USEPA 2000). Chloride is the most preferred anion used for the exchange of arsenic ions in the ion exchange process. The presence of high sulfate and total dissolved solids (TDS) concentrations may severely affect the efficiency of the ion exchange medium in removing arsenic from water due to severe competition. The anion preference of SBA from most to least preferred is given by (Clifford 1999):

$$HCrO_4^- > CrO_4^{2-} > ClO_4^- > SeO_4^{2-} > SO_4^{2-} > NO_3^- > Br^- > (HPO_4^{2-}, HAsO_4^{2-}, SeO_3^{2-}, CO_3^{2-})$$
$$> CN^- > NO_2^- > Cl^- > (H_2PO_4^-, H_2AsO_4^-, HCO_3^-) > OH^- > CH_3COO^- > F^-$$
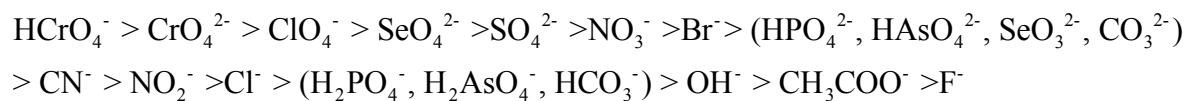
The biggest disadvantage of using the ion exchange process is the non-removal of As (III) species because of its uncharged behavior until pH of about 9 (pKa =9.22). This characteristic of As (III) anions necessitates a pre-oxidative step for the conversion of As

(III) to As (V) prior to removal from water. The removal of As (V) is independent of the initial concentration and pH of the liquid medium (Johnston and Heijnen 2001).

2.5.3 Adsorption

Adsorption is a physical/chemical process by which the target metal ions present in the contaminated water are adsorbed onto the surface of the adsorbents. Activated Alumina (AA) is the most widely used adsorbent for the removal of arsenic from water. Clifford (1999) showed the anion order preference of AA from the most to least preferred:

$$OH^- > H_2AsO_4^-, Si(OH)_3O^- > F^- > HSeO_3^- > SO_4^{2-} > CrO_4^{2-} >> HCO_3^- > Cl^- > NO_3^- > Br^- > I^-$$
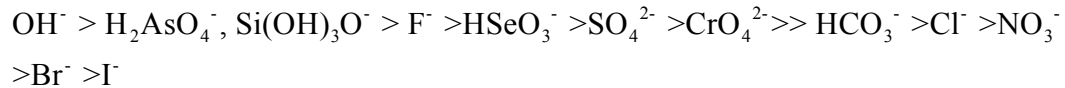
Batch adsorption isotherm studies are generally conducted to estimate the maximum adsorption capacity of the adsorbent prior to analyzing the effectiveness of the adsorbent in the complete removal of the contaminant in column studies. Ghosh and Yuan (1987), Jekel (1994), and Wasay et al. (1996) estimated the maximum adsorption capacity of AA to be in the range of 5 - 24 mg As adsorbed/g media at an equilibrium arsenic concentration range of 0.05 to 0.2 mg/L, respectively. There are several important factors affecting the adsorption process of As (V) ions on the AA such as the pH of contaminated medium, arsenic oxidation state, empty bed contact time, and competing ions, respectively (USEPA 2000). The optimum pH for maximum arsenic adsorption by AA is in the range of 5.5 -6.0 (Rosenblum and Clifford 1984). The details of the ligand exchange/adsorption process reactions between AA and As (V) ions are mentioned in chapter 6 (section 6.2.1).

2.5.4 Membrane Processes

Membranes are generally selective barriers allowing the passage of certain constituents with the rejection or exclusion of others in the water (USEPA 2000; Johnston and Heijnen 2001). A driving force in the form of pressure, concentration, electric potential, or temperature is required for the classification of the membrane process. Generally, high-pressure or low-pressure membranes are used for the treatment/removal of arsenic contaminated water. Microfiltration (MF), and ultrafiltration (UF) are generally grouped into the category of low-pressure membranes, whereas, nanofiltration (NF), and reverse osmosis (RO) are the high-pressure membranes, respectively (USEPA 2000). Low-pressure membrane for the removal of arsenic are generally operated at 10-30 psi, whereas, high-pressure membranes are operated at a pressure of 75-250 psi, respectively (Letterman, 1999). Shape and size of the arsenic compounds, and the chemical characteristics (charge and hydrophobicity) of the material and the feed water greatly influences the effectiveness of the membrane process in the removal of arsenic (USEPA 2000). Both MF and UF may not be viable techniques for the removal of arsenic from groundwater because of the ineffectiveness in the removal of most of the colloidal and particulate constituents of arsenic (USEPA 2000). Waypa et al. (1997) found that the RO and NF were very effective in decreasing an arsenic concentration of 0.05 mg/L by 90-100%. NF membranes due to their extremely small pore size were found to be very effective in removing most of the dissolved arsenic compounds. Studies showed that effective arsenic removal using RO and NF membranes would also require a pre-oxidative step for transforming As (III) to As (V) prior to the application of the removal techniques (USEPA 2000; Johnston and Heijnen 2001).

2.5.5 Alternate Strategies for Arsenic Removal

Apart from the convention treatment technologies for the removal of arsenic, there are several other alternative treatment techniques employed for arsenic remediation from contaminated water. Manning et al. (2002) showed the mechanism of As (III) and As (V) adsorption on synthetic birnessite (δ-MnO_2). The results of the study showed that oxidation of As (III) by MnO_2 caused an alteration to the surface resulting in the creation of several reaction sites for the adsorption on As (V) on the surface of birnessite. Nikolaidis et al. (2000) studied the adsorption capability of zero valent iron (Fe (0)) for the removal of arsenic from water. FeOOH produced on the surface as a result of the corrosion of Fe (0) can adsorb metalloids such as arsenic. However ions such phosphate, silicate, chromate, molybdate greatly interferes with the adsorption of arsenic by Fe (0) (Su and Puls 2001). Iron oxide coated sand (IOCS) is another material which has shown some tendency to remove arsenic from water (USEPA 2000). The column studies conducted by Benjamin et al. (1998) showed that IOCS was more efficient in the removal of As (V) ions compared to As (III). Competing ions such as sulfate, and chloride had the least effect on the adsorption of As (V) ions. The maximum As (V) adsorption occurred at pH of 5.5 with further increase in the pH causing significant decrease in the As (V) adsorption capacity. A study conducted by Driehaus et al. (1998) showed that granular ferric hydroxide (GFH) had a treatment capacity of 30,000 to 40,000 BV with residual As (V) concentration measuring less than 10 μg/L. The performance of the GFH media was better than AA at a pH $\geq$ 7.6. However, the As (V) retention capacity decreased with increasing pH, and which is very common with all anion adsorption (Driehaus et al. 1998). The only disadvantage in the implementation of this technique is the cost of GFH

media (\$4000 / ton). However, the GFH media can be reused for a longer time span compared to AA bed with a basic regeneration step.

2.6 Chemical Oxidation of As (III) to As (V)

Studies relating to arsenic contaminated water have shown that As (III) exhibits more toxicity and mobility than As (V), making it more difficult to remove from water (Rhine et al. 2006; Clifford 1990). Currently, most of the conventional treatment of arsenic contaminated water involves a pre-oxidation step oxidizing As (III) to As (V), and subsequent removal of As (V) through adsorption onto adsorbents (Clifford, 1990; Lievremont et al., 2003; Oremland and Stolz 2003). The chemical oxidation of As (III) to As (V) was first studied by Frank and Clifford (1986) utilizing chlorine, monochloramine, and oxygen. As (III) oxidation by chlorine was the fastest with 100 μg/L of As (III) oxidized by 1.0 mg/L of free chlorine in less than 5 seconds. The results (data not shown) also indicated partial oxidation of As (III) with monochloramine and the ineffectiveness of oxygen in oxidizing any added initial amount of As (III). The stoichiometric equations (Eq. (2-1), Eq. (2-2)) representing As (III) oxidation by chlorine and monochloramine are shown below (Frank and Clifford 1986):

$$H_3AsO_3 + NaOCl \rightarrow H_2AsO_4^- + Na^+ + H^+ + Cl^- \tag{2-1}$$

$$H_3AsO_3 + NH_2Cl + H_2O \rightarrow HAsO_4^{2-} + NH_4^+ + Cl^- + 2H^+ \tag{2-2}$$
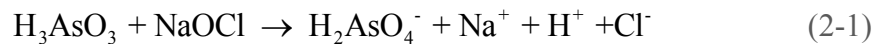
Based on the following equations, the stoichiometric requirement for chlorine was estimated to be 0.95 μg Cl_2/μg As (III), whereas for monochloramine it was 0.69 μg NH_2Cl/μg As (III). The optimum pH and time required for complete As (III) oxidation by chlorine was in the range of 6.3 -8.3 and 39 seconds. However, only 40% As (III)

oxidation by monochloramine was observed in the above pH range in the first 21 seconds (Ghurye and Clifford 2001).

The study of As (III) oxidation utilizing ozone (O_3), permanganate ($KMnO_4$), and chlorine (Cl_2) was previously studied by Amy et al. (2000). The results of the study stated that stoichiometric excess of these compounds can results in 100 % As (III) oxidation to As (V). Oxidation with ozone was fastest (15 seconds), whereas, for permanganate the time required for complete As (III) oxidation was 33 seconds (Ghurye and Clifford 2001). The following equation states As (III) oxidation by permanganate:

$$3H_3AsO_3 + 2MnO_4^- \rightarrow 3H_2AsO_4^- + 2MnO_2 + H_2O + H^+ \qquad (2\text{-}3)$$
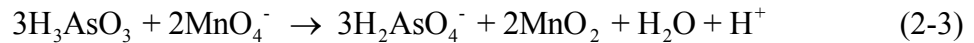
The stoichiometric requirement was estimated to be 1.06 µg MnO_4^- /µg As (III). The equation representing As (III) oxidation by ozone is given by:

$$H_3AsO_3 + O_3 \rightarrow H_2AsO_4^- + O_2 + H^+ \ (\text{pH} = 6.5) \qquad (2\text{-}4)$$
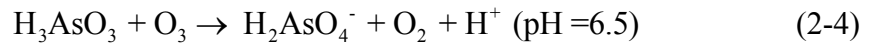
The stoichiometric requirement was calculated to be 0.64 µg O_3 /µg As (III).

Chlorine dioxide was also found to be very effective in the oxidation of As (III) to As (V) (Ghurye and Clifford 2001). However, in the pH range of 6.3-8.3, only 20-30% As (III) oxidation was observed in the first 21 seconds. The stoichiometric requirement based on the equations (Eq. (2-5), Eq. (2-6)) was estimated to be 1.80 µg As ClO_2/µg As (III) for 1 electron transfer, and 0.36 µg ClO_2/µg As (III) for 5-electron transfer respectively:

$$H_3AsO_3 + 2ClO_2 + H_2O \rightarrow H_2AsO_4^- + 2ClO_2^- + 3H^+ \ (\text{1-electron transfer}) \ (2\text{-}5)$$

$$5H_3AsO_3 + 2ClO_2 + H_2O \rightarrow 5H_2AsO_4^- + 2Cl^- + 7H^+ \ (\text{5-electron transfer}) \ (2\text{-}6)$$
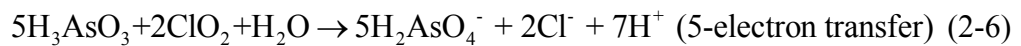
Solid phase oxidants such as birnessite (δ-MnO2) have also proven to be very useful in the oxidation of As (III) to As (V) at a optimum pH of about 6.5 (Manning et al. 2002). Other studies indicated that As (III) oxidation by birnessite was a surface phenomenon and that the rate limiting step in the surface mechanism was the adsorption of As (III) onto the oxide surface (Oscarson et al. 1983; Moore et al. 1990; Driehaus et al. 1995). Nesbitt et al. (1998) proposed a two step pathway for the oxidation of As (III) to As (V) by 7 Å birnessite with the aid of X-ray photoelectron spectroscopy (XPS):

$$2MnO_2 + H_3AsO_3 = 2MnOOH^* + H_3AsO_4 \qquad (2\text{-}7)$$
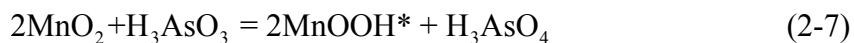
where MnOOH* is a Mn (III) intermediate reaction product. The final equation representing the transformation of As (III) to As (V) is given by:

$$2MnOOH^* + H_3AsO_3 + 4H^+ = 2Mn^{+2} + H_3AsO_4 + H_2O \qquad (2\text{-}8)$$
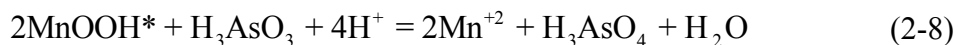
2.6.1 Other Methods of As (III) oxidation to As (V)

Hug and Leupin (2003) successfully conducted As (III) oxidation by oxygen and hydrogen peroxide (H_2O_2) with the aid of an iron catalyzed reaction. The study showed the simultaneous oxidation of Fe (II) and As (III) by O_2 and H_2O_2 and the non-inhibitory effect of $^.OH^-$ scavenger radical during the oxidation process. Emett and Khoe (2001) showed that rate of As (III) oxidation to As (V) can be increased several folds by O_2 in the presence of dissolved Fe (III) with the reaction solution illuminated to the near ultraviolet light. Dutta et al. (2005) showed the photocatalytic oxidation of As (III) to As (V) with $^.OH^-$ radical acting as the principal oxidant. Catherino (1967) performed electrochemical oxidation of As (III) to As (V), whereas Sengupta and Chakladar (1989) successfully used chromic acid for the oxidation process.

Chemicals used in the oxidation of As (III) to As (V) can result in the formation of byproducts which can be either harmful or difficult to remove from water (Ghurye and Clifford 1990). The usage of these chemical for the purpose of oxidation may not be very economical. Microbial oxidation of As (III) oxidation is not only considered an alternate strategy but a cost effective treatment of arsenic contaminated water.

2.7 Bioremediation of Contaminated Sites

Over the years, microorganisms have evolved mechanisms to remediate both metal and metalloid contaminants from water and wastewater. This special ability of the microorganisms is usually demonstrated by changes in the redox states of the corresponding metals / metalloids or by adsorption onto its surface. The net result of both the processes leads to the reduction in the mobility of these contaminants in the environment (Lovley and Coates 1997). The principal application of the bioremediation process can be subdivided into three major categories.

2.7.1 Biosorption of Metals

Biosorption is the process by which the metals / metalloids are absorbed onto the microbial surface of the living or the dead biomass. It is a very effective technique in immobilizing the metals present in the soils before entering the groundwater table. The economic viability and the effectiveness of biosorption method for the treatment of contaminated water and wastewater streams has been evaluated to be approximately the same as the ion exchange and chemical precipitation (Eccles H 1995; Lovley and Coates 1997). One such group of bacteria is *Saccharomyces cerevisiae*, a waste product of the industrial fermentation, found very useful in the absorption of metal contaminants (Volesky and May-Phillips 1995; Lovley and Coates 1997).

2.7.2 Biological Reduction of the Metal / Metalloid Contaminants

Several microorganisms are able to remediate metals / metalloids contaminants from water and wastewater by lowering the redox states of the corresponding contaminants. The potential use of specific microbes for the remediation of water and wastewater contaminated with metals and metalloids is being researched (Lloyd 2003). *Shewanella oneidensis* and *Geobacter metallireducens* are the first isolated microorganisms known to have exhibited growth during the reduction of Fe (III) or Mn (IV) (Myers and Nealson 1988; Lovley et al. 1987; Lovley 1989). Chirwa and Wang (1997) demonstrated biological reduction of Cr (VI) to Cr (III) using *Bacillus sp.* and *Pseudomonas fluorescens* LB 300 in fixed-film bioreactors. Microorganisms such as *W. succinogenes* and *Pseudomonas stutzeri* (Tomei et al. 1992; Lortie et al. 1992) have been also isolated to reduce Se (VI) and Se (IV) to Se^0 for the remediation of selenium contaminated water. Lovley et al. (1991) also demonstrated for the first time the biological reduction of the oxidized form of uranium, U (VI), to the insoluble form, U (IV), using the Fe (III)-reducing bacteria *G. metallireducens*.

2.7.3 Biological Oxidation of Metal /Metalloid Contaminant

Water and wastewater contaminated with metals/metalloids can be also remediated using microbes capable of increasing the redox states of the contaminants, rendering them insoluble or decreasing their toxicity in water. A very good example is the solubilization of metals in the sludge caused by low pH, produced as a result of microbial oxidation of elemental sulfur to sulfate (Shooner and Tyagi 1996; Jordan et al. 1996). Scientists discovered two rare groups of chemolithotrophic bacteria (*Acidithiobacillus ferrooxidans*, and *Thiobacillus ferrooxidans*) capable of oxidizing Fe^{+2}

to Fe^{+3} and derived energy for growth from the oxidation process (Molchanov et al. 2007; Okereke and Stevens Jr 1991).

2.8 Microbial Oxidation of As (III) to As (V)

Microbial oxidation of As (III) to As (V) was first observed in certain microorganisms, in the year 1918 in cattle-dipping tanks (Green 1918). A number of microorganisms capable of oxidizing As (III) to As (V) under both aerobic and anaerobic conditions have been isolated and identified since. Heterotrophic As (III) oxidation may represent a detoxification reaction on the cell's cytoplasmic (inner) membrane, whereas autotrophic As (III) oxidation releases energy that is used for CO_2 fixation and cell growth under both aerobic and anaerobic conditions (Anderson et al., 1992; Ilyaletdinov and Abdrashitova 1981; Santini et al., 2000). However, the autotrophic As (III) oxidation process may be preferred over heterotrophic one because of its lower nutritional requirements and lower potential for production of any harmful organic metabolites. The first heterotrophic As (III) oxidizing bacteria was described in 1918 (Green 1918), whereas an autotrophic As (III) oxidizing strain, *Pseudomonas arsenitoxidans*, was first reported in 1981 (Ilialetdinov and Abdrashitova 1981). Table 2.5 lists the several isolated heterotrophic and autotrophic As (III) oxidizing strains with their substrates and redox conditions for growth.

The novel chemoautotrophic *T.arsenivorans* strain b6 was first isolated by Battaglia Brunet et al. (2006) from a cheni disused gold mining site in France. Battaglia Brunet et al. (2006) reported the optimum pH, temperature, growth conditions, and As (III) oxidation ability of the strain b6. In the current study, As (III) oxidation was further

investigated by the chemoautotrophic *T.arsenivorans* strain b6 in continuous flow bioreactors under varying As (III) loading rates.

Table 2.5 As (III)-Oxidizing Microorganisms

Microorganism	Substrate/Redox condition	Source	References
Thiomonas arsenivorans sp. str. b6 (chemoautotroph)	Asparate, glutamate, pyruvate, succinate, glucose, raffinose, sucrose, sorbitol, yeast extract, sulfur, thiosulfate, tetrathionate, As (III) oxidation, and Fe (II) oxidation / aerobic and anerobic	Disused gold mining site in France	Battaglia-Brunet et al. (2006)
Strain CASO1 (autotroph)	As (III)/aerobic	Disused gold mining site in France	Battaglia-Brunet et al. (2002)
Agrobacterium/Rhizobium sp. str. NT-26 (chemolithoautotroph)	As (III), yeast extract, acetate, succinate, fumarate, pyruvate, malate, mannitol, sucrose, glucose, arabinose, fructose, trehalose, raffinose, maltose, xylose or galactose, lactate, salicin, glycerol, lactose, or inositol.	Gold mine in Northern Australia	Santini et al. (2000)
Ancyclobacter sp. str. OL-1 (chemoautotroph)	As (III), thiosulfate, sulfur, and sulfide (aerobic)	Onondaga lake (New York), and lagoon (Venezuela)	Garcia-Dominguez et al. (2008)
Thiobacillus sp. str. S-1 (chemoautotroph)	As (III), thiosulfate, sulfur, and sulfide , amonium (aerobic and anerobic)	Onondaga lake sediment (New York), and lagoon (Venezuela)	Garcia-Dominguez et al. (2008)

Table 2.5 (Continued)

Microorganism	Substrate/Redox condition	Source	References
Hydrogenophaga sp. str. CL-3 (chemoautotroph)	As (III), thiosulfate, sulfur, and sulfide, amonium, and nitrite (aerobic and anaerobic)	Onondaga lake sediment (New York), and lagoon (Venezuela)	Garcia-Dominguez et al. (2008)
Azoarcus sp. str. DAO1 (chemoautotroph)	As (III), bicarbonate, acetate, glucose, lactate, citrate, phenol, benzoate, *m*-xylene, and *p*-cresol/ anaerobic	Onondaga lake sediment (New York), Arthur kill sediment (NY/NJ harbour, and lagoon (Venezuela)	Rhine et al. (2006)
Sinorhizobium sp.str. DAO10 (chemoautotroph)	As (III), bicarbonate, acetate, glucose, and lactate/ anaerobic	Onondaga lake sediment (New York), Arthur kill sediment (NY/NJ harbour, and lagoon (Venezuela)	Rhine et al. (2006)
Sinorhizobium Ensifer sp.str. SDB1 (chemolithotroph)	As (III), glucose, fructose, galactose, sucrose, rhamose, alanine, glutamic acid, histidine, and proline	Sandong Mine area (Korea)	Lugtu et al. (2009)
Ectothiorhodospira sp. str. MLHE-1 (chemoautotroph)	As (III), hydrogen, sulfide, and acetate / anaerobic	Monolake (CA)	Oremland et al. (2002)

Table 2.5 (Continued)

Microorganism	Substrate/Redox condition	Source	References
Alkalilimnicola ehrlichii sp. str. (chemoautotroph)	As (III), hydrogen, sulfide, thiosulfate /facultatively aerobic and anerobic	Monolake (CA)	Hoeft et al. (2007)
Zoogloea sp.str.ULPAs 1 (chemoorganotroph)	lactate, acetate, peptone/aerobic	aquatic environment	Weeger et al. (1999)
Alcaligenes faecalis sp. str. O1201 (Heterotroph)	succinate, citrate, nutrient broth/aerobic	Soil sediment (OH)	Suttigarn (2005)
Agrobacterium albertimagni sp. str. AOL 15	Citrate, yeast extract, L-glutamate, and mannitol / aerobic	Hot creek (CA)	Salmassi et al (2002)
Thermus aquaticus sp. str. YT 1 (Heterotroph)	Sugars, organic acids, tryptone, yeast extract /obligate aerobe	Yellow stone (CA)	Brock and Freeze (1969)
Thermus thermophilus sp. (Heterotroph)	Yeast extract	Yellow stone (CA)	
Thermus sp. str. HR 13	Yeast extract , tryptone, and arsenate/ aerobic and anaerobic	Growler hot spring (CA)	Gihring and Banfield (2001)
Bosea thiooxidans sp. str. WAO	As (III), $S_2O_3^{2-}$, S^0, HCO_3^-, acetate, glucose, and lactate / aerobic	Newark's basin Lockatong formation, Trenton (NJ)	Rhine et al. (2008)

2.9 Arsenic Metabolism in Microorganisms

2.9.1 Arsenite Oxidase Enzyme

As (III) oxidation by heterotrophic bacterial strains is often considered a detoxification mechanism for tolerating high levels of As (III) concentrations in the water. However, studies have shown that certain microbes can use the energy released during As (III) oxidation to support cellular growth (Santini et al. 2000; Battaglia-Brunet et al. 2006). The enzyme catalyzing the As (III) oxidation process is called arsenite oxidase (Anderson et al. 1992; Ellis et al. 2001). The purification and characterization of the enzyme from the bacterial strain *Alcaligenes faecalis* (Legge and Turner 1954) was accomplished by Anderson et al. (1992). The enzyme is generally located on the outer surface of the inner membrane as observed in *Thiomonas* 3As (Duquesne et al. 2008), *Alcaligenes faecalis* (Anderson et al. 1992), and *Herminiimonas arsenicoxydans* str. ULPAs1 (Muller et al. 2003). However, the location of the enzyme found in the periplasmic space between the inner and outer membrane in *Hydrogenophaga* sp. str. NT-14 (Hoven and Santini 2004) and in *Rhizobium* sp. str. NT-26 (Santini et al. 2000) could be due to weak attachment to the periplasmic side of the cytoplasmic membrane (Duquesne et al. 2008).

2.9.2 Arsenite Oxidase Structure

Ellis et al. (2001) recently solved the structure of the arsenite oxidase using X-ray diffraction analysis. The structure consists of two major subunits. The large subunit, an 88-kDa polypeptide (825 amino acids residues) contains the Mo-pterin and HiPIP (High potential Iron Protein) 3Fe-4S center, whereas, the small subunit, a 14-kDa (134 amino acids) consists of the Rieske 2Fe-2S center (Anderson et al. 2001; Ellis et al. 2001)

(Figure 2.4). The orientation of the two pterins in the Mo-pterin cofactor is very similar to that of the other Mo-pterin cofactors in dimethyl sulfoxide (DMSO) reductase protein family (McEwan et al. 2002).

2.9.3 Arsenite Oxidase Reaction Cycle

Arsenite (As (OH) $_3$) is transported by aqua-glyceroporins through the funnel shaped opening of the large subunit structure and binds immediately to the Mo (VI) of the oxidized cofactor. The direct nucleophilic attack as a result of this association leads to the oxidation of As (III) to As (V) with the release of 2 electrons, and the subsequent reduction of Mo (VI) to Mo (IV) respectively (Figure 2.4). As (III) oxidation to As (V) is an exothermic reaction with release of significant amount of energy (Eq. (2-9)):

$$2H_3AsO_3 + O_2 \rightarrow HAsO_4^{2-} + H_2AsO_4^- + 3H^+ \ (\Delta G^{0'} = \text{-256 kJ/Rx}) \ (2\text{-}9)$$

Some strains have exhibited of utilizing the energy for cellular growth by fixing CO_2 using the well known Calvin-Benson-Bassham cycle (Jessup et al. 1998). Arsenate produced as a result of the oxidation process is released to the environment, whereas, Mo (IV) is reoxidized to Mo (VI) by the transfer of 2 electrons from Mo (IV) to the [3Fe-4S] HiPIP center. The two electrons are then transferred from the [3Fe-4S] HiPIP center to the Rieske [2Fe-2S] center of the small subunit. The small subunit is then finally reoxidized by the eventual transfer of these two electrons to azurin or cytochrome *c* of the oxygen-respiratory chain completing the reaction cycle of arsenite oxidase.
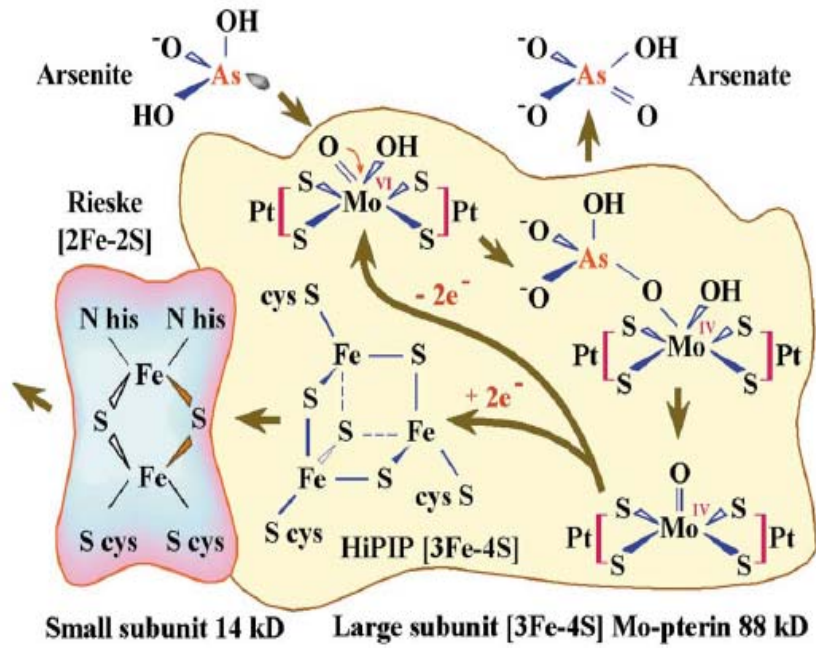
Figure 2.4 Proposed reaction pathway in arsenite oxidase obtained from *A.faecalis*
(Anderson et al. 1992; Ellis et al. 2001; Mukhopadhyay et al. 2002)

2.10 Calvin cycle: Carbon Metabolism in Chemolithoautotrophic Bacterial Strains

Most autotrophic microorganisms use the Calvin-Benson-Bassham cycle to fix CO_2 for cell synthesis (Shively et al. 1998). Obligate chemoautotrophs can fix CO_2 only by Calvin cycle, whereas, facultative chemoautotrophs in addition to the Calvin cycle possess the ability to exhibit growth on a wide range of substrates. Bryan et al. (2009) detected *cbbSL* genes encoding ribulose 1, 5-biphosphate carboxylase/oxygenase, leading to the belief that the *T. arsenivorans* strain b6 may be able fix CO_2 via the Calvin cycle.

2.10.1 Enzymatic Reactions of the Calvin Cycle

The Calvin cycle comprises of 13 enzymatic reactions as shown in Figure 2.5. The primary enzyme responsible for the fixation of CO2 is the ribulose-1, 5-biphosphate carboxylase / oxygenase (RuBisCO), which catalyzes the carboxylation of ribulose-1, 5-biphosphate (RuBP) leading to the formation of two molecules of 3-phosphoglycerate (McFadden, and Shively 1991; Tabita, F.R. 1988). The three glycolytic enzymes namely phosphoglycerate kinase, glyceraldehydes-3-phosphate dehydrogenase, and triosephosphate isomerase utilizes two molecules of ATP and two molecules of NADH for the conversion of the two molecules of 3-phosphoglycerate to glyceraldehydes-3-phosphate and dihydroxyacetone phosphate. A series of rearrangement reactions finally produces ribulose-5-phosphate (Jessup et al. 1998).

Two very similar metabolic units comprising of aldolase, a phosphatase, and a transketolase (APT) are the major component of the rearrangement reactions. Glyceraldehyde-3-phosphate and dihydroxyacetone phosphate is converted by the first metabolic unit into xylulose-5-phosphate and erythrose-4-phosphate. The second metabolic unit transforms dihydroxyacetonephosphate and erythrose-4-phosphate into

xylulose-5-phosphate and ribulose-5-phosphate. Xylulose-5-phosphate and ribose-5-phosphate are eventually converted to ribulose-5-phosphate by pentose epimerase and pentose phosphate isomerase. The final and the critical step in the Calvin cycle is performed by the unique enzyme phosphoribulokinase (PRK) for the regeneration of the RuBP at the expense of an ATP molecule (Jessup et al. 1998). Calvin cycle is a very expensive cycle because it utilizes nine molecules of ATP and six molecules of NADH (Nicotinamide adenine dinucleotide dehydrogenase) to produce one molecule of triose phosphate and three molecules of CO_2 respectively.

2.10.2 Evidence of CO_2 Fixation in *Thiomonas arsenivorans* Strain b6

Bryan et al. (2009) reported two very interesting findings about *T. arsenivorans* strain b6. Firstly, the primary proteins involved in CO_2 fixation (RuBisCo, and fructose-1, 6-biphosphate) were more abundant in the presence of arsenic. The study also revealed that the proteins involved in CO_2 fixation and enzymes involved in the glycolysis / neoglucogenesis were even expressed in the presence of organic substrates such as yeast. Another set of experiments conducted by Bryan et al. (2009) demonstrated the carbon fixation efficiency of the strain with increasing concentration of As (III) oxidized. The results of the study showed almost a linear relationship between carbon fixed and amount of As (III) oxidized in a solution consisting of 1.33 mM of As (III). The results also indicated that for every 1.33 mM of As (III) oxidized, 0.32 mM of carbon is fixed. The carbon fixation efficiency of 6% for *T. arsenivorans* strain b6 is very similar to the 5-10% fixation efficiency range of other autotrophic bacteria (Shock and Helgeson 1988).
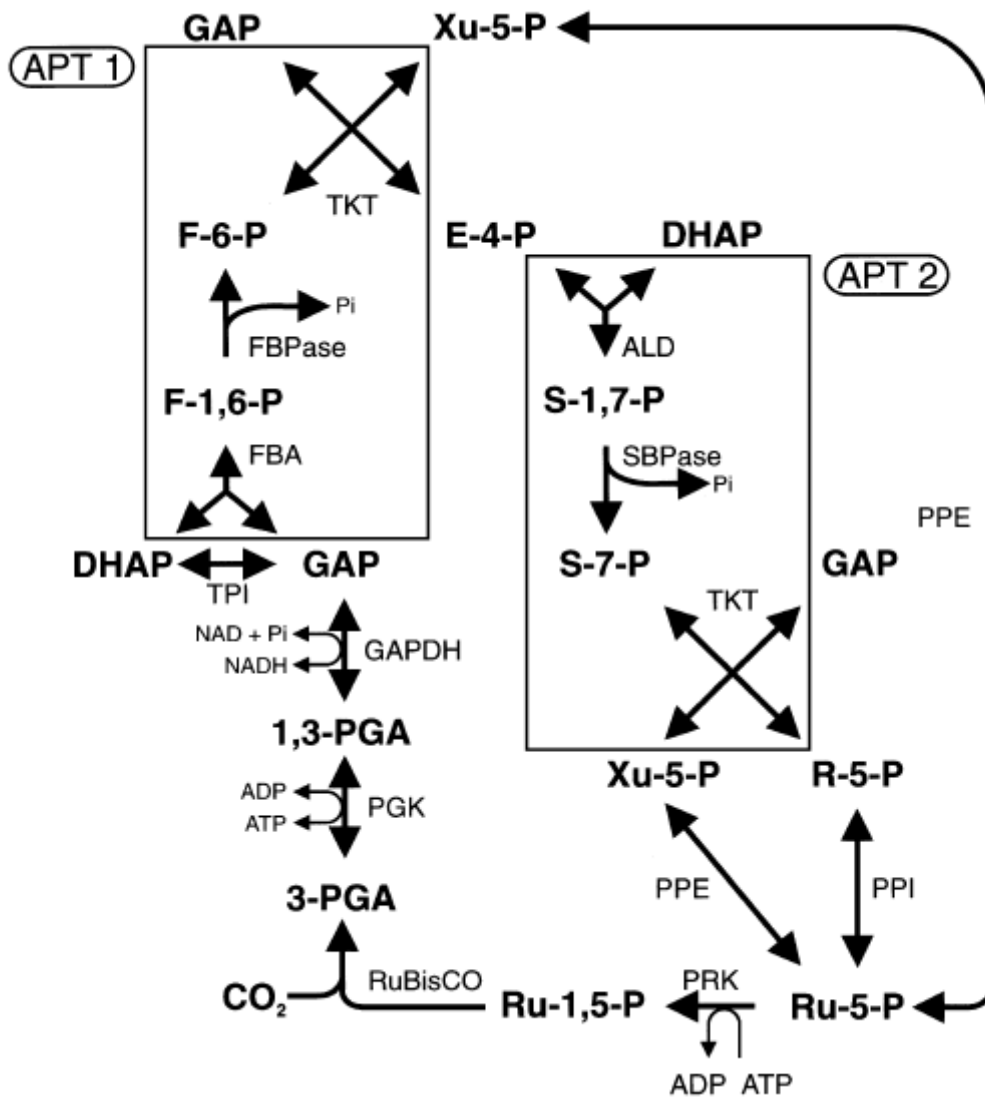
Figure 2.5 Calvin Cycle (Shively et al. 1998)

Chapter 3: Batch Reactor Study

3.1 Abstract

Arsenite (As (III)) oxidation by T.arsenivorans strain b6 was investigated in batch reactors at pH 6 and 30°C over As (III) concentrations ranging from 10 to 1,000 mg/L in the absence of added organic carbon. Strain b6 completely oxidized As (III) to arsenate (As (V)) during exponential growth phase for lower levels of As (III) concentrations ($\leq$ 100 mg/L). At higher levels of 500 and 1000 mg/L, As (III) oxidation was observed mostly in the exponential phase but continued into the stationary phase of growth. The Haldane substrate inhibition model was used to estimate biokinetic parameters for As (III) oxidation. The best fit parameters of half saturation constant K_s = 33.2 $\pm$ 1.87 mg/L, maximum specific substrate utilization rate k = 0.85 $\pm$ 0.18 mg As (III)/mg dry cell weight / hour, substrate inhibition coefficient K_i = 602.4 $\pm$ 33.6 mg/L, yield coefficient Y = 0.088 $\pm$ 0.0048 mg cell dry weight/mg As (III), and endogenous decay coefficient k_d = 0.006 $\pm$ 0.002 hour^{-1} were obtained using the Adams-Bashforth-Moulton algorithm and nonlinear regression technique. Sensitivity analysis revealed that Y and K_i are the most sensitive to model predictions, while k_d is the least sensitive to model simulation at both low and high concentrations of As (III).

3.2 Introduction

Batch reactors are suspended growth reactors generally used for investigational and treatability studies of pollutant degradation in water and soil. The reactors are filled with appropriate amount of contaminated liquid, specific bacterial culture known to degrade the particular pollutant of interest, and essential nutrients for the bacterial growth (Rittmann 2001). The contents of the reactors are kept in suspension by incubating the

reactors on a shaker at fixed rotation speed. Based on the aerobic / anaerobic nature of the contaminant degradation, batch studies are generally conducted in an oxygen rich / anoxic environment. The operation of the batch reactors are generally terminated once the measured level of the contaminant is below the MDL (Method Detection Limit) or the concentration remains the same in consequent sample measurements.

There are several advantages of using batch reactors for investigational research studies for removal of metal contaminants from water:

1. Batch reactors are generally very easy to operate compared to continuous flow bioreactors. The non-requirement of pumps and the minimal chances of bacterial contamination during the degradation make the process very economical and reliable.

2. Research studies have shown batch reactors to be highly efficient in the removal of individual wastewater contaminants (Rittmann 2001).

3. The concept of sequencing batch reactors, where batch reactors are operated in a parallel manner have gained a lot of importance and momentum as a part of the design strategy in remediating contaminated water. Several studies have demonstrated very high removal efficiency of contaminants with the application of the sequencing batch reactor process (Strous et al. 1998; Munch et al. 1996; Woolard and Irvine 1995; and Zeng et al. 2003).

4. The ease of operation makes it possible to operate several (n $\geq$ 3) identical batch reactors at the same time. The measured data are generally expressed as average $\pm$ SD (standard deviation), the most reliable manner of representing experimental observations.

In the current research, batch studies were conducted using the novel chemoautotrophic Thiomonas arsenivorans strain b6 to investigate As (III) oxidation to

As (V) under varying environmental conditions. The novelty of the strain b6 was the use of As (III) as the sole source of energy for growth and the usage of carbon dioxide (CO2) for cell synthesis (Battaglia-Brunet et al. 2006).

The specific objectives of the batch reactor study are as follows:

1. To investigate the optimal conditions (pH and temperature) for the biological oxidation of As (III) to As (V) using pure batch cultures of T.arsenivorans strain b6. The batch studies were conducted under five different pHs (4, 6, 7, 8, and 9) and four different temperatures (10°C, 20°C, 30°C, and 40°C) for evaluating the optimum pH and temperature for oxidizing As (III) to As (V).

2. To test the effect of dissolved oxygen (DO) on the rate of biological oxidation of As (III) under optimal pH and temperature conditions.

3. To investigate whether CO_2 was limiting during the oxidation of As (III) to As (V) by pure cells of the T.arsenivorans strain b6. Batch studies were conducted with and without the addition of 500 mg/L of sodium bicarbonate ($NaHCO_3$) to the growth media containing As (III).

4. To assess the As (III) oxidation ability of T.arsenivorans strain b6 under a wide range (10 mg/L – 1,000 mg/L) of initial As (III) concentrations. The purpose of this approach was to explore the toxicity level of As (III) which inhibited the growth of strain b6 leading to significant reduction in the As (III) oxidation rate.

5. To investigate the effect of different initial cell concentrations of T.arsenivorans strain b6 on the oxidation rate of As (III). The objective was to evaluate whether increase in the initial cell concentration improved the overall biological As (III) oxidation rate.

6. To determine the intrinsic biokinetic parameters (k maximum specific As (III) oxidation rate $[MM_x^{-1}T^{-1}]$; K_s As (III) half velocity constant $[ML^{-3}]$; Y Yield coefficient $[M_sM_x^{-1}]$; k_d is the endogenous decay coefficient $[T^{-1}]$) using a kinetic model and the As (III) oxidation data obtained from the batch study. The Haldane model was tested and solved using a nonlinear least-square estimation technique and the Adams-Bashforth-Moulton algorithm.

7. To verify the applicability of the Haldane model and the obtained best-fit parameters. Specifically, model simulations were obtained for a broader range of initial As (III) concentrations by varying the initial observed biomass concentrations within the acceptable analytical precision of ± 20%.

8. To evaluate the sensitivity of the model to changes in the parameters for both low and high initial As (III) concentrations (10 mg/L and 1,000 mg/L). A plot of the sensitivity coefficients against the independent variable, t is beneficial in assessing the sensitivity of the model prediction to changes in the parameters and correlation between the obtained kinetic parameters.

3.3 Materials and Methods

3.3.1 Bacterial strain and growth medium

Thiomonas arsenivorans (LMG 22795T) b6 was obtained from the BCCM[TM]/ LMG collection center in Belgium. The details of isolation, identification and growth aspect of strain b6 were described before (Battaglia-Brunet et al. 2006; Altschul et al. 1997; Katayama et al. 2006; Moreira et al. 1997). Strain b6 was grown using a modified CSM medium (MCSM) consisting of two solutions (Battaglia-Brunet et al. 2002, 2006). Solution A contained 0.5g of K_2HPO_4, 0.5g of KH_2PO_4, 0.5g of NaCl, 0.5g of yeast

extract, 0.05 g of $(NH4)_2SO_4$, and 1 mL of trace elements solution in 500 ml of deionized distilled water. The pH of solution A was adjusted to 6 with H_2SO_4. Solution B contained 0.1g of $CaCl_2$ and 0.1g of $MgSO_4$ in 500 mL of deionized distilled (DD) water. Both the solutions A and B were autoclaved at 121°C for 15 minutes, cooled and then mixed. The trace elements solution was prepared by adding 6.5 mL of HCl (25%), 1.5 g of $FeCl_2.4H_2O$, 60mg of H_3BO_3, 100 mg of $MnCl_2.4H_2O$, 120 mg of $CoCl_2.6H_2O$, 70 mg of $ZnCl_2$, 25mg of $NiCl_2.6H_2O$, 15 mg of $CuCl_2.2H_2O$ and 25 mg of $Na_2MoO_4.2H_2O$ to 1L of DD water. The medium used for As (III) oxidation study was a modified MCSM medium to which 5g/L each of K_2HPO_4 and KH_2PO_4 were added as a buffer and no yeast extract was added.

3.3.2 As (III) oxidation experiment

3.3.2.1 Optimal pH and Temperature Study

The optimal conditions for As (III) oxidation by strain b6 were first investigated at five different pHs (4, 6, 7, 8, and 9) and four temperatures (10°C, 20°C, 30°C, and 40°C). Inocula of the strain b6 were first grown overnight in the MCSM medium. Once the cells reached the exponential growth phase, they were harvested by centrifugation at 4500 x g for 20 mins and at 4˚C. The harvested cells were washed three times with 0.85% NaCl before use in the experiments. 10% (v/v) of the obtained pure strain b6 were introduced into 250 mL Erlenmeyer flasks containing the modified MCSM medium with 100 mg/L of As (III). The mouth of the flasks were then capped with sterile cotton plugs and incubated on a shaker (120 rpm) at 30°C in the dark. The pH range (4 − 9) was adjusted in the modified (MCSM) medium with 1N NaOH or 6N H_2SO_4 containing 5g/L each of the buffer K_2HPO_4 and KH_2PO_4. Samples were collected at appropriate intervals

to determine As (III), As (V) and viable cell concentrations. The optimal temperature for As (III) oxidation was also investigated using the same procedure over a range of 10 - 40 $\pm$ 1.5°C. All the experiments were run in triplicates.

3.3.2.2 Biological and Chemical Control Study

As (III) oxidation was also investigated using biological control (cells of T.arsenivorans strain b6 killed by autoclaving at 121°C for 15 minutes) and chemical control (modified MCSM medium only) conditions. The batch studies were run in triplicates and at optimal pH and temperature conditions. The studies were essential to ascertain that As (III) transformation to As (V) occurred only due to enzymatic reactions resulting from the synthesis of enzymes by pure cells of T.arsenivorans strain b6.

3.3.3 Analytical Method

3.3.3.1 Sample Handling and Quality Control

Samples from the bioreactor were collected using 1 mL sterile disposable pipets (Fisher Scientific CO., Pittsburgh, PA) at appropriate time intervals. The collected samples were immediately centrifuged at 10,000 rpm for 10 mins using a microcentrifuge (Brinkmann Instruments Inc, West bury, NY). The supernatant was acidified using 1 % HNO_3 (pH < 2) and preserved in 4 °C for no more than 7 days prior to analysis of As (III), As (V) and total As (APHA 1995). Microbial analysis involved determining the viable suspended cell concentrations and biomass dry weight measured as volatile suspended solids (VSS). The biological samples were analyzed immediately in order to prevent any changes in the actual cell concentrations at the time of sample collection.

The glassware apparatus for arsenic analyses were rinsed with concentrated HNO_3 to remove any stains which might interfere with the true absorbance reading of the

arsenic samples. After rinsing, the glassware were washed with Micro-90 detergent (IPC, Burlington, New Jersey) and tap water in a water bath. They were again rinsed in deionized distilled water (Millipore, Bedford, MA) and oven dried at 105°C for at least 1 hour prior to using for the analyses.

Prior to analyses of the preserved samples in one big batch comprising of seven samples each of As (III), As (V), and total As, new calibration curves were established to eliminate any bias during corresponding absorbance measurement (APHA 1995).

3.3.3.2 As (III), As (V), and Total As Determination

As (III), As (V), and total As were analyzed using a silver diethyldithiocarbamate method (SDDC) (3500-As B, APHA 1995). The method was slightly modified by adding 1 g of sodium borohydride to 0.01 N NaOH (Fisher scientific CO., Pittsburg, PA) instead of 1 N NaOH solution (Suttigarn and Wang 2005). This was essential for obtaining different distinguishable color absorbance readings for varying arsenic concentrations of the samples. The nitrogen flow rate inside the arsine generator was maintained at 100 ± 5 mL / min with a flow meter (Gilmont$^@$ Instrument, Model 316 SS). The glass wool placed in the scrubber was continuously monitored and replaced when needed. The black or grayish color of the glass wool indicated the ineffectiveness in removing H_2S, which caused potential interference with the true absorbance reading of the arsenic samples (APHA 1995). As (III), As (V), and total As concentrations in mg/L were determined from the absorbance values using their respective calibration curve as shown below:

$$\text{mg As /L} = \frac{\mu\text{g As (from calibration curve)}}{\text{mL sample in generator flask}} \text{ x (Dilution factor)} \qquad (3\text{-}1)$$

The method detection limit (MDL) for arsenic using the SDDC method is 1 mg/L.

3.3.3.3 pH and Dissolved Oxygen Determination

pH was measured in situ using a pH meter (Denver Instrument, Denver, CO) equipped with an ATC Combo, Silver/Silver chloride electrode. The pH meter was calibrated with standard buffers of 4 and 7 and disinfected by 95% ethanol before use. DO was determined in situ using a DO meter (YSI 550A, Yellow Springs, Ohio), also calibrated and disinfected with 95% ethanol before use.

3.3.4 Biomass Analysis

3.3.4.1 Viable Suspended Cell Count

The suspended viable cell concentration was determined according to the spread plate technique outlined in section 9215C of the standard methods for the examination of water and wastewater (APHA 1995). The agar medium for the spread plate method comprised of the modified MCSM medium (including yeast extract) and 15 g of Difco ^{TM} Nutrient Agar (Becton, Dickinson and Company, Sparks, MD). The agar medium was autoclaved at 121°C for 15 mins and then spread over a number of 100 x 15 cm petri dishes to solidify over time.

Samples of volume 1 mL were withdrawn from the batch reactors at appropriate time intervals and transferred to clean (autoclaved at 121°C for 15 mins) borosilicate test tubes containing 9 mL of the dilution water. The constituents of the dilution solution were essentially the same as the modified MCSM medium but without the addition of yeast extract, As (III), and nutrient agar. The resulting solution was further diluted using the serial dilution technique outlined in the standard methods for the examination of water and wastewater (APHA 1995). 100 μL of the sample was withdrawn from each of the borosilicate test tubes of dilution factors ranging from 10^6 to 10^8, and transferred to

the solidified agar medium on the agar plates. The samples were then spread on the agar medium using sterile bent rods. After spreading, the agar plates were inverted and kept in a walk-in temperature room at 30°C for at least 48 hours before counting the number of colonies on the plate. The colonies were counted using a colony counter (Quebec Colony Counter, model 3330, American Optical, Co., Buffalo, N.Y.). A maximum relative standard deviation of ± 20 % was established for the analysis of replicate biomass samples.

3.3.4.2 Biomass Dry Weight

Batch reactors containing 500 mL of the MCSM medium with yeast extract were inoculated with 10% V/V of pure cells of T.arsenivorans strain b6, and then placed on a rotary shaker at 120 rev/min and 30°C. The purpose of this study was to obtain significant amount of cell density for establishing an appropriate correlation between biomass dry weight and viable suspended cell concentration. Samples were collected at different time intervals of the log phase growth of the culture to analyze for suspended viable cell concentrations and their corresponding biomass dry weight measured as volatile suspended solids (VSS). The method for the measurement of cell density as VSS is outlined in section 2540E of standard methods for the examination of water and wastewater (APHA 1995). A correlation was established between the viable cell count and biomass dry weight with a conversion factor of 6.604×10^{-8} mg dry weight / L· cell (Appendix C, Figure C-5).

3.4 As (III) Oxidation Kinetic Analysis

The data indicate that As (III) oxidation is coupled to the growth of strain b6 with inhibition observed at higher levels of As (III) concentrations. Consequently, the Haldane expression was used to analyze As (III) oxidation by this strain:

$$-\frac{dS}{dt} = \frac{kSX}{K_s + S + \frac{S^2}{K_i}}$$
(3-2)

where S is the As (III) concentration $[ML^{-3}]$, t is the incubation time $[T]$, k is the maximum specific As (III) utilization rate $[MM_x^{-1}T^{-1}]$, X is the cell concentration $[ML^{-3}]$, K_s is the saturation constant $[ML^{-3}]$, and K_i is the inhibition coefficient $[ML^{-3}]$. The net growth rate of strain b6 is described by:

$$\frac{dX}{dt} = Y(-\frac{dS}{dt}) - k_d X$$
(3-3)

where Y is the cell yield coefficient $[M_s M_x^{-1}]$ and k_d is the endogenous decay coefficient $[T^{-1}]$. Initial estimate of Y was evaluated independently from the substrate and growth data whereas parameters k, K_s, and K_i were obtained using a linearized form of Eq. (3-3) without the endogenous decay coefficient at high ($S \gg K_s$) and low ($S \ll K_i$) As (III) concentrations (Onysko et al. 2000; Shuler and Kargi 2002). The initial guess value of k_d was determined from the stationary phase growth data by linear regression using Eq. (3-4) below:

$$\frac{dX}{dt} = -k_d X$$
(3-4)

Kinetic parameters were determined by a computerized numerical integration technique with MATLAB (7.0) using the Adams-Bashforth-Moulton algorithm (Klecka and Maier

1985, 1988). This algorithm was employed for the numerical integration by fitting the differential equations (3-2) and (3-3) to the shape of the substrate depletion versus time curve. The optimized model parameters were obtained by minimizing the residual sum of squares (SSE) between observed data and model calculated values as given by:

$$SSE = \sum_{i=1}^{n} (S_i^{obs} - S_i^{pred})^2 \qquad (3\text{-}5)$$

where S_i^{obs} is the observed As (III) concentration in the i th sample, and S_i^{pred} is the corresponding model prediction of As (III) for the same sample point. A fourth order Runge-Kutta numerical method (Suttigarn and Wang 2005) was applied to generate simulation curves by using MATLAB 7.0

3.5 Sensitivity Analysis

Parameter sensitivity measures the sensitivity of the dependant variable (S) to changes in each of the parameters and is desirable for nonlinear regression analysis. It predicts the uniqueness and relative precision of the estimated parameters from the model. The sensitivity coefficients ($\frac{dS}{dK_s}$, $\frac{dS}{dK_i}$, $\frac{dS}{dK_d}$, $\frac{dS}{dY}$, $\frac{dS}{dk}$) are obtained by calculating the approximate (numerical approximation) first derivatives of the model predictions with respect to each parameter (Smith et al. 1997, 1998). The sensitivity coefficient of the parameter K_s is given by:

$$\frac{\partial S_i^{pred}}{\partial K_s} = \frac{S_i^{pred}(K_s^{p} + \Delta K_s) - S_i^{pred}(K_s^{p})}{\Delta K_s} \qquad (3\text{-}6)$$

where K_s^{p} is the best estimate of K_s, ΔK_s is a small variation of the best estimated value K_s^{p} whereas $S_i^{pred}(K_s^{p} + \Delta K_s)$ and $S_i^{pred}(K_s^{p})$ are the model predictions at i the data

point time for both $K_s{}^p$ and $K_s{}^p + \Delta K_s$ values, respectively. In a similar manner, the rest of the sensitivity coefficients for the parameters (k, K_i, Y, k_d) are obtained from the model predictions. These coefficients are then plotted against the independent variable (t) to estimate the range of the independent variable over which the model is most sensitive to changes in parameters (Robinson and Tiedje 1983).

Since the linear correlation between the model parameters can result in large uncertainties in estimation of unique values from the model (Liu and Zachara 2001), uncertainties in the best estimates of K_s, K_i, Y, k and k_d expressed as the standard error were calculated using the method described by Smith et al.(1997, 1998). The method consists of finding the mean square fitting error (σ^2) and inverse of a p x p matrix containing the sensitivity coefficients of each parameter as well as the correlation coefficients between them (Smith et al. 1997, 1998; Dmitriou-Christidis et al. 2007). The mean square fitting error σ^2 is expressed as:

$$\sigma^2 = \frac{1}{n-p} SSE \qquad (3\text{-}7)$$

where n is the total number of observed data points and p is the number of fitted parameters.

3.6 Results and Discussion

3.6.1 Effect of pH

The pH range for strain b6 growth was previously reported at 4-7.5 (Battaglia-Brunet et al. 2006). In this study, the optimal pH for As (III) oxidation by strain b6 was investigated at 5 different pHs (4, 6, 7, 8 and 9) at an initial As (III) concentration of 100 mg/L. The data in Figure 3.1a show that the amount of As (III) oxidized was 98.8 ± 2.5

% at pH 6 and 13.2 ± 1.9 % at pH 9, respectively after 72 hours of incubation. A significant amount of As (III) (90.5 ± 1.8 %) was also oxidized at pH 4 in the same time period. However, a rapid decline in the rate of As (III) oxidation was observed at pH > 6. Biological oxidation of As (III) at low pH ranges was also reported with other species. As (III) oxidation by strain *Sulfolobus acidocaldarius* was reported at pH of 2- 4 (Shelin and Lindstorm 1992). However, the optimal pH for As (III) oxidation by most known As (III)-oxidizing species is near neutral range (Suttigarn and Wang 2005; Philips and Taylor 1976; Salmassi et al. 2002; Turner 1949, 1954, 1954).

3.6.2 Effect of Temperature

Strain b6 was reported to grow at a temperature range of 20-30˚C (Battaglia-Brunet et al. 2006). In this study, As (III) oxidation was investigated at 4 different temperatures (10, 20, 30, and 40°C) with the optimal observed at 30°C (Figure 3.1b). The amount of As (III) oxidized was 98.9 ± 2.1 % at 30ºC after 72 hours of incubation.

The growth range of most known As (III) oxidizing species is reported to be 25 - 37°C (Suttigarn and Wang 2005; Philips and Taylor 1976; Salmassi et al. 2002). However, *Thermus* strain HR13 and *Sulfolobus acidocaldarius* strain BC oxidized As (III) at very high temperatures of 70 and 65°C, respectively (Shelin and Lindstorm 1992; Gihring and Banfiled 2001). As (III) oxidation at 4°C was also reported with *Pseudomonas putida* strain 18 (Abdrashitova et al. 1985).

a

b
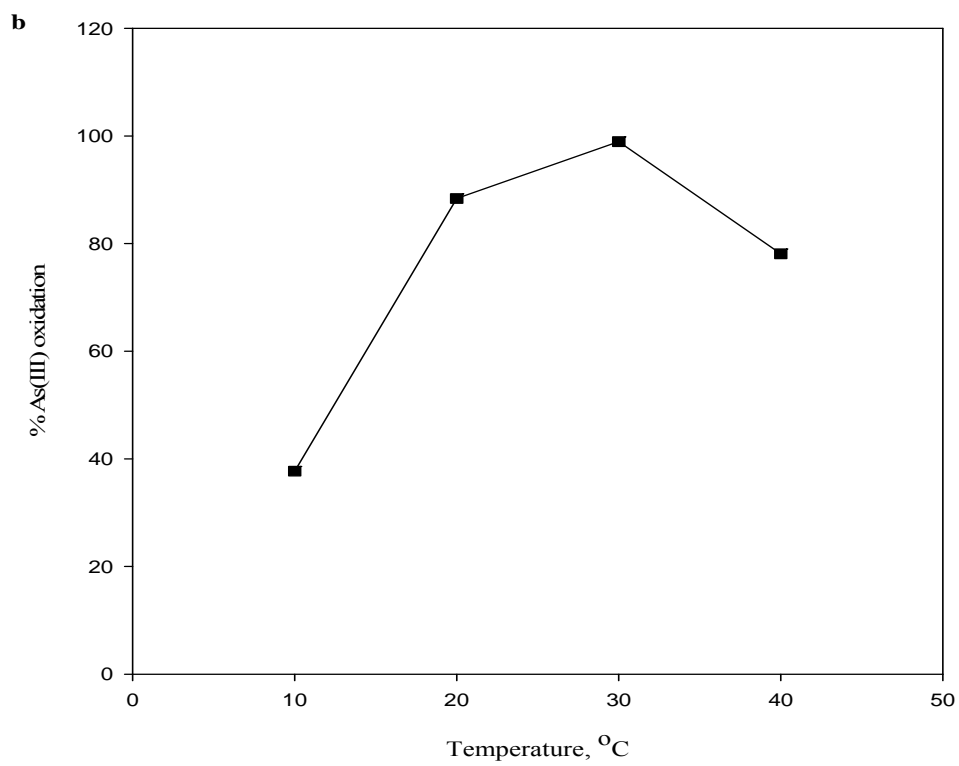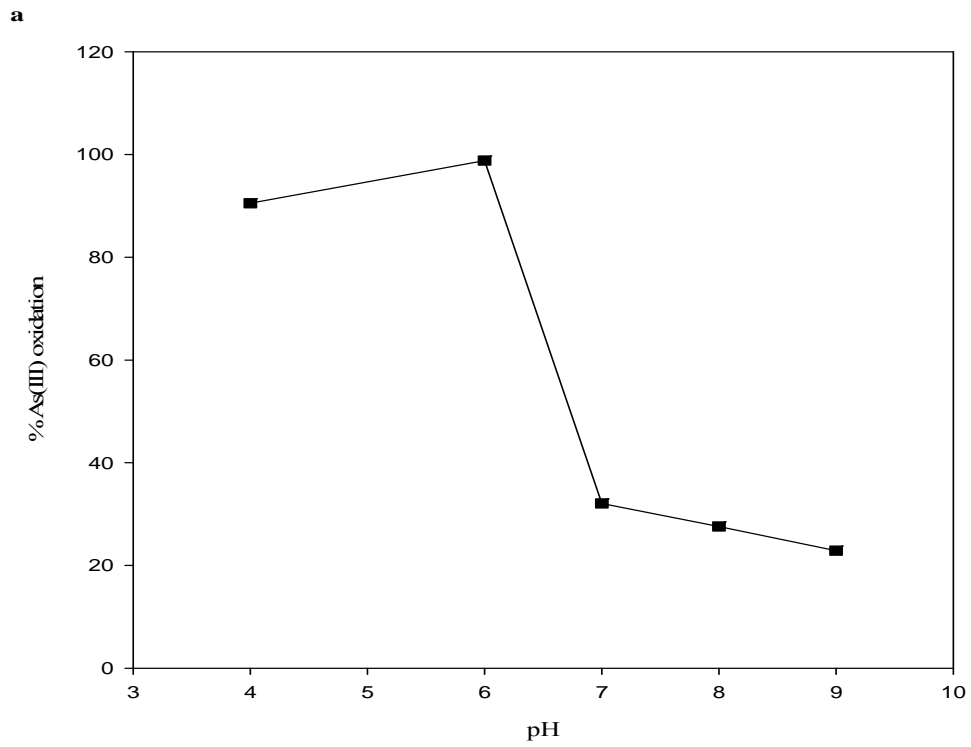
Figure 3.1 Effect of pH (a) and temperature (b) on As (III) oxidation by strain b6

52

3.6.3 Biological and Chemical Control for As (III) Oxidation

As (III) oxidation was investigated in batch reactors by killed cells of *T.arsenivorans* strain b6 containing 100 mg/L of As (III) added to the modified MCSM medium. The data in Figure 3.2a clearly show the absence of any As (III) oxidation to As (V) over the 96 h period. The relative standard deviation (RSD) value (4.18%) was well within the acceptable analytical error of ±15% in accordance with the modified SDDC (Silver DiethylDithio Carbamate) method. The results clearly indicate the lack of abiotic transformation of As (III) to As (V) in the absence of active cells of *T.arsenivorans* strain b6.

Chemical control of As (III) to As (V) was conducted in batch reactors containing 100 mL of the modified MCSM medium and an initial As (III) concentration of 100 mg/L. The data in Figure 3.2b show insignificant change in the level of initial added As (III) in the reactor. The RSD of the measured data was only 4.15%, therefore indicating the absence of any chemical oxidation of As (III) to As (V) under the present batch conditions.

Both the chemical and biological control batch studies conclusively proved that only live cells of *T.arsenivorans* strain b6 can transform As (III) to As (V). The optimal conditions are maintained to achieve maximum As (III) oxidation efficiency during specific reactor processes.

a

b
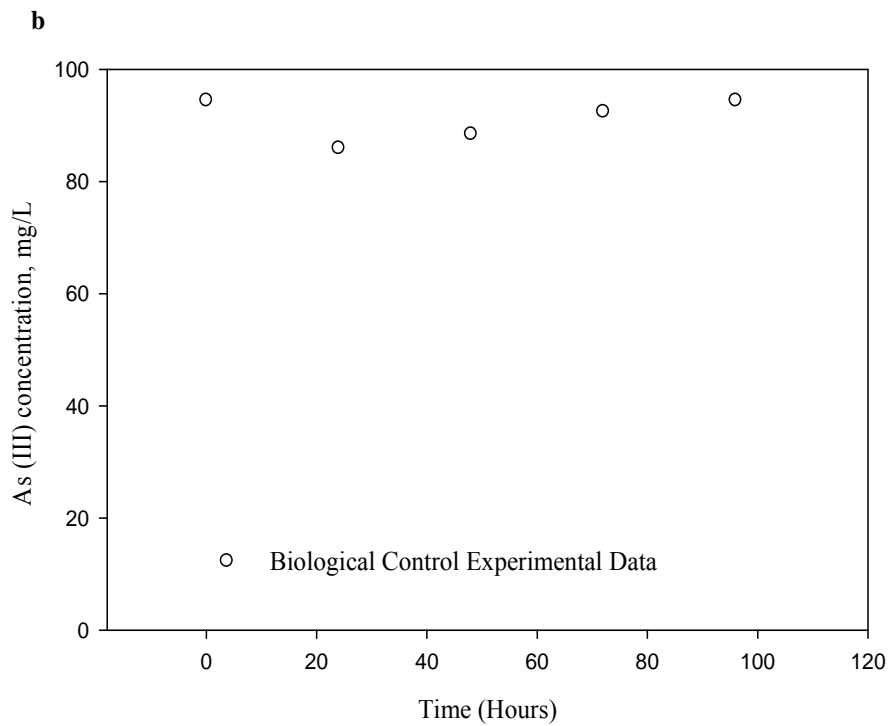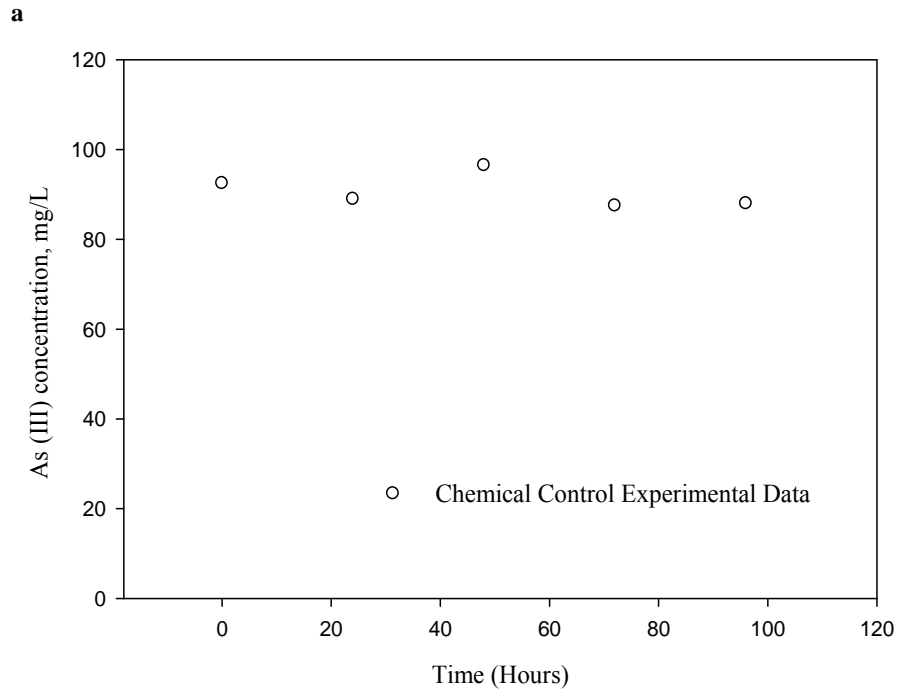
Figure 3.2 a) Chemical Controls and b) Biological Controls for As (III) oxidation in batch reactors containing 100 mg/L of As (III) at pH of 6.0

3.6.4 Effect of Dissolved Oxygen

To evaluate the effect of dissolved oxygen on As (III) oxidation, the rate of As (III) oxidation in cultures with diffused air aeration and with shaking only was investigated at the optimal conditions of pH 6 and 30˚C. The initial As (III) concentration was maintained at 100 mg/L. The DO for both cultures at the beginning of the experiment was maintained at near saturation levels of 8.0 mg/L. After 72 hours incubation, DO levels of 4.26 ± 0.16 mg/L and 2.5 ± 0.18 mg/L were observed with diffused air aeration and with shaking, respectively. However, the rate of As (III) oxidation with or without diffused air aeration did not differ significantly (Figure 3.3). The amount of As (III) oxidized was 94.2 ± 3.35 % (1.24 mg/L.hour) and 95.7 ± 3.34 % (1.26 mg/L.hour) , respectively, for air aeration and shaking, suggesting that DO was not a limiting factor for As (III) oxidation by strain b6.

3.6.5 Effect of Inorganic Carbon

To determine whether CO_2 was limiting for As (III) oxidation, the rate of As (III) oxidation was investigated with and without adding sodium bicarbonate (500 mg/L) to the modified MCSM medium at pH 6 and 30˚C. The same initial As (III) concentration of 100 mg/L was maintained in the flasks before the start of the experiment. Results indicate that the oxidation rates for both cultures did not differ significantly (Figure 3.4). The rate of As (III) oxidation averaged at 1.04 and 1.13 mg As (III) / L.hour with and without sodium bicarbonate supplement, respectively. Thus, the rate of As (III) oxidation by strain b6 was probably not limited by inorganic carbon.
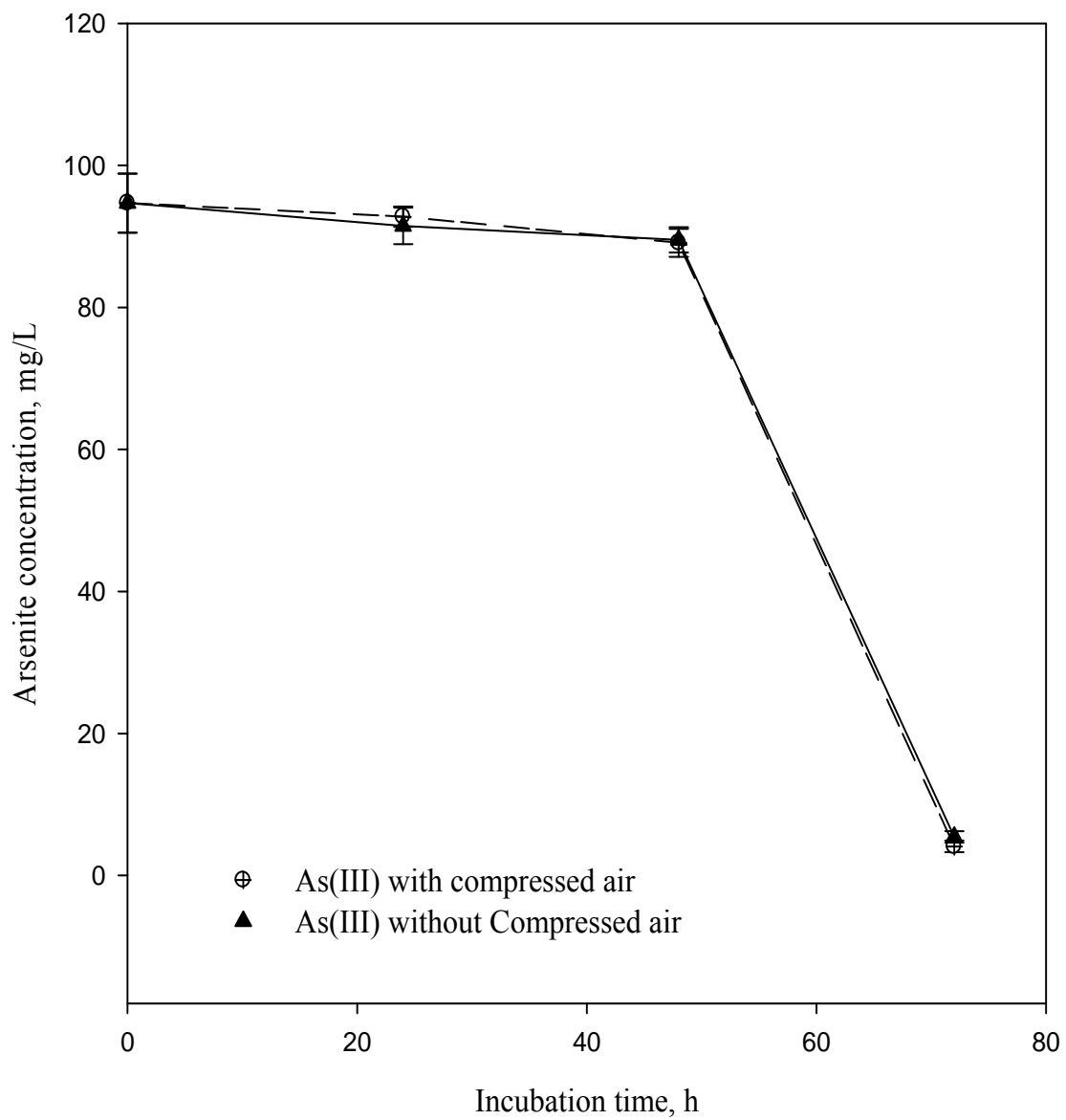
Figure 3.3 As (III) Oxidation with and without diffused air aeration (initial As (III) concentration =100 mg/L, pH =6.0, temperature = 30°C)
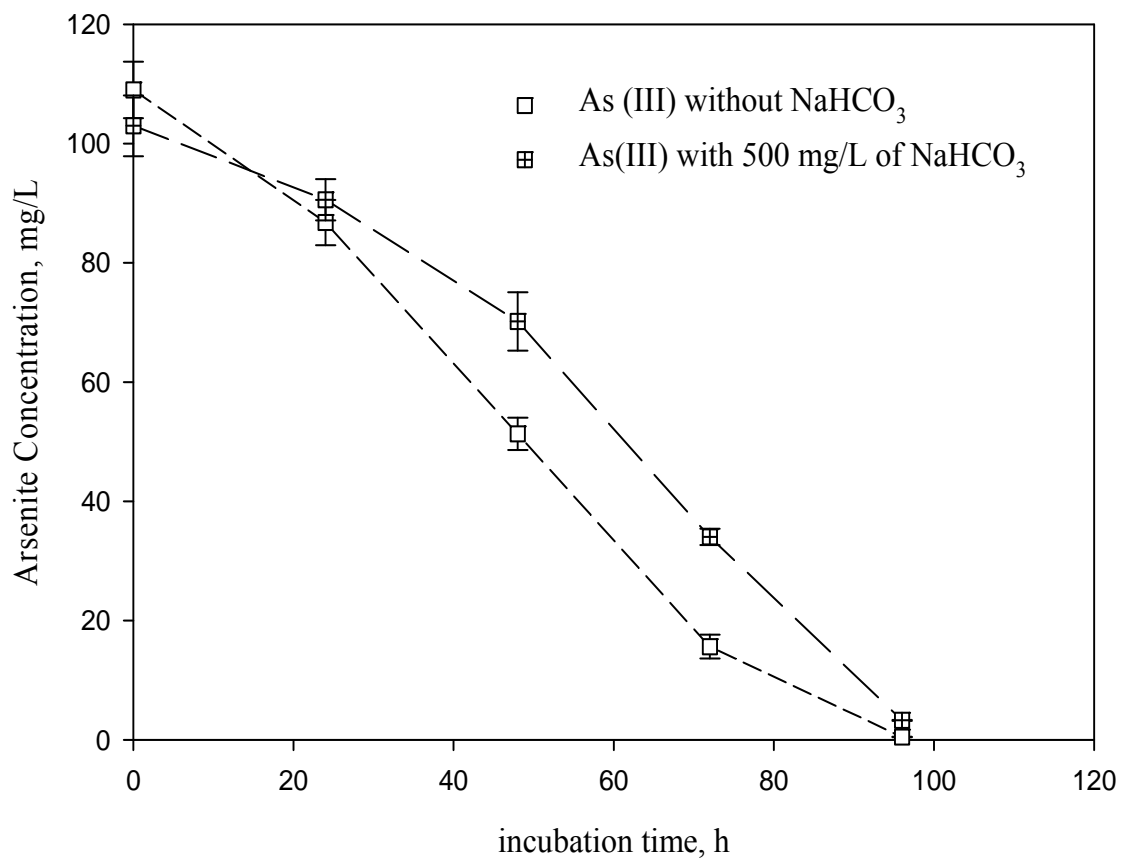
Figure 3.4 Arsenite Oxidation with and without Sodium Bicarbonate in modified MCSM medium (initial As (III) concentration =100 mg/L, temperature = 30°C)

3.6.6 Effect of As (III) Concentrations

As (III) oxidation by pure cultures of *T.arsenivorans* strain b6 was investigated in batch reactors at a wide range of initial As (III) concentrations of 10, 50, 100, 500 and 1,000 mg/L at pH 6 and 30ºC. Samples were collected at appropriate time intervals to analyze for the dissolved As (III) level and the corresponding cell concentrations. The data in Figures 3.5a and 3.5b show that both As (III) oxidation and cell growth were preceded by a lag of about 48 and 72 hours at As (III) concentrations of 500 and 1000 mg/L, respectively. The lag may be due to As (III) toxicity at such high concentrations or the need for induction time before As (III) oxidation occurs (Suttigarn and Wang 2005). During the induction time, cells of *T.arsenivorans* strain b6 produce the necessary enzymes to match the varying levels of As (III) concentrations in the batch reactors (Storer and Gaudy 1969).

However, the lag phase was not significant for lower initial As (III) concentrations of 10, 50 and 100 mg/L with As (III) oxidation observed during the exponential phase of growth of the strain b6. The absence of a lag phase at such low levels of As (III) may also indicate insignificant As (III) inhibition on the growth of the strain b6 during the oxidation process. For initial As (III) concentration of 500 mg/L, simultaneous oxidation of As (III) accompanied by cell growth was observed after the lag phase and lasted until 168 hours (Figure 3.5b). However, in the 1000 mg/L of As (III) culture, a decrease in the cell density was initially observed during the first 72 hours, followed by growth until 144 hours.
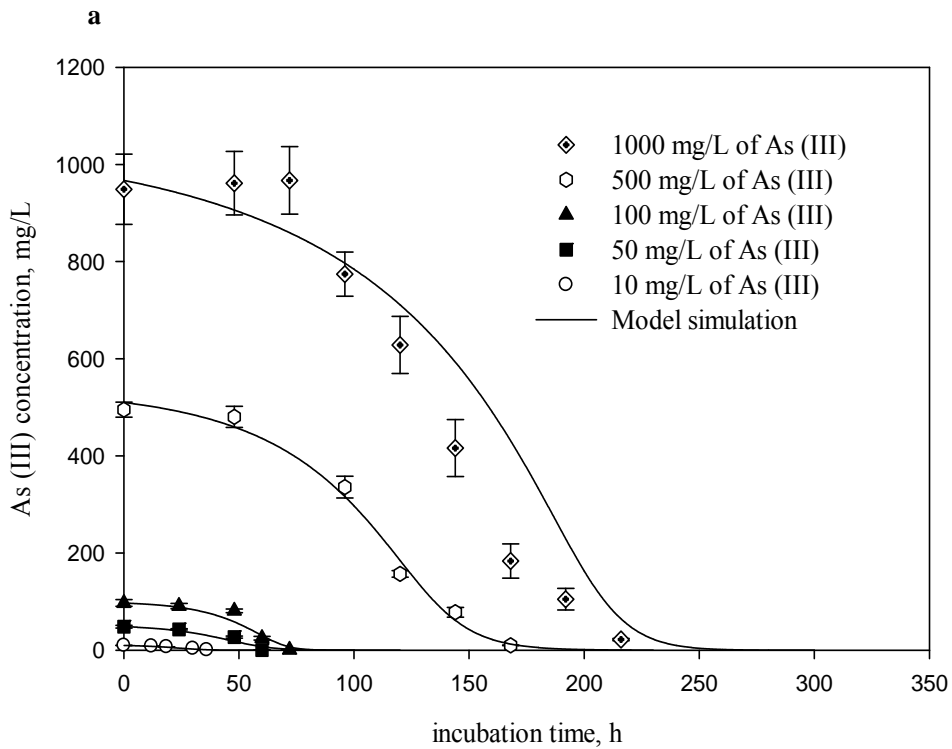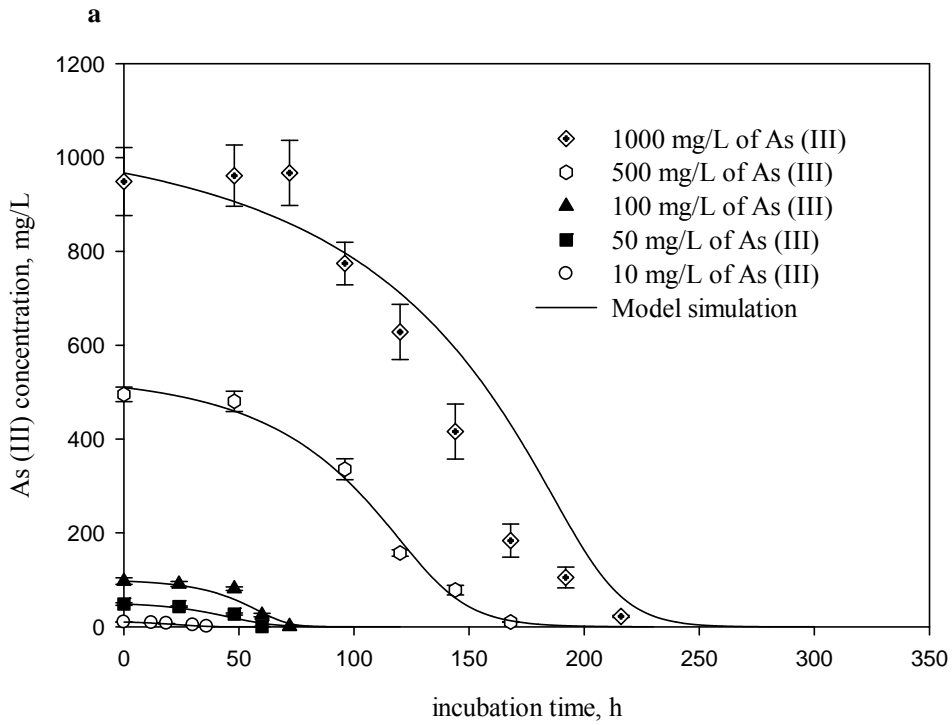
Figure 3.5 a) Effect of As (III) concentration on As (III) oxidation, b) Effect of As (III)

concentration on growth of strain b6 under the varying As (III) concentrations.

3.6.7 Fate of As (III)

The fate of As (III) was investigated at the optimal pH 6 and 30°C. The data in Figure 3.6 show the disappearance of As (III) with concomitant production of As (V), with As (III) being completely oxidized by the strain b6 in less than 80 hours. The total measured concentrations of As (III) and As (V) (for t = 0, 24, 48, 72 hours) was not statistically different at the 95% confidence level to the added initial concentration of As (III) in the reactor. No As (III) oxidation was observed with the killed controls in the modified MCSM medium during the 72 hours of incubation. In addition, no significant As (III) oxidation was observed in the chemical controls that contained no added cells. Thus, the studies conclusively prove that enzymatic reactions associated with microbial cells of *T.arsenivorans* strain b6 are responsible for the oxidation of As (III) to As (V).

3.6.8 Effect of Varying Initial Cell Concentrations on As (III) Oxidation

Batch studies were also conducted to assess the effect of varying initial cell densities (1% v/v, 10% v/v, 20% v/v, and 40% v/v) of *T.arsenivorans* strain b6 on As (III) oxidation in the MCSM medium containing 100 mg/L of As (III). The data in Figure 3.7 show that increasing the initial cell densities in the batch environment improved the overall As (III) oxidation rate. A maximum average As (III) oxidation rate of 2.63 mg As (III)/L·hr was obtained in the batch experiment containing 100 mg/L of As (III) and inoculated with 40% v/v ($16.7 \times 10^8 \pm 2.1 \times 10^8$ cells /mL) of cells of *T.arsenivorans* strain b6. There was a lag of 48 h prior to the start of As (III) oxidation in batch reactors inoculated with 1% v/v of cells of strain b6. A delay of 24 h was also observed in the two reactors inoculated with initial cell densities of 10% v/v, and 20%v/v of cells of strain b6.
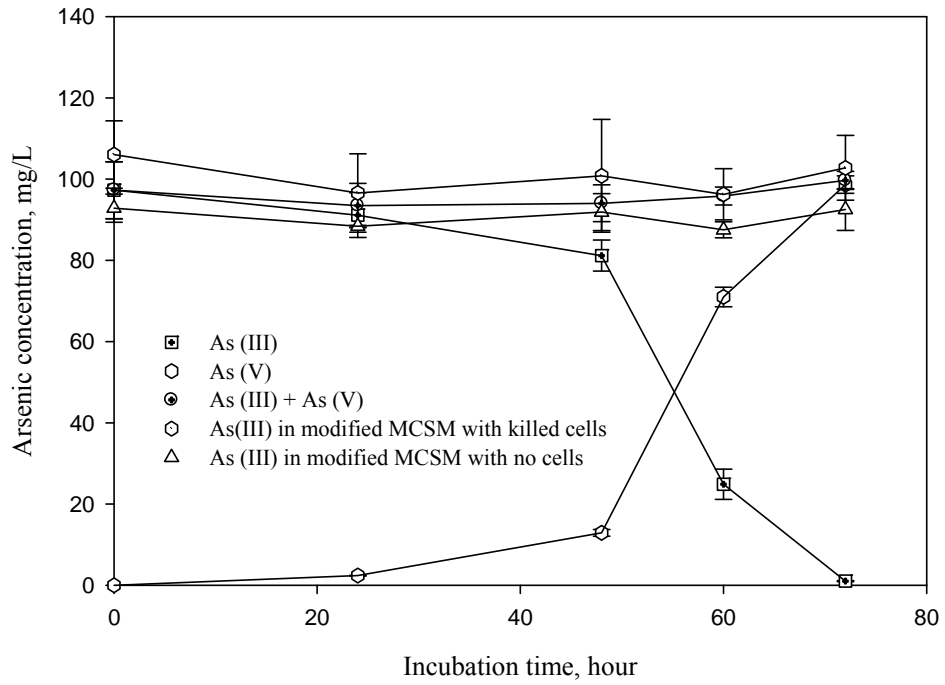
Figure 3.6 As (III) oxidation with concomitant production of As (V).

The delay could be due to the time required for the synthesis of new enzymes to match the current As (III) level prior to the start of the enzymatic oxidation process. Average As (III) oxidation rates of 1.29 mg As (III)/L.hr (1% v/v cell density), 1.45 mg As (III)/L.hr (10% v/v cell density), and 1.88 mg As (III)/L.hr (20% v/v cell density), were obtained from the study.
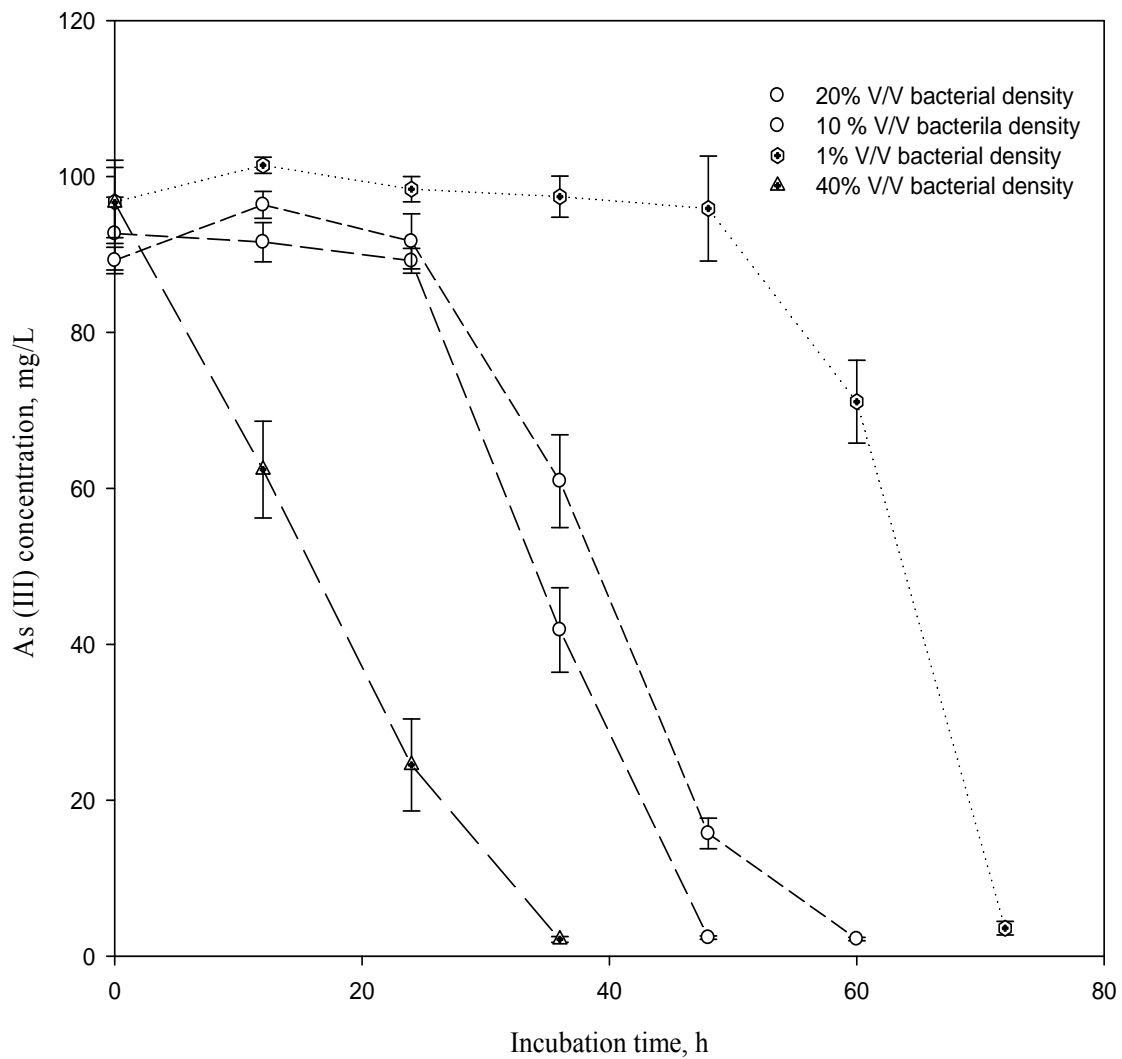
Figure 3.7 Effect of varying initial cell concentrations on As (III) oxidation rate (Initial

As (III) concentration =100 mg/L, pH =6.0, temperature = 30°C)

3.6.9 Kinetics of As (III) Oxidation

Kinetic parameters obtained at a high As (III) to biomass ratio ($S_o/X_o > 20$) are termed as intrinsic parameters (Grady et al. 1996). Estimation of parameters at such a high ratio results in estimation of unique parameter values since it reduces the degree of correlation between k, K_s, Y prevalent at low ratios (Robinson and Tiedje 1983; Dmitriou-Christidis et al. 2007; Seagren et al. 2003). In this study, best fit values of the five intrinsic parameters (k, K_s, K_i, Y and k_d) were estimated by fitting the model Eqs. (3-2) and (3-3) to the As (III) oxidation curve obtained at 500 mg/L ($S_o/X_o = 41.4$). The method of estimation involved varying the trial (or initial estimates) of the parameters along with initial cell mass concentration independently to obtain the best fit simulation (minimal SSE) for the observed data (Klecka and Maier 1985, 1988).

The best fit ($R^2 = 0.98$) parameter values for As (III) oxidation by strain b6 were obtained using the data shown in Figure 3.5a and listed in Table3-1.The variability in the estimated parameters can be attributed to three key factors: (1) the expression of the enzyme system being controlled by the manner of preparation of pure culture of the species prior to the experiment, (2) mathematical routine employed for the estimation of the parameter values, and (3) ratio of S_o/X_o which influences history of the pure culture and the uniqueness of estimated parameters (Grady et al. 1996; Seagren et al. 2003). The third factor (S_o/X_o) is a major factor for uniquely estimating parameter values from the model in this study. For a low ratio of S_o/X_o, the kinetics obtained will be closely related to the physiological state of the cell before start of the experiment. This is due to complete depletion of the substrate before significant synthesis of new enzymes.

However, for a high S_o/X_o ratio and S_o being higher than anticipated K_s value, the physiological state of the cell may change due to synthesis of new enzymes accompanying substrate depletion. Under such conditions, the measured kinetics is a true representation of the cells ultimate capabilities compared to that before the kinetic test (Grady et al. 1996).

In order to verify the applicability of the model, the obtained kinetic parameters were applied to a broader range of initial As (III) concentrations. The best fit parameters were used to simulate As (III) concentrations at 10, 50, 100 and 1000 mg/L. Excellent fit between the model simulation and the measured data was obtained for three of the four data sets (10, 100, 1000 mg/L, Figure 3.5a). R^2 of 0.92 was obtained for the As (III) oxidation curve of 1000 mg/L, whereas R^2 of 0.92 and 0.93 were determined for As (III) concentrations of 10 and 100 mg/L, respectively. However, the fit of model simulation to the experimental data obtained at 50 mg/L of As (III) was not excellent ($R^2 = 0.89$) as compared to the results obtained with higher initial As (III) concentrations.

The best fit K_s (33.2 ± 1.87 mg/L) obtained in this study was higher than the K_s (4.575 mg/L) reported for another chemoautotrophic strain NT-26 (Santini et al. 2004). A low K_s (0.225 ± 0.165 mg/L) was reported by Salmassi et al.(2002) with a heterotrophic strain *Agrobacterium albertimagni* AOL15 utilizing citrate as the organic source of carbon. Literature regarding the kinetic parameters for As (III) oxidation by other autotrophic strains is scarce. However, a similar K_s (33.75 mg/L) was reported earlier with heterotrophic strains *Pseudomonas arsenitoxidans* and *Alcaligenes faecalis* strain YE56 (Philips and Taylor 1976; Turner and Legge 1954). Although the mechanism of As (III) oxidation may be different in heterotrophic and autotrophic strains, this comparison

at least shows the relative affinity for non-growth and growth substrate As (III). Other K_s

values, ranging from 2.63 to 15 mg/L were also reported for heterotrophic strains as

O1201 (Suttigarn and Wang 2005) and NT-14 (Hoven and Santini 2004). A direct

comparison of the best fit maximum specific substrate utilization rate k (0.85 ± 0.18 mg

As (III) / mg dry weight of cells / hour) obtained in this study to that reported for strain

NT-26 (2.4 μmol arsenite oxidized / mg protein-min) (Santini and Hoven 2004) was

difficult due to the difference in biomass analysis. However, the best fit k value obtained

in this study compares very well to the k (0.47 mg / mg dry weight/hour) obtained with a

heterotrophic strain *Alcaligenes faecalis* strain O1201 (Suttigarn and Wang 2005).

Although a comparison of other best fit parameters (K_i, Y, k_d) for As (III)

oxidation is not possible due to the lack of published information, the value obtained for

Y (0.088 ± 0.0048 mg dry cell weight/mg As (III)) is generally in the range of those

reported with several non-As (III) oxidizing autotrophic strains (0.076 ± 0.011 mg cell

mass/mg SCN^-, 0.087 mg biomass/mg SCN^-, 0.063 g biomass/g N and 0.056 g biomass/g

N) (Ahn et al. 2004; Hung and Pavlostathis 1999; Keen and Prosser 1987).

Previous studies often assume a value for the parameter k_d (Klecka and Maier

1985, 1988) or simply ignored it to simplify model analysis (Hung and Pavlostathis

1999), due to its insignificant effect on the model outcome. However, in this study, the

effect of the parameter k_d on the model prediction was further investigated by using its

optimized value as the initial guess for the non-linear fit of the model Eq. (3-3) to the

specific growth rate data of the strain b6 under different initial As (III) concentrations

(Figure 3.8). The other optimized parameter values were kept same during this analysis.

However, the obtained best fit k_d value (0.007) was well within the range of the k_d value

(0.006 ± 0.002 hr^{-1}) optimized using As (III) data shown in Figure 3.5a. The non-linear fit (Figure 3.8) indicates that optimum growth of strain b6 occurs at 46.9 mg/L of As (III) and the specific growth rate quickly decrease at higher As (III) concentrations.

3.6.10 Sensitivity Analysis

The sensitivity coefficients of the best fit parameters were evaluated at both low and high initial As (III) concentrations (10 and 1000 mg/L). The obtained sensitivity coefficients were then plotted against the independent variable, t to measure the sensitivity and correlation between obtained kinetic parameters. The data in Figure 3.9 clearly show a good separation between all the five sensitivity coefficients over most of the progressive curve for low values of S_o/X_o = 0.8 and S_o/K_s = 0.3. Previous studies have reported the problem of parameter identifiability in the first order region (S_o/K_s = 0.04) due to high degree of correlation between the parameters (k, K_s, Y) (Robinson and Tiedje 1983). However, the lack of proportionality between the obtained sensitivity coefficients indicates unique estimates of these parameters at this low level of As (III) concentration. Figure 3.9 also shows the considerable influence of the parameters k, K_s and Y to model prediction, with Y being the most sensitive of all parameters. The maximum influence of the parameters k and K_s is observed during the time range of 4-5 hours, after which the sensitivity decreases for the remaining time period. However, the sensitivity of Y influences the model outcome until the first 20 h before reaching a constant value. The analysis also suggests that the Haldane model (equations 3-2 and 3-3) is relatively insensitive to changes in K_i and k_d which was reflected by the lower values

of their coefficients. The optimal k_d value, however, was further confirmed and verified using the growth data as indicated in Figure 3.8.

For higher values of $S_o/X_o = 82.9$ and $S_o/K_s = 30.1$, the sensitivity coefficients of K_i and K_s have the greatest influence on model prediction during the time intervals of 180-190 and 200-205 hours (Figure 3.10). This is consistent with previous studies, where K_i is highly sensitive to model outcome at high substrate concentrations (Hung and Pavlostathis 1999). The parameters k_d, k and Y have the least effect on the model predictions for the entire time range as is indicated by the low values of their coefficients obtained from model simulation. Although Figure 3.10 shows the curves look proportional (very low degree of proportionality), the good separation between each coefficient suggests that parameter estimates by the method of nonlinear least square analysis is unique even at high concentrations of As (III).

3.6.11 Summary and Conclusions

This study showed that the *Thiomonas arsenivorans* strain b6 was able to oxidize As (III) concentrations as high as 1000 mg/L in the absence of an added carbon source. As (III) oxidation took place during the exponential growth of the strain b6 for As (III) concentrations of 10, 50 and 100 mg/L. However, for As (III) concentrations of 500 and 1000 mg/L, As (III) oxidation was observed mostly during the exponential phase but continued into the stationary phase of growth. Neither dissolved oxygen level nor inorganic carbon source was observed to limit the rate of As (III) oxidation. The Haldane substrate inhibition equations adequately described the kinetics of As (III) oxidation over a wide range of initial As (III) concentrations. Sensitivity analysis indicated Y and K_i to

be the most sensitive at low and high initial As (III) concentrations. However, the model

was insensitive to changes in k_d at both the low and high concentrations.

Table 3.1 Best estimates of model parameters and their standard errors

Parameters	Description	Best estimate	Standard error
K_s	Saturation constant (mg /L)	33.2	1.87
K_i	Inhibition coefficient (mg/L)	602.4	33.6
k	Maximum specific oxidation rate (mg As (III)/mg biomass dry weight/hour)	0.85	0.18
Y	Yield coefficient (mg biomass/mg As (III))	0.088	0.0048
k_d	death or decay rate (h^{-1})	0.006	0.002
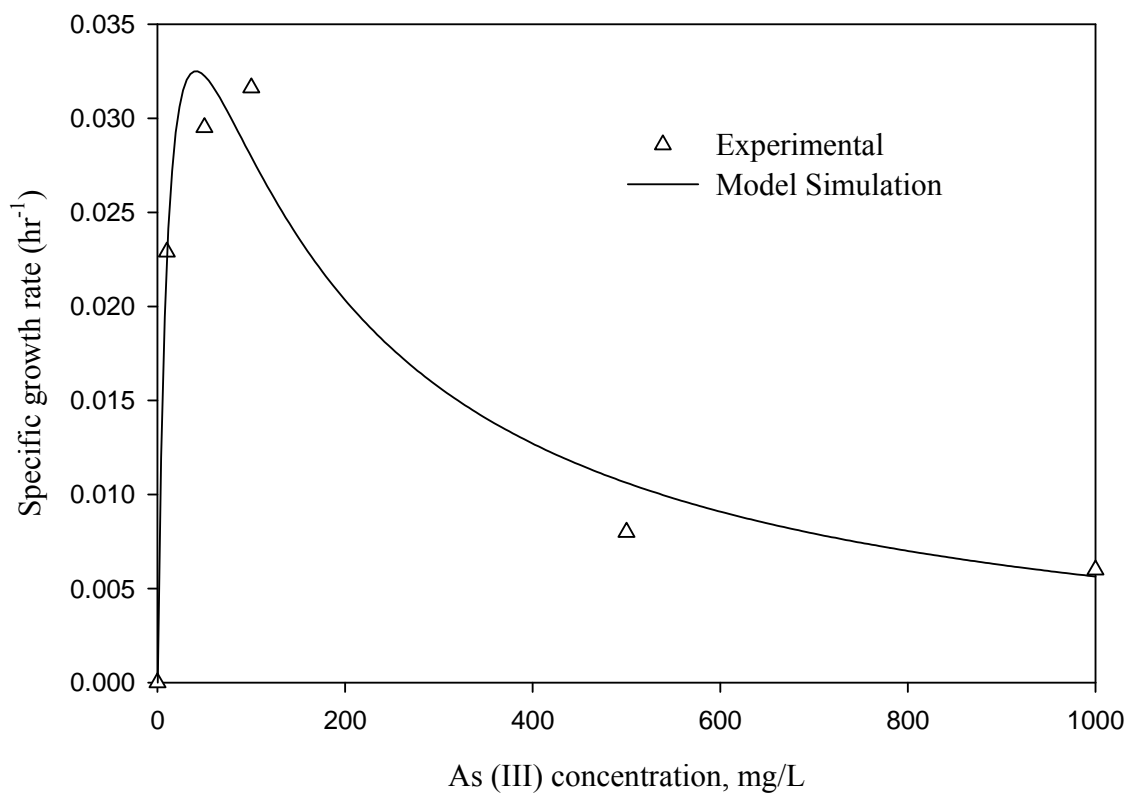
Figure 3.8 Relationship between As (III) concentration and specific growth rate of *T. arsenivorans* strain b6.
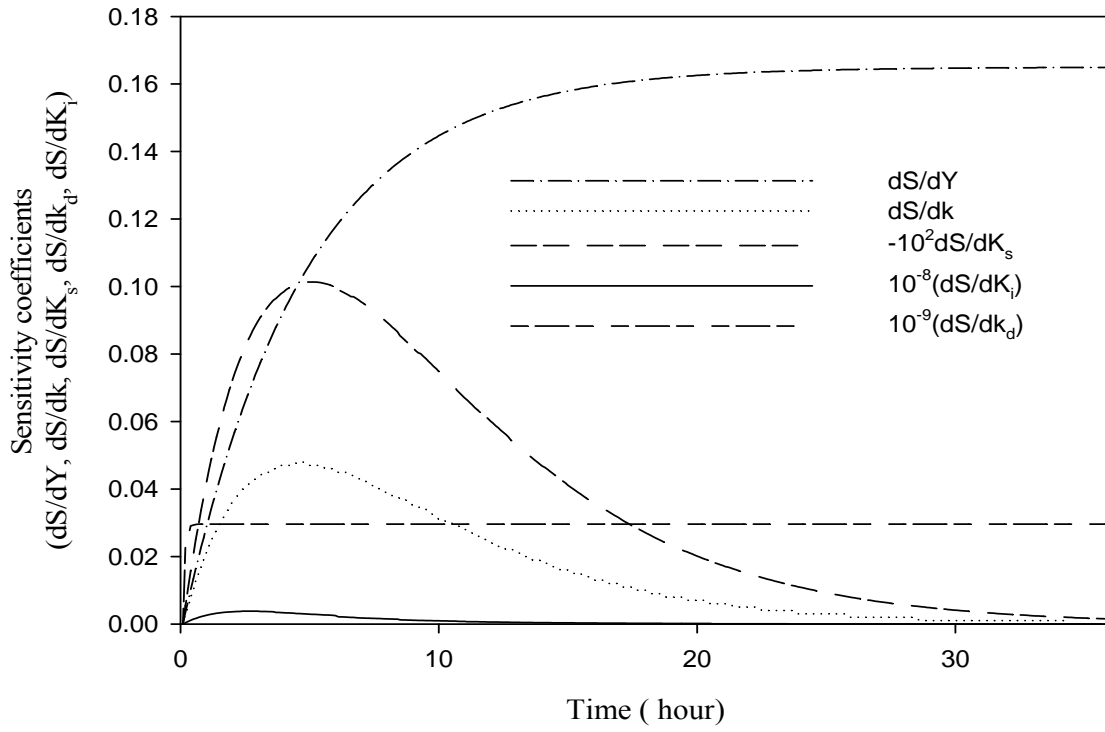
Figure 3.9 Sensitivity analysis at S_o/X_o =0.8 and S_o/K_s = 0.3
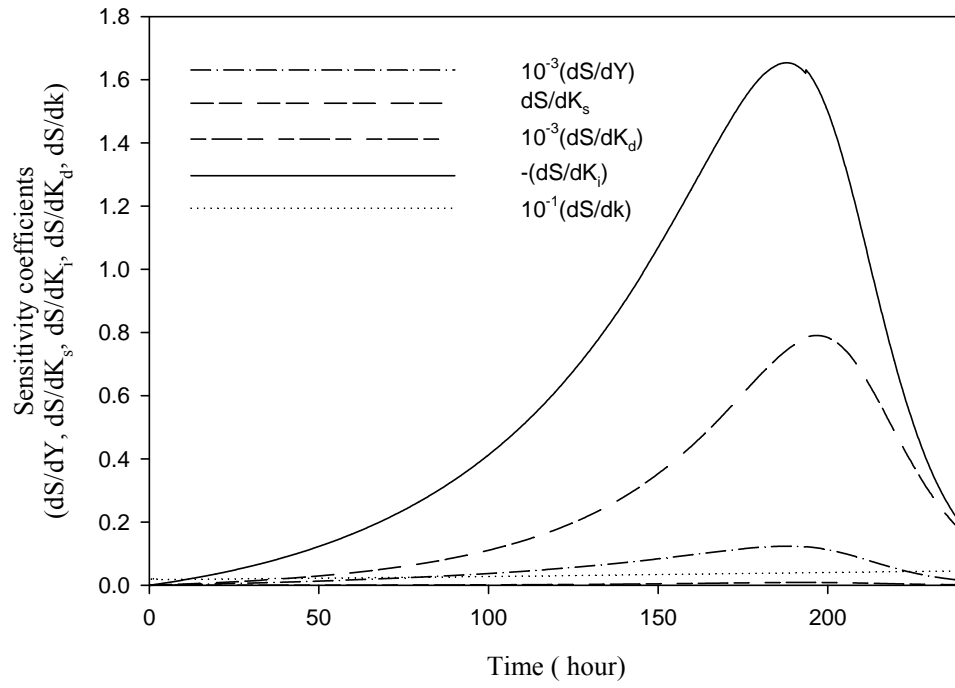
Figure 3.10 Sensitivity analysis at $S_o/X_o = 82.9$ and $S_o/K_s = 30.1$

Chapter 4: Continuous Stirred Tank Reactor (CSTR)

4.1 Abstract

As (III) oxidation by a chemoautotrophic bacterium, *Thiomonas arsenivorans* strain b6, was evaluated in a continuous stirred tank reactor (CSTR) under a range of influent As (III) concentrations (2,000 - 4,000 mg/L) and hydraulic retention times (HRTs) (21.7 - 74.9 h). Five steady-states were obtained after the CSTR was continuously operated for 115 days with over 99% As (III) oxidized under the optimal growth conditions for strain b6 at pH 6 and 30 $^{\circ}$C. The culture exhibited strong resilience by recovering from an As (III) overloading of 4,847.4 ± 290.9 mg/day/L operated at a HRT of 21.7 h. Arsenic mass balance analysis revealed that As (III) was mainly oxidized to As (V), with unaccounted arsenic well within the analytical measurement error. The best estimates of biokinetic parameters for As (III) oxidation were obtained using the steady-state data and the Monod expression based model (k = 5 mg As (III)/mg dry cell weight /h; K_s = 20.1 mg/L; k_d = 0.008 h^{-1}; and Y = 0.011 mg cell dry weight/mg As (III)). The Monod model and the reactor mass balance successfully simulated both the steady-state and transient phases of CSTR operation. Sensitivity analyses defined Y and k to be the most sensitive to model predictions, whereas k_d and K_s were least sensitive to model simulations of As (III) oxidation under steady-state conditions. A model adequacy test performed on all the five phases also demonstrated the prediction accuracy of the model in simulating the obtained transient and steady-state data from the bioreactor operation.

4.2 Introduction

A CSTR (*continuous-flow stirred-tank reactor*) also referred to as a *chemostat*, is a chemical reactor generally used to culture microorganisms under a continuous flow of fresh nutrient supply and constant environmental conditions (Rittmann 2001). The contents of the CSTR are always completely mixed (homogenous) and the concentration of the growth limiting substrate is essentially the same in the effluent and inside of the reactor. However, the application of such bioreactors in the aerobic and anaerobic treatment of primary wastes, biological sludges, and industrial wastes are of profound interest.

There are several advantages in using a CSTR for the biological treatment of industrial wastes comprising of organic and inorganic contaminants. One of the biggest advantages of using the chemostat culture is the overall control on the generation time or the maintenance of a constant growth rate of the microorganisms in the culture vessel. The continuance of a constant growth rate between 0 to μ_{max} (maximum specific growth rate) is generally achieved by varying the feed flow rate of the nutrient medium to the bacteria in the CSTR (Adams and Hansche 1973). Another advantage of using the CSTR is the reliability of the parameter estimates obtained under optimized and steady-state conditions compared to non steady-state batch environment (Wang and Suttigarn 2007). The elimination of parameters identifiability as a result of the simplified kinetics is an added advantage of using the *chemostat* to measure the response of the microorganism to changes in the environment (Commandeur et al. 1995; Shuler and Kargi 2002).

The preliminary treatment of arsenic contaminated water generally involves the oxidation of As (III) to As (V) by chemical or biological means due to the acute toxicity

and mobility of As (III) compared to As (V) ions. This study is the first to report As (III) oxidation in a continuous-flow bioreactor by a chemoautotrophic bacterial culture with detailed steady-state as well as dynamic analysis. The specific objectives of the study were as follows:

1. To investigate the responses of the continuous culture of chemoautotrophic *Thiomonas arsenivorans* strain b6 in oxidizing As (III) to As (V) under variable influent As (III) concentrations and HRTs in the CSTR. More specifically, the study was conducted to measure the potential of the bioreactor in transforming As (III) to As (V) under high As (III) loading rates and also to assess the resilience of the *chemostat* culture under As (III) overloading conditions.

2. To compute the biokinetic parameters (k, K_s, k_d, and Y) using the steady-state data obtained from the various operating conditions and an overall reactor mass balance relationship. The parameters were essentially estimated by performing linear regression analyses using Sigma Plot 10 application software (SPSS Inc) and the observed steady-state data.

3. To evaluate the applicability of the computed parameters in simulating the obtained steady-state data under variable HRTs (Hydraulic residence times). A good fit between the data and model predictions would indicate strong reliability of the parameter estimates.

4. To assess the potential application of these biokinetic parameters in predicting the observed transient and as well as the steady-state responses in the CSTR under varying As (III) loading rates. A paired *t-test* was also performed to measure whether the

difference between the model predicted and observed data were statistically significant at the 95% confidence level (α =0.05).

5. To perform sensitivity analysis for measuring the effect on model predictions by changes in the parameters. Parameter sensitivity is an important aspect of the modeling analysis because it indicates the applicability of the obtained parameters and the usage of the model under varying environmental conditions.

6. To conduct model adequacies check for detecting any model inadequacy or instability in predicting the observed data from all the phases of the CSTR operation.

4.3 Materials and Methods

4.3.1 Bacterial Strain and Feed Composition

The same *T.arsenivorans* (LMG 22795T) strain b6 described in the batch study (section 3.3.1) was used in the CSTR study. The feed to the CSTR was a modified CASO1 selective medium (MCSM) to which 5 g/L each of K_2HPO_4 and KH_2PO_4 were added as buffer, while the yeast extract was eliminated to ensure autotrophic growth conditions (Chapter 3; Section 3.3.1). The concentration of As (III) in the feed varied between 2,000 and 4,000 mg/L under a constant HRT of 74.9 h for the first two phases (I and II). For the remaining five phases (III-VII), the HRT was varied between 21.7 h and 74.9 h while the As (III) concentration was maintained in the feed at 4,000 mg/L.

4.3.2 Bioreactor System

The CSTR consisted of a 14 L fermentor (Modular Microferm series MF-114, New Brunswick Scientific, Edison, NJ) equipped with mechanical stirring, temperature controller, and airflow regulator (Figure 4.1). The CSTR was operated with a working volume of 4 L under completely mixed and fully aerated conditions. The pH and the

temperature were maintained at the optimum growth conditions for *T.arsenivorans* strain b6 (30 $^{\circ}$C and pH 6) (chapter 3; sections 3.6.1, 3.6.2). Double-headed peristaltic and master flex pumps (Cole-Parmer, Chicago, IL) were calibrated to obtain the desired HRT. Autoclavable Nalgene brand platinum-cured silicon tubings (Nalgene Nunc International, Rochester, NY) were used as interconnections for carrying fluid and air into the reactor. The reactor and connecting tubings were autoclaved at 121°C for 30 mins and assembled in a sterile hood (Steril Gard, Class II type A/B3, Baker Company, Sanford, ME) using 95% ethanol for sterilization. A microfilter of 0.3 μm (Whatman, Florham Park, NJ) was installed on the influent airline to prevent contamination. All connecting tubings were replaced periodically to prevent undesirable growth and contamination. The CSTR was operated continuously for 115 days under a range of influent As (III) concentrations (2,000 - 4,000 mg/L) and HRTs (21.7 - 74.9 h) (Table 4.1).
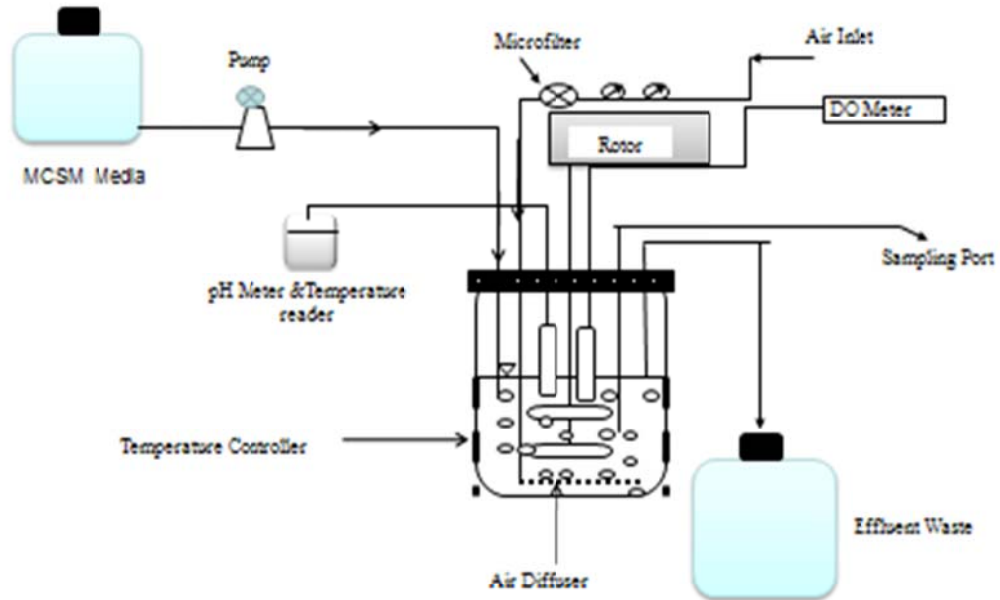
Figure 4.1 CSTR Bioreactor System for As (III) oxidation to As (V)

Table 4.1 Summary of Operating Conditions for the CSTR Bioreactor System

Phase	Duration (day)	Influent As (III) (mg/L)	HRT (Hr)	T (°C)	pH	DO (mg/L)
I	42-65	2,071.59 ± 41.21	74.9	30.74±1.36	5.56±0.18	6.37±0.17
II	65-77	4,130.99 ± 162.50	74.9	30.04±0.31	5.68±0.09	6.28±0.12
III	77-87	4,165 ± 123.48	60	29.95±0.14	5.62±0.08	6.28±0.04
IV	87-99	4,195.37 ± 114.30	48	29.44±0.44	5.32±0.10	6.21±0.03
V	99-105	4,194.72 ± 260.32	38.4	29.78±0.24	5.30±0.10	6.23±0.05
VI	105-106	4,241.44 ± 254.56	21.7	29.87±0.05	5.28±0.20	6.22±0.04
VII	106-115	4,238.21 ± 253.20	74.9	29.74±0.27	5.66±0.10	6.22±0.04

4.3.3 Tracer Study

A tracer study was conducted to assess the fluid characteristics of the CSTR using a stirring speed of 160 revolutions per minute and methylene blue as a tracer. A methylene blue concentration of 10 mg/L was fed continuously into the reactor containing 4L of DDW (Deionized Distilled Water) under a flow rate of 53.41mL/hr (τ=74.9 hr). Samples were collected at appropriate time intervals and analyzed for methylene blue levels in the reactor by measuring the absorbance at 664 nm using a spectrophotometer (Spectronic Instrument, Rochester, NY). The observed effluent methylene blue breakthrough curve was then compared with the tracer response from an ideal completely mixed reactor based on Eq. (4-1):

$$\frac{C}{C_o} = (1\text{-}e^{\text{-}t/\tau}) \qquad\qquad (4\text{-}1)$$

where C and C_o are influent and effluent methylene blue concentrations, t is the time of sample measurement and τ is the HRT based on the feed flow rate Q.

4.3.4 Analytical Methods

Samples were collected at appropriate time intervals and immediately centrifuged at 10,000 rpm for 10 mins using a microcentrifuge (Brinkmann Instruments Inc, West bury, NY). The supernatant was acidified using nitric acid (pH < 2) and preserved in 4 °C for no more than 7 days prior to analysis of As (III), As (V) and total As (APHA 1995). A modified silver diethyldithiocarbamate method (Suttigarn and Wang 2005) was used for arsenic analyses using a spectrophotometer (Spectronic Instrument, Rochester, NY). pH and dissolved oxygen (DO) were monitored daily with adjustments to maintain an

optimized environment during the operation. pH was measured *in situ* using a pH meter (Denver Instrument, Denver, CO) equipped with an ATC Combo, Silver/Silver chloride electrode. The pH meter was calibrated with standard buffers of 4 and 7 and the probe disinfected by 95% ethanol before use. DO was determined *in situ* using a DO meter (YSI 550A, Yellow Springs, Ohio) which was also calibrated and disinfected with 95% ethanol before each use.

Samples were also collected for the determination of suspended viable cell concentrations, and biomass dry weight measured as volatile suspended solids (VSS). The details of the VSS method has been outlined in the section 2540 E of the *standard methods for the examination of water and wastewater* (APHA 1995). The spread plate technique (section 9215 C APHA 1995) used for the determination of suspended viable cell concentrations has been described in section 3.3.4.1 of chapter 3.

4.4 Steady-State Data Analysis

The steady-state data were analyzed by a kinetic based model developed for the completely mixed reactor using material balance analysis on the cell and As (III) respectively.

$$V\frac{dX}{dt} = QX_i - QX + (\mu)XV \qquad (4\text{-}2)$$

$$V\frac{dS}{dt} = QS_i - QS - \frac{\mu}{Y}XV \qquad (4\text{-}3)$$

where Q = influent flow rate $[L^3T^{-1}]$; X_i and X = biomass concentration in the feed and the reactor, respectively $[M_xL^{-3}]$; μ = specific growth rate of strain b6 $[T^{-1}]$; V = volume of the reactor $[L^3]$; and S_i = the influent As (III) concentration $[ML^{-3}]$ to the CSTR; S =

As (III) concentration in the reactor $[ML^{-3}]$; and Y = cell yield coefficient $[M_sM_x^{-1}]$. The Monod expression (Eq. (4-4)) and the maximum specific As (III) oxidation rate, k $[MM_x^{-1}T^{-1}]$ (Eq. (4-5)) are integrated into the above mass balance equations (4-2) and (4-3) to obtain steady-state ($V\dfrac{dS}{dt} = 0$ and $V\dfrac{dX}{dt} = 0$) expressions for effluent As (III) concentration (Eq. (4-6)) and biomass concentration as a function of HRT ($\tau=\dfrac{V}{Q}$) (Eq. (4-7)) :

$$\mu=\frac{\mu_m S}{K_s+S}-k_d \qquad (4\text{-}4)$$

$$k=\frac{\mu_m}{Y} \qquad (4\text{-}5)$$

$$S=\frac{K_s(\dfrac{1}{\tau}+k_d)}{(kY-k_d-\dfrac{1}{\tau})} \qquad (4\text{-}6)$$

$$X=\frac{(\dfrac{1}{\tau})(S_i-S)(K_s+S)}{kS} \qquad (4\text{-}7)$$

where μ_m = maximum specific growth rate constant $[T^{-1}]$; K_s = As (III) half velocity constant $[ML^{-3}]$; k_d = death or decay rate of strain b6 in the reactor $[T^{-1}]$; τ = HRT [T], which is equal to the mean cell residence time (θ_x) in a completely mixed suspended cells bioreactor under steady-state conditions (Rittman and McCarty 2001). The biomass productivity (P_x), effluent As (V) concentration, As (V) productivity (P_s) and specific As (III) oxidation rate ($q_{As(III)}$) are defined in equations (4-8) - (4-11) below:

$$P_x = \frac{X}{\tau} \qquad (4\text{-}8)$$

$$[As(V)] = S_i - S = S_i - \frac{K_s(\frac{1}{\tau} + k_d)}{(kY - k_d - \frac{1}{\tau})} \qquad (4\text{-}9)$$

$$P_s = (\frac{1}{\tau})[As(V)] \qquad (4\text{-}10)$$

$$q_{As(III)} = \frac{P_s}{X} \qquad (4\text{-}11)$$

where P_x = biomass productivity $[ML^{-3}T^{-1}]$; $[As\,(V)]$ = As (V) concentration $[ML^{-3}]$; P_s = As (V) productivity $[ML^{-3}T^{-1}]$; and $q_{As(III)}$ = specific As (III) oxidation rate $[MM_x^{-1}T^{-1}]$. The mass balance equations (4-2) and (4-3) indicate that steady state determination in a CSTR is controlled by the parameters k, K_s, k_d and Y within the range of operating HRTs. The best-fit kinetic parameters were estimated by applying least-square minimization technique to the steady-state data against the model equations (4-12) and (4-13), obtained by substituting and rearranging equations (4-2) – (4-5):

$$\frac{X\tau}{S_i - S} = (\frac{K_s}{k})\frac{1}{S} + \frac{1}{k} \qquad (4\text{-}12)$$

$$\frac{1}{\tau} = \frac{Y(S_i - S)}{X\tau} - k_d \qquad (4\text{-}13)$$

4.5 Nonsteady-state Data Analysis

The As (III) and cell mass balance over the entire CSTR (Eq. (4-2) and Eq. (4-3)) integrated with the modified Monod expression (Eq. (4-4)) and the biokinetic parameters obtained using the steady-state data and equations (4-12) and (4-13), were solved

numerically using MATLAB (7.0) to simulate the transient responses of the bioreactor system towards increased As (III) loadings during phases II-V. The applicability of the model was then verified using data obtained with a different influent As (III) concentration (phase I).

The maximum permissible analytical error for the measurement of biomass concentration was ± 20% as described in the QA/QC guidelines (Appendix A). The observed biomass was used as the initial trial value but varied (within ±15%) to obtain the best fit As (III) value for all the five phases (Table 4.2).

4.6 Results and Discussion

4.6.1 Tracer Results

The tracer response of the CSTR under the given methylene blue loading is shown in Figure 4.2. The observed data of $\frac{C}{C_o}$ vs $\frac{t}{\tau}$ matches very well with the ideal completely mixed characteristic curve of a CSTR. The results also confirm the validity of the completely mixed assumption in the operation of the CSTR under varying As (III) loading rates.

4.6.2 Performance of the CSTR

Reactor Start-Up (0-42 days): The process of As (III) oxidation in the CSTR was initiated by adding 40 mL of harvested overnight grown cells of *T.arsenivorans* strain b6 to 4 L of modified MCSM medium containing 300 mg/L of As (III) in the absence of any added organic carbon source. Once a stable effluent As (III) level (0.4 mg/L) was established in the reactor, the influent As (III) concentration was then progressively increased from 500 to 1,000 mg/L under a constant HRT of 74.9 h. The

stepwise increase in the influent As (III) level during the start-up phase was to acclimate the culture to high As (III) concentrations and also establish significant biomass in the CSTR. Autotrophic cultures are generally very slow growing in nature and can utilize only 5-10% of the total available energy for carbon fixation and growth (Shock and Helgeson 1988).

During the start-up phase, the average stable effluent As (III) concentrations ranged between 0.4 ± 0.1 mg/L and 4.4 ± 0.3 mg/L under the influent As (III) concentration range of 300 – 1,000 mg/L, respectively. The As (III) oxidation efficiency of the bioreactor maintained steady at 99% during operation of this phase. pH, DO, and temperature were closely monitored with adjustments to maintain optimum growth conditions of the *T.arsenivorans* strain b6 during the start-up operation.

Phases I-VII (42-115 days): After the start-up phase, the CSTR was operated for an extended period of 73 days under varying As (III) loading rates. The first two phases (I and II) were operated under the same HRT (74.9 h), while the influent As (III) concentration was increased from 2,000 mg/L in phase I to 4,000 mg/L in phase II. A power outage on day 54 caused a spike in the effluent As (III) concentration to 13.54 mg/L (Figure 4.3; Figure 4.9). However, the effluent As (III) level quickly recovered to its steady-state level (11.13 mg/L) once the normal operating conditions were restored.

Steady-state conditions in the reactor were defined as the variation in the measured effluent parameters remained within $\pm 15\%$ after operating for at least three times the HRT for each phase. According to Jensen (2001) and Foggler (1999), the time taken to reach steady-state conditions in a completely mixed continuous flow bioreactor

exhibiting first-order kinetics is at least three to four times the hydraulic residence times (HRTs).

The steady-state effluent As (III) concentrations measured at 11.1 ± 0.8 mg/L and 19.6 ± 1.4 mg/L, for the first two phases (I and II), respectively (Table 4.3). pH values of 5.6 ± 0.2 (phase I) and 5.7 ± 0.1 (phase II) were maintained, whereas DO levels averaged at 6.4 ± 0.2 (phase I) and 6.3 ± 0.1 (phase II), respectively. The As (III) oxidation efficiency of the reactor in both the phases remained steady at 99.5%.

The HRT was gradually decreased in phases III-VI while operated under the same influent As (III) concentration of 4,000 mg/L. The steady-state DO and pH averaged at 6.2 mg/L and 5.4 ± 0.2, respectively, during phases III-V. The steady-state effluent As (III) concentrations measured at 24.1 ± 0.6 mg/L (phase III), 26.9 ± 0.4 mg/L (phase IV), and 31.4 ± 0.4 mg/L (phase V), respectively (Table 4.3). The increase in As (III) loading rates through decreased HRTs did not have any significant effect on the As (III) removal efficiency until a critical HRT of 21.7 h was reached on day 106 (phase VI), when the effluent As (III) concentration increased to 395.4 mg/L. To prevent complete washout of the cells and also to assess the resilience of the CSTR culture, the HRT was increased to 74.9 h on day 106 while maintaining the same influent As (III) concentration of 4,000 mg/L (phase VII). The system was able to recover at the end of day 115 as effluent As (III) decreased to a low value of 20 mg/L (Figure 4.3).

4.6.3 Fate of As (III) in the Bioreactor System

An arsenic mass balance analysis was conducted over the CSTR to analyze the fate of As (III) in the CSTR. Cumulative values of influent As (III), effluent As (III), and sum of effluent As (III) and As (V) were plotted for the entire experimental duration of

115 days as shown in Figure 4.4. The difference between the cumulative influent As (III) and sum of cumulative effluent As (III) and As (V) was approximately 11.7%, which was within the analytical error of $\pm15\%$. Furthermore, a correlation coefficient (R^2) of 0.99 was obtained between the linear regression plot of cumulative effluent total As and sum of cumulative effluent As (III) and As (V) with a measured difference of less than 10% (Figure 4.5). These analyses clearly show that the measured differences between each of the cumulative variables (As (III), As (V), As (III) and As (V), total As) were always within the analytical error of $\pm15\%$, indicating that nearly all the As (III) fed to the reactor was oxidized to As (V) by *T.arsenivorans* strain b6.

Table 4.2 Input biomass levels for transient phases simulations

Phases	Observed biomass (mg VSS/L)	Simulated Biomass (mg VSS/L)	% Variation
I	20.2[a]	22.2	9.9
II	23.2	26.2	12.9
III	26.5	30.1	13.6
IV	30.2	30.8	1.99
V	32.4	34.6	6.8

[a] value calculated from the conversion factor between viable cells/mL and mg VSS/L
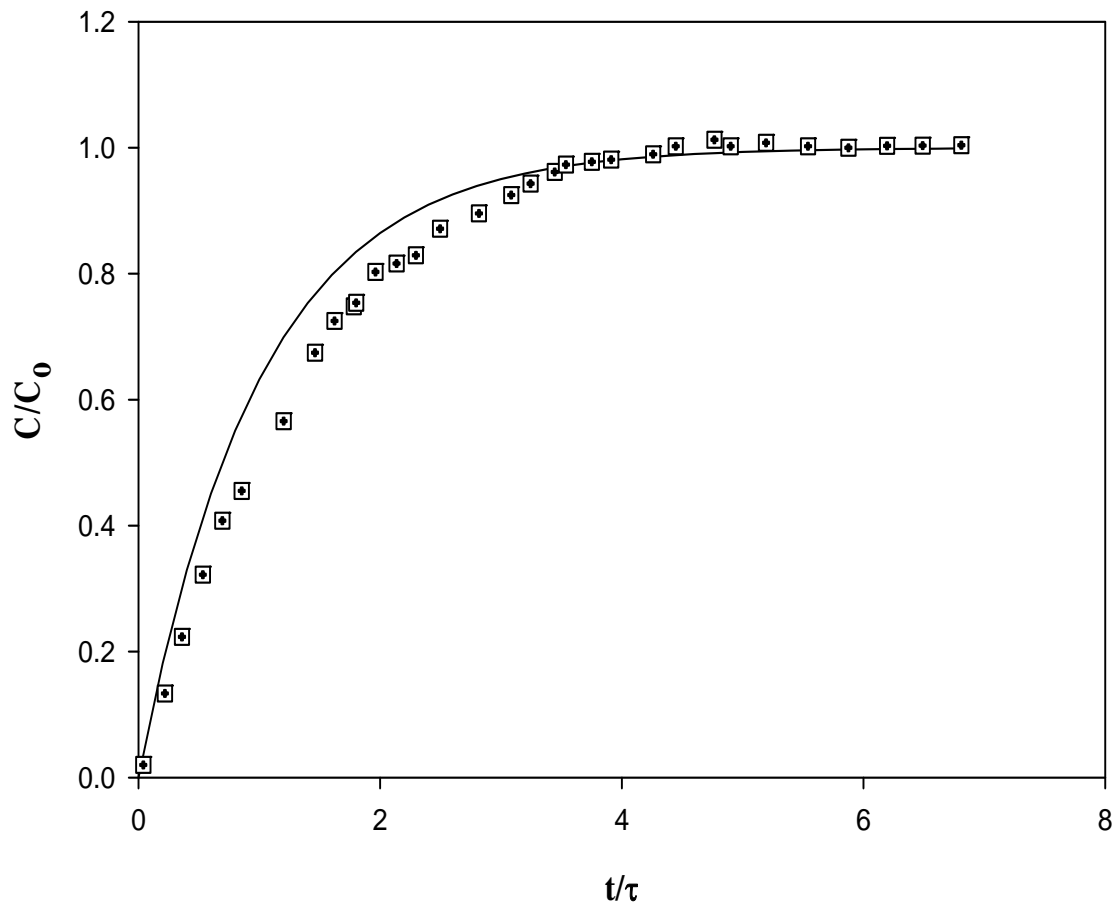
Figure 4.2 Tracer study response in the CSTR for verifying complete mixed characteristics.

Table 4.3 Summary of operating conditions and steady-state performance of the CSTR

Phase	Duration (days)	HRT (Hrs)	Influent As (III) (mg/L)	As (III) loading rate (mg/day/L)	Effluent As (III) (mg/L)	Effluent As (V) (mg/L)	Average As (III) removal (%)	viable cell count/mL	Biomass mg VSS/L
I	42-65	74.9	2,071.6±41.1	663.9±13.2	11.1±0.8	1,801.6±46.6	99.5±0.03	$5\times10^8\pm1\times10^8$	20.2^b
II	65-77	74.9	4,130.9±162.5	1,324.0±52.1	19.6±1.4	3,495.8±157.8	99.4±0.01	$9.3\times10^8\pm1.5\times10^8$	23.1
III	77-87	60	4,165±123.5	1,700.2±50.4	24.1±0.6	3,600.1±137.4	99.4±0.0	$1.2\times10^9\pm2.1\times10^8$	26.5
IV	87-99	48	4,195.4±114.3	2,097.7±57.1	26.9±0.4	3,795.3±156.9	99.4±0.01	$1.8\times10^9\pm1.4\times10^8$	30.2
V	99-105	38.4	4,194.7±260.3	2,796.5±173.5	31.4±0.4	3,652.9±162.2	99.3±0.04	$1.9\times10^9\pm7.2\times10^8$	32.4
VI	105-106	21.7	4,241.4±254.6	4,847.4±290.9	---------[a]	--------[a]	----------[a]	---------[a]	--------[a]
VII	106-115	74.9	4,238.2±253.2	1357.9±81.1	------[c]	--------[c]	-------[c]	---------[c]	-------[c]

a- Failure Phase (No steady state values)

b-value calculated from the conversion factor between biomass dry weight and viable cells /mL

c-Recovery Phase
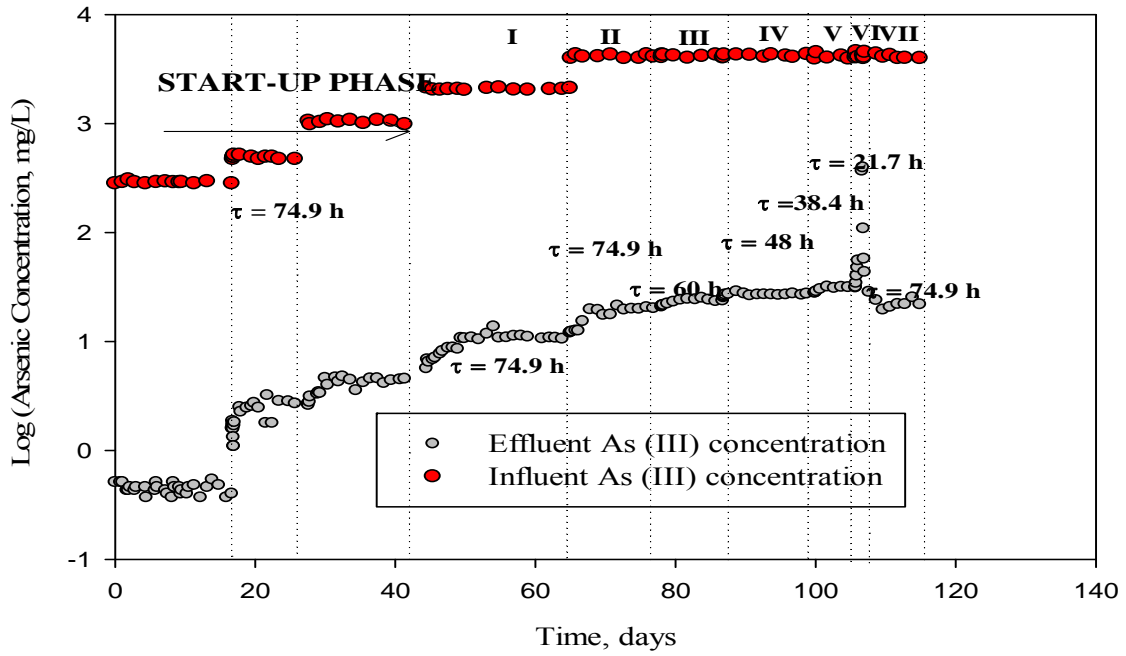
Figure 4.3 As (III) Oxidation in the CSTR bioreactor system
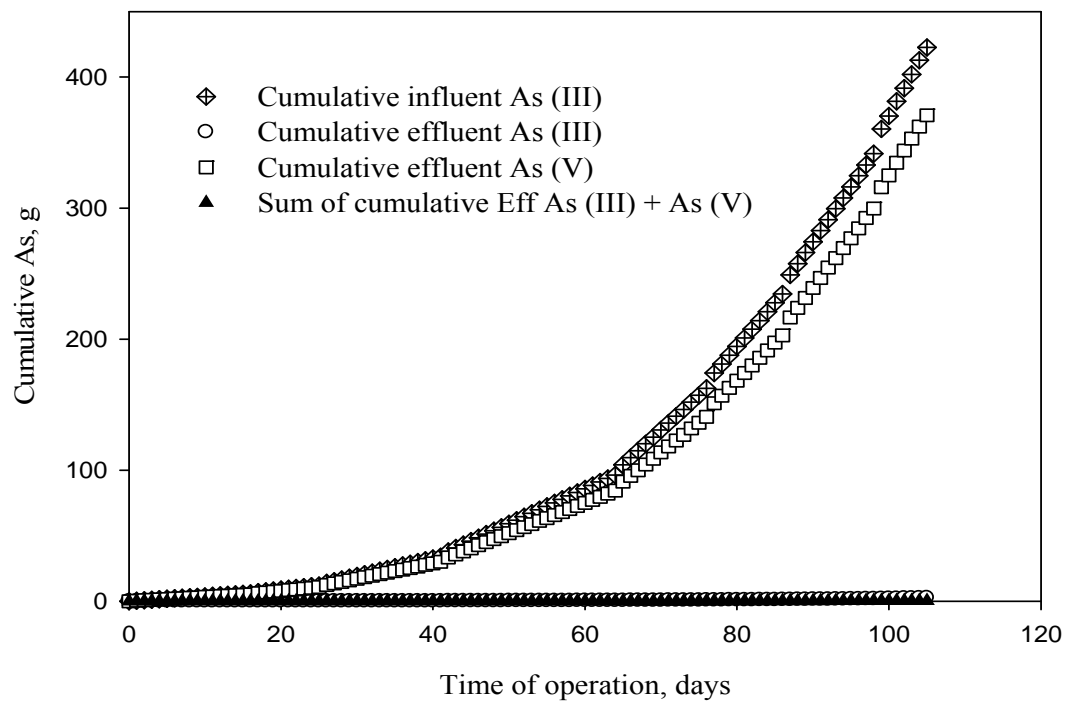
Figure 4.4 Arsenic Mass Balance in the CSTR
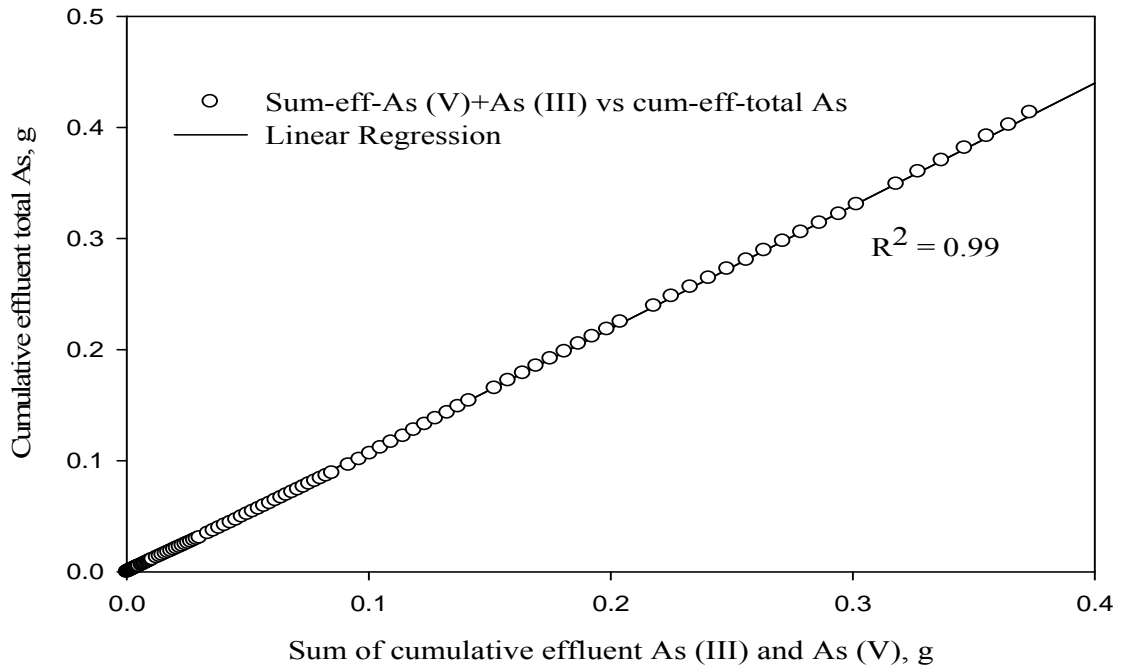
Figure 4.5 Comparison of cumulative effluent total As and sum of cumulative effluent As (III) and As (V).

4.6.4 Steady-State Analysis

4.6.4.1 Biokinetic Parameters Estimation

Biokinetic parameters k, K_s, k_d and Y were determined using the steady state data obtained in phases II-V, under a constant influent As (III) concentration of 4,000 mg/L and HRTs varying between 38.4 h and 74.9 h. A linear regression analysis between the plot of $\frac{X\tau}{S_i-S}$ versus $\frac{1}{S}$ using Eq. (4-12) yielded k = 5 mg As (III)/ mg cell dry weight/h and K_s = 20.1 mg/L, respectively, with R^2 = 0.981(Figure 4.6a). The maximum specific As (III) oxidation rate k was much higher than that obtained earlier (0.85 ± 0.18 mg As (III)/ mg cell dry weight/h) with batch cultures of the same strain b6 (chapter 3 section 3.6.9). The variability in the estimated values of the same parameter could be due to culture history prior to the start of the experiment or the mathematical routine employed to obtain the parameters as discussed by Grady et al. (1996). A nonlinear regression technique was used to obtain parameters from the batch study, whereas, a linearized approach is employed to obtain the same from the continuous flow study. The As (III) half-velocity constant K_s, had the same order of magnitude compared to its estimated value (33.2±1.87 mg/L) from the batch study (section 3.6.9, chapter 3). However, in a similar study with *Alcaligenes faecalis* strain O1201 using citrate as the carbon and energy source (Wang and Suttigarn 2007); the value of K_s (70 mg/L) was at least 3 times higher than that obtained in the present study, suggesting that the autotrophic strain b6 has a higher affinity towards As (III) than the heterotrophic *A.faecalis* strain O1201. The strain O1201 exhibiting lower affinity towards As (III) validated the fact that

heterotrophic strains oxidizes As (III) to As (V) for detoxification reason rather than use the available energy for the purpose of growth (Santini et al. 2000).

The K_s value for *T.arsenivorans* strain b6 was also lower than those reported for other heterotrophic arsenite oxidizing strains ranging from 34 - 115 mg/L (Turner 1949, 1954; Turner and Legge 1954; Osborn and Ehrlich 1976).

The other two parameters $Y = 0.011$ mg dry weight of cells / mg As (III) and $k_d =$ 0.008 h^{-1} were obtained from a linearized plot using Eq. (4-13) with R^2 of 0.891(Figure 4.6b). The obtained cell yield coefficient Y was approximately eight times lower than the value ($Y = 0.088 \pm 0.0048$ mg cell dry weight/mg As (III)) estimated in the batch study as described in the section 3.6.9 of chapter 3. This may be again due to the linearized approach used for estimation in this study compared to the non-linearized estimation technique in the batch study. However, the value of decay coefficient k_d (0.008 h^{-1}) estimated in this study is comparable to the value (0.006±0.002 hr^{-1}) obtained from the batch experiment. The close proximity between the estimated values of Y and k_d in this study indicates that the culture decay in the CSTR operated with long HRTs is significant.

The variability in the estimated kinetic parameters obtained in batch and the CSTR cultures of *T.arsenivorans* strain b6 (this study) can be due to the method of estimation or the history of the specific culture prior to the start of the experiment as discussed before by Grady et al.(1996). Although batch operation is easier and economical compared to CSTR operation, the kinetic parameters obtained at steady-state conditions in the CSTR are more accurate and reliable than that obtained in batch study

(Gallifuoco et al. 2002). This is because continuous cultures at steady-states are under better controlled and optimized environments than that of transient growth conditions in batch study (Wang and Suttigarn 2007). Another advantage of CSTR over batch reactor is the dilution of the feed As (III) concentration to the reactor. This explains the reason for no significant inhibition observed for the range of influent As (III) concentrations (2,000-4,000 mg/L) fed to the CSTR in this study. However, significant inhibition was observed on As (III) oxidation for As (III) concentrations greater than 500 mg/L using pure cultures of the same strain b6 in batch reactors (Figure 3.5a, chapter 3).
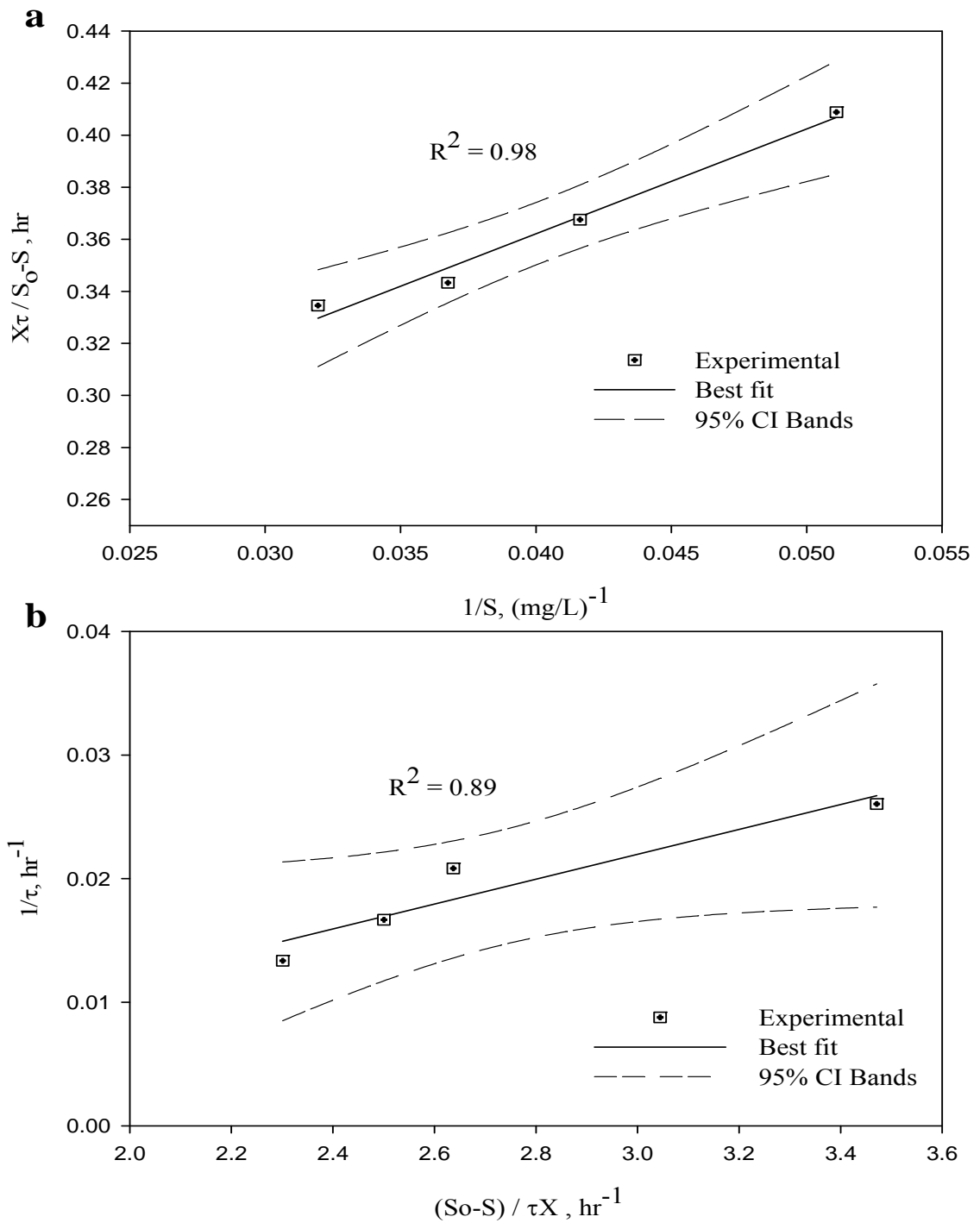
Figure 4.6 a) Linear regression analysis for the determination of k and K_s b) Linear regression analysis for the determination of k_d and Y.

4.6.4.2 Performance Evaluation using the Steady-State Model

The expressions (Eqs. (4-6) - (4-11)) derived from the mass balance were used to analyze steady-state results using the parameter values estimated from Eqs. ((4-12) - (4-13)) and data obtained in phases II-V. Figure 4.7a shows the comparison between the model simulation and the measured steady-state effluent As (III) concentrations for the entire operating range of HRTs (38.4 h-74.9 h). The experimental results represent the average effluent As (III) levels obtained at the operating HRTs of 38.4 h, 48 h, 60 h and 74.9 h, respectively. Using steady state expression (Eq. (4-6)) along with the obtained biokinetic parameters, effluent As (III) concentrations were calculated and compared to the data obtained at steady-state conditions. Analyses were also conducted for biomass production, biomass productivity, As (V) production, percentage conversion of As (III) to As (V), and the specific As (III) oxidation rate under steady-state conditions. Very good agreement was observed between the model prediction and the effluent As (III) concentrations (Figure 4.7a). The model was also able to capture the general trend in biomass concentration, although slightly overestimating its values at HRTs of 74.9 and 60 h (Figure 4.7b). However, the difference between the measured and predicted biomass concentrations at these two HRTs were statistically insignificant ($p = 0.3449$, H = 0; $p1 = 0.6667$ H1 = 0) at 95% confidence level. The group values (p, H and $p1$, H1) were obtained from the two sample t-test and Wilcoxin Rank Sum test, respectively.

At the critical HRT of 21.7 h, the model analysis is consistent with the experimental observation in predicting the complete washout of the cells of strain b6 (Figure 4.3 and Table 4.3) due to inability of the culture to reproduce quickly enough to maintain itself under the short HRT. Complete washout of the cells was prevented by

quickly increasing the HRT from 21.7 h to 74.9 h on day 106 when a decrease in the cell density and a rapid increase in the effluent As (III) concentration were observed. The model also predicted that an increased flow rate (lower HRT) through the reactor would results in higher biomass productivity (Figure 4.7c) until reaching the critical HRT of 21.7 h, at which the productivity declined due to loss of viable cell mass.

Similar results were observed with As (V) productivity in the reactor (Figure 4.7d). The productivity increased until the critical HRT (21.7 h) was reached. The As (V) productivity decreases rapidly at HRTs $\leq$ 21.7 h due to loss of biomass.

The data in Figure 4.7e indicate the efficiency of the CSTR in converting As (III) to As (V). Although the model overestimated at the operating HRTs, this deviation from the model simulation was within the acceptable analytical error of $\pm$ 15%. At HRTs $\leq$ 21.7 h, the efficiency of the CSTR decreased due to rapid loss of viable cell mass. Furthermore the projected specific As (III) oxidation rate under various HRTs (Figure 4.7f) also indicates that the specific As (III) oxidation rate reached its maximum value close to the critical HRT of 21.7 h. This increase in the As (III) oxidation rate is related to the increase in biomass productivity with decreasing HRTs as indicated in Fig. 4.7c until reaching the critical HRT of 21.7 h.
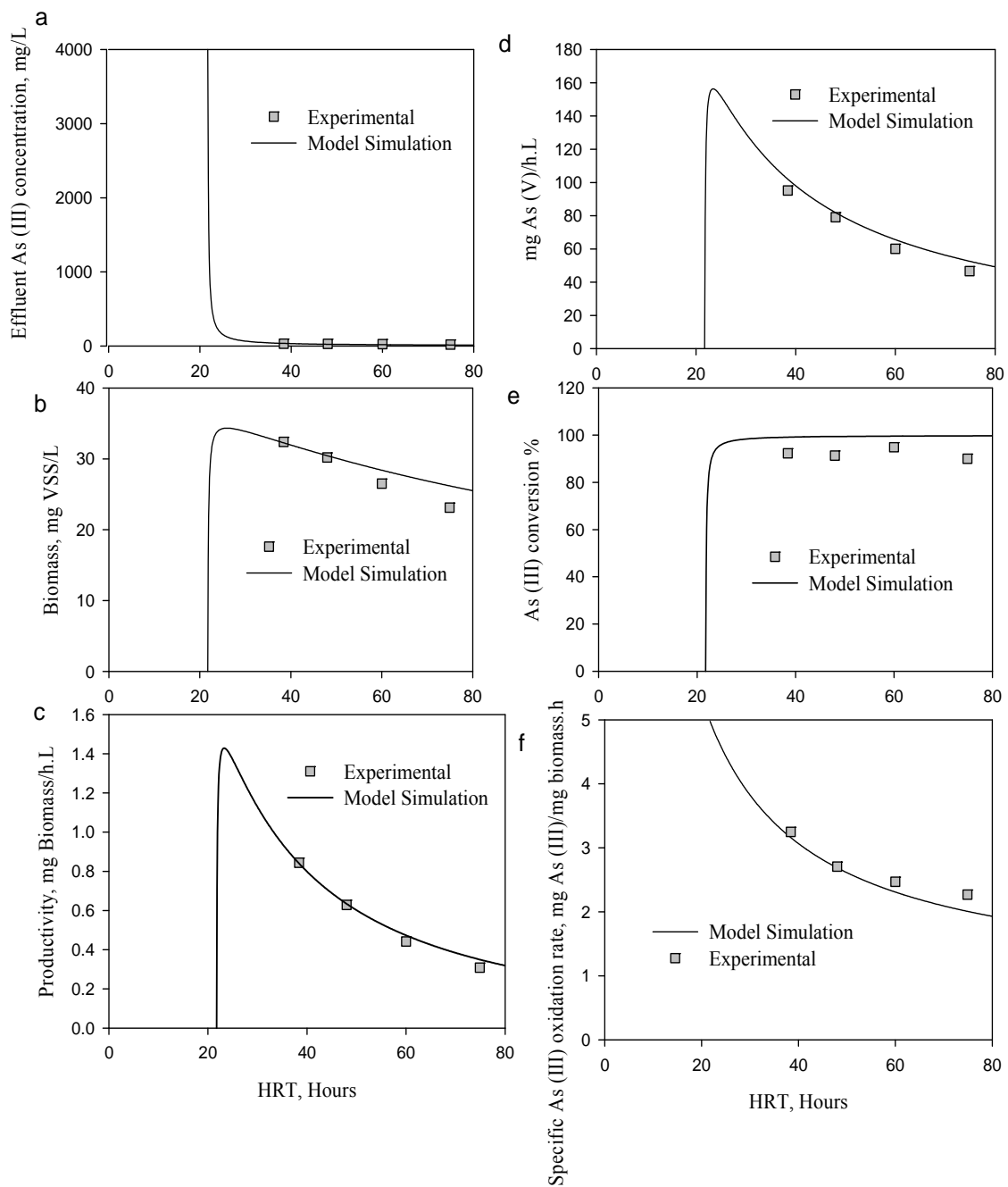
Figure 4.7 Simulated and experimental results of a) effluent As (III) concentrations, b) biomass concentrations, c) Biomass productivity, d) steady-state As (V) productivity, e) As (III) conversion to As (V), and f) Specific As (III) oxidation rate on biomass under different HRTs in the CSTR.

4.6.5 Non steady-state performance analysis

Equations (4-2) and (4-3) coupled with the modified Monod expression (Eq. (4-4)) and the obtained best-fit parameters were used to simulate the transient responses of the CSTR under varying As (III) loading rates. Good agreement between the model predictions and the experimental data was observed for phases II-V (Figure 4.8). The model accurately predicted the transient trends for phases II and III, although slightly underestimating the steady-state effluent As (III) levels (Figures 4.8a and 4.8b). The model predicted steady-state effluent As (III) levels of 18.04 mg/L (phase II) and 23.7 mg/L (phase III) are within ± 15% the observed values of 19.6 mg/L and 24.1 mg/L (Table 1), respectively for phases II and III. This variation was statistically insignificant ($p = 0.32$ and $p = 0.81$) and may be attributed to error involved in sampling and laboratory analyses. The model predicted both the transient and steady-state performance for the remaining two phases (IV, V) with an even higher accuracy (Figure 4.8 c and Figure 4.8 d), with the deviation of the model simulations from the experimental values statistically insignificant ($p = 0.29$ for phase IV; $p = 0.5$ for phase V).

The model and the parameters obtained using steady-state data in phases II-V were verified using the experimental data obtained from phase I under an influent As (III) concentration of 2,000 mg/L increased from 1,000 mg/L under a constant HRT of 74.9 h. Although the difference between the model and experimental data is significant (Figure 4.9 $p = 0.0039$), the model was able to simulate the trend of the effluent As (III) in response to the increased As (III) loading.

A sensitivity analysis was performed on the kinetic model using the approach of Gooijer de et.al (1991). The sensitivity procedure revolved around set-point values (steady-state) of the governing parameters used in the model evaluation for all the five steady-state phases. The value of each parameter was varied 0.5-1.5 times the set-point value independently keeping all the other parameters and variables constant. The model predicted effluent As (III) concentrations for the variation in parameter values were plotted in a dimensionless form by comparing it with the corresponding effluent As (III) levels at steady-state conditions.

A representative sensitivity analysis using data obtained in phases II-V of this study was shown in Figure 4.10. The results clearly show that the sensitivity of the model prediction to changes in the parameters was very similar in pattern for all the phases (II-V). The data clearly indicate that the parameters Y and k have a high impact on the predicted effluent As (III) levels in the CSTR as compared to K_s and k_d (Figure 4.10). The sensitivity of the model outcome to changes in these two parameters Y and k was mostly significant when varied 0.5-0.8 times their set-point values, compared to the rest of the variation range (0.8-1.5). The observation that the model is sensitive to Y may be attributed the closeness of estimated values of Y and k_d. The influence of the yield coefficient (Y) becomes less significant on the reactor performance than the decay coefficient (k_d), when its parameter is at 0.5 times the set-point value. As a result, the magnitude of predicted effluent As (III) level increased several folds compared to its value at steady-state condition. Similarly, reduction of the magnitude of specific As (III) oxidation rate, k, by 0.5 times leads to an increase in the predicted level of effluent As

(III) in the reactor due to the reduction of As (III) uptake by cells in the reactor. Similar results were also observed for the other four phases as shown in figure 4.10.

4.6.6 Model Adequacy check

The appropriateness of the model fit to the transient and steady-state data obtained from phase II-V of the CSTR operation were determined by means of two diagnostic plots: (1) model predicted effluent As (III) concentration versus observed effluent As (III) levels at each HRT, and (2) a normal probability plot of the residuals e_i. Two additional statistical tests (a paired t-test and a chi-square goodness-of-fit test) were also employed to test whether the difference between the model predicted effluent As (III) levels and the observed effluent As (III) concentrations were statistically significant at the 95% confidence level ($\alpha = 0.05$).

The correlation coefficient between the model predicted and observed effluent As (III) values obtained by means of a linear regression analysis are listed in Table 4.4 and the corresponding plots are shown in Figures 4.11a, 4.12a, 4.13a, 4.14a, and 4.15a, respectively. Except for the validation data (phase I, $R^2 = 0.67$), the model adequately described the general trend of the response of the CSTR operated under varying HRTs. The statistical test results (Table 4.4) also clearly show that the measured difference between the model predicted and observed effluent As (III) values was not statistically significant at the 95% confidence level ($\alpha = 0.05$) except for the data in phase I. However, the model was still successful in depicting the transient and steady-state trend of the observed effluent As (III) data in phase I. Except phase I, the statistical tests also demonstrate the strong performance of the model in predicting the observed effluent As (III) values for phases II-V (Table 4.4).

The normal probability plots used for checking any model inadequacies are shown in Figures 4.11b, 4.12b, 4.13b, 4.14b, and 4.15b, respectively. The normal probability plot for the validation phase (I) suggest the presence of one more outliers or some inadequacies in the normality assumption of the observed data (Montgomery 2001). The flattening of the data at the two extreme indicate the distribution having thinner tails than the normal.

However, the normality assumption validates the data obtained in phases II-V of the CSTR operation as shown in the corresponding plots. The coupling of the mass balance equations with the Monod model was not perfect but adequate in describing As (III) -oxidation to As (V) in the CSTR operated under varying HRTs.
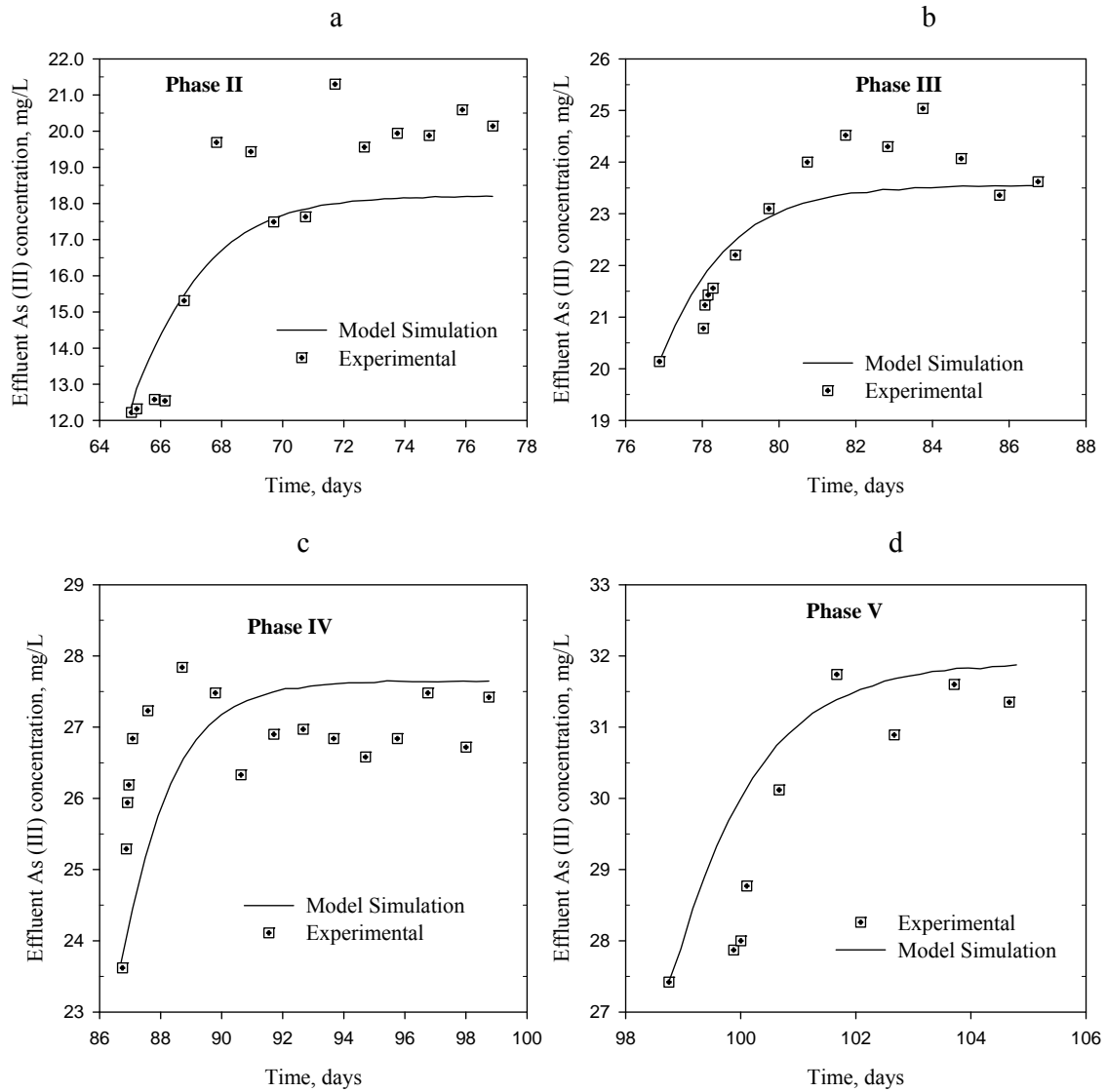
Figure 4.8 Simulation of the transient and steady-state conditions in the CSTR for a)

phase II, b) phase III, c) phase IV, and d) phase V.
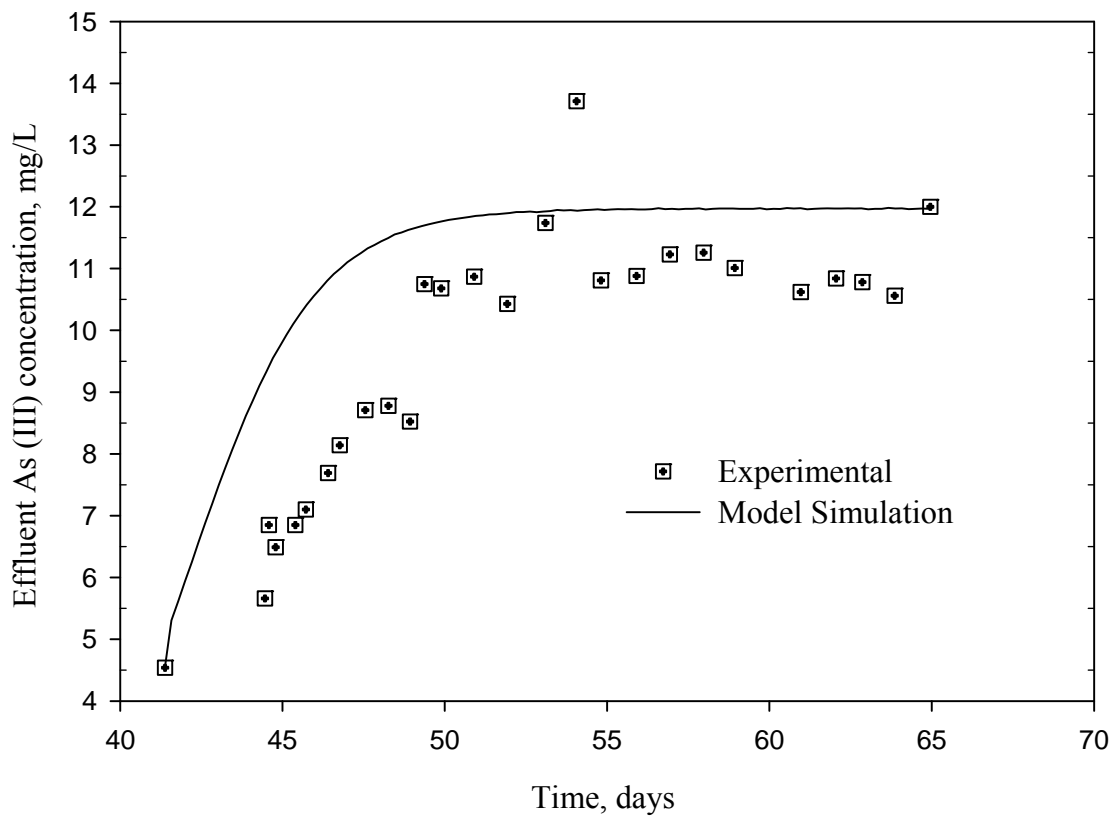
Figure 4.9 Model validation on the experimental dataset obtained from phase I of the

CSTR operation.
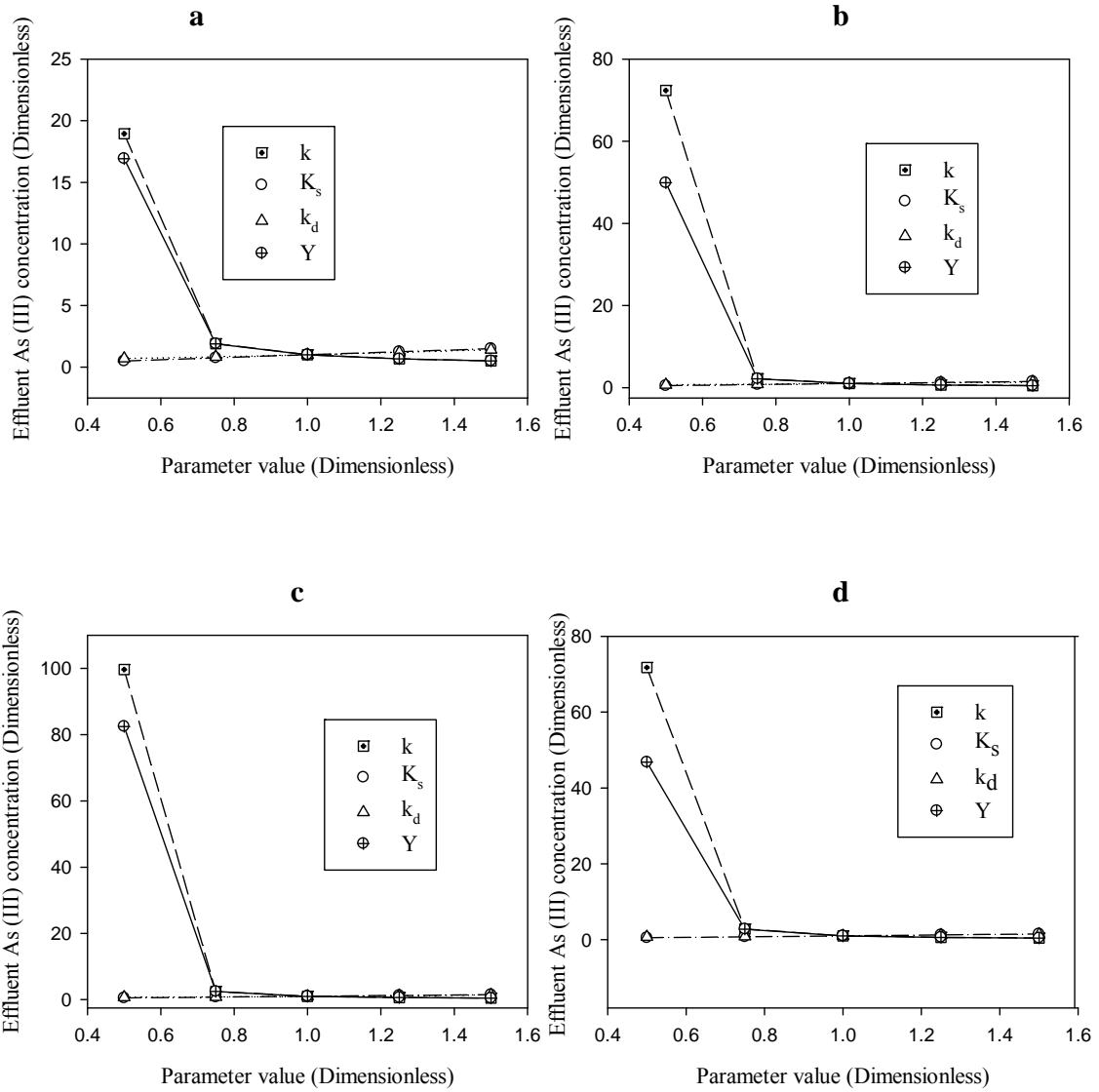
Figure 4.10 Sensitivity analyses for phases II-V of the CSTR bioreactor system
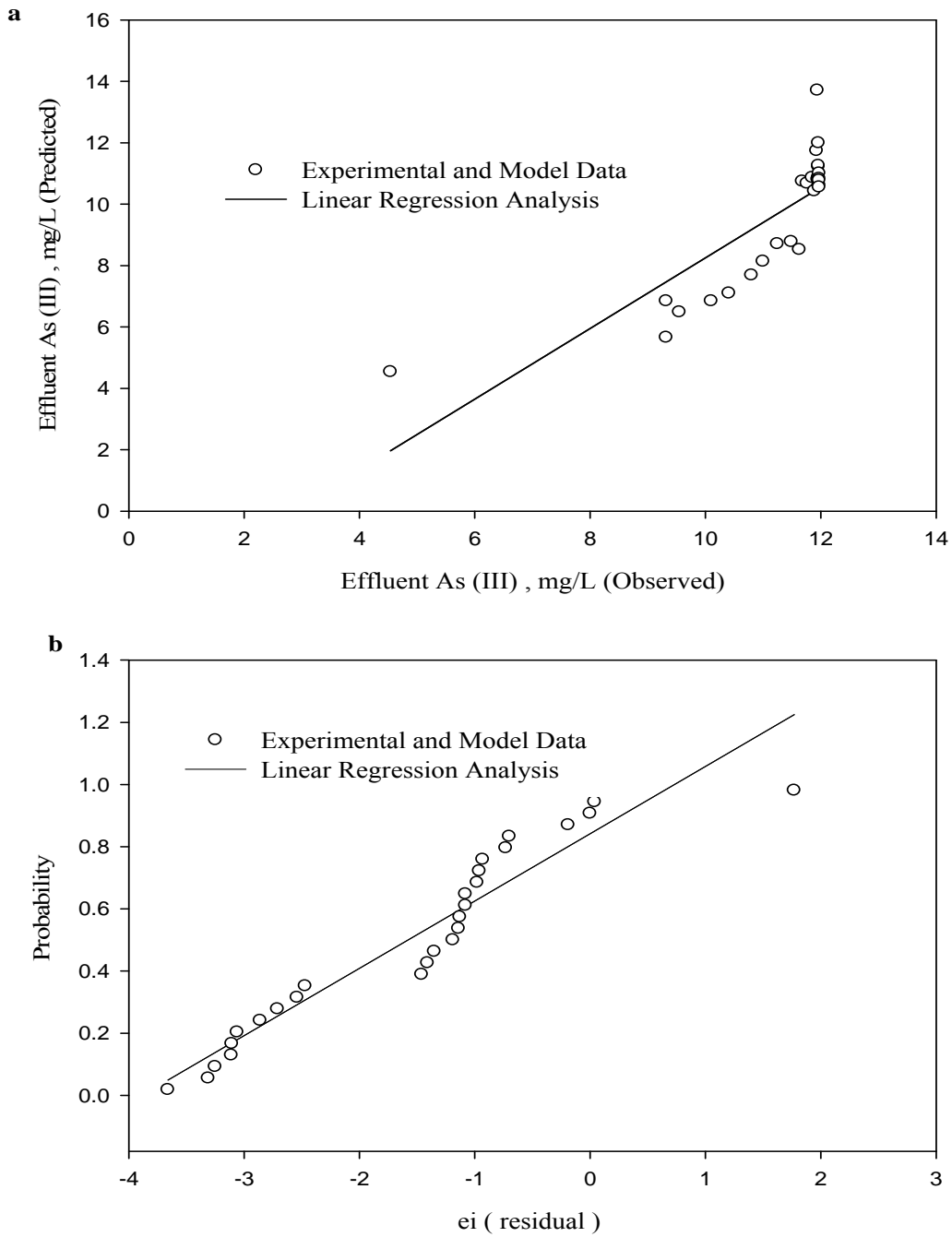
Figure 4.11 Plots for assessing the validity of the fitted model to the phase I data a) model predicted and observed effluent As (III) concentrations, and b) normal probability plot of the residuals (e_i).
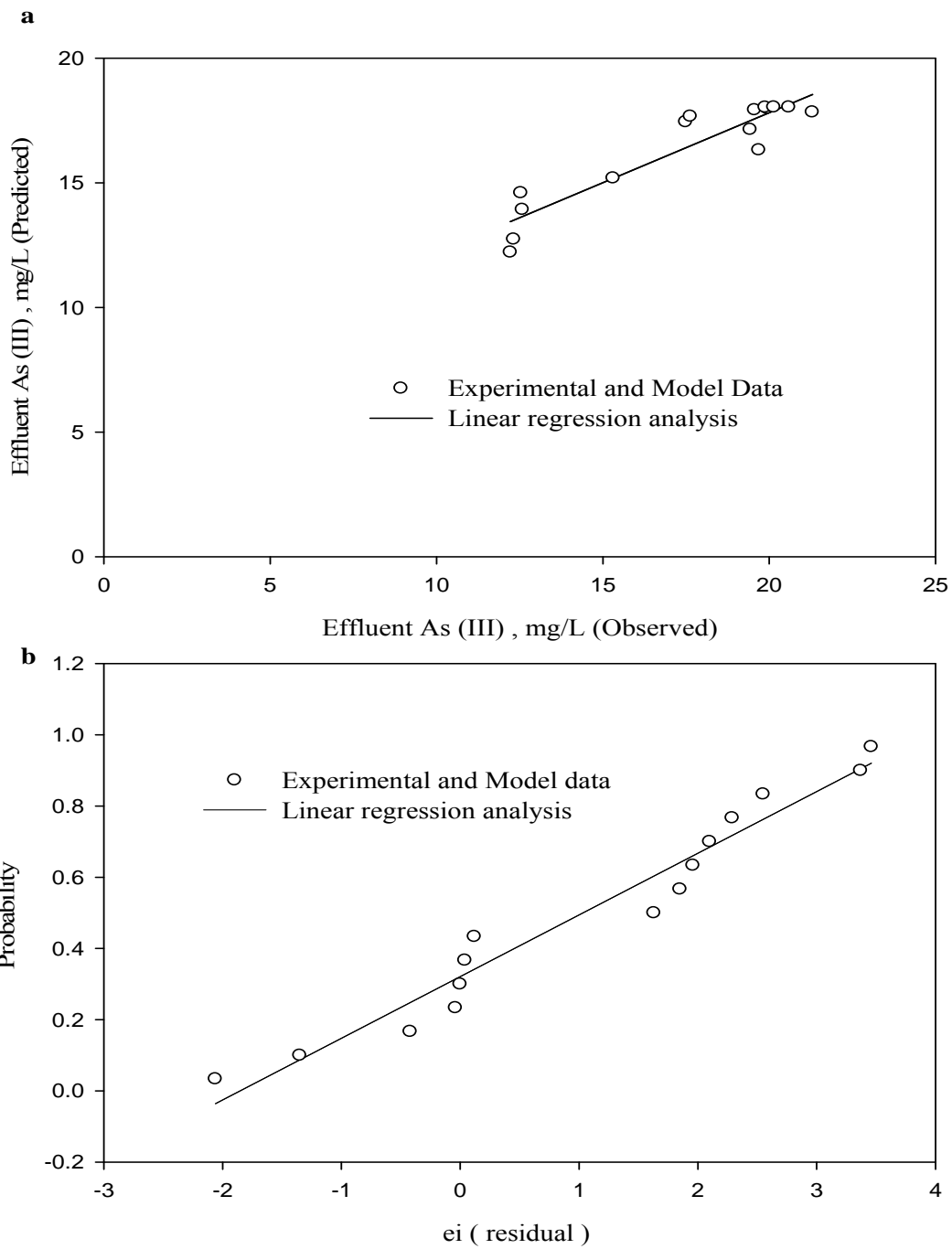
Figure 4.12 Plots for assessing the validity of the fitted model to the phase II data a) model predicted and observed effluent As (III) concentrations, and b) normal probability plot of the residuals (e_i).
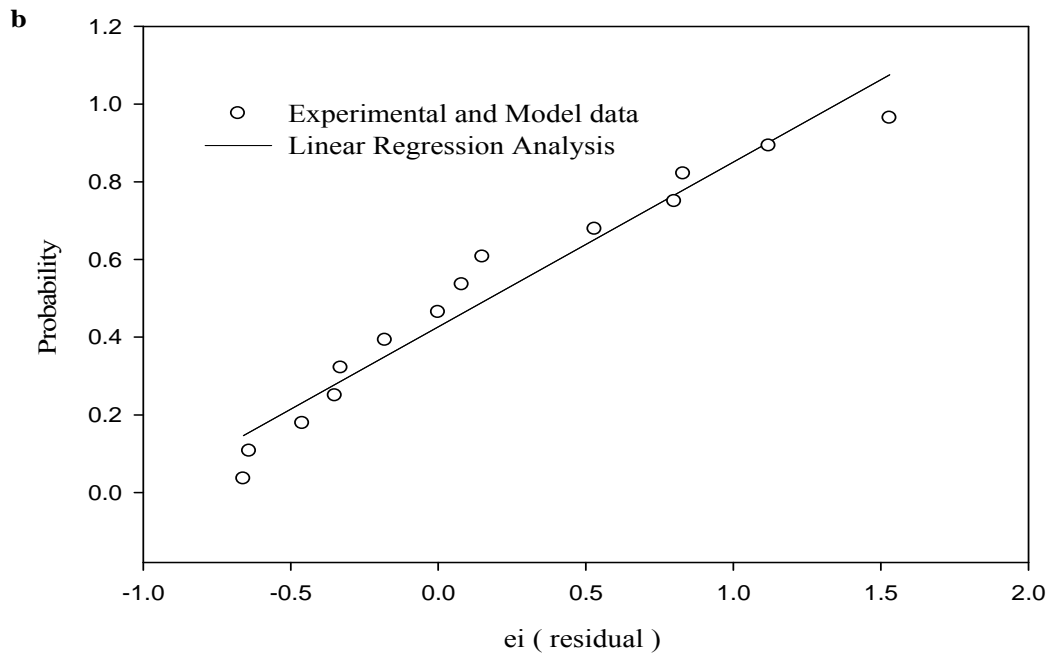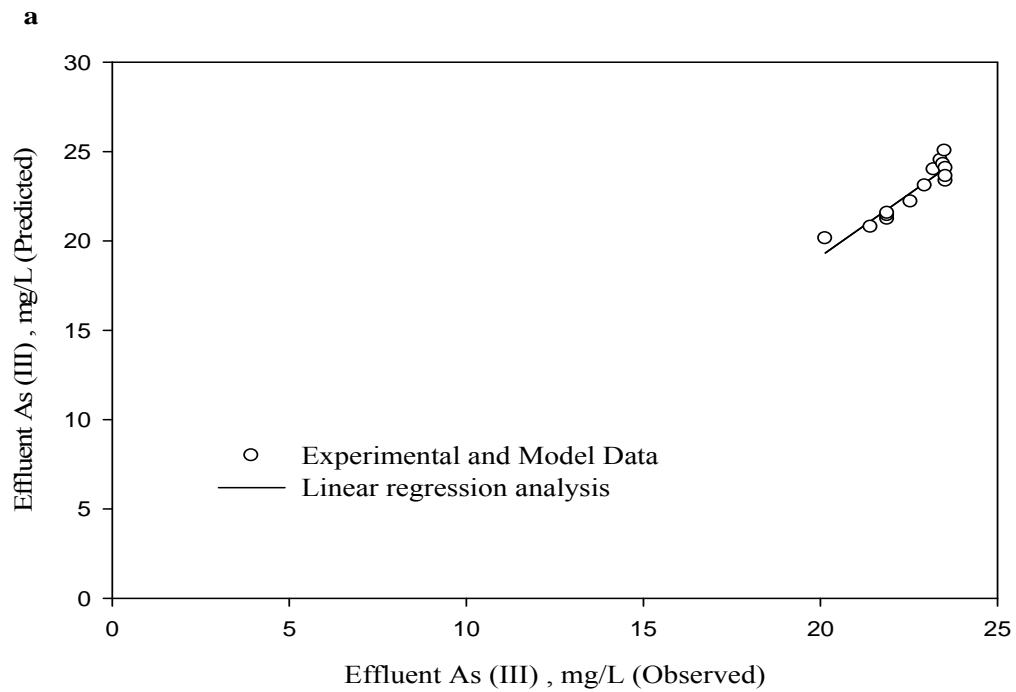
Figure 4.13 Plots for assessing the validity of the fitted model to the phase III data a) model predicted and observed effluent As (III) concentrations, and b) normal probability plot of the residuals (e_i).
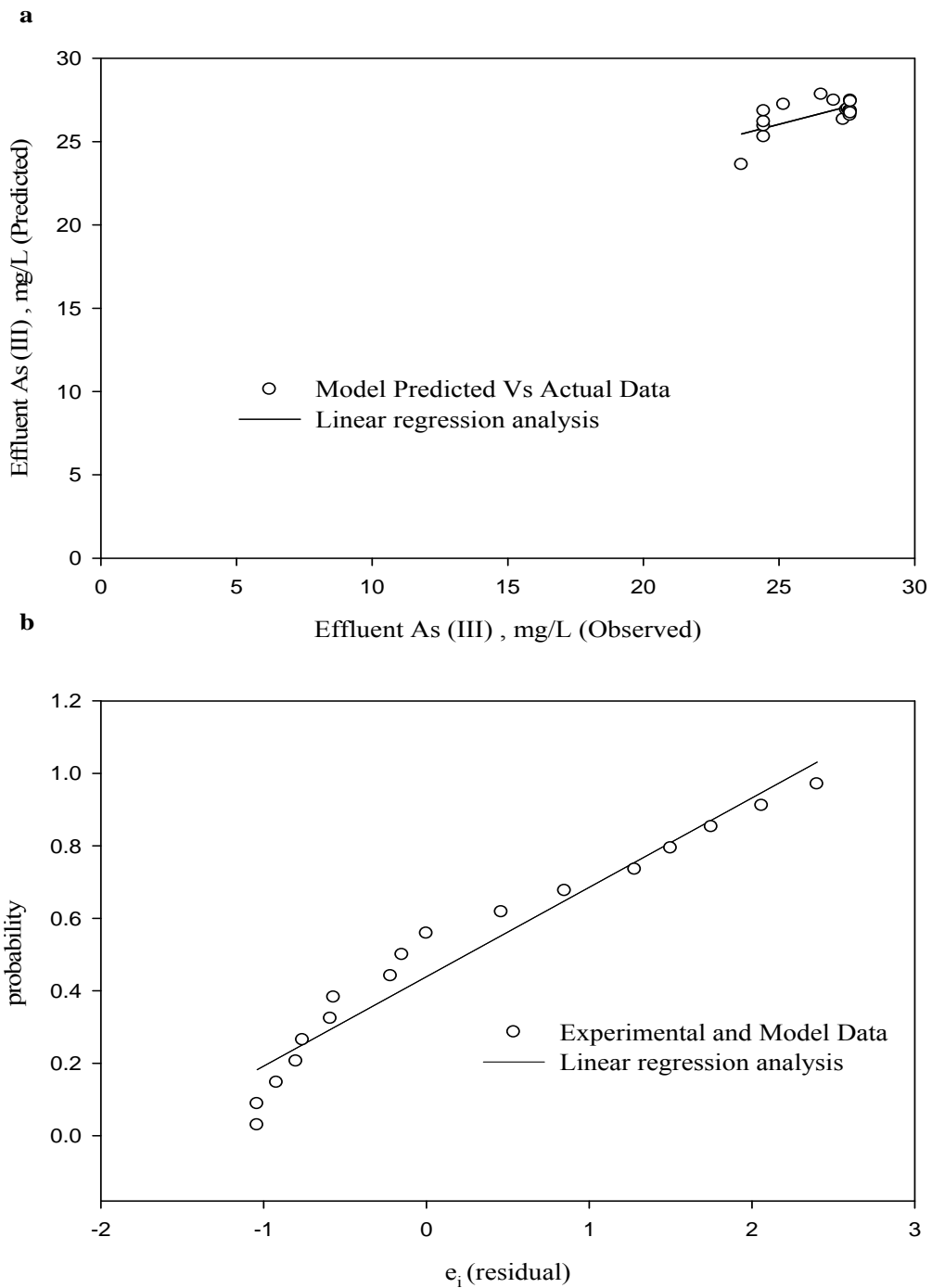
Figure 4.14 Plots for assessing the validity of the fitted model to the phase IV data a) model predicted and observed effluent As (III) concentrations, and b) normal probability plot of the residuals (e_i).

a

b
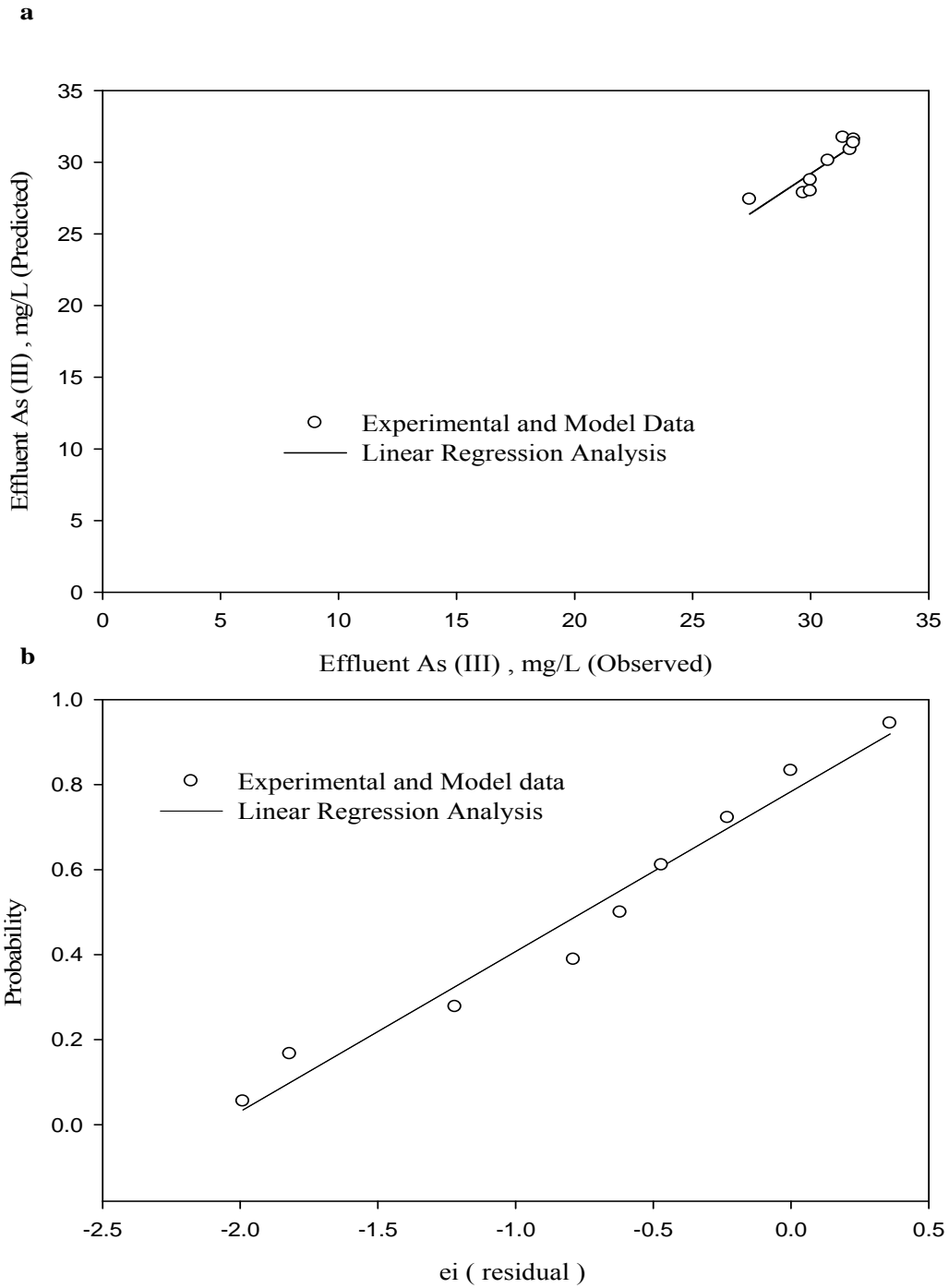
Figure 4.15 Plots for assessing the validity of the fitted model to the phase V data a) model predicted and observed effluent As (III) concentrations, and b) normal probability plot of the residuals (e_i).

Table 4.4 Statistical tests for evaluating model fit to the experimental data

Phase	HRT (hr)	R^2 (model predicted versus observed effluent As (III) values)	Paired t-test (α=0.05)	Chi-square goodness-of-fit test (α=0.05)
I	74.9	0.67	0.36	0.99
II	74.9	0.86	0.03	0.99
III	60	0.87	0.36	1
IV	48	0.87	0.39	1
V	38.4	0.8	0.36	1

4.7 Summary and Conclusions

The bacterial strain *T.arsenivorans* b6 oxidized As (III) in the CSTR under a wide range of influent As (III) concentrations (2,000 – 4,000 mg/L) and HRTs (21.7-74.9 h). The CSTR was unstable under an As (III) loading rate of 4,847.4 ± 290.9 mg/day/L and HRT of 21.7 h, but quickly recovered once the As (III) loading rate was reduced by increasing the HRT to 74.9 h. The major mechanism of As (III) removal in the CSTR was oxidation to As (V) by the *T.arsenivorans* strain b6. The obtained biokinetic parameters (k, K_s, k_d and Y) and reactor mass balance based expressions integrated with the Monod model satisfactorily predicted both the transient and steady-state As (III) oxidation in the CSTR. Sensitivity analyses revealed k and Y are the most sensitive to mode predictions compared to K_s and k_d for all the five steady-state conditions. The model adequacy check clearly demonstrated the appropriateness of the model fit to the observed data obtained by operating the CSTR under varying HRTs.

Chapter 5: Fixed-film Reactor Study

5.1 Abstract

As (III) oxidation by the chemolithoautotrophic bacterium *Thiomonas arsenivorans* strain b6 was investigated in a fixed-film reactor under variable influent As (III) concentrations (500 – 4,000 mg/L) and hydraulic residence times (HRTs) (0.2 – 1 day) for a duration of 137 days. Seven steady-state conditions were obtained with As (III) oxidation efficiency ranging from 48.2% to 99.3%. The strong resilience of the culture was exhibited by the recovery of the bioreactor from an As (III) overloading of 5000.4 ± 373 mg As (III) / L.day operated at an HRT of 0.2 day. An arsenic mass balance revealed that As (III) was mostly oxidized to As (V) with unaccounted arsenic (≤ 4 %) well within the analytical error of measurement. A predictive flux model was used to determine the biokinetic parameters by fitting the modified Monod expression against the observed steady-state flux data obtained from operating the bioreactor under a range of HRTs (0.2 – 1 day) and a constant influent As (III) concentration of 500 mg/L. Parameters $k = 4.24 \pm 0.63$ mg As (III) / mg cells.hr, and $K_s = 13.2 \pm 5.6$ mg As (III)/L were obtained using a non-linear estimation routine and employing the Marquardt-Levenberg Algorithm. Sensitivity analysis revealed k to be more sensitive than K_s to model simulations of As (III) oxidation under steady-state conditions.

5.2 Introduction

5.2.1 Biofilm

Biofilms are defined as communities of bacteria attached to a solid substratum and embedded in a "glycocalyx" matrix consisting of self excreted extracellular polymeric substances (EPS). EPS is one of the key components of the biofilm matrix

because it mediates the process of adhesion between the bacterium and the attachment surface (Donlan and Costerton 2002). According to some genetic studies conducted by Watnick and Kolter (1999), the biofilms of single species are formed in several multiple steps. These steps resulting from the association between the bacterium and the attachment surface and other microorganisms already present on the surface finally leads to the formation of the three-dimensional biofilm matrix (Watnick and Kolter 2000). Biofilms formed under extremely high shear conditions are stronger and resistant to mechanical breakage than biofilms formed under low shear conditions (Donlan and Costerton 2002).

EPS of the biofilm matrix is also termed as the "house of the biofilm cells", because it is responsible for keeping all the cells together (Watnick and Kolter 2000). This biofilm matrix helps to maintain a constant growth of microorganisms on the attachment surface by supplying nutrients to the bacteria in the biofilm community through its adsorption property. Several studies have been conducted to investigate and understand the complex structure of the EPS and its components (Flemming et al. 2007). EPS basically controls the environment around the attached cells by affecting the "water content, charge, sorption properties, hydrophobicity, and mechanical stability" (Flemming and Wingender 2002). The EPS consists of polysaccharides, proteins, glycoproteins, glycolipids, and in some cases, certain amounts of extracellular DNA (e-DNA) (Flemming et al. 2007).

Several theories have been proposed to rationale the need for biofilm formation (Watnick and Kolter 2000; Rittmann 2001; Donlan and Costerton 2002). However, the most common and widely accepted theory is the creation of the microenvironment, which

helps to counter severe pH changes in the bulk liquid and also to resist toxic substances from entering the biofilm matrix. Rittmann (2001) also stated that the close spacing of the cells in the matrix was important for effective transport of essential nutrients across the cells.

5.2.2 Biofilm Reactors

Packed bed reactors are the most common type of biofilm reactors. In these reactors, the cells are usually attached to a stationary medium, and are generally used for aerobic and anaerobic treatment of wastewater (Rittmann 2001). Fluidized-bed reactor, another kind of biofilm reactor, is also commonly employed for wastewater treatment. The cells in the fluidized-bed reactors are immobilized, and are kept in suspension under a very high effluent recycle flow rate. This high recycle rate is essential for maintaining the necessary fluidization velocity for achieving optimum performance during the wastewater treatment process. However, very high fluidization velocity can also result in losses of these particles or the detachment of cells from the media under abrasion or turbulence (Rittmann 2001). The Rotating biological contactor RBC is the other biofilm reactor commonly used for aerobic wastewater treatment. The RBC can be also used for anaerobic treatment of wastewater by submerging the reactor or by covering it so as to prevent the entrance of oxygen into the contactors. The biggest advantage of the packed bed reactor over the other reactors is the capacity to withstand higher substrate loading rate due to the presence of strong attachment force between the cells and the surface.

5.2.3 Importance of Effluent Recirculation in Biofilm Reactors

Effluent recycle is very important in biofilm operations. The recycle leads to a reduction of the mass transfer resistance in the reactor due to the even distribution of

biomass resulting from the homogenous concentration profile of the substrate in the reactor (Choi and Silverstein 2007). Effluent recycle also leads to dilution / reduction of influent substrate concentration in the reactor. This decreases the acclimation time of the attached cells in the bioreactor to the varying hydraulic / substrate loading. Finally, effluent recycle helps to oxygenate and maintain a constant upflow rate in the bioreactor (Rittmann 2001; Choi and Silverstein 2007).

5.2.4 Objectives of the Biofilm Study

The objectives of the fixed-film reactor study were as follows:

(1) To evaluate the potential of As (III) oxidation in the fixed-film reactor under a wide range of As (III) loading rates. The bioreactor was continuously operated under variable influent As (III) concentrations (500 - 4,000 mg/L) and HRTs (hydraulic residence time) (0.2 - 1 day) for a period of 137 days. The efficiency of the reactor in converting As (III) to As (V) was evaluated.

(2) To estimate the intrinsic biokinetic parameters k (maximum specific As (III) oxidation rate [$MM_x^{-1}T^{-1}$), and K_s (As (III) half velocity constant [ML^{-3}]). The parameters were obtained using the steady-state conditions (phases: I-IV) and the predictive flux equation derived from the pseudo analytical solution of the biofilm model given by Atkinson and Davies (1974).

(3) To compute the growth potential values of the biofilm reactor under the different As (III) loading rates (phases I-VIII). The effect of the mass-transfer resistance on the overall performance of the fixed-film reactor was also evaluated.

(4) To investigate whether carbon was limiting for As (III) oxidation under high As (III) loading rates in the bioreactor. A statistical technique was employed to evaluate the

difference in the obtained effluent As (III) data with and without the additional carbon source.

5.3 Materials and Methods

5.3.1 Bacterial Strain and Feed Composition

Both the culture and feed composition used in the biofilm reactor study have been described before in section 3.3.1 in chapter 3.

5.3.2 Fixed-Film Bioreactor

Biological oxidation of As (III) to As (V) was investigated in a bench-scale fixed-film bioreactor under different As (III) loading rates. Pure cultures of *T.arsenivorans* strain b6 were immobilized by attachment to spherical glass beads. The reactor was operated with effluent recycle to maintain completely mixed conditions inside the bioreactor. The HRT of the reactor was varied between 0.2 – 1 day under a constant influent As (III) concentration of 500 mg/L for the first four phases of operation (phases I-IV). The remaining phases (V-VIII) were operated under a range of influent As (III) concentrations (1,000 mg/L- 4,000 mg/L) at a constant HRT of 1 day.

5.3.2.1 Reactor Configuration and Operating Conditions

The biofilm reactor was constructed from a acrylic column (internal diameter : 2.3 ± 0.01 cm, height : 20.1 ± 0.04 cm) packed with 2997 spherical pyrex glass beads (Fisher Scientific Co, Pittsburg, PA) averaging 3 mm in diameter (Figure 5.1). The total external surface area available for cell attachment in the packed bed reactor was 847.4 cm^2 with the empty bed volume of the reactor measuring at 83.7 mL. The components of the pump and the connecting tubings were autoclaved at 121°C for 30 mins. The interior of the

reactor was rinsed in 95% ethanol and dried before assembling the components under a germ free hood (Steril Gard Class II Model, The Baker Company, Stanford, ME).

Biological growth in the feeding tubes was minimized by close monitoring and periodical replacement. Bolted flanges and rubber gaskets were used on the top and bottom of the reactor to prevent leakage of the effluent from the reactor. Pre-calibrated peristaltic pumps (Masterflex, Cole-Parmer Inst. Co., Niles, Illinois) were used for the influent and recycle flows and the reactor was operated in an up-flow mode to ensure near completely submerged conditions in the reactor. A recirculation / influent flow ratio of 50:1 was maintained to ensure near completely mixed conditions in the reactor. The empty bed HRTs in the reactor were 1.0, 0.48, and 0.2 day under three feed flow rates of 83.7, 172.8, and 423.8 mL /d, respectively. A compressed air flow rate of 200 mL / min was maintained during operation of Phase III in order to investigate the effect of DO on the performance of the fixed-film reactor.
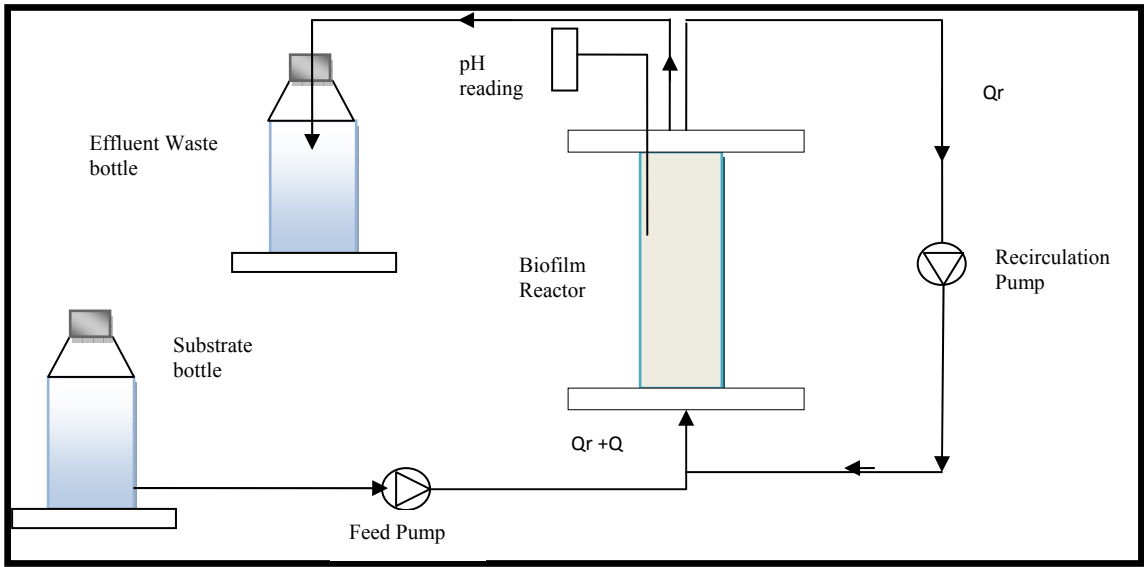
Figure 5.1 Schematic of the fixed film reactor system.

5.3.3 Tracer Study

Tracer studies were conducted to determine the flow characteristics in the biofilm reactor. Sodium arsenite ($NaAsO_2$) solution was used as the tracer with influent As (III) concentration measuring at 20 mg/L and an influent based flow rate of 7.2 mL/hr (HRT = 0.48 day). The observed effluent As (III) concentrations were then compared to the tracer response curve for an ideal completely mixed reactor using Eq. (5-1):

$$\frac{C}{C_o} = (1 - e^{-t/\tau})$$
(5-1)

where C and C_o are influent and effluent As (III), t is the time of sample measurement and τ is the HRT based on the feed flow rate Q. As (III) was measured using the modified silver diethyldithiocarbamate method (chapter 3; section 3.3.3.2). The same experiment was repeated with methylene blue dye (tracer) at an initial concentration of 10 mg/L to verify the optimum recycle ratio obtained earlier. The effluent methylene blue concentration was measured at a wavelength of 664 nm using the spectrophotometer (Spectronic Instrument, Rochester, NY), and the breakthrough curve was also compared to the ideal tracer response curve of a completely mixed reactor shown by Eq. (5-1).

5.3.4 Control Study

The column reactor was packed with fresh oven-dried glass beads and operated under an influent As (III) concentration of 100 mg/L at a HRT of 1 day for a period of 14 days. This control study was performed to investigate whether the glass beads or the walls of the acrylic column reactor were able to oxidize / adsorb As (III) present in the influent feed to the reactor. Samples were collected every day from the reactor and analyzed for influent As (III), effluent As (III), and As (V), respectively.

5.3.5 Reactor Startup

The reactor and its components were assembled under a laminar flow hood (Steril Gard, class II type A/B3, Baker Company, Sanford, ME), and packed with autoclaved oven- dried solid glass beads (Fisher scientific Co, Pittsburg, PA). The reactor was then inoculated with 30 mL of overnight grown cultures of *T. arsenivorans* strain b6. Subsequently, the reactor was operated under an influent As (III) concentration of 500 mg/L and HRT of 1day for 15 days until visible cell attachment was observed on the glass beads. During the startup phase, samples were collected and analyzed for effluent As (III), As (V) and total As using the modified silver diethyldithiocarbamate method (chapter 3, section 3.3.3.2). Optimum operating conditions were maintained in the reactor by frequent monitoring of pH and DO (Dissolved oxygen). pH was maintained at ~ 6.0 using 1N NaOH solution.

Samples were also collected for determining the viable suspended cells in the effluent from the reactor. Once a biofilm was clearly established on the glass beads, the bioreactor was then operated under various operating conditions as listed in Table 5.1.

5.3.6 Steady-State Determination in the Biofilm Reactor

The biofilm reactor was continuously operated for at least 14 days to ensure steady-state conditions before changing the As (III) loading rate. The study conducted by Foggler (1999) and Jensen (2001) showed that the time taken by a completely mixed reactor to reach 95% of its steady-state concentration is at least three to four times the HRT. In the present study, the operation periods ranged from 14 - 70 times the HRTs and thus satisfying the steady-state assumptions for the entire operational phases.

The relative standard deviation (RSD or RSD %) of the steady-state data for each phase of the reactor operation was also evaluated. The RSD values were always less than the permissible analytical error for arsenic analyses (section 3500-As B, APHA 1995) and biomass measurement (APHA 1995), respectively.

5.3.7 Analytical Methods

5.3.7.1 Sample Handling and Quality Control

Samples from the bioreactor were collected using 1 mL sterile disposable pipets (Fisher Scientific CO., Pittsburgh, PA) at appropriate time intervals. The collected samples were immediately centrifuged at 10,000 rpm for 10 mins using a microcentrifuge (Brinkmann Instruments Inc, West bury, NY). The supernatant was acidified using 1 % HNO_3 (pH < 2) and preserved in 4 °C for no more than 7 days prior to analysis of As (III), As (V) and total As (APHA 1995). Microbial analysis involved determination of the total protein content of bacterial cells, and attached / suspended viable cell concentrations for each steady-state phase. The biological samples were analyzed immediately to prevent any changes that may occur after collection.

Table 5.1 Operating Conditions Of the Biofilm Reactor

Phase	Duration (days)	Influent flow rate Q (mL/hr)	HRT (day)	pH	Influent As (III) (mg/L)	DO (mg/L)
I	1-9	3.5	1	5.2 ± 0.1	473.2 ± 29.3	2.8 ± 0.1
II	9-36	3.5	1	5.5 ± 0.3	466 ± 24.4	2.5 ± 0.2
III	36-62	7.2	0.5	5.1 ± 0.3	489.5 ± 10.7	3.1 ± 0.1
IV	62-78	17.4	0.2	5.3 ± 0.1	510.7 ± 24.4	2.4 ± 0.2
V	78-80	17.4	0.2	-----[a]	1000.1 ± 74.6	-----[a]
VI	80-97	3.5	1	5.1 ± 0.4	1000 ± 34.9	1.9 ± 0.1
VII	97-120	3.5	1	5.1 ± 0.3	2208.8 ± 79.2	1.5 ± 0.1
VIII	120-137	3.5	1	5.1 ± 0.2	4146.3 ± 98.6	1.2 ± 0.1

------[a] Not measured (overloading phase of the biofilm reactor)

The glassware used for arsenic analyses were first rinsed with concentrated HNO_3 to remove any contaminants which might interfere with the absorbance reading of the arsenic samples. After rinsing, the glassware was washed in a water bath with Micro-90 detergent (IPC, Burlington, New Jersey). The washed glassware were again rinsed in deionized distilled water (Millipore, Bedford, MA) and then oven dried at 105°C for at least 1 hour prior to the analyses.

For protein analysis, the microreaction vessels (Supelco, Inc., Bellefonte, PA) were washed, rinsed, and oven dried prior to use. The 1.5 mL centrifuge tubes (Fisher Scientific CO., Pittsburg, PA) used for protein analysis and viable cell counts were first autoclaved at 121°C for at least 15 mins, and then stored under the germ free hood (Steril Gard Class II Model, The Baker Company, Stanford, ME) before each use.

Arsenic analyses were conducted in one batch of seven samples each for As (III), As (V), and total As, respectively. A new standard / calibration curve was prepared for arsenic species and protein concentration prior to analysis to eliminate any bias during measurement (APHA 1995).

5.3.7.2 As (III), As (V), and Total As Determination

As (III), As (V), and total As were analyzed using a silver diethyldithiocarbamate method (SDDC) as described in section 3.3.3.2 in chapter 3.

5.3.7.3 pH and Dissolved Oxygen Determination

pH was measured *in situ* using a pH meter (Denver Instrument, Denver, CO) equipped with an ATC Combo, Silver/Silver chloride electrode. The pH meter was calibrated with standard buffers of 4 and 7 and disinfected by 95% ethanol before use.

DO was determined *in situ* using a DO meter (YSI 550A, Yellow Springs, Ohio), also calibrated and disinfected with 95% ethanol before use.

5.3.8 Biomass Analysis

5.3.8.1 Viable Suspended Cell Count

The suspended viable cell concentration was determined according to the spread plate technique outlined in section 9215C of the *standard methods for the examination of water and wastewater* (APHA 1995). The details of the method are described in section 3.3.4.1 (chapter 3).

5.3.8.2 Attached Cell Count

Once steady-state operating conditions were obtained, 6 glass beads each from top and bottom of the reactor were removed under the laminar flow hood (Steril Gard Class II Model, The Baker Company, Stanford, ME). The removed glass beads were then replaced by equal number of fresh sterile ones while keeping the rest of the beads and the liquid undisturbed in the reactor. Each of the removed glass bead was placed inside a 10 mL microreaction vessel containing 1 mL MCSM (without yeast extract) solution. Six glass beads (top and bottom) were used for the determination of viable attached cell count, whereas, the rest were used for protein analysis of the attached cells.

5.3.8.2.1 Viable Attached Cell Count

The glass beads in the tightly closed 10 mL vessels were shaken vigorously in a vortex mixer (Fisher Vortex Genie 2, Fisher Scientific Co, PA) for 5-10 mins to achieve cell detachment. Samples (1.0 mL) from each microreaction vessel were serially diluted in 30-mL test tubes containing 9.0 mL of MCSM (without yeast extract) solution. The

diluted samples of 1.0 mL were then transferred to the solidified agar medium on the agar plates for colony counting.

5.3.8.2.2 Protein Measurement

The vessels containing glass beads for protein analysis were also shaken in a similar manner for the occurrence of cell detachment. Samples (1.0 mL) from each vessel were transferred to 1.5 mL centrifuge tubes (Fisher Scientific Co., Pittsburg, PA). The cell pellet obtained by centrifuging the samples at 10,000 g for 20 mins was then analyzed for protein concentration.

Bradford reagent (Bradford 1976) sample (0.5 mL) was added to the cell pellet in the centrifuge tube and the contents were mixed for 15 s, followed by incubation at room temperature for at least 5 mins. Deionized distilled water (0.5 mL) was then added to the tube and the contents mixed for 5 s and incubated for 30 mins. The absorbance reading of the samples was measured at 594 nm in a spectrophotometer (Spectronic Instrument, Rochester, NY). The true absorbance value of the collected samples was estimated by measuring the difference between the measured and the control (1:1 ratio of Bradford reagent and deionized distilled water) values. The protein concentration in mg/L was then computed using a standard calibration curve obtained by treating different dilutions of bovine serum with Bradford reagent (Sundkvist et al. 2008).

5.4 Basic Biofilm Model

5.4.1 Properties

The physical properties and characteristic concentration profiles of an idealized biofilm (Figure 5.2) are listed as follows:

1. The biofilm has a uniform biomass density X_f ($M_x L^{-3}$).

2. The biofilm is homogenous in nature with a uniform biofilm thickness (L_f) throughout the reactor.

3. The external mass transport resistance is represented by the effective diffusion layer of thickness (L), whereas, the internal mass transport resistance is due to molecular diffusion.

4. The consequence of the mass transport resistance leads to the lowering of the actual bulk As (III) concentration (S) to a value (S_f) inside the biofilm.

5. A deep biofilm is characterized by the substrate concentration approaching zero at a certain point in the biofilm, whereas, in a shallow biofilm, the concentration (S_f) remains above zero at all points in the biofilm matrix.

6. A fully penetrated biofilm is characterized by identical substrate concentrations at the outer (S_s) and attachment (S_w) surfaces.

7. The increase in the biofilm thickness is due to growth of the biofilm itself with attachment from suspended cells negligible.

Diffusion layer   Biofilm

Bulk liquid

X_f,
Biofilm density

L L_f

Fully penetrated

S

Shallow

S   S

Deep

S_s

S_f S_w

z
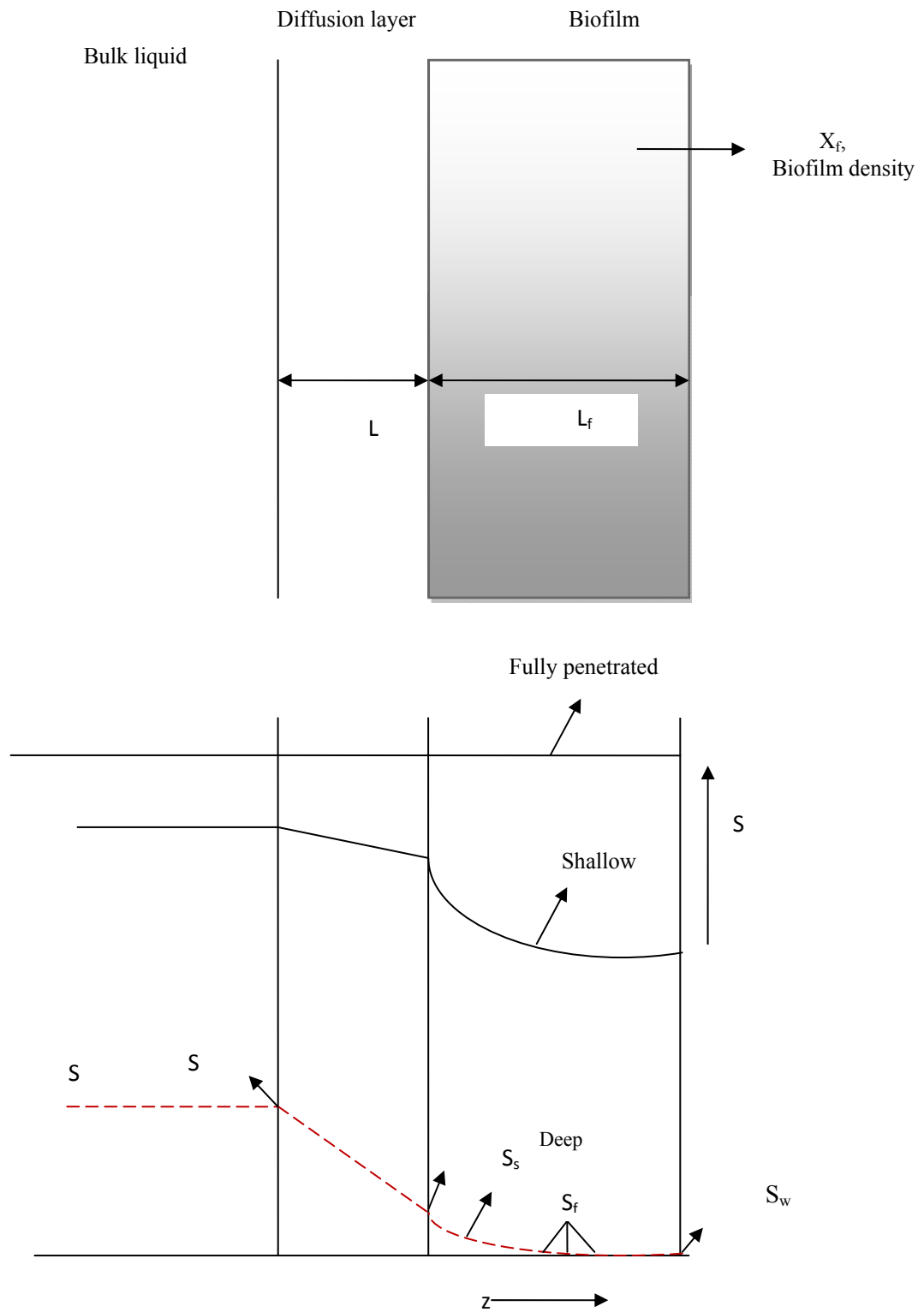
Figure 5.2 Idealized biofilm profile (Rittmann 2001)

5.5 Liquid–Phase Parameters

5.5.1 Effective Diffusivity

The diffusivity of As (III) in water was estimated using the Nernst-Haskell equation (Longsworth, 1972):

$$D_{As(III)} = \frac{RT}{F^2} \cdot \frac{\lambda}{|z|} \tag{5-2}$$

where $D_{As(III)}$ = diffusion coefficient of As (III) in water $(cm^2 s^{-1})$, T = absolute temperature (K), R = universal gas constant (J/mol K), F = Faraday's constant (C g mol), λ = Electrolytic conductance $(cm^2$ ohm c), and $|z|$ is the charge on the ion. The value of electrolytic conductance (λ) was obtained from the table of ionic conductivity and diffusion at infinite dilution (section 5, CRC handbook 2009). As per the CRC handbook guidelines (CRC Handbook 2009 section 5), the listed electrolytic conductance (λ) value at 25°C should be increased by 3% for every 1°C temperature rise in the medium.

5.5.2 Porosity of the Medium Bed

The porosity of the packed bed was estimated using the direct volumetric method:

$$\varepsilon = \frac{V_V}{V_T} \tag{5-3}$$

where V_V is the volume of the void-space in the medium bed, and V_T is the total or bulk volume of the medium bed. The porosity of the medium bed was assumed constant for the purpose of model calculations under different operating conditions.

5.5.3 Absolute Viscosity of Water

The absolute viscosity of water (μ) used for model calculation was obtained at 30°C from the CRC handbook (2009).

5.5.4 Modified Reynolds Number and Schmidt Number

The modified Reynolds number (Re_m) was calculated using the following equation (Jennings 1975):

$$Re_m = \frac{2\rho d_p u}{(1-\varepsilon)\mu} \tag{5-4}$$

where Re_m = the modified Reynolds number, ρ = density of water (g/cm^3), d_p = diameter of the solid medium bed, u = superficial velocity (cm/d), ε = porosity of the medium bed, and μ = absolute viscosity (g/cm-d).

The superficial velocity (u) was estimated according to the following relationship between the feed flow rate and the cross sectional area of the flow stream:

$$u = \frac{Q}{A_c} \tag{5-5}$$

where Q is the feed flow rate to the reactor (cm^3/d), and A_c is the cross sectional area of the flow stream (cm^2). The calculated modified Reynolds number of 1.66 was well within the acceptable limits typical for water ($1 \le Re_m \le 30$) (Rittmann 2001).

The Schmidt number was calculated using the following equation:

$$Sc = \frac{\mu}{\rho D_{As(III)}} \tag{5-6}$$

5.5.5 Effective Diffusion layer

The thickness of the effective diffusion layer (L) or the external mass transfer layer was estimated using the empirical formula reported by Jennings (1975) for porous media:

$$L = \frac{D_{As(III)} (Re_m)^{0.75} Sc^{0.67}}{5.7u} \qquad (5\text{-}7)$$

The thickness value of the effective diffusion layer (L) used for steady-state data analysis was estimated by substituting the other liquid phase parameter coefficients into the Eq. (5-7).

5.5.6 Molecular Diffusivity of As (III) in the biofilm

The molecular diffusivity (D_f) of As (III) in the biofilm was estimated according to Williamson and McCarty (1976) by using the ratio:

$$\frac{D_f}{D_{As(III)}} = 0.8 \qquad (5\text{-}8)$$

5.5.7 Biofilm Specific Surface Area

The biofilm specific surface area was estimated using the following relationship:

$$a = \frac{nA}{V} \qquad (5\text{-}9)$$

where a is the biofilm specific surface area (L^{-1}), n is the number of glass beads in the reactor, A is the surface area of a glass beads (L^2), and V is the empty bed volume of the reactor (L^3).

5.5.8 Biofilm Thickness and Biofilm Density

The biofilm thickness and the biofilm density were computed from the following equations (Rittman et al.1986) assuming biofilm mass to be 99% water by weight:

$$L_f = \frac{W_w}{\rho n A (0.99)} \tag{5-10}$$

$$X_f = \frac{W_d}{A L_f} \tag{5-11}$$

where W_w is the wet weight of the biofilm (M), ρ is the density of water (ML^{-3}), n is the number of glass beads in the packed bed reactor, X_f is the biofilm density (ML^{-3}), and W_d is the biofilm dry weight (M).

5.5.9 Model Inputs for Steady-State Analysis

The parameters listed in Table 5.2 were used as inputs of the predictive flux model for analyzing the steady-state flux data obtained under steady-state conditions.

5.6 Steady-state Analysis

5.6.1 Steady-State Mass Balance on As (III)

The steady-state mass balance on As (III) in the completely mixed packed bed reactor is described by:

$$QS_o - QS_e - J_{exp} a V = 0 \tag{5-12}$$

where Q is the steady-state flow rate ($L^3 T^{-1}$), S_o is the influent As (III) concentration (ML^{-3}), S_e is the effluent As (III) concentration (ML^{-3}), J_{exp} is the observed steady-state As (III) flux ($M/L^2.T$) into the biofilm, a is the biofilm specific surface area (L^{-1}), and V is the reactor volume (L^3).

The steady-state As (III) flux expression calculated from Eq. (5-12) for the various steady-state conditions in the packed bed reactor is given by:

$$J_{exp} = \frac{S_o - S_e}{\tau a} \qquad (5\text{-}13)$$

where τ is the empty bed detention time (T) $= \dfrac{V}{Q}$

5.6.2 As (III) Volumetric Loading Rate

The As (III) volumetric loading rate was calculated based on Eq. (5-14):

$$VL = \frac{QS_o}{V} \qquad (5\text{-}14)$$

where VL is the volumetric As (III) loading rate ($MT^{-1}L^{-3}$), Q is the influent As (III) flow rate to the reactor ($L^3 T^{-1}$), S_o is the influent As (III) concentration (ML^{-3}), and V is the volume of the reactor (L^3).

5.6.3 As (III) Applied Surface Loading Rate

The As (III) applied surface loading rate was estimated using Eq. (5-15) shown below:

$$J_{As(III)} = \frac{QS_o}{M_s (a/M)} \qquad (5\text{-}15)$$

where $J_{As(III)}$ is the mass of As (III) applied per unit of biofilm surface area per unit of time ($ML^{-2}T^{-1}$), M_s is the total mass of glass beads in the reactor (M), and a/m is the surface area per unit mass of the glass beads ($L^2 M^{-1}$).

5.6.4 As (III) Oxidation Rate

The As (III) oxidation rate was evaluated using the following Eq. (5-16):

$$v = \frac{S_o - S_e}{\tau} \qquad (5\text{-}16)$$

where v is the As (III) oxidation rate ($ML^{-3}T^{-1}$), τ is the HRT (T), and S_e is the effluent

As (III) concentration (ML^{-3}).

Table 5.2 Model Inputs for the Steady-State Data Analysis

Parameters	Description	Units	Values
$D_{As(III)}$	Diffusivity coefficient of As (III) in water	cm^2s^{-1}	1.01×10^{-5}
ε	Porosity of the medium bed	------	0.46
μ	Absolute viscosity of water	g/cm.day	689.47
Re_m	Modified Reynolds number	------	1.66
Sc	Schmidt number	-------	785.37
L	Effective diffusion layer thickness	cm	0.012 - 0.019
D_f	Molecular diffusivity	cm^2/day	0.702
a	Biofilm specific surface area	cm^{-1}	13.18
X_f	Biofilm density	mg/cm^3	~10
L_f	Biofilm thickness	cm	0.002 - 0.007

5.6.5 Components of the steady-state biofilm model

A recycle ratio of 50 was used to maintain completely mixed conditions during the bioreactor operation. The influent As (III) concentration S_o at the inlet of the reactor was estimated using the following mass balance equation:

$$S_o = \frac{QS_o + Q_r S_e}{Q + Q_r} \qquad (5\text{-}17)$$

where Q_r is the recycle flow rate (L3T-1).

The As (III) concentration at the biofilm/liquid interface (S_s) (ML-3) was determined from the Fick's first law:

$$S_s = S_e - \frac{L J_{exp}}{D} \qquad (5\text{-}18)$$

where L the thickness of the external mass transfer diffusion layer, S_e is the effluent As (III) concentration (ML^{-1}), and D is the diffusion coefficient of As (III) in water (L^2/ T).

The effectiveness factor (η), "which is the ratio of the actual flux to the flux that would occur in a fully penetrated biofilm" (Rittmann 2001), was estimated using Atkinson's numerical solution to the biofilm model (Atkinson and Davies, 1974):

$$\eta = 1 - (L_f (\frac{kX_f}{K_s D_f})^{-0.5}) \tanh(L_f (\frac{kX_f}{K_s D_f})^{0.5})(\frac{\varphi}{\tanh\varphi} - 1) \ \ \text{If} \ \ \varphi < 1 \qquad (5\text{-}19)$$

$$\eta = \frac{1}{\varphi} - (L_f (\frac{kX_f}{K_s D_f})^{-0.5}) \tanh(L_f (\frac{kX_f}{K_s D_f})^{0.5})(\frac{\varphi}{\tanh\varphi} - 1) \ \ \text{If} \ \ \varphi \geq 1 \qquad (5\text{-}20)$$

The Thiele modulus (φ) was calculated using the following expression (Atkinson and Davies 1974):

$$\varphi = L_f \left(\frac{kX_f}{K_s D_f} \right)^{0.5} \left(1 + \frac{2S_s}{K_s} \right)^{-0.5} \qquad (5\text{-}21)$$

where k is the maximum specific As (III) oxidation rate ($M_s/M_x.T$), K_s is the saturation

constant (ML^{-3}), and D_f is the diffusion coefficient of As (III) in the biofilm (L^2T^{-1}). The

biofilm was considered fully penetrated if η was estimated to be ≈ 1.

5.6.6 Predicted Flux Model and the Optimization Algorithm

The As (III) mass balance for a steady-state concentration profile in the biofilm

can be described as:

$$0 = D_f \frac{d^2 S_{As(III)}}{dz^2} - \frac{kX_f S_{As(III)}}{K_s + S_{As(III)}} \qquad (5\text{-}22)$$

The pseudo-analytical solution of the above equation can be expressed according

to Atkinson and Davies (1974):

$$J_{prAs(III)} = \frac{\eta L_f S_s kX_f}{K_s + S_s} \qquad (5\text{-}23)$$

where $S_{As(III)}$ is the As (III) concentration in the biofilm, and $J_{prAs(III)}$ is the model

predicted As (III) flux in the biofilm. The biomass density (X_f) used in Eq. (5-23) was

calculated from the biomass dry weight (mg VSS). The biokinetic parameters k and K_s

in Eq. (5-23) were estimated using a nonlinear regression analysis with Sigma Plot 10

application software (SPSS Inc). The software uses Marquardt-Levenberg algorithm

(Marquardt 1963) to estimate the optimized value of the parameters by minimizing the

residual sum of squares between the observed flux (Eq. (5-13)) and the predicted flux

(Eq. (5-23)) and is given by the equation:

$$\min \sum_{i=1}^{n} \left(J_{exp,i} - J_{prAs(III),i}(k, K_s) \right)^2 \qquad (5\text{-}24)$$

where n= number of data pairs.

5.6.7 The overall *biofilm-loss coefficient,* b'

The over-all biofilm loss coefficient, b' (T^{-1}) consists of two parts: b (cell decay coefficient) (T^{-1}), and b_{det} (specific biofilm-detachment rate coefficient) (T^{-1}). The decay coefficient b is very similar to the decay coefficient of cells in suspended growth reactor processes. The biofilm-detachment coefficient, b_{det} represents the loss of cells from the attached surface due to tangential shear forces, axial forces (pressure fluctuations), or physical abrasion between the attached surface and the walls of the bioreactor (Rittmann 2001). Rittmann (1982b) developed two separate expressions for the detachment coefficient of biofilms cells from smooth surfaces considering shear stress as the primary force causing the detachment. The first expression is valid for $L_f < 0.003$ cm and is given by:

$$b_{det} = 8.42 \times 10^{-2} \times \sigma^{0.58} \qquad (5\text{-}25)$$

where $\sigma =$ liquid shear stress in units of dyne/cm^2. The shear stress is computed for fixed beds of porous media from the following equation:

$$\sigma = \frac{200 u \mu (1-\varepsilon)^2}{dp^2 \varepsilon^3 a (7.46 \times 10^9)} \qquad (5\text{-}26)$$

where $u =$ superficial liquid velocity (cm/day), $\mu =$ absolute viscosity (g/cm-day), $\varepsilon =$ medium bed porosity, $d_p =$ diameter of the solid medium (cm), and $a =$ specific surface area of the biofilm carrier (1/cm).

The second expression for the biofilm-detachment coefficient was developed for smooth surfaces and is valid for $L_f > 0.003$ cm:

$$b_{det} = 8.42 \times 10^{-2} \left(\frac{\sigma}{1 + 433.2(L_f - 0.003)} \right)^{0.58} \qquad (5\text{-}27)$$

Finally, the overall biofilm-loss coefficient, b' is the sum of b and b_{det}:

$$b' = b_{det} + b \qquad (5\text{-}28)$$

The value of the decay coefficient b was obtained from the CSTR study described in section 4.6.4.1 in chapter 4.

5.6.8 Biofilm yield coefficient (Y)

The biofilm yield coefficient (Y) can be estimated by conducting a mass balance on biomass under steady-state conditions and the overall biofilm-loss coefficient from the following expression (Rittmann 2001):

$$Y = \frac{X_f L_f b'}{J_{exp}} \qquad (5\text{-}29)$$

5.7 Model evaluation and reliability of the parameter estimates

The reliability of the parameter estimates was assessed by the 95% confidence intervals of the evaluated parameters. The 95% confidence intervals were obtained from the standard errors of the estimated parameters. Multiple starting points (different initial estimates of the parameters) were used for the optimization routine to confirm that the parameter values converged to global minima and not local minima.

The coefficient of correlation (R^2) between the predicted $J_{prAs(III)}$ and the observed J_{exp} was obtained using a linear regression analysis plot .Two additional statistical tests were performed on the model calibration: a paired *t*- test and a chi-square goodness-of-fit

test (Schnoor 1996). These two statistical tests were performed to investigate whether the observed and the model predicted As (III) flux were statistically different at the 95% confidence level.

The parameters k and K_s obtained using the data from the first four phases of operation and the non-linear estimation routine were used to predict the steady-state As (III) flux for the remaining three phases of operation. The model validation was essential to establish the uniqueness of the parameter estimates obtained from the non-linear estimation approach.

5.8 Mass Transfer

The effect of mass transfer resistance on the overall biofilm performance was investigated using the dimensionless variable K^*. The variable K^* represents one of the three dimensionless variables used for expressing the pseudo analytical solution of the Eq. (5-22) (Saez and Rittmann 1992):

$$K^* = \frac{D}{L} \sqrt{\frac{K_s}{kX_f D_f}} \qquad (5\text{-}30)$$

The dimensionless variable compares the external mass transport to the maximum substrate utilization rate in the biofilm.

5.9 Growth Potential

The relative importance of cell growth under different operating conditions versus loss of biomass due to decay and detachment was investigated using the dimensionless variable S_{min}^*. High growth potential ($S_{min}^* \ll 1$) indicated that the biomass growth was significantly higher than biomass loss, whereas low growth potential ($S_{min}^* \gg 1$) indicated

that the biomass loss through decay and detachment was significantly higher than cell growth under the various As (III) loading rates. Low growth potential also demonstrated the difficulty of maintaining stable, steady-state biomass in the reactor. S_{min}^{*} was estimated from $\dfrac{S_{min}}{K_{s}}$, whereas S_{min} was calculated using the following equation:

$$S_{min} = \frac{K_{s}b'}{Yk - b'} \qquad (5\text{-}31)$$

In Eq. (5-31), b' is the overall biofilm-loss coefficient, which is the sum of biofilm loss through decay and detachment, and Y is the net bacterial growth yield in the biofilm reactor under the different operating conditions (Saez and Rittmann 1992). Rearrangement of equation (5-31) yields the following expression for growth potential S_{min}^{*}:

$$S_{min}^{*} = \frac{1}{\dfrac{Yk}{b'} - 1} \qquad (5\text{-}32)$$

A mass balance analysis on active biomass at any position inside the biofilm can be written as:

$$\frac{d(X_{f}dz)}{dt} = Y\frac{kS_{As(III)}}{Ks + S_{As(III)}}(X_{f}dz) - b'X_{f}dz \qquad (5\text{-}33)$$

where dz is the thickness of a differential section of biofilm (L).

When steady-state operating conditions were obtained, the biomass per unit surface area ($X_{f}L_{f}$) was constant in time even though biomass at any one location may not be at

144

steady-state. The concept can be expressed by setting the integrated form of Eq. (5-33) for the entire biofilm thickness equal to zero:

$$0 = \int_0^{L_f} \frac{d(X_f dz)}{dt} = \int_0^{L_f} Y \frac{kS_{As(III)}}{K_s + S_{As(III)}} X_f dz - \int_0^{L_f} b' X_f dz \qquad (5\text{-}34)$$

The total reaction rates per unit area of biofilm may be represented by the integral of $r_{ut} dz$, while the integral ($r_{ut} dz$) equals to the flux of As (III) into the biofilm, and the multiplication of the same integral by the yield coefficient (Y) gives the growth rate per unit surface area:

$$\int_0^{L_f} Y \frac{kS_{As(III)}}{K_s + S_{As(III)}} X_f dz = Y \int_0^{L_f} (-r_{ut}) dz = YJ_{exp} \qquad (5\text{-}35)$$

The biomass loss averaged across the biofilm is represented by:

$$\int_0^{L_f} b' X_f dz = b' X_f L_f \qquad (5\text{-}36)$$

According to the fundamental law of steady-state biofilm, the growth of new biomass per unit surface area (YJ_{exp}) is balanced by biofilm loses per unit area ($b'X_f L_f$) and the resulting expression is given by the following equation (Rittmann 2001):

$$X_f L_f = \frac{J_{exp} Y}{b'} \qquad (5\text{-}37)$$

Substituting Eq. (5-35) into Eq. (5-30) gives us the final expression of the growth potential:

$$S_{min}^* = \frac{1}{\dfrac{X_f L_f k}{J_{exp}} - 1} \qquad (5\text{-}38)$$

145

5.10 Results and Discussion

5.10.1 Tracer study

The data in Figure 5.3 clearly show that tracer response curves generated at a $Qr / Q = 50$ using As (III) and methylene blue matched well with the ideal completely mixed characteristic curve. The difference between the observed data and the ideal tracer response curve was statistically insignificant at the 95% confidence level ($\alpha = 0.05$) for both As (III) ($p = 0.34$), and methylene blue ($p = 0.87$), respectively.

The completely mixed regime in the reactor was also investigated at a recycle ratio of 13.1 under the same HRT of 0.48 day using As (III) as the tracer as shown in Figure 5.3. The agreement between the observed data and the tracer response curve was not very good with the difference statistically significant ($p = 0.01$) at the 95% confidence level.

The results of the study conclusively proved that operation of the biofilm reactor at a recycle ratio of 50 would ensure completely mixed conditions under the different As (III) loading rates.
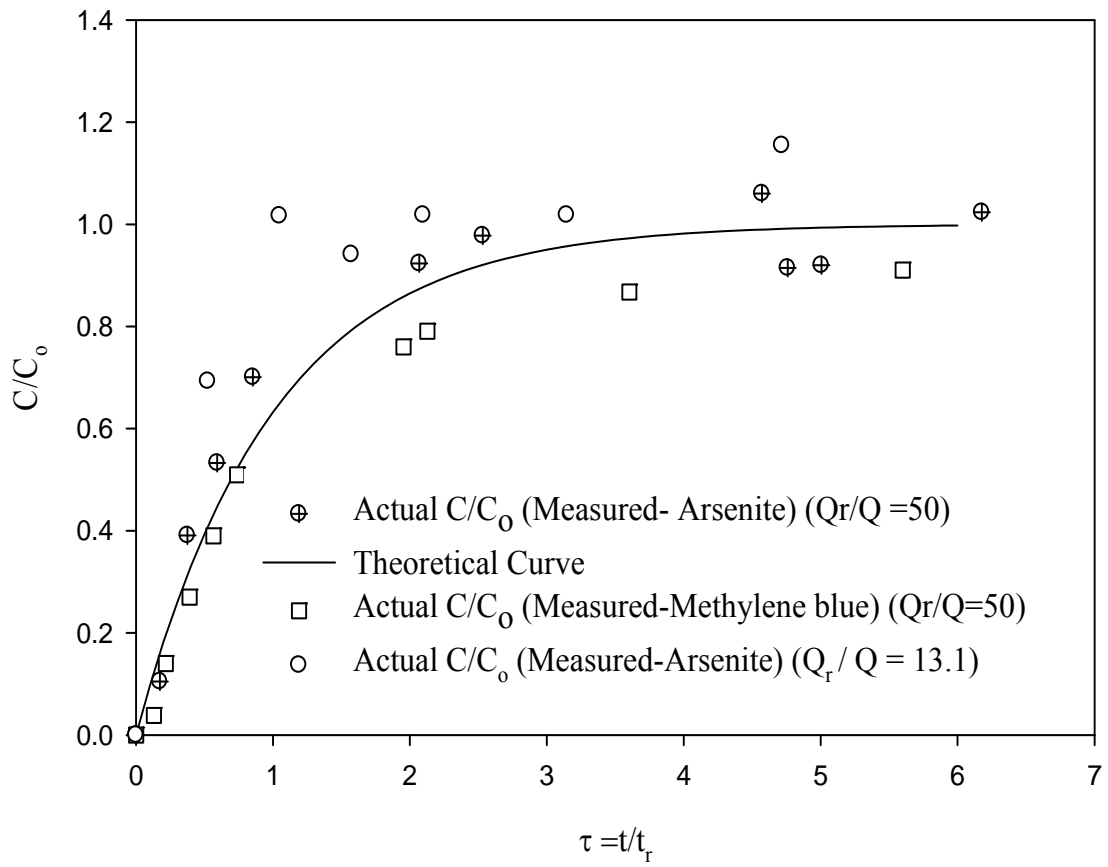
Figure 5.3 Tracer study to determine the optimum recycle rate

5.10.2 Chemical Control Experiment

The reactor was operated under an influent As (III) concentration of 100 mg/L and a HRT of 1 day to investigate whether abiotic mechanisms such as adsorption and chemical oxidation are significant in the bioreactor. Figure 5.4 showed that the measured influent and effluent As (III) levels in the reactor were statistically insignificant ($p = 0.37$). The arsenic analyses also included measurement of As (V) in the effluent from the reactor. The As (V) concentrations measured at different time intervals were below its corresponding method detection limit (MDL) of 1 mg/L. The results of the control experiment clearly demonstrated that abiotic As (III) oxidation to As (V) was not significant in the fixed-film bioreactor.

5.10.3 Performance Analysis of the Biofilm Reactor

Phase I (Days 1-9): Once cell attachment was established on the glass beads, the biofilm reactor was operated under an influent As (III) concentration of 500 mg/L and a HRT of 1day at pH of 5.2 ± 0.1 and DO of 2.8 ± 0.1 mg/L during this phase of operation (Table 5.3). The average steady-state effluent As (III) and As (V) levels measured at 3.2 ± 0.2 mg/L, and 452.6 ± 5.4 mg/L, respectively (Table 5.3). The measured steady-state viable cell count was $2.17 \times 10^8 \pm 2.64 \times 10^7$ cfu / bead, and the total biomass dry weight calculated using the conversion factor of 6.604×10^{-8} mg dry weight/ L. cells was 63.78 ± 5.18 mg VSS, respectively (chapter 3 section 3.3.4.2). Under the phase I operating conditions, the reactor was highly efficient in converting nearly all the As (III) (99.3%) fed to the reactor to As (V).
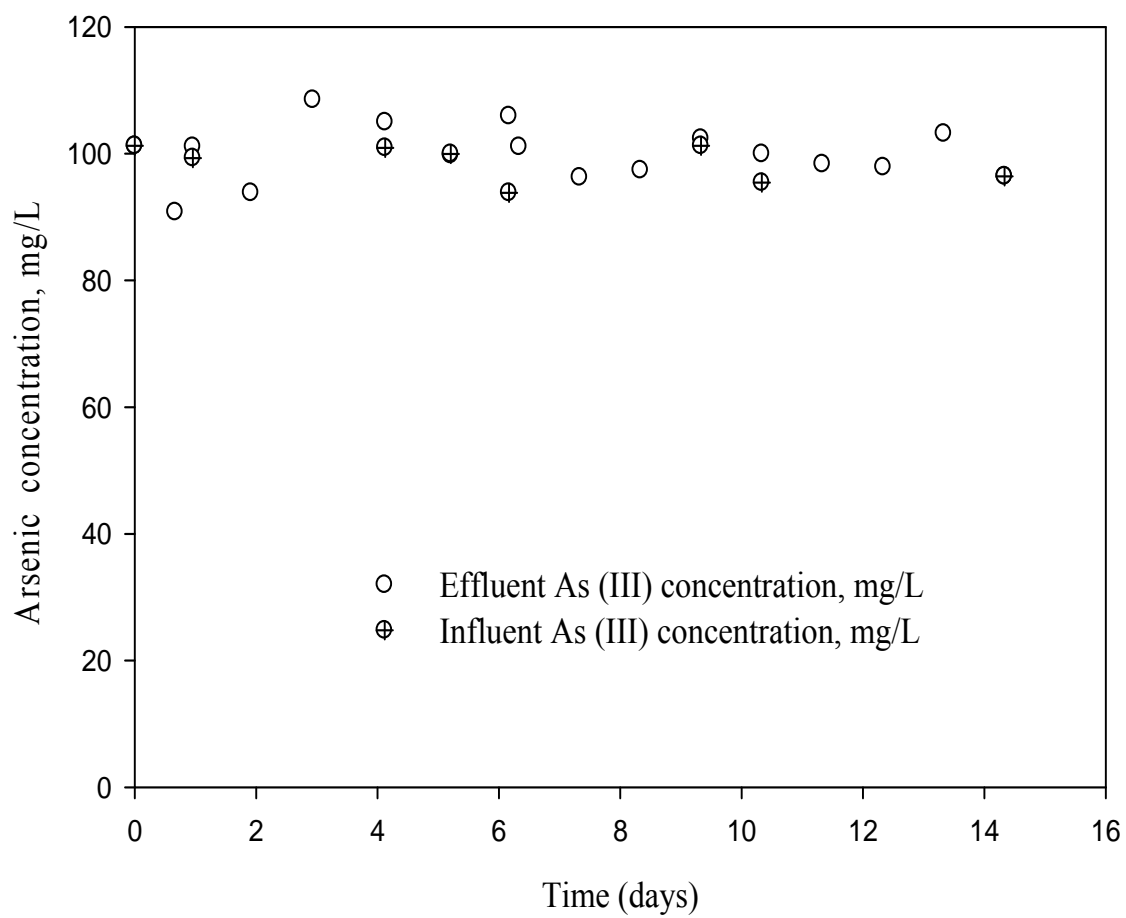
Figure 5.4 Control study for As (III) oxidation in the Biofilm reactor

Phase II (Days 9-36): The operating conditions for this phase were the same as phase I, except that an additional source of carbon in the form of sodium bicarbonate ($NaHCO_3$) was added to the feed MCSM medium. Such high level (500 ppm) of $NaHCO_3$ was added to the feed solution in order to investigate whether As (III) oxidation was limited by the carbon source.

The measured average steady-state effluent As (III) level (2.76 ± 0.33 mg/L) in this phase did not differ significantly ($p = 0.3$) as compared to the effluent As (III) level of 3.2 ± 0.2 mg/L obtained in phase I (Table 5.3) at the 95% confidence level ($\alpha = 0.05$). A pH of 5.5 ± 0.3 was maintained, whereas, an average of DO of 2.5 ± 0.2 mg/L was recorded during the steady-state condition (Table 5.1). The As (III) oxidation efficiency (99.4%) of the reactor in this phase was similar to the 99.3% efficiency obtained in phase I. In addition, difference between the computed attached biomass values (68.69 ± 7.42 mg VSS; 63.77±5.18 mg VSS) obtained in phases II and I were statistically insignificant ($p = 0.22$) at the 95% confidence level. This observation was also validated by the minimal increase (17 -20%) in the measured protein concentration values (3.2 ± 1.1 mg; 4 ± 1.2 mg) from phases I and II.

The reactor performance was slightly affected by unstable operating conditions occurred during days 13 to 16 due to a significant biological growth in the feed bottle. This lead to clogging of the reactor and pump tubings and lowering of the influent As (III) concentration to the biofilm reactor. These problems were corrected on day 14 by feeding the reactor with freshly prepared medium and replacing the contaminated tubings.

Phase III (Days 36-62): To evaluate the performance of the packed-bed reactor at a higher As (III) loading rate (1008.9 ± 22.14 mg As (III) /L.day), the HRT was decreased from 1.0 to 0.5 day while maintaining the influent As (III) concentration at 500 mg/L (Table 5.1). The response of the reactor to such a higher volumetric loading rate was characterized by steep increase in the effluent As (III) level to 83.51 mg/L (Figure 5.5) before subsiding to stable effluent level of 10.25 ± 0.58 mg/L (Table 5.3).

To ensure that DO was not limiting for As (III) oxidation, the feed reservoir was aerated by compressed air in the phase. The effluent DO measured at 3.1 ± 0.1 mg/L, whereas the pH measured at 5.1±0.3, respectively. The introduction of the aeration line in the reservoir had insignificant effect on the effluent As (III) level, and the biomass growth, respectively. The computed biomass value was 73.11 ± 8.75 mg VSS, whereas the corresponding attached viable cell count measured at 2.59 x 10^8 ± 4.45x10^7 cfu / bead, respectively (Table 5.4). The percentage increase in biomass in phase III compared to phase II was minimal (6.4%). However, the measured protein concentration showed significant increase from phase II to III (Table 5.5). This may be because of accumulation of dead cells on the attached surface giving a higher total protein concentration reading. The bioreactor still exhibited high As (III) oxidation efficiency (97.9%) under the high volumetric As (III) loading rate employed for this phase.

Phase IV (Days 62-78): The As (III) loading rate in this phase was increased to 2580.6 ± 123.24 mg/L.day by decreasing the HRT to 0.2 day under the same nominal influent As (III) concentration of 500 mg/L. The effluent As (III) concentration increased to 229.11 mg/L (Figure 5.5) before decreased to an average steady-state effluent As (III) level of 64.1±3.8 mg/L, respectively. The data in Table 5.3 also indicate that the biofilm

reactor was always operated in the high load region as characterized by increase in the effluent As (III) levels with increase in the As (III) loading rates (Heath et al. 1992). pH was maintained at 5.3 ± 0.1, whereas as the measured steady-state DO level decreased by only 2.25% compared to phase III (Table 5.1).

The steady-state attached biomass concentration of 75.9 ± 12.6 mg VSS was statistically insignificant ($p = 0.66$) compared to the phase III steady-state biomass concentration (73.11 ± 8.75 mg VSS).The statistical analysis was also supported by the measured viable cell count of $2.7 \times 10^8 \pm 6.4 \times 10^7$ cfu / bead, which was very close to the measured value in phase III. However, the protein concentration increased by 27.7% from phase III to IV of operation (Table 5.5). In addition, the As (III) oxidation efficiency of the reactor dropped from 97.9% (phase III) to 87.5% in this phase, suggesting As (III) inhibition on the biological growth of the cells under such high As (III) loading rate.

Phase V (Days 78-80): In this phase, the As (III) loading rate was further increased to 5295.4 ± 376.8 mg As (III) / L·day by increasing the influent As (III) concentration from 500 mg/L to 1000 mg/L under the same HRT of 0.2 day. However, within one day of operation, the effluent As (III) level quickly increased to 845.82 mg/L which was very close to the influent As (III) concentration (1000.1 ± 74.6 mg/L) (Figure 5.5). This breakthrough of As (III) was the result of As (III) overloading. Biomass concentration, pH, and DO were not measured during the failure phase of the reactor.

Phase VI (Days 80-97): In order to test the resilience of the biofilm reactor, the HRT was increased to 1.0 day on day 80 while maintaining the same influent As (III) concentration at 1000 mg/L. The bioreactor system recovered completely on day 96 with effluent As (III) level at 13.1 ± 0.4 mg/L and an As (III) oxidation efficiency of 98.7%

(Table 5.3). The steady-state biomass concentration measured at 24.2 ± 0.9 mg VSS representing a reduction of 68.1% from its previous steady-state level observed in phase IV. The protein concentration also dropped almost 42% from its previous steady-state measured level (Table 5.4). Significant loss of biomass may have occurred through detachment due to high shear force under the increased flow rate (0.42 L/day) in phase V. The DO level (1.9 ± 0.1 mg/L), however, did not change significantly as compared to its level in phase IV (Table 5.1). pH was maintained at 5.1 ± 0.4 during this phase of operation.

Phase VII (Days 97-120): Once the recovery phase was complete, the reactor was then operated under an influent As (III) concentration of 2,000 mg/L at a HRT of 1 day. The effluent As (III) level rose to 1343.6 mg/L (Figure 5.5) under the current As (III) loading rate of 2208.6 ± 79.09 mg As (III) / L·day, before reaching a steady-state effluent As (III) concentration of 153.8 ± 23.8 mg/L in the reactor (Table 5.3). The data in Figure 5.5 may also indicate that As (III) oxidation rate was independent of the influent As (III) concentration (zero order process) under such high As (III) level in the reactor. This kind of growth situation ($\mu = \mu_m$) is very unlikely but is one of the limiting cases ($S \gg K_s$) following the Monod expression (Maier 2009). The high level of steady-state effluent As (III) in the bioreactor may indicate As (III) inhibition on the biological growth of the cells of strain b6. The inhibition may limit enzyme production required for As (III) binding and consequent oxidation to As (V).

There was a minimal drop in the DO level in the reactor from its previous steady-state level (Table 5.1). pH was maintained fairly constant at 5.1 ± 0.3 with the As (III) oxidation efficiency measuring at 93.1 %. The steady-state viable cell count and the

computed biomass dry weight were $1.35 \times 10^6 \pm 4.8 \times 10^5$ cells / bead, and 22.43 ± 0.1 mg VSS, respectively (Table 5.4).

Phase VIII (Days 120-137): In order to assess the operating range of the influent As (III) level in the reactor, the As (III) loading rate was further increased to 4145.9 ± 98.47 mg As (III) / L·day by increasing the influent As (III) concentration to 4,000 mg/L under the same HRT (1.0 day). The effluent As (III) level quickly rose to 1893.80 mg/L within a day of the new operating condition (Figure 5.5). However, the effluent As (III) concentration subsided and stabilized around a high level of 2147.4 ± 174.1 mg/L. This may be due to insufficient DO (1.5 ± 0.1 mg/L) or As (III) inhibition towards biological activities in the reactor. However, the amount of As (III) oxidized in this phase of operation was almost the same as that in the previous phase, indicating consistent performance of the bioreactor. The biological activity of the cell was clearly inhibited by the high level of As (III) toxicity as observed in the measured steady-state cell concentration ($2.5 \times 10^5 \pm 2.2 \times 10^5$ cells /bead). The computed steady-state biomass level remained almost the same (22.21 ± 0.04 mg VSS) compared to its level in phase VII (Table 5.4). The protein concentration also registered a net drop of 54.4% from phase VI through phase VIII (Table 5.5). This extremely high As (III) loading rate also resulted in the reduction of the steady-state As (III) oxidation efficiency to 48.2%.

5.10.4 As (III) Oxidation Efficiency of the Biofilm Reactor

The As (III) oxidation efficiency of the biofilm reactor ranged from 97.9 to 99.3% for the first three phases of the reactor operation (Figure 5.6). The efficiency of the reactor dropped to 87.9% under an increased As (III) loading rate of 2580.6 ± 123.24 mg/L.day in phase IV. Once the culture recovered from an As (III) overloading of 5295.4

± 376.78 mg /L.day (phase V), the oxidation efficiency of the bioreactor measured at 98.7% (phase VI), and 93.1% (phase VII) under the corresponding As (III) loading rates of 999.9 ± 34.85 mg/L.day, and 2208.6 ± 79.2 mg /L.day, respectively (Figure 5.6). However, the As (III) oxidation efficiency of the biofilm reactor dropped to 48.3% under an As (III) loading rate of 4145.9 ± 98.47 mg/L.day (phase VIII). This lowering of the oxidation efficiency could be attributed to insufficient DO or the inhibition of biological growth by such high influent As (III) level of 4146.3 ± 98.6 mg/L (Table 5.3).

5.10.5 As (III) Oxidation Rates versus As (III) loading Rates

The data in Figure 5.7 clearly showed the increase of the As (III) oxidation rate in the biofilm reactor with increase in the As (III) loading rate for the first four phases of reactor operation. Although the As (III) oxidation efficiency in phase IV was lower compared to the previous three phases, the As (III) oxidation rate reached a maximum of 2229.75 mg As (III)/day.L under the critical As (III) loading rate of 2580.6 ± 123.24 mg/L.day (Figure 5.7). The oxidation rate dropped significantly during an As (III) overloading in phase V. For the last two phases (VII and VIII), the As (III) oxidation rates were very similar measuring at 2054.19 and 1998.58 mg As (III)/day.L respectively (Figure 5.7).

Table 5.3 Fixed-film bioreactor steady-state performance data

Phase	Duration (days)	HRT (Hrs)	pH	Influent As (III) mg/L	Effluent As (III) mg/L	As (III) loading rate mg/L.day	As (III) surface loading rate $(mg/m^2.day)$	Effluent As (V) mg/L	DO mg/L	Average As (III) oxidation %
I	1-9	24	5.2±0.1	473.2±29.3	3.17±0.24	473.2 ±29.26	472.5±29.3	452.6±5.4	2.8±0.1	99.3
II	9-36	24	5.5±0.3	466±24.4	2.8±0.3	465.9 ± 24.36	465.3±24.4	437.1±20.6	2.5±0.2	99.4
III	36-62	12	5.1±0.3	489.5±10.7	10.3±0.6	1008.9 ± 22.14	1005.1±22	441.8±29.2	3.1±0.1[b]	97.9
IV	62-78	5	5.3±0.1	510.7±24.4	64.1±3.8	2580.6 ± 123.24	2535.2±121.4	411.6±4.9	2.4±0.2	87.5
V	78-80	5	-----[a]	1000.08±74.6	------[a]	5295.4 ± 376.78	4963.6±371	------[a]	-----[a]	------[a]
VI	80-97	24	5.1±0.4	1000±34.9	13.1±0.4	999.9 ± 34.85	998.4±34.8	871.4±17.1	1.9±0.1	98.7
VII	97-120	24	5.1±0.3	2208.8±79.2	153.8±23.8	2208.6 ± 79.09	2205.3±79.1	1694.2±80	1.5±0.1	93.1
VIII	120-137	24	5.1±0.2	4146.3±98.6	2147.4±174.1	4145.9 ± 98.47	4139.8±98.4	1910.6±198.3	1.2±0.1	48.2
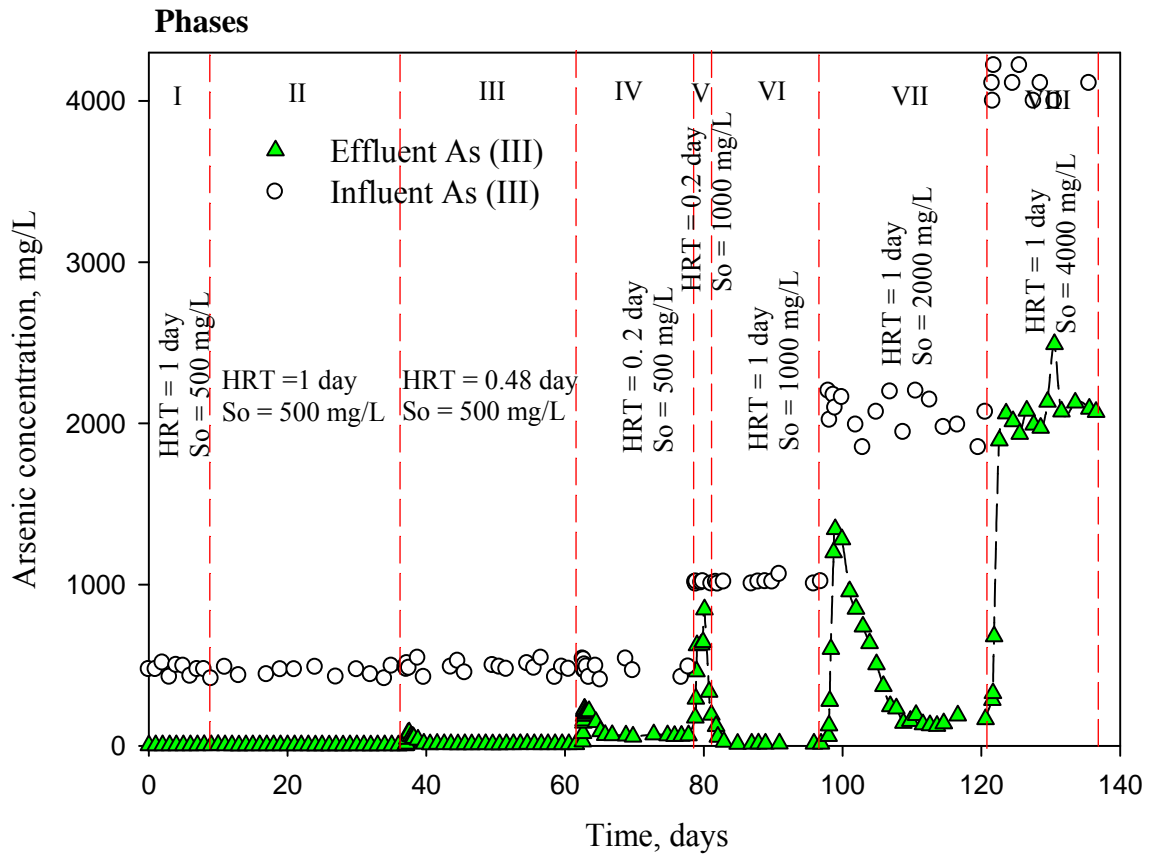
Figure 5.5 As (III) oxidation in the biofilm reactor system by the chemoautotrophic strain *T.arsenivorans* b6

Table 5.4 Steady-state biomass distribution in the packed bed reactor

Phase	As (III) loading rate $(mg/m^2.day)$	Viable suspended cell count (no in the reactor)	Total suspended cells in reactor $(mg\ VSS)^b$	Viable attached cell count (no in the reactor)	Total attached cells in the reactor $(mg)^b$
I	472.5±29.3	2.1×10^8	0.42	$6.3 \times 10^{11} \pm 7.91 \times 10^{10}$	63.7±5.2
II	465.3±24.4	4.1×10^8	0.7	$7.02 \times 10^{11} \pm 1.1 \times 10^{11}$	68.7±7.4
III	1005.1±22	9.6×10^8	1.42	$7.7 \times 10^{11} \pm 1.3 \times 10^{11}$	73.1±8.7
IV	2535.2±121.4	2.8×10^9	3.84	$8 \times 10^{11} \pm 1.9 \times 10^{11}$	75.9±12.6
V	4963.6±371	--------[a]	-------[a]	--------[a]	--------[a]
VI	998.4±34.8	3.7×10^8	0.6	$3 \times 10^{10} \pm 1.4 \times 10^{10}$	24.2±0.9
VII	2205.3±79.1	7×10^6	0.16	$4.1 \times 10^9 \pm 1.3 \times 10^9$	22.4±0.4
VIII	4139.8±98.4	4×10^5	0.15	$7.4 \times 10^8 \pm 6.6 \times 10^8$	22.2±0.1

-------[a] values not available since stead-state not achieved.

[b] values obtained using a correlation coefficient of $6.604 \times 10^{-8} + 7.445$ mg dry weight /L.cells ($R^2 = 0.90$)

Table 5.5 steady-state biomass distribution in the
pure culture bioreactor

Phase	As (III) loading rate (mg/L.day)	Total suspended cells in reactor (μg protein) [b]	Viable suspended cell count (No. in the Reactor)	Total attached cells in the Reactor (mg protein) [1b]	Viable attached count /bead (No. in Reactor) [1]
I	472.5±29.3	24.1 ± 4.6	2.1×10^8	3.2 ± 1.1	1.7×10^8
II	465.9±24.4	22.4 ± 4.4	4.1×10^8	4 ± 1.2	2.3×10^8
III	1008.9±22.1	19.8 ± 3.4	9.6×10^8	8.3 ± 0.5	3.4×10^8
IV	2580.6±123.2	20.5 ± 3.8	2.8×10^9	10.6 ± 1.3	3.6×10^8
V	5295.4 ± 376.8	------[a]	------[a]	------[a]	------[a]
VI	999.8 ± 34.8	18.5 ± 2.4	3.7×10^8	5.7 ± 0.9	6×10^6
VII	2208.6 ± 79.2	10.3 ± 2.5	7×10^6	3.1 ± 0.6	4×10^5
VIII	4149.5 ± 98.5	10.6± 3.1	4×10^5	2.6 ± 0.6	5×10^5

[a]   No steady state value obtained
        precision given as standard
[b]   deviation

[1]   number of samples N (2 locations x 6 beads top &
        bottom) = 12
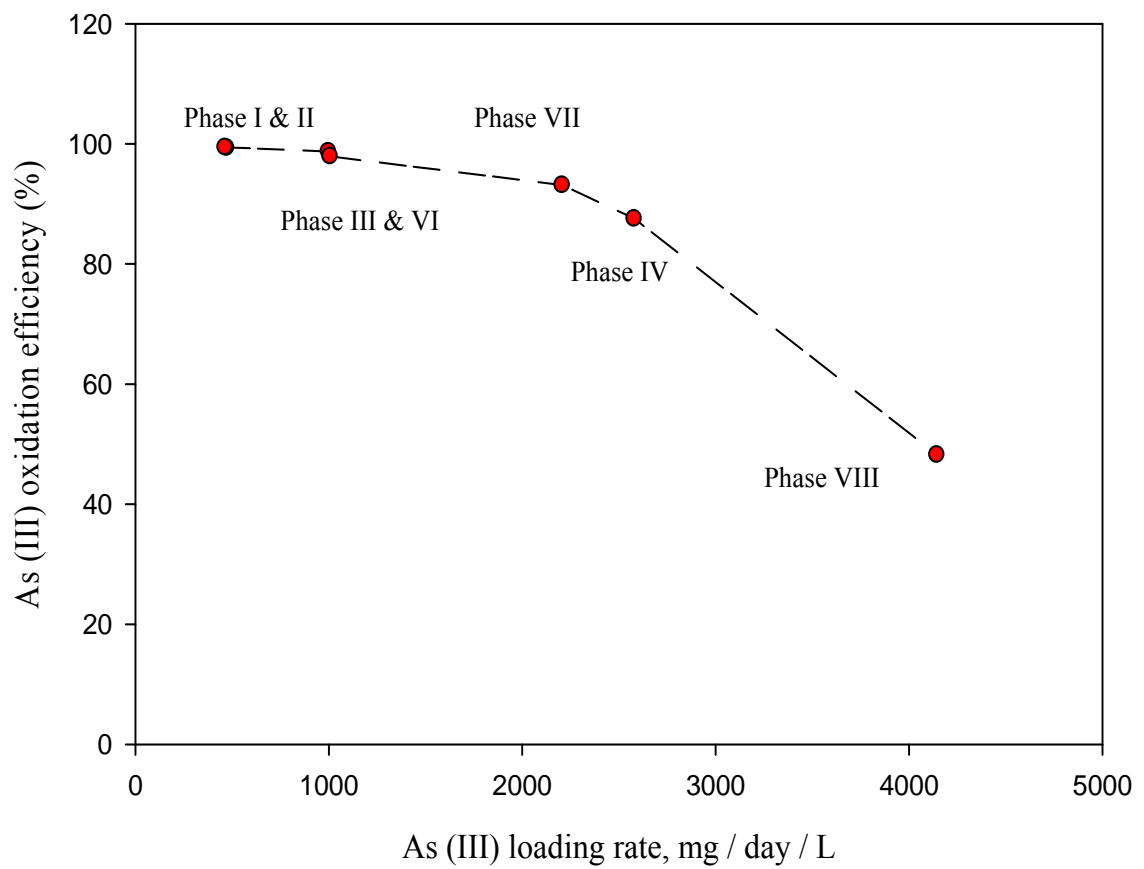
Figure 5.6 Plot of As (III) oxidation efficiency of the biofilm reactor versus varying As (III) loading rates.
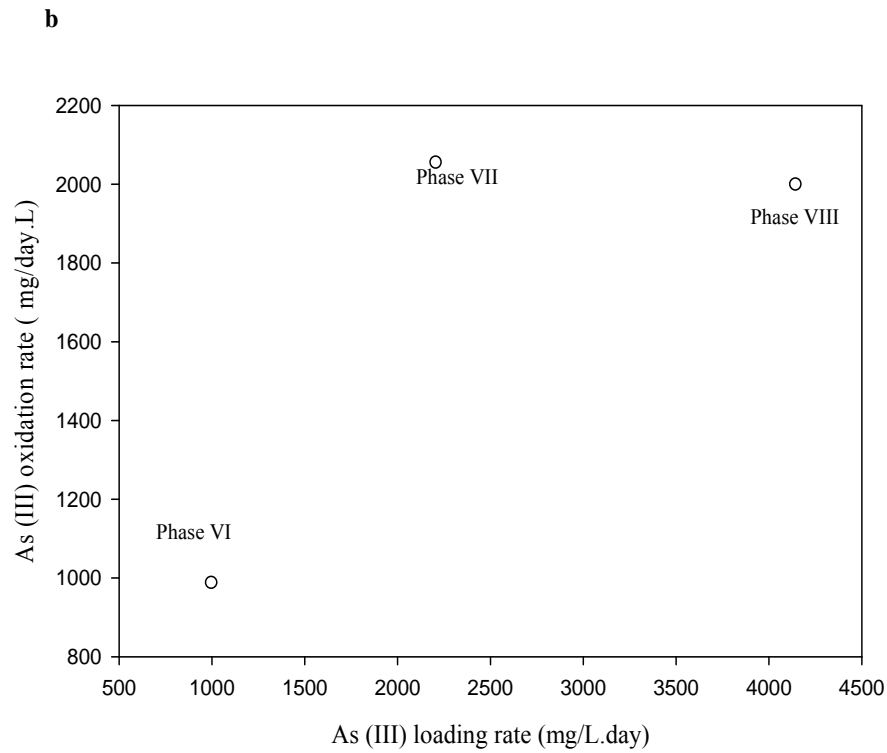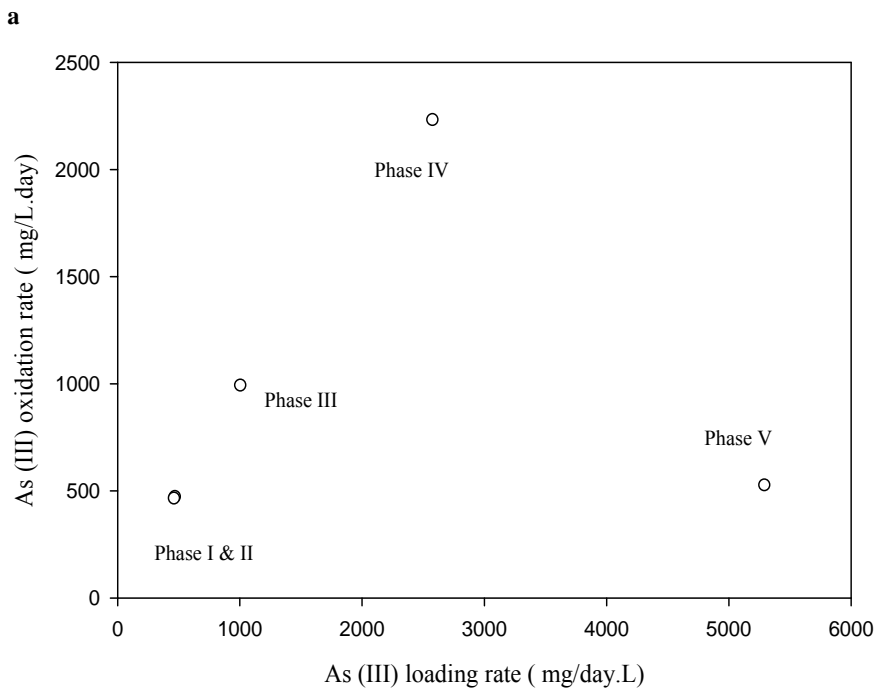
Figure 5.7 Plot of As (III) oxidation rates versus As (III) loading rates a) phase I-V, b) phase VI-VIII.

5.10.6 Arsenic Mass Balance

An arsenic mass balance analysis was performed over the biofilm reactor to analyze the fate of As (III) in the bioreactor. Cumulative values of influent As (III), effluent As (III), effluent As (V), and sum of effluent As (III) and As (V) was plotted (Figure 5.8) for the entire operation of the biofilm reactor. The difference between the cumulative influent As (III) and sum of cumulative effluent As (III) and As (V) was only 4%. The difference was within the acceptable analytical error of ±15% indicating that the loss of arsenic by means of adsorption and precipitation can be ignored. Furthermore, the data in Figure 5.6 and 5.7 clearly show a very good correlation (R^2= 0.99, R^2= 0.99) between the measured cumulative effluent total As and influent As (III) versus the sum of cumulative effluent As (III) and As (V). This mass balance analysis suggested that nearly all the As (III) was oxidized to As (V) in the biofilm reactor.

5.10.7 Oxygen Uptake

The chemoautotrophic bacteria *T. arsenivorans* strain b6 utilizes O_2 as an electron acceptor in the oxidation As (III) to As (V) (Battaglia-Brunet et al 2006). The strain b6 exhibits growth by using CO_2 (source of carbon) and energy released from the oxidation process for cell synthesis (Bryan et al. 2009). Therefore, the utilization rate of O_2 is an indicator of the biological activity of the strain b6 in the biofilm reactor. The theoretical oxygen demand for As (III) oxidation can be determined from the following stoichiometric relationship:

$$H_3AsO_3 + 0.5O_2 \xrightarrow{T.arsenivorans \text{ strain b6}} 0.5HAsO_4^{2-} + 0.5H_2AsO_4^- + 1.5H^+ \quad (5\text{-}39)$$
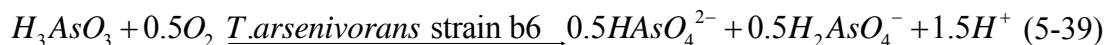
According to Eq. (5-39), one mole of As (III) requires 0.5 moles of O_2 for the complete oxidation of As (III) to As (V). The cumulative theoretical oxygen demand was

calculated based on the difference between the influent and effluent As (III) level and the feed flow rate to the reactor, and then compared to the measured cumulative oxygen demand for each phase as shown in Figures 5.11 and 5.12 respectively.

The cumulative theoretical oxygen demand was almost 19.8 ± 2.1 times higher than the measured oxygen consumption for the first four phases of operation (Table 5.6). However, this difference in the oxygen demand widened by factors ranging from 31 in (phase VI) to 51 (phase VIII).

The difference could be attributed to sulfate (SO_4^{2-}) acting as an electron acceptor during As (III) oxidation to As (V) under slightly anaerobic conditions according to the following equation:

$$4\ AsO_3^{3-} + SO_4^{2-} + 2H^+ \rightarrow 4\ AsO_4^{3-} + H_2S \qquad (5\text{-}40)$$

The study conducted by Battaglia-Brunet et al (2006) showed the absence of any growth of the *T.arsenivorans* strain b6 in the presence of nitrate (NO_3^-). However, the possibility of nitrate being used as a complement in the presence of oxygen has not been previously investigated, and nitrate content was not measured during the biofilm reactor operation. Another possibility is the simultaneous use of sulfate and oxygen as electron acceptors during As (III) oxidation. The possibility of multiple electron acceptors and one single electron donor during biodegradation process was previously demonstrated by Curtis (2003).

The pathway and oxidation of As (III) in the enzyme arsenite oxidase with the subsequent release of As (V) was shown in a study conducted by Mukhopadhyay et al. (2002). As (III) oxidation is followed by the release of 2 electrons which eventually reaches oxygen (electron acceptor) at the end of the respiratory chain via several

intermediates. The distance between the [3Fe-4S] HiPIP center and the [2Fe-2S] center is comparable enough to need the service of these intermediates for the transfer of electrons (Mukhopadhyay et al. 2002). The intermediates consist of hydrogen bonds with amino acids and/or water molecules. The final transfer of electrons to the first coupling protein of the aerobic respiratory chain may be severely affected / inhibited by these intermediates (Silver and Phung 2005). The disruption in the flow of electrons may result in higher DO in the effluent of the reactor because of inadequate production of water as a result of lower rate of reduction of the oxygen molecule.

The potential reason behind the large difference between the theoretical and actual oxygen demand cannot be exactly ascertained without further studies. Future research can focus on the simultaneous use of multiple electron acceptors during As (III) oxidation process or the bacterial choice of electron acceptor during anaerobic conditions in the bioreactor operation.

	Influent As (III)
⊕	Effluent As (III)
▣	Sum of cumulative effluent As (III) and As (V)
◈	Effluent As (V)
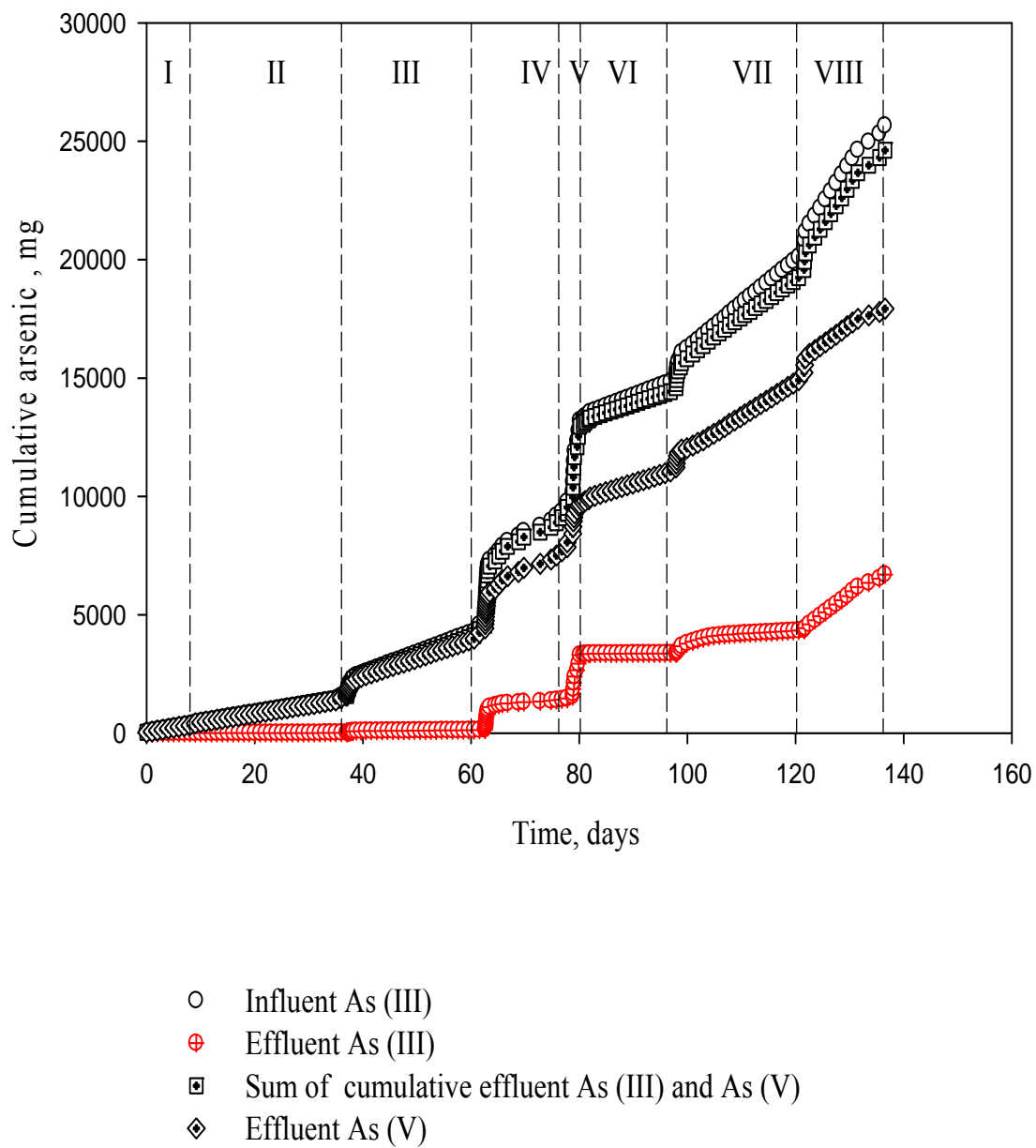
Figure 5.8 Arsenic mass balance in the biofilm reactor system
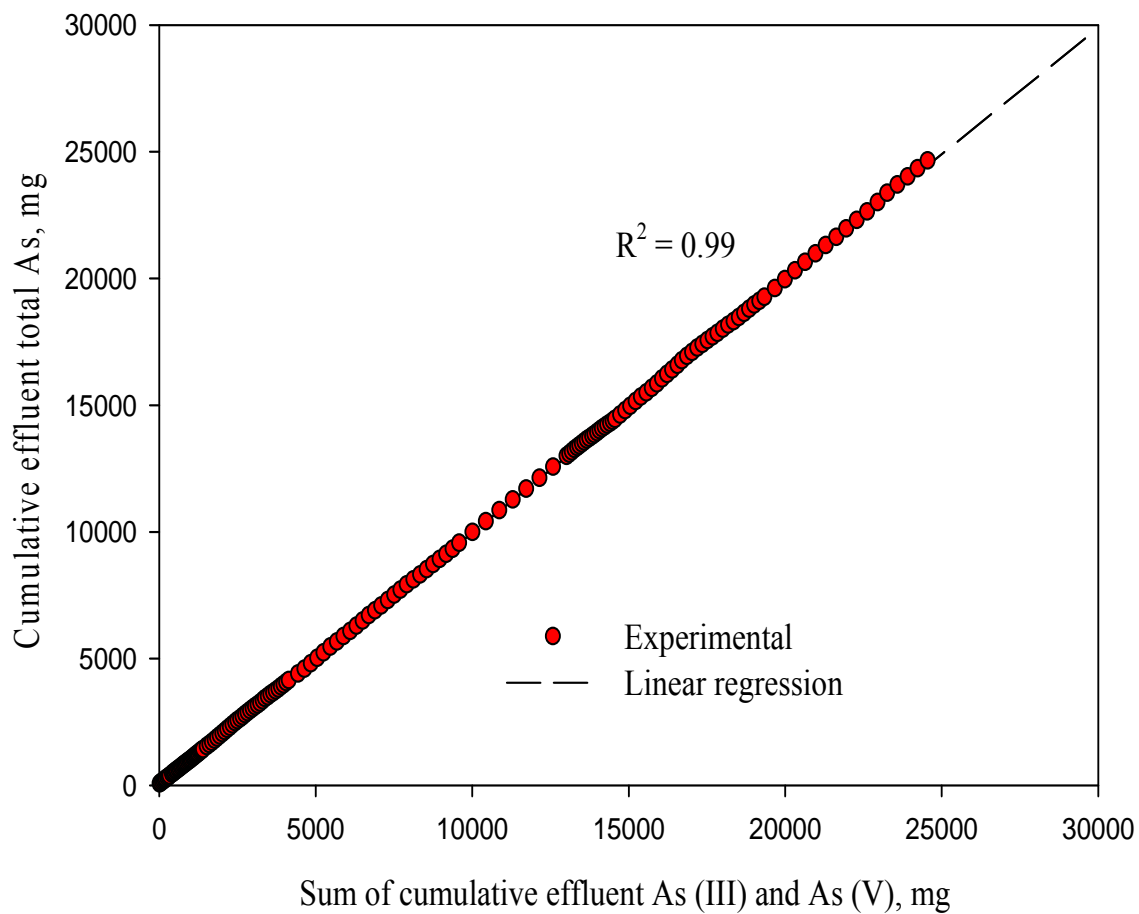
Figure 5.9 Comparison of effluent total As versus sum of cumulative effluent As (III) and As (V)
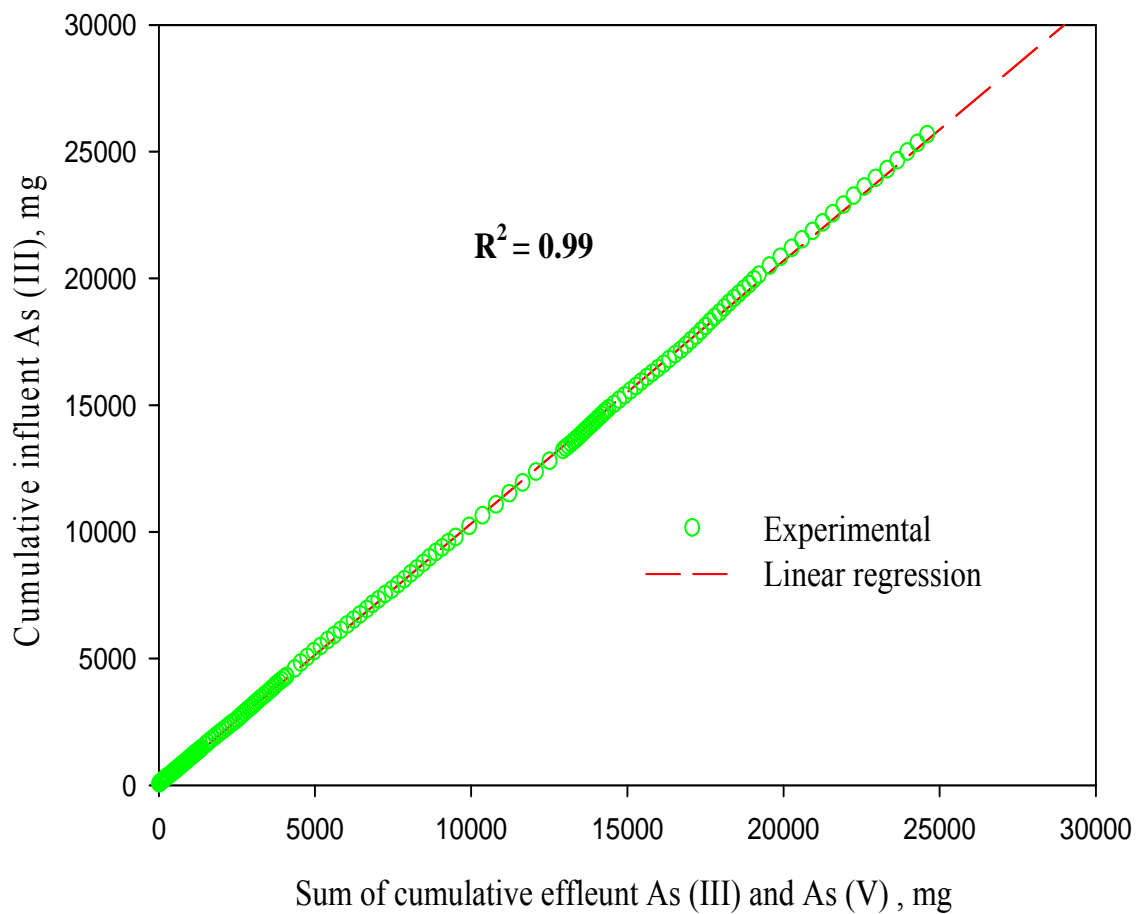
Figure 5.10 A comparison of the cumulative influent As (III) versus sum of cumulative effluent As (III) and As (V) in the biofilm bioreactor
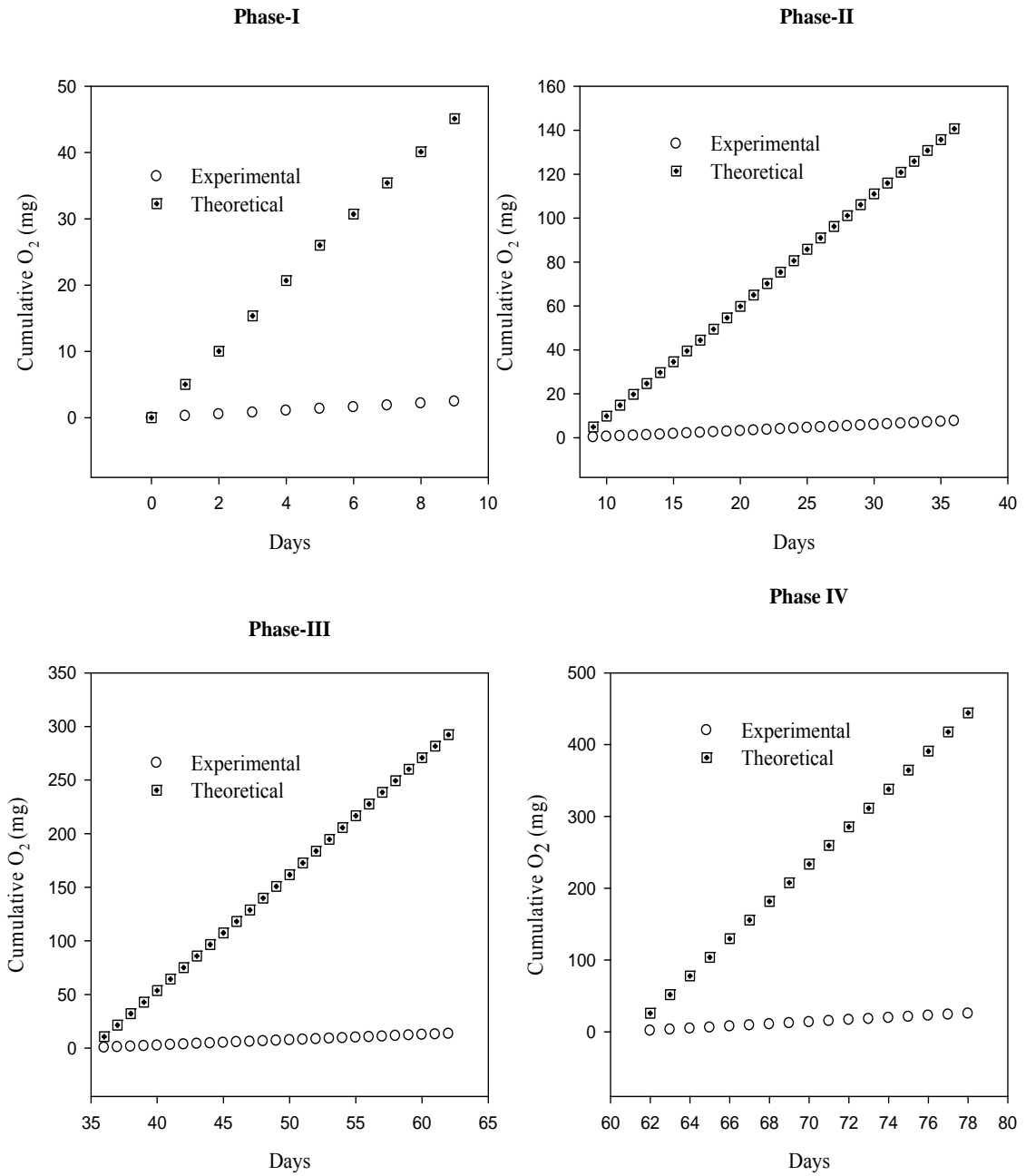
Figure 5.11 Comparison of theoretical and actual oxygen demand in the biofilm reactor system (phases I-IV)
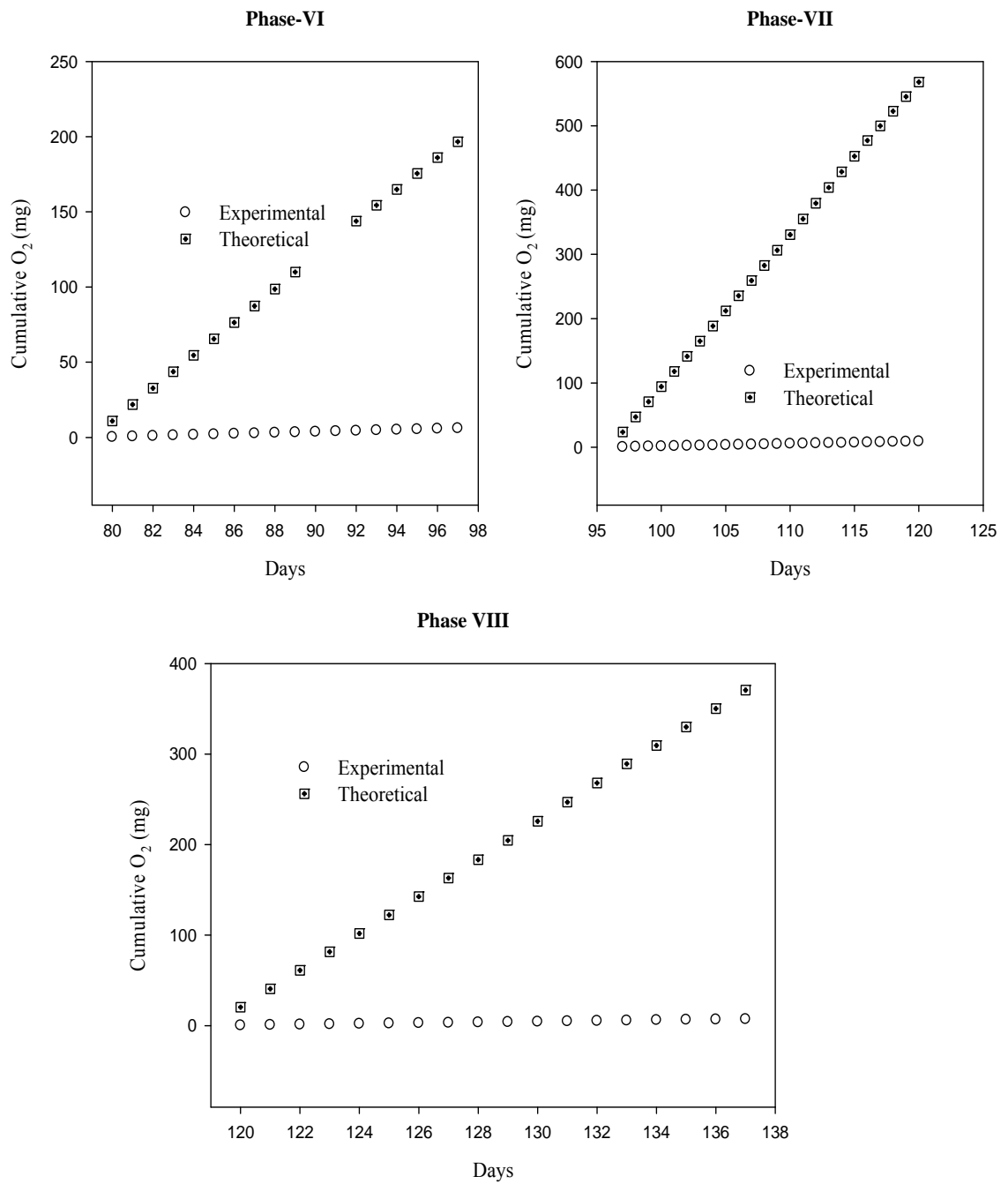
Figure 5.12 Comparison of theoretical and actual oxygen demand in the biofilm reactor system (phases VI-VIII)

Table 5.6 Steady-state oxygen mass balance in the biofilm reactor

Phase	Duration (days)	Influent flow rate Q (mL/hr)	HRT (day)	DO uptake (mg O_2 / day) ± SD^b	Theoretical DO (mg O_2/day) ± SD^b
I	1-9	3.5	1	0.24±0.08	5.01±0.26
II	9-36	3.5	1	0.27±0.02	5.02±0.12
III	36-62	7.2	0.48	0.49±0.02	10.59±0.11
IV	62-78	17.4	0.2	1.49±0.06	23.36±0.51
V	78-80	17.4	0.2	------[a]	-----[a]
VI	80-97	3.5	1	0.34±0.01	10.92±0.28
VII	97-120	3.5	1	0.38±0.01	21.98±0.65
VIII	120-137	3.5	1	0.40±0.10	20.59±0.35

-----[a] DO values not measured

------[b] SD : standard deviation

5.10.8 Estimation techniques of biofilm parameters

Rittmann et al. (1986) proposed a method of measuring the kinetic parameters from biofilm experiments using the measured influent and effluent substrate concentrations under steady-state conditions. The substrate concentrations obtained from the study were normalized, plotted and then visually compared to a series of a design curves. This was a highly inaccurate approach for determining the parameters because it involved large errors from sampling and visual comparison. Nguyen and Shieh (1995) treated a fluidized bed reactor as a batch process and used the data for estimating the parameters. However, the method had several limitations. First of all, the method was very tedious because separate batch experiments had to be conducted for each data point, to be used during the estimation procedure. Secondly, linearization of the non-linear Monod model was performed to determine the intrinsic parameters (Nguyen and Shieh 1995). Linearization of a non-linear model results in unknown transformation of measurement errors, which makes it difficult to evaluate the uncertainties in rate coefficients obtained from the linearized approach (Eisenthal and Cornish-Bowden 1974; Hanes 1932; Robinson 1985). Zhang and Huck (1996) modified Rittman and McCarty's biofilm equations (1980a) to develop an expression for the flux (J) as a function of the bulk substrate concentration (S_b). The model parameters were then estimated using the flux expression and a non-linear routine. The uncertainties estimates in the parameter values were also evaluated using the Jackknife technique (Zhang and Huck 1996). The authors concluded in their study that this method was severely limited by the large uncertainties in the parameter estimates. Parameters obtained from batch experiments are sometimes applied to biofilm systems (Livingston and Chase 1989; Rittmann and

McCarty 1980b; Williamson and McCarty 1976). However, this is a highly inaccurate method of estimation because the species physiology and composition in biofilm systems are different than in suspended growth systems (Grady et al. 1996; Van Loosdrecht et al. 1990). Riefler et.al (1998) fitted a mechanistic mathematical model to the dissolved oxygen concentration profile in the biofilm system to determine the intrinsic biokinetic parameters.

In this study, the parameters (k, K_s) were obtained using a very similar approach adopted by Smets et.al (1998). The method involved using a combination of equations developed by Atkinson and Davies (1974) for the numerical solution of the biofilm model. The measured As (III) flux into the biofilm under various operating conditions was fitted to a predictive flux expression ($J_{prAs(III)}$), which is a function of the As (III) concentration at the biofilm/liquid interface (S_s). The parameters were also characterized by their corresponding 95% confidence levels.

5.10.8.1 Parameter Estimation Technique

The averaged (variations $\leq \pm 15\%$) steady-state effluent As (III) concentrations measured from the first four phases of the reactor operation were used to compute the (J_{exp}, S_s) data pair for the estimation of biokinetic parameters. Sigma Plot 10 (SPSS Inc), which employs a non-linear optimization routine Marquardt-Levenberg algorithm (Marquardt 1963) was used to estimate the parameters by minimizing the residual sum of squares between the observed flux (Eq. (5-13)) and the model simulation (Eq. (5-24)), respectively.

The optimized parameters obtained from the non-linear estimation routine and steady-state data are listed in Table 5.7. The covariance % (asymptotic standard error) was reasonably small suggesting closely bound 95% confidence intervals for the parameters. The 95% confidence intervals of the parameters were obtained from their respective standard errors. However, the lack of knowledge of the joint variability of the fitted parameters can limit the use of single-parameter confidence intervals for modeling purposes (Laurence et.al.1997). The high value of the dependencies (0.65) as shown in Table 5.7 indicates a strong degree of correlation between the obtained parameters. However, such high degree of correlation between K_s and k is commonly seen in both suspended and biofilm modeling involving Monod kinetics (Holmerg 1982; Lobry and Flandrois 1991; Riefler et al. 1995; Robinson and Tiedje 1983; Laurence et.al. 1997).

The non-linear estimation routine was repeated for different initial starting values of the parameters. The Marquardt-Levenberg algorithm uses these initial guess values of the parameters as the starting point of the estimation procedure. The algorithm keeps on making better guesses until the difference between the residuals sum of squares no longer decreases significantly. The data (Appendix E1) show the different initial starting and final converged values of the parameters k and K_s. The values clearly indicate that the estimation routine converged to global minima rather than local minima.

Table 5.7 Optimized parameters obtained from the steady-state

Parameters	Values	CV % [a]	Dependencies [b]
k , mg As (III)/cells.hr	4.24	7.57	0.65
K_s , mg As (III)/L	13.2	21.5	0.65

[a] CV%: the relative asymptotic standard error of the parameters

[b] Dependency of the parameter = 1-(variance of the parameter, other parameter constant)/ (variance of the parameter, other parameter changing)

5.10.8.2 Parameter Estimates

The estimated biokinetic parameters (k and K_s) in this study are the first ones reported for As (III) oxidation by the novel chemoautotrophic bacterium *T. arsenivorans* strain b6 in a biofilm reactor . The maximum specific As (III) uptake or oxidation rate k (4.24 ± 0.63 mg As (III) / mg cells.hr) was very close to the k value of 5 mg As (III) / mg cell.hr obtained earlier in the continuous flow bioreactor study of As (III) oxidation by the same chemoautotrophic *T. arsenivorans* strain b6 (section 4.6.4.1). However, As (III) oxidation by the batch cultures of the same strain b6 yielded a k value of 0.85 ± 0.18 mg As (III) / mg cells.hr (section 3.6.9). Different reactor configuration can significantly influence the estimation of the parameter values. The physiology and composition of the species is quite different in biofilm and suspended growth batch systems (Grady et al. 1996; Van Loosdrecht et al. 1990). The variation could be also due to the history of the culture prior to the kinetic tests (Grady et.al 1996). In addition, different estimation routines / techniques (linear versus non-linear) could also result in large variation in the parameter values. However, the As (III) affinity towards the bacterial cells measured as K_s varied very little under two different experimental conditions (continuous flow versus fixed film processes). The K_s value (13.2 ± 5.58 mg/L) obtained from steady-state conditions in the biofilm reactor was slightly lower than the K_s value of 20.1 mg/L obtained from the CSTR study (section 4.6.4.1), even though the values were of the same order of magnitude. The slight variation can be due to the difference in the employed mathematical technique (linear versus non-linear optimization) for the determination of the parameters. Such difference could also be attributed to the affinity of the attached

cells of *T.arsenivorans* strain b6 towards As (III) being higher compared to the cells in batch and continuous flow studies as exhibited by a comparably lower value.

A sensitivity analysis on the parameters showed that k was more sensitive to model predictions than the saturation constant K_s (Figure 5.13). This is in accordance with the results observed for As (III) oxidation in a continuous flow bioreactor (section 4.6.5). A twofold change in the parameter value of k was more sensitive to the prediction of As (III) flux into the biofilm than a twofold change in the parameter K_s. The estimated value of the effectiveness factor (η) ranged between 0.99 - 1.0 indicating the presence of a fully penetrated biofilm in the reactor (Zeng and Zhang 2005). Negligible external mass transfer resistance in a fully penetrated biofilm may lead to higher As (III) uptake/oxidation rate resulting in higher As (III) flux into the biofilm per unit surface area.

5.10.9 Evaluation of the Model Fit

The model fit (Figure 5.14) was evaluated by means of a linear regression analysis of the plot between observed and model predicted As (III) flux values. A correlation coefficient of $R^2 = 0.99$ suggested a good fit between the model and the experimental data (Figure 5.15). Two statistical tests (two-tailed paired *t*-test, and chi-square goodness of-fit-test) were also performed to evaluate any significant difference between the observed and predicted As (III) flux values. The two-tailed *p*-value (0.63 > 0.05) and the chi-square goodness of-fit test result ($p = 1$) showed that the difference between model predicted and obtained As (III) flux values were statistically insignificant at the 95% confidence level.
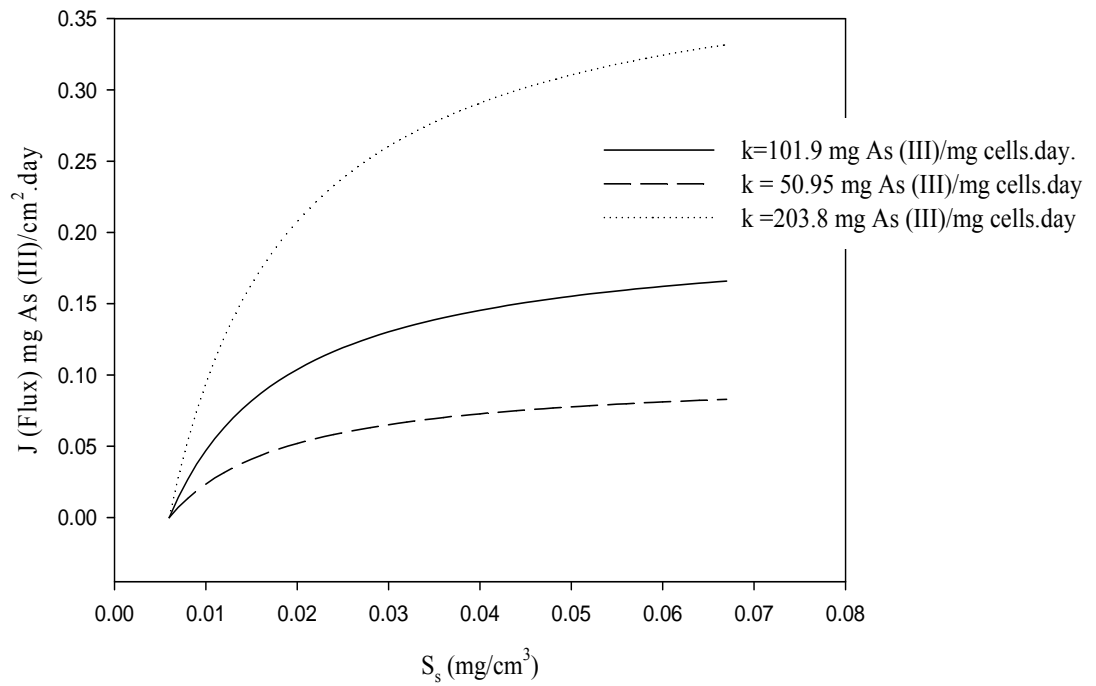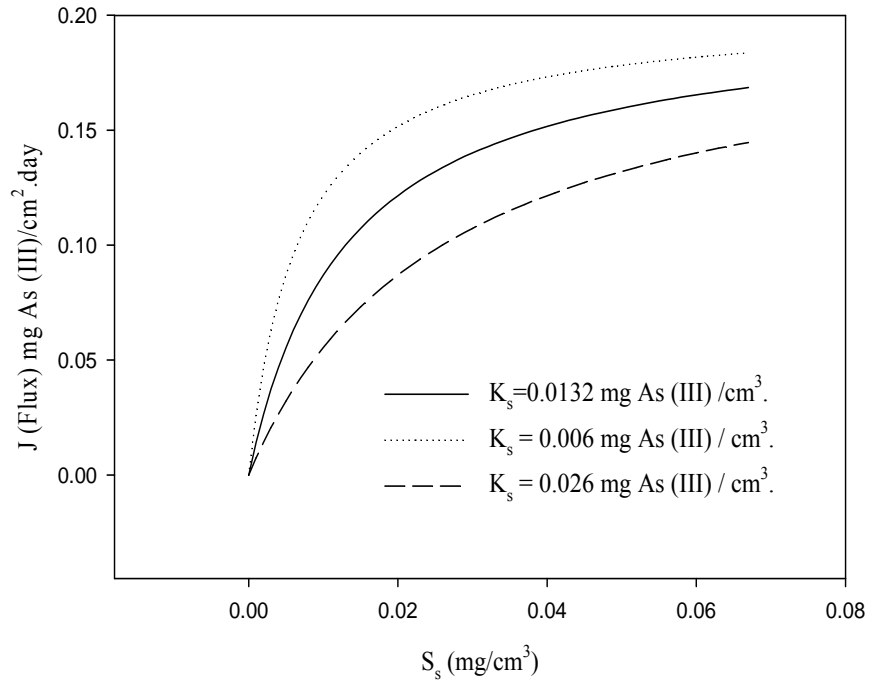
Figure 5.13 Sensitivity of the obtained parameters (k and K_s) to model predictions
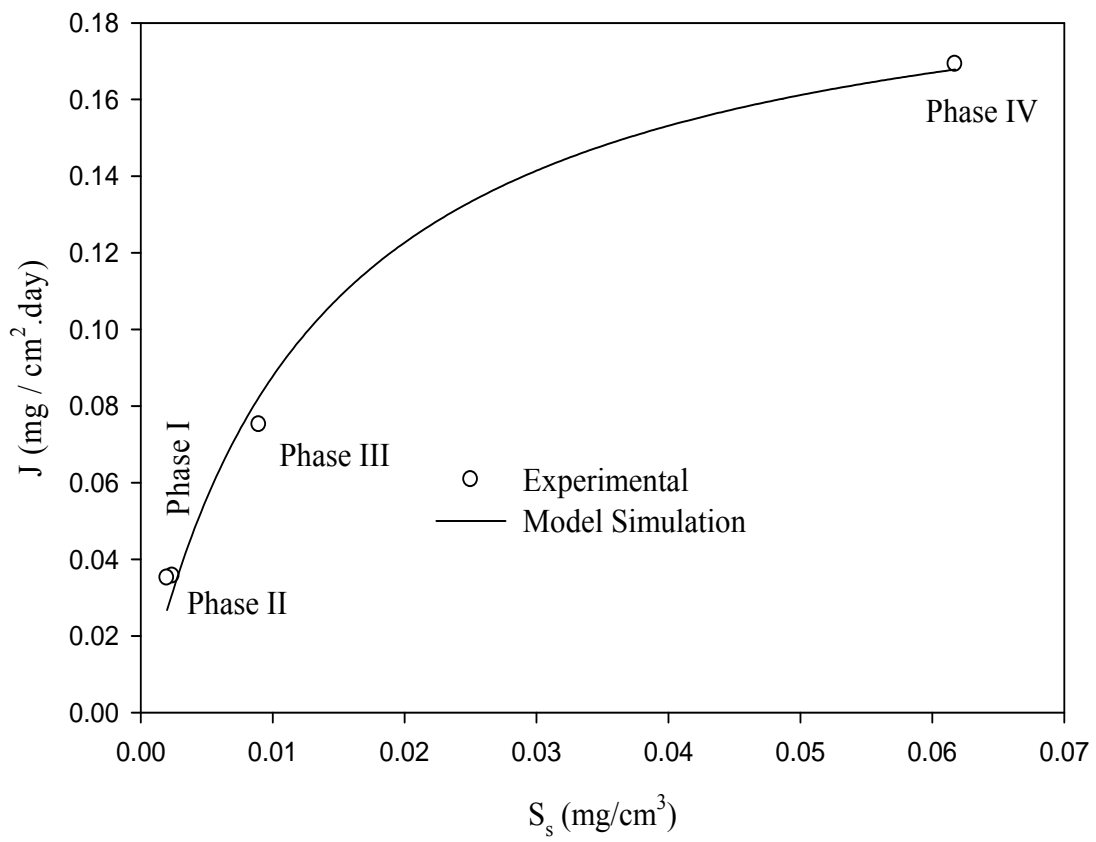
Figure 5.14 J_{exp} versus S_s and model best fit for parameters estimation.
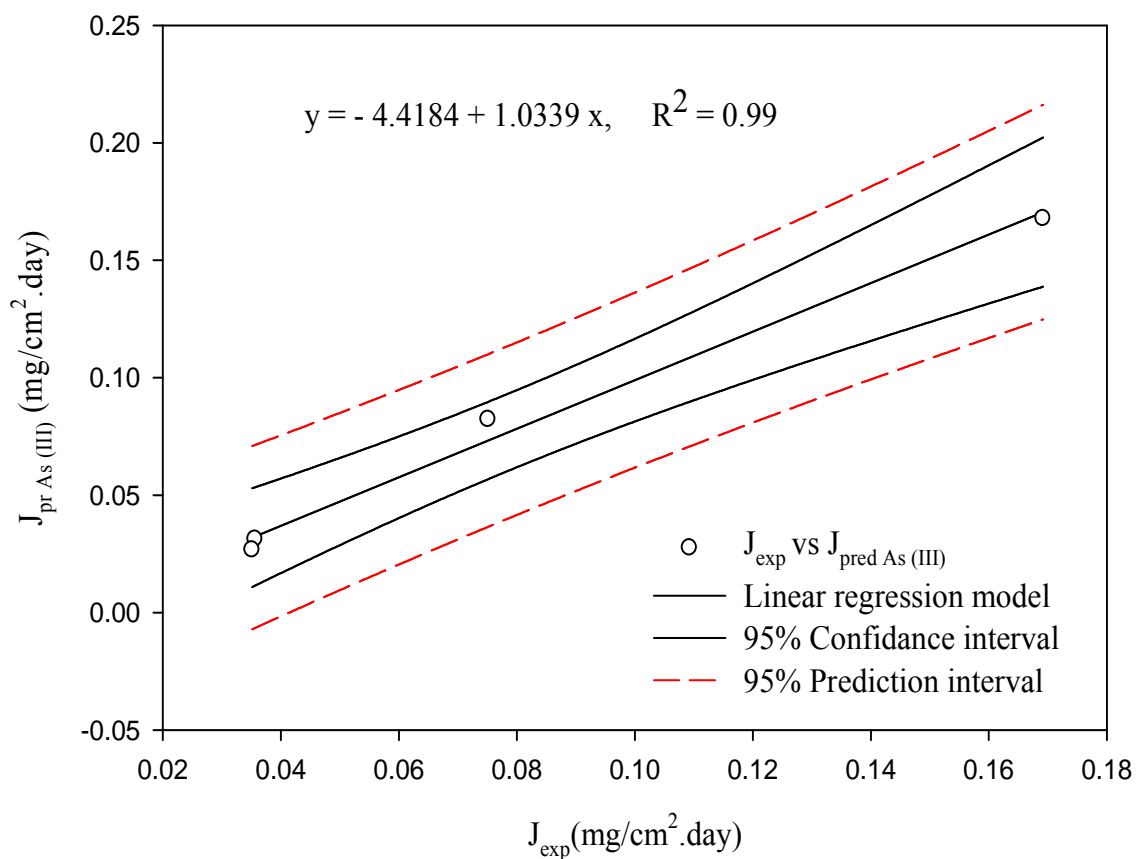
Figure 5.15 Linear regression analysis between the observed and the predicted flux values

5.10.10 Validation of the Model

The flux model (Eq. (5-23)) and the obtained best-fitted kinetic parameters (k, K_s) along with reactor specific parameters listed in Table 5.2 were used to predict the steady-state As (III) flux values for the remaining three phases (VI-VIII) of operation. The biofilm thickness (L_f) was estimated using Eq. (5-10), whereas, the biofilm density (X_f) was calculated using Eq. (5-11) respectively. Results in Table 5.8 show that the model predicted As (III) flux values were an order of magnitude lower compared to the observed values. The poor model prediction accuracy may be attributed to: (i) As (III) overloading during phase V caused by significant loss of biomass. It was earlier reported that large disturbances can result in transient changes to the cells' physiological state or the macromolecular composition of the cells (Grady et al. 1996). As a result of the altered physiological state of the cell, the kinetic parameters obtained from the first four phases may not be valid or applicable for the last three phases of operation. Another possibility is the inhibition of Protein synthesizing system (PSS) by the presence of high levels of As (III) in the reactor. PSS is a very important functional component of the macromolecular composition of the bacterial cells. It plays a very crucial role in the cells' metabolic process since it controls the rate of synthesis of catabolic enzymes essential for the oxidation of As (III) to As (V). Such high level of toxicity may negatively impact or inhibit the synthesis of PSS components. The kinetics obtained under conditions of minimal changes to the physiology of cells (phases I-IV) may not accurately represent the altered physiological state of the cells for the last three phases of operation.

Table 5.8 Validation of the flux model for the last three phases

Phase	L_f (cm)	X_f (mg/cm^3)	$P=X_fL_f$	S_s (mg/cm^3)	J_{obs} (mg/cm^2.day)	J_{pred} (mg/cm^2.day)	J_{obs}/J_{pred}
VI	0.0029	0.0856	0.0002	0.02	0.07	0.01	4.96
VII	0.0027	0.0793	0.0002	0.17	0.15	0.02	7.71
VIII	0.0027	0.0786	0.0002	2.16	0.15	0.02	7.15

5.10.11 Mass Transfer

The diffusivity of As (III) in water (0.87 cm^2/day) was estimated using the Nernst-Haskell equation (Longsworth 1972), whereas, the diffusivity coefficient of As (III) in biofilm (0.70 cm^2/day) was estimated using Eq. (5-8). The thickness of the effective external mass transfer layer (L cm) estimated using the empirical formula reported by Jennings (1975) varied very little (0.12-0.19 cm) under the different operating conditions. This may be due to the minimal variation in the particle dimension and superficial velocity (Barth F. Smets et al.1999).

The effect of mass transfer resistance in the fixed film reactor under different operating conditions was evaluated using the dimensionless variable $K*$. The value of $K*$ ranged from 1.18 - 1.71 for the first four phases and 1.91-2.00 for the last three phases of operation, respectively. The first four phases of operation were accompanied by progressive increase in the influent flow rates of As (III) into the reactor. The increase in the superficial velocity increased the external mass transport rate by decreasing the external mass transfer resistance. As a result, As (III) oxidation efficiency exceeding 96% was demonstrated during the four phases. Higher values of $K*$ reported for the last three phases of operation confirmed that external mass transfer resistance had little effect on the over-all bioreactor performance.

5.10.12 Growth Potential

The importance of biomass growth versus loss of biomass through decay and detachment was compared using the dimension less parameter S_{min}^*, referred to as growth potential. The estimation of the overall biofilm loss coefficient (b') posed a potential problem in the calculation of the growth potential under the different operating conditions

(Barth F Smets et.al 1999). The detachment coefficient (b_{det}), may be estimated using a combination of the Eqs. (5-25, 5-26, 5-27, 5-28) as suggested by Rittmann (1982 b). However, the endogenous decay coefficient (b), which is also used for the estimation of the overall biofilm loss coefficient, is generally not measured in fixed-film reactor processes (Barth F Smets et al. 1999). Any assumption of the value of b, leads to significant uncertainty and error in correctly predicting the growth potential values of the microorganisms during the operation of the fixed bed reactor process.

A new approach adopted by Barth F Smets et.al (1999) was employed in this study to estimate the growth potential values for all the steady-state phases (I-IV, VI-VIII). The advantage of using this method was that the method was completely dependent on the steady-state reactor conditions such as the biofilm density (X_f), biofilm thickness (L_f), best-fit parameter k, and the observed As (III) flux (J_{exp}) into the biofilm, respectively. The results obtained from this study show that the performance of the fixed-bed reactor process may be limited by the growth potential of the microorganisms based on the computed values of S_{min}^* ranging from 0.21 - 0.48 for the first three phases of operation. The values may also indicate that the maximum net positive growth rate ($Yk-b'$) was greater than the overall biofilm loss rate (b'), which was validated by the increase in the biofilm thickness and biofilm density. However, the growth potential computed for the fourth phase was low (2.11) indicating significant loss of biomass through detachment caused due to high shear force. The observance was also validated by decrease in the As (III) oxidation efficiency of the reactor from 99.3% (phase I) to 87.5%

(phase IV). Extremely high values of the growth potential make it difficult to maintain steady-state biomass in the reactor.

Negative values (< 0) of the growth potential were obtained for the last three phases of the reactor operation. As reported earlier, both the parameters (k, K_s) failed to accurately predict the observed As (III) flux values due to changes in the physiological state of the cells for the phases VI-VIII. The estimation of the growth potentials (Eq. (5-38)) without using the true intrinsic k value representative of the reactor conditions during the last three phases may lead to the computation of improbable negative values. The growth potential values obtained from the first two phases of this study were very close to the earlier reported growth potential value of 0.17 in a study of autotrophic nitrification (Rittmann 1994). Higher flow rates (lower HRTs) leading to substantial loss of biomass in the reactor lowers the growth potential (≥ 1) in the reactor. The growth potential values can be substantially increased in a biofilm reactor by improving reactor conditions such as higher yield coefficient, greater As (III) oxidation rate, and lowering the overall loss of biofilm, respectively.

5.11 Summary and Conclusions

The potential of As (III) oxidation in a fixed-film reaction was investigated using cells of *T.arsenivorans* strain b6 under varying As (III) loading rates. The As (III) oxidation efficiency of the reactor varied from 48.2% to 99.3%, with seven steady-state conditions obtained. The bioreactor successfully recovered from an As (III) overloading of 5000.4 ± 373 mg As (III) / L.day operated at an HRT of 0.2 day. An arsenic mass balance revealed that all the As (III) fed in the reactor was oxidized to As (V) with unaccounted arsenic being very insignificant (≤ 4 %). An oxygen mass balance for each

phase revealed significant difference between the theoretical and actual oxygen consumption by the strain b6. Biokinetic parameters K_s and k were estimated using a modified Monod model and the obtained steady-state flux data. However, the estimated parameters failed to validate the steady-state performance of the reactor for the last three phases of operation. The sensitivity of the parameter k was definitely more significant to model simulations compared to the parameter K_s as revealed by the sensitivity analysis.

Chapter 6: Preliminary Study of Arsenic Removal in a Bioreactor Packed with Granular Activated Alumina

6.1 Abstract

The potential application of the coupling of biological As (III) oxidation to As (V), and adsorption of As (V) by Activated Alumina (AA) beads was investigated in both a one-stage and a two-stage reactor process. A novel chemoautotrophic *Thiomonas arsenivorans* strain b6 was used for the biological oxidation of As (III) to As (V). The one-stage bioreactor used granular AA as the contact medium for strain b6 cells and was operated under two influent As (III) concentrations (60 mg/L and 100 mg/L) and a constant HRT of 1.0 day for 12, 6 days respectively. The As (III) oxidation and As (V) removal patterns in the reactor under the two influent As (III) concentrations were very similar. The two-stage system consisted of a bioreactor packed with glass beads for the biological oxidation of As (III) to As (V), and subsequent granular AA column for the removal of As (V). The two-stage system was operated under a very high influent As (III) concentration of 500 mg/L and a HRT of 1 day. The overall As removal in both the one-stage and two-stage column processes may be limited by the presence of ionized species such as PO_4^{3-}, SO_4^{2-}, and Cl^-, which compete with As (V) for the adsorption sites on AA. The operation of both the systems under such high influent As (III) concentrations and the difficulties in maintaining the pH close to the range 5.5 - 6.0 for optimum As (V) removal may also affect the overall performance.

6.2 Introduction

Arsenious acid (H_3AsO_3) has pKa values of 9.22, 12.13, and 13.4 whereas arsenic acid (H_3AsO_4) has pKa values of 2.20, 6.97, and 11.53, respectively (Healy et al. 1999). The pKa values for arsenate clearly suggest that both $H_2AsO_4^-$ and $HAsO_4^{2-}$ are the two most predominant forms present in water at the pH range of 6-9. In this study, the pH was maintained close to 6.0 (the optimum pH for strain b6), and thus $H_2AsO_4^-$ would be the most likely predominant form present in the water.

The preliminary treatment of arsenic contaminated water generally involves oxidation of arsenite (As (III)) to arsenate (As (V)). This initial treatment of arsenic polluted water is essential because As (III) is more toxic and mobile than As (V) in water (Smedley and Kinniburgh 2002; Oremland and Stolz 2003). The oxidative pretreatment can be achieved using both chemical and biological means. However, chemical oxidation of As (III) to As (V) may produce harmful by products such as trihalomethanes (THMS) during the treatment process as reported by Gallard and Von Gunten (2002). Biological oxidation of As (III) is a potential alternative strategy and may be more economical than chemical oxidation methods.

Little attention has been paid to the removal of As (V) formed through biological oxidation. As (V) produced as a result the oxidation process generally can be removed by adsorption using the following mineral based compounds such as amorphous aluminum hydroxide; Aluminum and Iron (Fe) oxides and clay minerals; Activated Alumina Grains; Goethite; titanium dioxide suspensions; and granular ferric hydroxide (GFH) (Anderson et al. 1976; Goldberg 2002; Lin and Wu 2000; Grafe et al. 2001; Dutta et al. 2004; and Badruzzaman et al. 2004). Lievremont et al. (2003) conducted a batch study of As (III)

oxidation to As (V) using the β-*proteobacterium* strain ULPAs1 in the presence of chabazite and Kutnahorite minerals. The method was highly efficient in removing 90% of the total As (V) ions produced during the oxidation process.

The effectiveness of various adsorbents in the removal of As (V) ions can be severely limited by various physical, chemical, and biological factors. One of the major reasons limiting the As (V) removal efficiency of these materials is the presence of phosphates (PO_4^{3-}), which competes for the same adsorption sites on the adsorbent. Katsoyiannis et al. (2004) used *Leptothrix ochracea*, a prominent manganese oxidizing bacterium, to mediate low levels (35 and 42 µg/L) of As (III) oxidation to As (V), and then removal of As (V) by adsorption on biogenic manganese oxides. However, the effectiveness of As (V) removal was severely limited by the presence of high concentration of PO_4^{3-} ions in the liquid medium of the reactor.

6.2.1 Mechanism of As (V) adsorption on AA

The adsorption of arsenate ($H_2AsO_4^-$ or $HAsO_4^{2-}$) on activated alumina (AA) is a surface phenomenon, wherein the hydroxides present on the surface are exchanged for the incoming arsenate ions (Clifford and Ghurye 2002; Clifford 1990). However, this adsorption process is more appropriately termed as *ligand exchange* reaction. The *ligand exchange* using AA for As (V) removal is an example of a weak-base anion exchange process. The most commonly used AA for water treatment is generally a mixture of amorphous and gamma aluminum oxide (γ-Al_2O_3). This is prepared by the dehydration of precipitated Aluminum hydroxide (Al (OH)$_3$) at temperatures of 300-600°C.

Both the internal and external surfaces of the AA are involved in the *ligand exchange* process, and are very sensitive to any changes in pH of the influent medium.

The point of zero charge (pH_{pzc}) of the AA's generally range between 8.2 and 9.1, and is highly dependent on the material composition of the AA (Stumm and Morgan 1981; Bowlers and Huang 1985; Clifford and Ghurye 2002; Clifford 1990). The surface of the AA is very positively charged at any pH values below pH_{pzc}, and the excess amount of available hydrogen ions facilitates the adsorption of As (V) ions onto the AA surface. The optimum range of pH for arsenate adsorption on the AA surface is 5.5 - 6.0 as reported in several studies using AA for arsenic removal from ground water (Clifford and Ghurye 2002; Clifford 1990; Lin and Wu 2001; Chen and Gupta 1978).

The establishment of positive charges on AA facilitating the adsorption of As (V) ions is usually accomplished by preacidification with HCl or H_2SO_4. This *ligand exchange*/adsorption process is represented by the following set of equations (Clifford and Ghurye 2002):

$$\overline{Alumina \cdot HOH} + HCl \rightarrow \overline{Alumina \cdot HCl} + HOH \qquad (6\text{-}1)$$
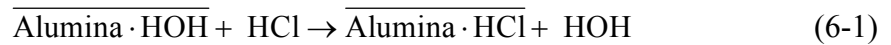
Eq. (6-1) represents the formation of acidic (protonated) Alumina by pre-treating with HCl. The chloride ions (Cl^-) of the protonated alumina surface are strongly displaced by the incoming arsenate ions under the operating pH maintained at the desired optimum range of 5.5 - 6.0. This part of the chemical reaction is given by the following Eq. (6-2):

$$\overline{Alumina \cdot HCl} + H_2AsO_4^- \rightarrow \overline{Alumina \cdot HH_2AsO_4} + Cl^- \qquad (6\text{-}2)$$
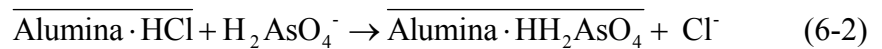
The over bar represents the solid phase of the complex.

6.2.2 Factors Affecting Arsenate Adsorption on Activated Alumina

6.2.2.1 Oxidation State of Arsenic in the Water

To achieve near complete removal of arsenic from water, it is preferred to convert As (III) to As (V) through an oxidation process (Clifford and Ghurye 2002; Clifford 1990). A study conducted by Clifford and Ghurye (2002) using two bench-scale mini columns packed with AA showed that the arsenic breakthrough curve from 100 µg/L As (III)-fed column reached 50 µg As/L after passing through only 300 bed volumes (BV). However, the breakthrough concentration of 50 µg/L occurred in the 100 µg/L of As (V)-fed column after treating 23, 400 BV.

6.2.2.2 Influence of pH, Sulfate, and Hardness on the Uptake Capacity of AA

The adsorption of As (V) ions on AA is a highly pH dependant surface phenomenon. The arsenic speciation also depends on the pH and Eh of the surrounding environment. In the pH range of 6-9, As (V) species are usually present in the form of $H_2AsO_4^-$ and $HAsO_4^{2-}$ based on the dissociation of arsenic acid ($H_3AsO_4^-$) exhibiting pKa values of 2.2, 7.0, and 11.5. However, arsenious acid (H_3AsO_3), the other most predominant arsenic specie is generally neutral by nature in that same pH range based on a pKa value of 9.2 (Clifford and Ghurye 2002). The optimum pH for maximum arsenate adsorption or *ligand exchange* was found to be in the range of 5.5-6.0 based on several pilot-scale column studies (Clifford and Lin 1991; Clifford et al. 1997, 1998; Clifford and Wu 2001; Simms et al. 2000; Rosenblum and Clifford 1984; Frank and Clifford 1986; Clifford and Lin 1995; Lin and Wu 2000). The studies also showed that significant decrease in the As (V) uptake by AA occurred with increase in pH above the optimum range. The decrease in the adsorption capacity of the AA could be due to decrease in the

number of positively charged sites on the AA surface with increase in pH of the surrounding medium.

The equilibrium isotherm studies conducted by Clifford and Ghurye (2002) showed that sulfate in comparison to chloride ions strongly reduced the arsenate adsorption capacity of the AA in a given liquid medium. This is the reason as to why hydrochloric acid (HCl) is generally preferred for pH adjustment during the course of the experiment instead of sulfuric acid (H_2SO_4).

A recent study by the same authors (Clifford and Ghurye 2002) also demonstrated that the As (V) uptake capacity of the AA may increase by almost 30-50% at pH of 7.3 in a sample of hard water measuring 250 mg/L as $CaCO_3$ compared to 5 mg/L as $CaCO_3$ at the same total dissolved solids (TDS) level.

6.2.2.3 Effect of Competing Ions

The arsenate adsorption capacity of the AA is severely affected by the presence of competing anions such as chloride (Cl^-), nitrate (NO_3^-), sulfate (SO_4^{2-}), phosphate (PO_4^{3-}), and silicate ($H_3SiO_4^-$).

The dissociation constant of the weak acid H_4SiO_4 is 9.77 indicating that the concentration of the anion $H_3SiO_4^-$ increases with increase in the pH of the water. The anion $H_3SiO_4^-$ is a very strong ligand competing with As (V) for the adsorption sites on AA. A study conducted by Clifford and Wu (2001) showed that the adsorption capacity of the AA decreased by almost 75% from 0.55 to 0.15 mg As (V)/g alumina by adding 15 mg/L of silica to the raw water. However, the effect of silicate anions decreases with decrease in the pH values of the surrounding medium.

Out of the three anions (Cl^-, PO_4^{3-}, and NO_3^-), phosphate is the strongest competitor of As (V) for the adsorption sites on the AA surface. A study conducted by Tripathy and Raichur (2008) showed the adverse effects of varying concentrations (0 - 100 mg/L) of PO_4^{3-} ions on 10 mg/L As (V) adsorption on AA. They found that PO_4^{3-} concentration of 25 mg/L caused 8% reduction in the As (V) adsorption efficiency of the AA, whereas, a concentration of 100 mg/L decreased the As (V) uptake capacity by 27% at a pH of about 7.0.

6.2.2.4 Characteristics of the Design Process

The four most important process variables that affect the arsenate uptake capacity of the AA are as follows: (i) adsorbent dosage, (ii) size of the adsorbent particle, (iii) flow rate of the influent As (III) contaminated water, and (iv) empty bed contact time (EBCT). Both the size of the alumina particles and the EBCT can significantly affect the AA adsorption capacity. It was reported that finer particles of AA (28 x 48 mesh, 0.6-3 mm) have a higher arsenic uptake capacity, less likely arsenic leakage, and longer operation time of AA column compared to larger particles of AA with dimension 14 x 28 mesh (1.18 -0.6 mm) (Simms and Azizian 1997; Clifford and Lin 1991; 1995). The same study also reported that life of the AA column was linearly proportional to EBCT values ranging from 3 - 12 mins.

6.2.4.5 Objectives of the study

1. To conduct a preliminary study for evaluating the potential of a one-stage reactor in the complete removal of arsenic from water. The one-stage reactor consisted of immobilized cells of *T.arsenivorans* strain b6 on granular AA. The performance of biological As (III)

oxidation and As (V) adsorption was investigated in the one-stage reactor under varying influent As (III) concentrations (60 – 100 mg/L) at a HRT of 1 day.

2. To investigate the potential of a two-stage reactor system for treating very high influent As (III) level (500 mg/L) using separated biological oxidation and adsorption processes. The reactors were operated continuously at a HRT of 1 day until arsenic breakthrough was observed in the effluent.

6.3 Materials and Methods

6.3.1 Bacterial Strain and Feed Composition

The *T.arsenivorans* strain b6 as described in section 3.3.1 was used in this study. The feed to the biofilm reactor was a modified MCSM medium to which 5 g/L each of K_2HPO_4 and KH_2PO_4 were added as buffer, while eliminating the addition of yeast extract to ensure autotrophic growth conditions.

6.3.2 One-stage Reactor

Granular Activated Alumina (AA) (Sigma Aldrich USA) beads averaging 3mm were pre-acidified with the aid of a magnetic stirrer in an erlenmeyer flask containing a solution of 1N H_2SO_4. All the AA particles were also initially screened for 3 mm sizes due to the varying irregularly shaped sizes in the particular lot.

A schematic of the reactor setup is shown in Figure 6.1.The reactor was constructed from an acrylic column of internal diameter 2.3 ± 0.01 cm with a height 20.1 ± 0.04 cm (empty bed volume = 83.7 mL). The reactor was packed with approximately 3000 AA particles with an estimated available external surface area of 847.4 cm^2 for cell attachment and As adsorption process.

The effluent recycled was accomplished by using an adjustable peristaltic pump (6-600 rpm) (Cole Parmer Instrument Co). The reactor was operated with Q_R / Q ratio of 100 to establish completely mixed conditions. The reactor was then inoculated with 30 mL of overnight grown pure cells of *T.arsenivorans* strain b6. The feed to the reactor consisted of MCSM medium with yeast extract (Difco Lab, MD USA) and the reactor was operated for at least 4 days under a HRT of 1 day until cell attachment was visible on the AA surface.

Once cell attachment was observed on the AA, the reactor was then fed continuously with an influent As (III) concentration of 60 mg/L (without yeast extract) at a HRT of 1.0 day. The reactor operations were terminated once the As (V) breakthrough curve was observed. The reactor and its components were then dismantled and thoroughly cleaned by washing, autoclaving at 121°C for 15 mins, and oven dried before reassembled for the next experimental run. After packed with fresh pre-acidified AA, the reactor was operated under an influent As (III) concentration of 100 mg/L at a HRT of 1 day.

Liquid phase samples were collected for analyzing As (III), As (V) and total As concentrations. At the end of each experimental run, samples were also collected for viable cell concentrations and attached cell mass on the AA. The viable cell concentration was measured using the spread plate technique as mentioned in section 9215C of the *standard methods for the examination of water and wastewater* (APHA 1995). The details of the procedure have also been described in chapter 3 (section 3.3.4.1).

The attached biomass on the AA was determined at the end of each experimental run. 12 AA beads (6 from the top and 6 from the bottom of the reactor) were collected by

opening the reactor under a germ free chemical hood (Steril Gard Class II Model, The Baker Company, Stanford, ME). The attached biomass was measured as mg VSS (Volatile suspended solids) by measuring the difference between the dry weights of the sampled AA particles before and after washing with sterile deionized distilled water. The sampled AA beads were first oven dried for 30 mins at 105ºC and cooled in a dessicator before being weighed. They were then washed with sterile distilled water, oven dried again at 105°C, cooled and then finally weighed. The attached biomass value was computed from the loss in weight of the AA samples through washing. The 12 beads collected for biomass determination were replaced by freshly prepared pre-acidified AA beads prior to the next phase of the experiment.
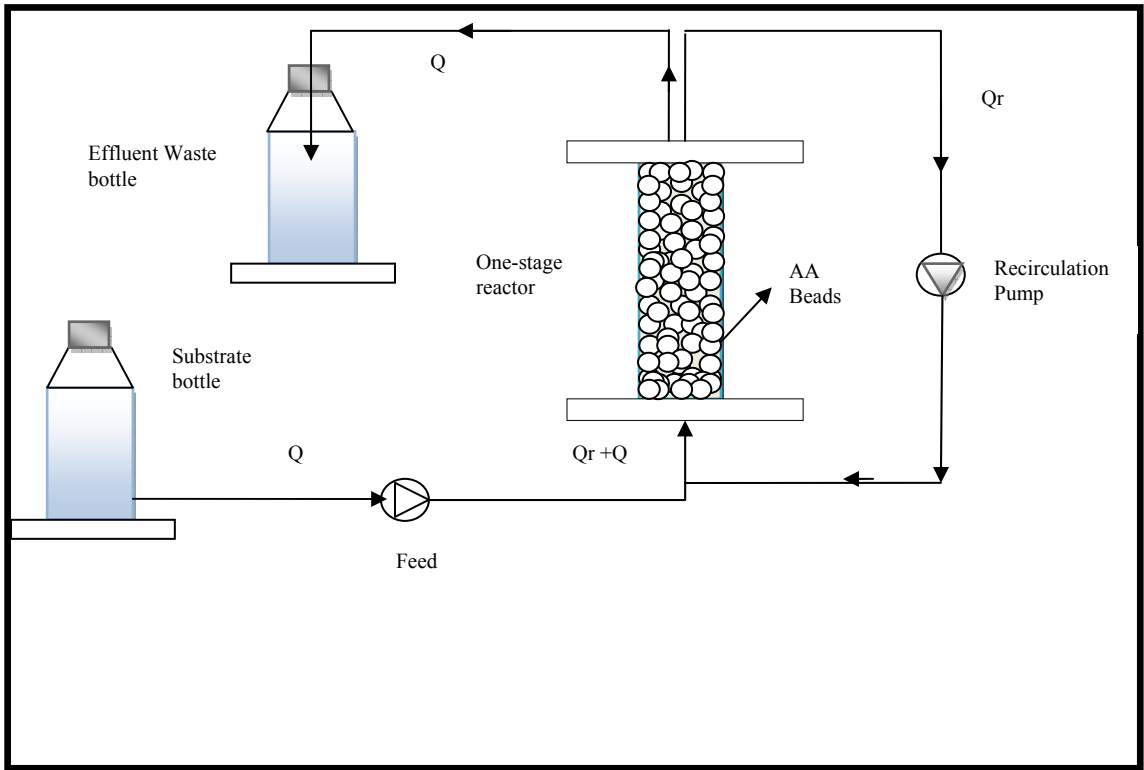
Figure 6.1 One-stage reactor system for the complete removal of arsenic from water.

6.3.3 Two-Stage Column Reactor

A schematic of the two-stage column reactor setup is shown in Figure 6.2. The first reactor (R1) was utilized for the biological oxidation of As (III) to As (V), whereas, the second reactor (R 2) was used for the adsorption of As (V).

6.3.3.1 Operating Conditions and the Reactors Configuration

Two identical reactors were constructed from an acrylic column (internal diameter: 2.3 ± 0.01 cm and height 20.1 ± 0.04 cm). The reactor R1 was packed with approximately 3000 clean oven dried 3mm glass beads with an estimated total external surface area of 847.4 cm^2. This reactor was inoculated with cells of *T.arsenivorans* strain b6 and was operated under an influent As (III) concentration of 500 mg/L at a recycle ratio of 50 to ensure completely mixed condition. The reactor R2 was also packed with 3000 AA beads (diameter: 3mm) with computed external surface area of 847.4 cm^2 for the adsorption of As (V). The specific physical properties of AA are given in Table 6.1 (Sircar et al. 1996).The AA beads were pH adjusted or pre-acidified by rinsing in 0.1N HCl prior to packing the reactor R2. After the attainment of steady-state conditions, the effluent As (III) and As (V) from R1 was treated as the influent feed for the AA beads in R2.

6.3.3.2 Reactor Startup

Reactor R1 and its components were assembled under a laminar flow hood (Steril Gard, class II type A/B3, Baker Company, Sanford, ME), and packed with autoclaved oven dried solid glass beads (Fisher scientific Co, Pittsburg, PA). 30 mL of overnight grown and harvested pure cells of *T. arsenivorans* strain b6 were inoculated inside R1 during the assembly process. Bolted flanges and rubber gaskets were used at the top and

bottom of both the reactors to prevent leakage of the effluent arsenic during the reactor operation. Pre-calibrated peristaltic pumps (Masterflex, Cole-Parmer Inst. Co., Niles, Illinois) were used in the influent and recycle lines and the reactor was operated in an up-flow mode to ensure completely submerged conditions in the reactor. The pump and the connecting tubings of both the reactors were autoclaved at 121°C for 30 mins, whereas, the inside of the reactors rinsed in 95% ethanol and dried prior to the assembly process under the germ free hood (Steril Gard Class II Model, The Baker Company, Stanford, ME).

The reactor R1 was operated under the influent As (III) concentration of 500 mg/L at HRT of 1.0 day until cell attachment was visible under stable operating conditions. The reactor R2 was then fed with the effluent from R1. Samples collected from R2 were analyzed for As (III), As (V), total As, suspended and attached biomass concentration, and TOC (Total Organic Carbon).

6.3.4 Analytical Methods

6.3.4.1 Sample Handling and Quality Control

Samples from both the reactors were collected using 1 mL sterile disposable pipets (Fisher Scientific CO., Pittsburgh PA) at appropriate time intervals. The samples from R-1 was immediately centrifuged at 10,000 rpm for 10 mins using a microcentrifuge (Brinkmann Instruments Inc, West bury, NY). The supernatant was acidified using 1 % HNO_3 (pH < 2) and preserved in 4 °C for no more than 7 days prior to analysis of As (III), As (V) and total As (APHA 1995). However, the samples from R2 were first filtered using 0.2 µm PTFE filters (Fisherbrand Co., PA).
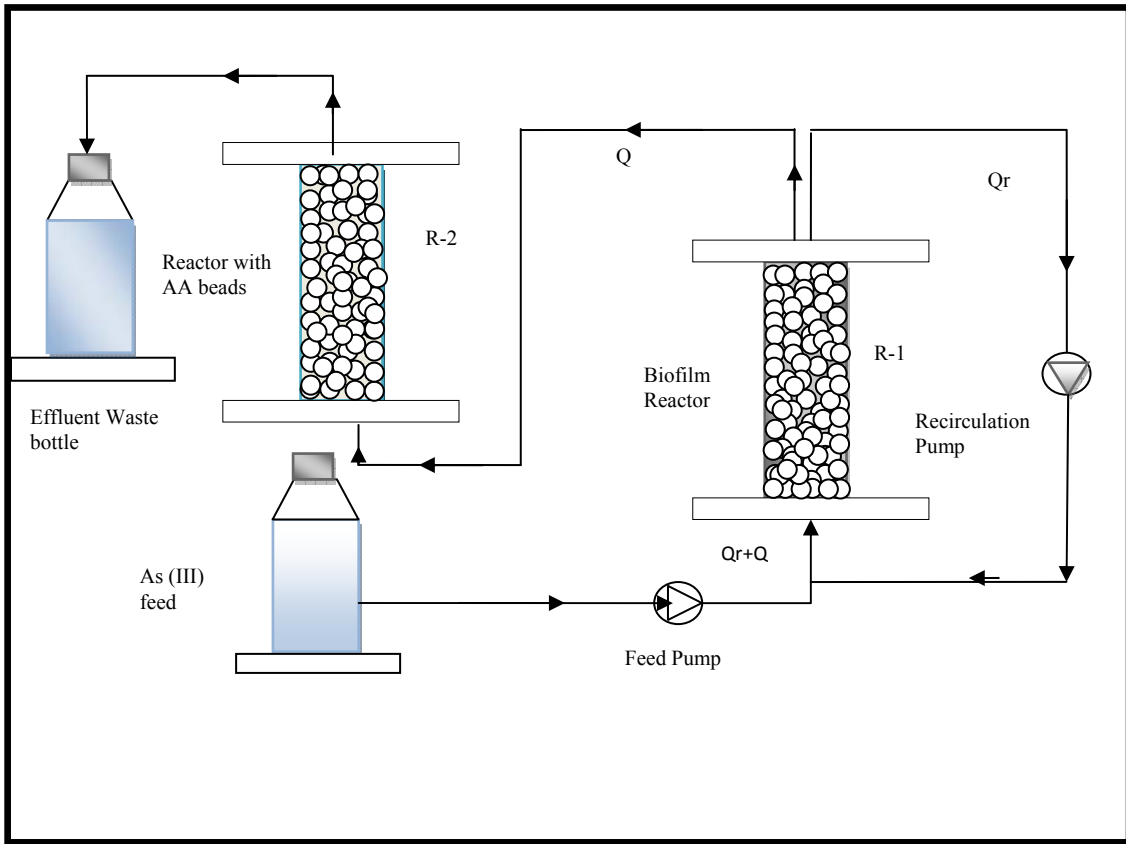
Figure 6.2 Two-stage reactor system for the removal of high level of arsenic from water.

Table 6.1 Physical properties of activated alumina (Sircar et al. 1996)

Properties	AA-300 (4 x 8 mesh)
BET Area (m^2/g)	330
Pore Volume (cm^3/g)	0.44
Bulk Density (g/cm^3)	0.84
Particle Density (g/cm^3)	1.34
Mean Pore Diameter (Å)	65

The filtrate was then centrifuged to eliminate remaining any bacterial cells. Samples for viable cell counts were collected and analyzed immediately to prevent any changes prior to the analysis. The protocol for the preservation of TOC samples prior to analysis was similar to that of As (III) and As (V) respectively.

6.3.4.2 As (III), As (V), and Total As Determination

The method for determining As (III), As (V), and total As by the modified silver diethyldithiocarbamate method (Suttigarn and Wang 2005) is described in section 3.3.32 in chapter 3.

6.3.4.3 pH and Dissolved Oxygen Determination

The pH in R2 was very closely monitored so as to maintain an optimum pH range of 5.5-6.0 for maximal As (V) adsorption by the AA beads. Similarly, the pH in R1 was maintained close to 6.0 using 0.1 N NaOH for optimal biological oxidation of As (III) to As (V).

pH was measured *in situ* using a pH meter (Denver Instrument, Denver, CO) equipped with an ATC Combo, Silver/Silver chloride electrode. The pH meter was calibrated with standard buffers of 4 and 7 and the pH probe was disinfected by 95% ethanol before each use. Dissolved oxygen (DO) in R1 was determined *in situ* using a pre-calibrated DO meter (YSI 550A, Yellow Springs, Ohio) with the probe also disinfected with 95% ethanol before use.

6.3.4.4 TOC Analysis

Samples collected from both R1 and R2 were analyzed for TOC (Total Organic Carbon) using a Total Organic Carbon Analyzer (TOC-5000 ACE, Shimadzu scientific). The TOC of the samples was measured using this following equation:

$$\text{TOC (mg/L)} = \text{TC (Total Carbon)} - \text{IC (Inorganic Carbon)} \qquad (6\text{-}3)$$

6.3.5 Biomass Analysis

At the end of the experimental runs, beads were collected from the top and bottom of the reactors and analyzed for viable attached (section 5.3.8.2) and viable suspended cell concentrations (section 3.3.4.1) in accordance with the guidelines outlined in the *standard methods for the examination of water and wastewater* (APHA 1995).

6.4 Data Analysis

6.4.1 Adsorption Isotherms

A preliminary experiment was conducted to estimate the time required for the establishment of As (V) adsorption equilibrium with the AA beads. The AA used for the experiment was pretreated by rinsing with 0.1 N HCl before use. Varying adsorbent doses (33 g/L – 167 g/L) were placed in borosilicate test tubes containing 15 mL of 500 mg/L As (V) concentration. The solution in the test tubes comprised of the same MCSM medium used for the column experiment with the addition of 500 mg/L of As (V) concentration. The tubes were shaken in an orbital mixer (Glas-Col, IN) for at least 96 h until an equilibrium condition was attained with a constant As (III) concentration in the liquid medium of the tubes. The pH was monitored and adjusted during the study using 0.1 M HCl solution (Bouguerra et al. 2009). Samples were collected at appropriate time intervals and filtered through 0.2 μm PTFE filters (Fisher Scientific Co., PA) before analyzing for As (V) concentrations.

6.4.2 Adsorption Equilibrium Isotherms

Adsorption isotherms are very important in explaining the interaction between the adsorbent (AA) and the adsorbate (As (V)) in aqueous solution. This information is very

useful in the optimum use of the adsorbent for the treatment of arsenic contaminated water (Tang et al. 2009). Important information regarding the adsorption and the extent of the surface area involved in the process is also obtained from the shape of the adsorption isotherms (Faust and Aly 1987). The adsorption isotherms were investigated using two major adsorption isotherm models: Langmuir Adsorption Isotherm and Freundlich Adsorption Isotherm.

6.4.2.1 Langmuir Adsorption Isotherms

The following four important assumptions were incorporated while formulating the Langmuir Adsorption Isotherm model (Faust and Aly 1987):

1. Adsorption of the molecules takes place on definite sites on the adsorbent's surface.

2. The isotherm is valid for monolayer (single molecule) of the adsorbate on each of the definitive sites.

3. The geometry of the surface determines the fixed area of each site.

4. All the adsorption sites have the same adsorption energy.

The Langmuir adsorption isotherm model equation is given as:

$$\frac{C_e}{q_e} = \frac{1}{bq_m} + \frac{C_e}{q_m} \qquad (6\text{-}4)$$

Eq. (6-6) can be modified as shown below:

$$\frac{1}{q_e} = \frac{1}{q_m} + \frac{1}{bq_mC_e} \qquad (6\text{-}5)$$

where q_e = mass of As (V) adsorbed per unit weight of AA (mg/g); q_m = amount of As (V) adsorbed per unit weight of AA required for monolayer coverage of the surface, also called the maximum monolayer capacity; C_e = equilibrium As (V)

concentration in the solution (mg/L); and b = constant related to the affinity of the binding sites.

Hall et al., (1966) proposed a separation factor or equilibrium parameter "r" to describe some of the essential features of the Langmuir isotherm according to the following equation:

$$r = \frac{1}{(1 + b \cdot C_o)} \tag{6-6}$$

where

r = the dimensionless parameter

C_o = initial As (V) concentration in mg/L.

6.4.2.2 Freundlich Adsorption Isotherm

The Freundlich adsorption isotherm is an empirical model which dictates the heterogeneity of the AA adsorbent surface and is given by the equation (Bouguerra et al. 2009):

$$q_e = K \cdot C_e^{1/n} \tag{6-7}$$

K , n are Freundlich constants related to adsorption capacity and adsorption intensity.

6.5 Results and Discussion

6.5.1 Performance analysis of the one-stage reactor

The one-stage reactor was operated under an influent As (III) concentration of 60 mg/L at a HRT of 1 day. The first 12 h of operation was characterized by a rapid increase in the effluent As (V) level to 6.7 mg/L, before decreasing to a stable concentration of 1.37 mg/L (Figure 6.3). The initial increase in As (V) in the effluent could be due to a higher As (III) oxidation rate than the rate of As (V) adsorption by AA. The data in

Figure 6.3 also show the trend of arsenic breakthrough curve starting at only 24 h of the experimental run.

A very slow upward movement of the adsorption zone reflected by the gradual increase in the effluent As (V) levels before complete breakthrough of As (V) in the reactor was also exhibited by the data in Figure 6.3. The attached biomass on the AA beads measured at 0.98 ± 0.45 mg VSS/L, whereas, the DO measured at 3.67 mg/L at the end of the reactor operation.

The pH inside the reactor was adjusted at least twice a day with 0.1 N HCl solution. The actual pH measured during this run averaged at 8.9 ± 0.35 as shown in Figure 6.4. The instability of the AA beads used in this experiment was also observed with gradual disintegration of the beads noticed at the end of day 2 operation. This could be attributed to reactions between the AA surface and the HCl added for pH adjustment.

Similar pattern of the As (V) breakthrough curve was also observed under an influent As (III) concentration of 100 mg/L (Figure 6.5). A peak As (V) concentration of 11.9 mg/L was observed after 12 h of operation before reaching a low of 2.04 mg/L at the end of 96 h. The experiment was terminated after observing an As (V) concentration of 20.5 mg/L after 144 h of continuous operation (Figure 6.5). The average biomass measured at 0.24 ± 0.2 mg VSS/L, whereas, the DO measured at 2.97 mg/L respectively. The existing problem of large pH fluctuations (Figure 6.6) and disintegration of the AA beads was also observed in this experimental run. These two operating problems along with the probable competition from PO_4^{3-} for the same adsorption sites severely limited the performance of the reactor.
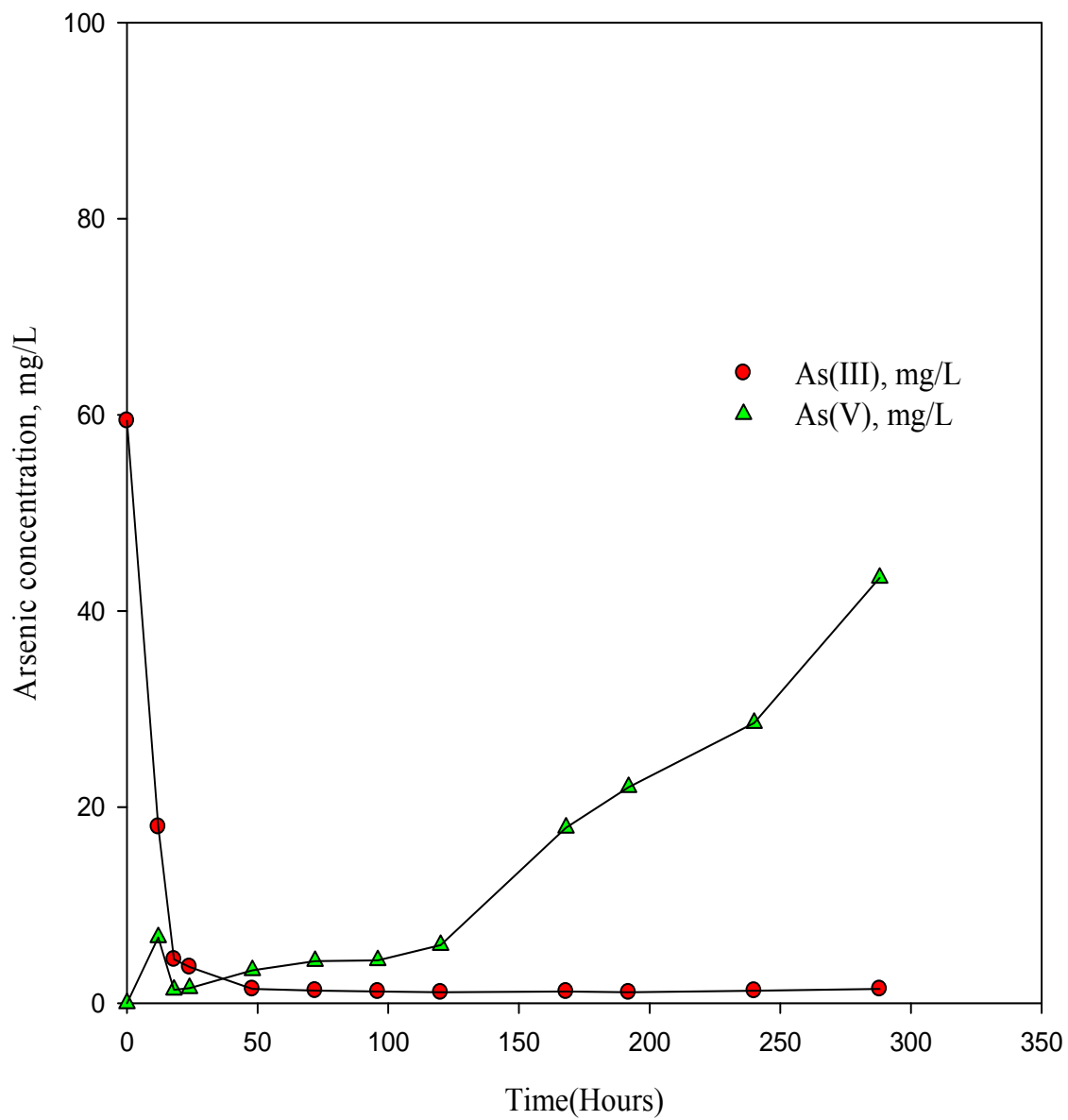
Figure 6.3 Performance of the column reactor under an influent As (III) concentration of
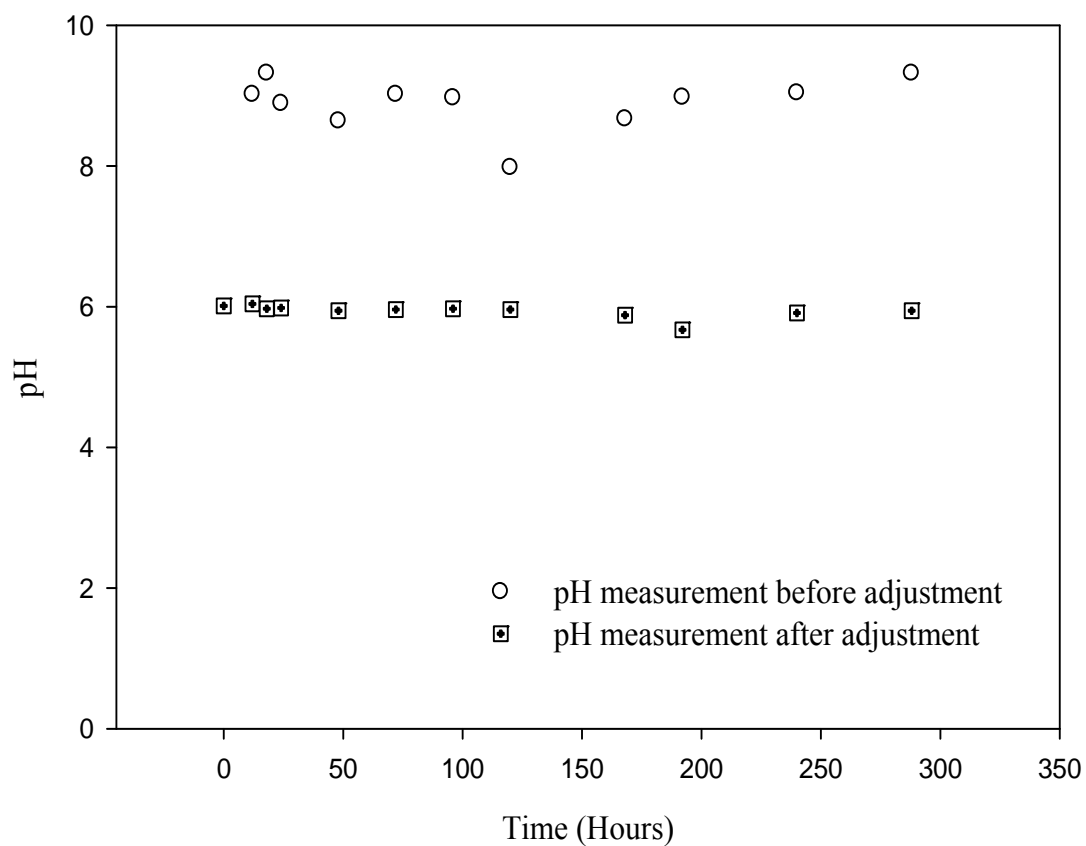
60 mg/L.

Figure 6.4 pH variations in the AA packed column reactor operated under an influent As (III) concentration of 60 mg/L.
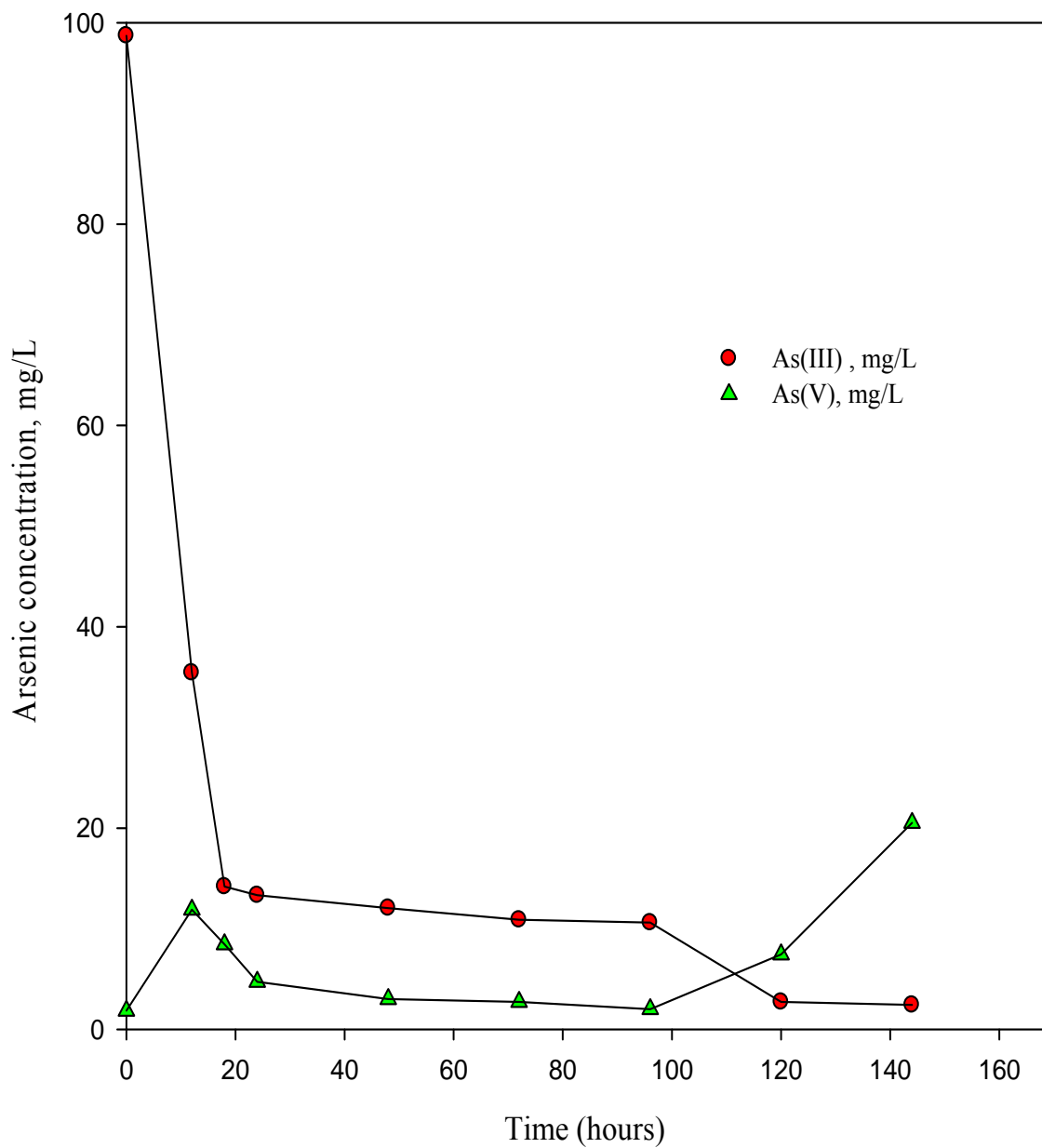
Figure 6.5 Performance of the AA column reactor under an influent As (III)

concentration of 100 mg/L.
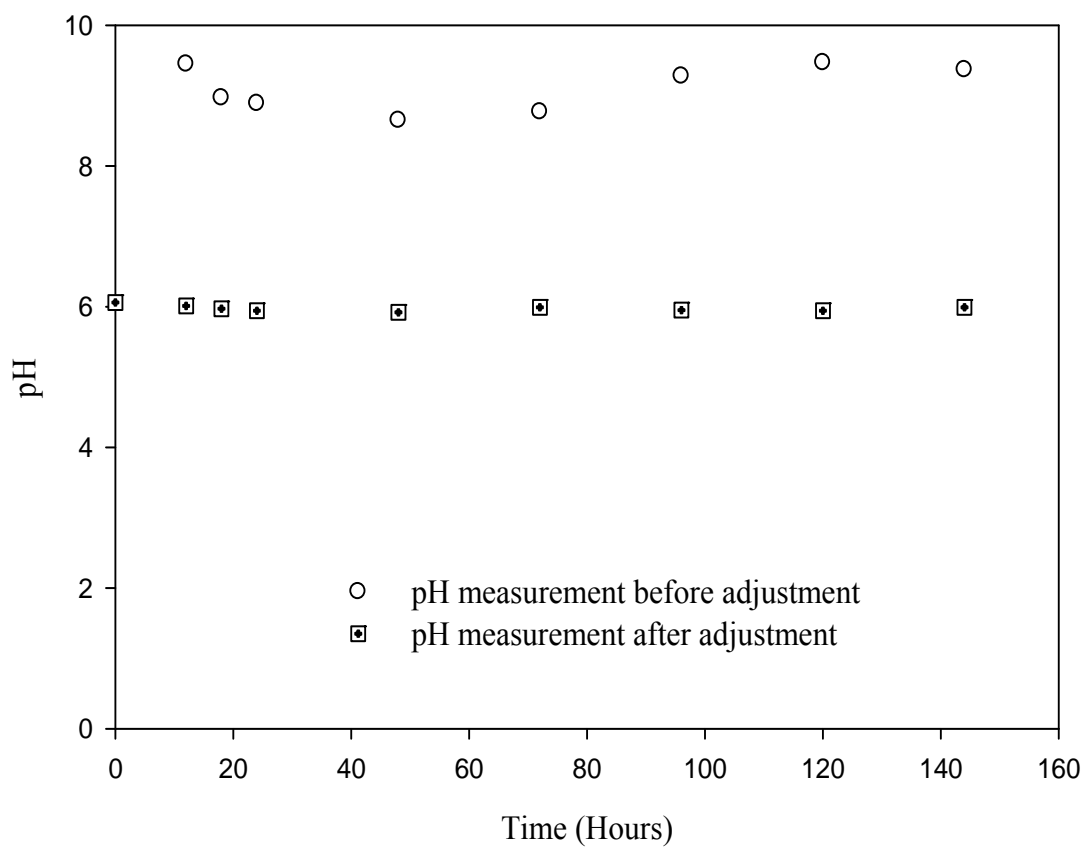
Figure 6.6 pH variations in the packed AA column reactor operated under an influent As (III) concentration of 100 mg/L.

6.5.2 Performance Analysis of the Two-stage Reactor

The performance of the two-stage reactor system was evaluated under an influent As (III) concentration of 500 mg/L at a HRT of 1 day for 41 days. The effluent steady-state As (III) and As (V) levels in the R1 averaged at 2.96 ± 0.39 mg/L, and 460.45 ± 20.35 mg/L, respectively. An average pH of 5.8 ± 0.15 and DO of 3.70 ± 0.17 was maintained during the entire R1 operation. It was also observed that the average effluent As (III) level in R1 was very similar to the average effluent As (III) of 3.17 ± 0.24 mg/L obtained in phase I of biofilm reactor operation (section 5.10.3). The operating conditions in phase I of the biofilm reactor experiment (section 5.3.2.1) were employed for the two-stage reactor experiment. The difference between the measured effluent As (III) levels in this study compared to the biofilm study was statistically insignificant ($p = 0.62$) with an average relative percent difference of 11.3 % (< 15%). The steady-state suspended cell concentration in R1 measured at 7.3 x 10^7 ± 1.5 x 10^7 cfu/mL. The confirmation of cell attachment on the glass beads was followed by the passage of the effluent As (III) and As (V) from R1 in an up-flow mode to the reactor R2 packed with AA beads on day 24 of the reactor operation.

During day 24 to 31 of R2 operation, the average effluent As (V) and As (III) concentrations were below their detection limits of 1 mg/L. The data in Figure 6.7 clearly indicated that both As (III) and As (V) from R1 were removed from R2. The actual pH measured at 7.23 ± 0.29 before adjustment with 0.1 N HCl and averaged 5.72 ± 0.48 which was within the optimum pH range of 5.5 - 6.0 with adjustment (Figure 6.8).

From day 31 onwards, the effluent As (V) levels in R2 started increasing and the breakthrough curve for As (V) was observed on day 41(Figure 6.7). The data in Figure

6.7 also showed that the effluent As (III) and As (V) were maintained at constant levels in R1 all throughout the reactors operation until day 41when As (V) breakthrough occurred. The reactors were thereafter dismantled and beads from R1 collected and analyzed for biomass.

The data in Figure 6.7 also showed the upward movement of the primary adsorption zone of As (V) along the column length with time. No arsenic was detected in the effluent from R2 for at least 9 days into the reactor operation. However, with the gradual saturation of the adsorption sites, the adsorption zone moved upward along the length of R2. Due to the continuous upward movement of the adsorption zone, more and more detectable amount of As (V) ions were observed in the effluent until an As (V) breakthrough was observed on day 41.

The data representing the ratio of effluent As (V) concentrations to the initial As (V) concentrations ($\frac{C}{C_o}$) in R2 were plotted against the bed volumes of AA as shown Figure 6.9.The As (V) breakthrough on the S-shaped or sigmoidal curve corresponded to the maximum allowable As (V) concentration. The point of column exhaustion (Kundu et al. 2004) on the sigmoidal curve corresponds to a C/C_o ratio of 0.95. Fornwalt and Hutchins (1996) reported that the operation of a single column would be more feasible when the position of the column exhaustion and the breakthrough point were very close to each other. However, if the breakthrough occurred much earlier than column exhaustion, then installation of multiple columns would be more feasible in the complete removal of arsenic. In this study, both the point of exhaustion and As (V) breakthrough

were very close to each other, indicating the feasibility of operating a single column

reactor for adsorption removal of arsenic from the effluent of R1 (Figure 6.9).

The similarity between As (V) ions and phosphate ion (PO_4^{3-}) makes PO_4^{3-} the

strongest competitor of As (V) for the same adsorption sites on AA (Williams et al.,

2003). Both arsenic and phosphorus appear in the same group (column) of the periodic

table. In this study, phosphate buffer ($H_2PO_4^-$ and HPO_4^{2-}) may have competed with

either $H_2AsO_4^-$ or $HAsO_4^{2-}$ for the adsorption sites on AA. The reason for an early

breakthrough of As (V) in R2 could be due to the high concentration (2500 mg/L) of

K_2HPO_4 and KH_2PO_4 used for pH buffering in R1. Such high concentrations of

phosphates were needed to maintain a pH in the optimum range of 5.5-6.0 for biological

oxidation of As (III). The presence of phosphates generally reduces the adsorption

efficiency of adsorbents including AA as reported in several other studies investigating

the chemical removal of arsenic from water (Zhang et al., 2003; Tripathy and Raichur

2008; Dixit and Hering 2003). Tripathy and Raichur (2008) reported that the adsorption

efficiency of the alum-impregnated activated alumina (AIAA) decreased by almost 27%

under a phosphate (PO_4^{3-}) concentration of 100 mg/L. Jain et al. (2000) reported that in

the presence of arsenic-to-phosphate ratio of 1:10, the adsorption capacity of amorphous

iron oxide (HFO) decreased from 100% to 60% for As (V) ions, whereas As (III)

adsorption decreased from 95% to almost 50% under the same ratio.
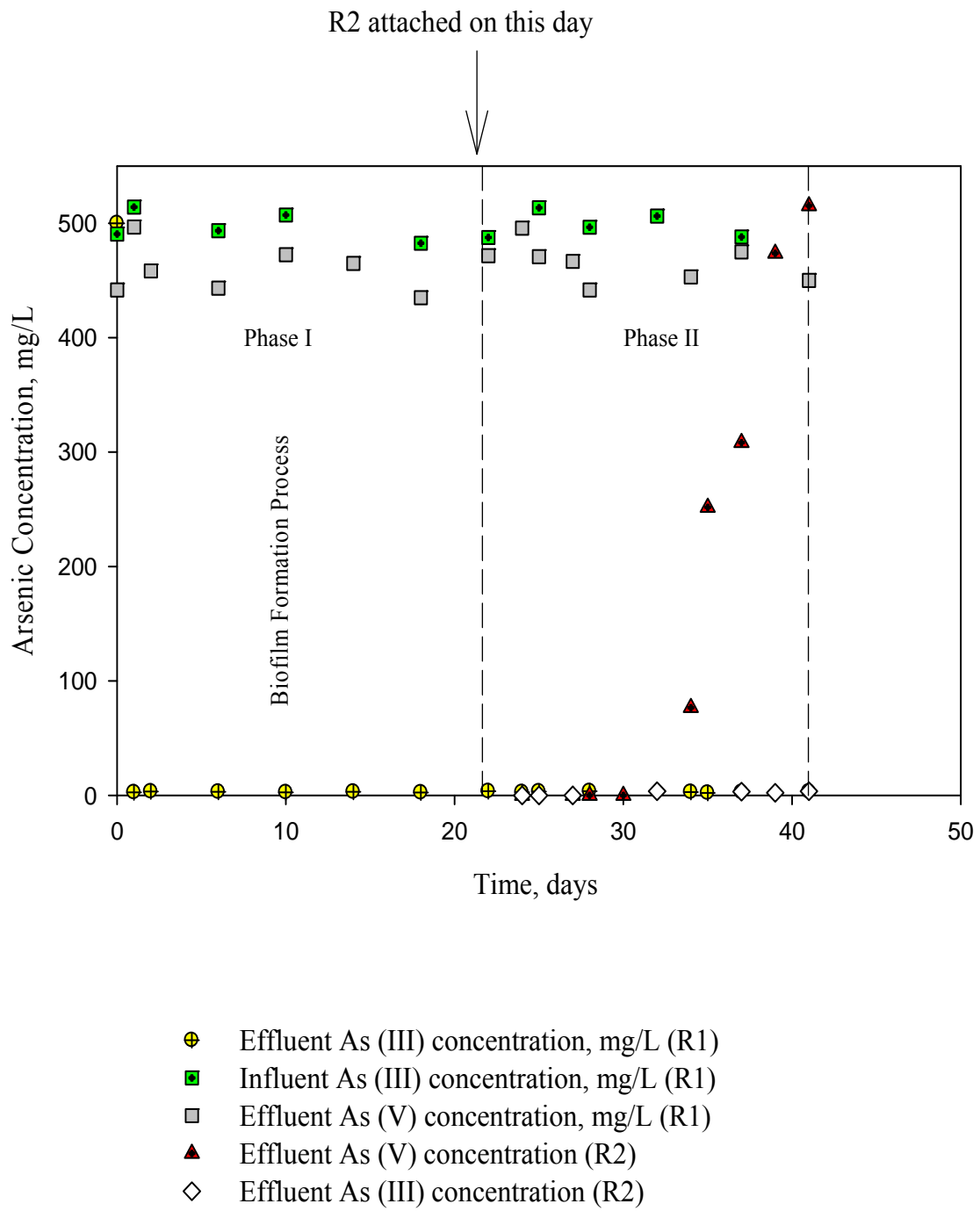
Figure 6.7 Performance of the two-stage reactor system for complete removal of arsenic
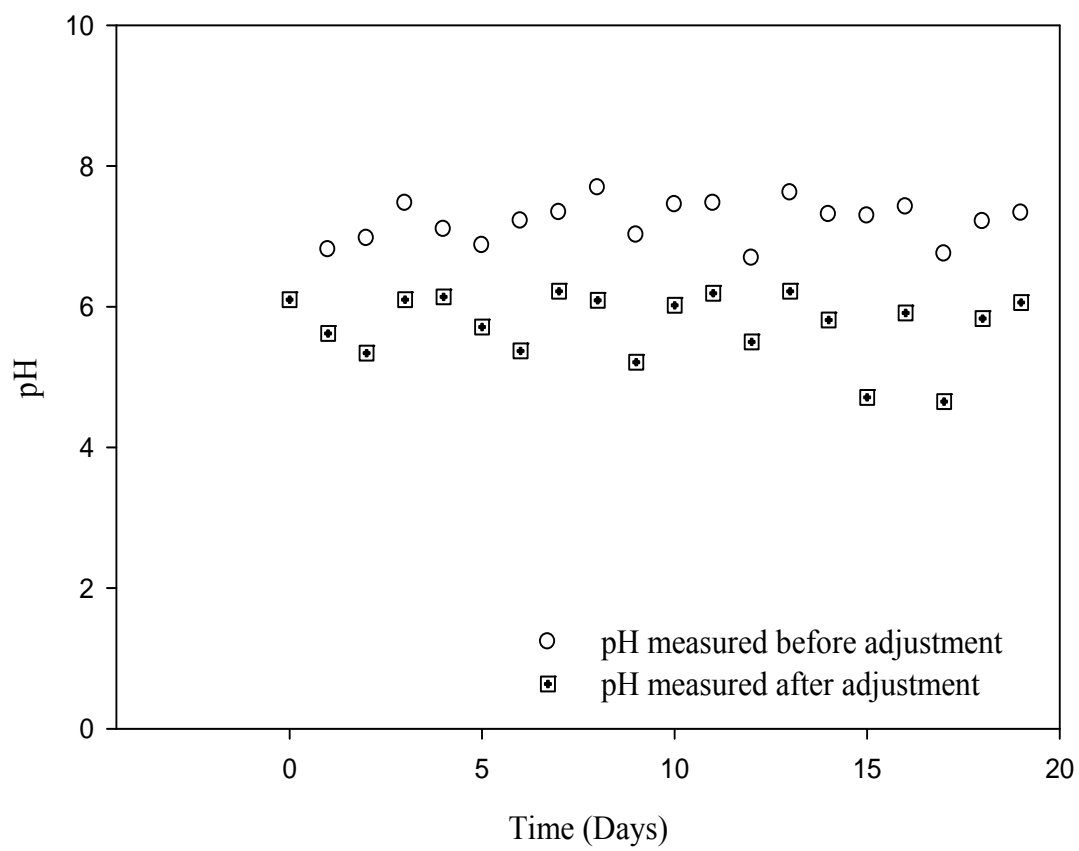
Figure 6.8 pH variations in R2 column reactor operation
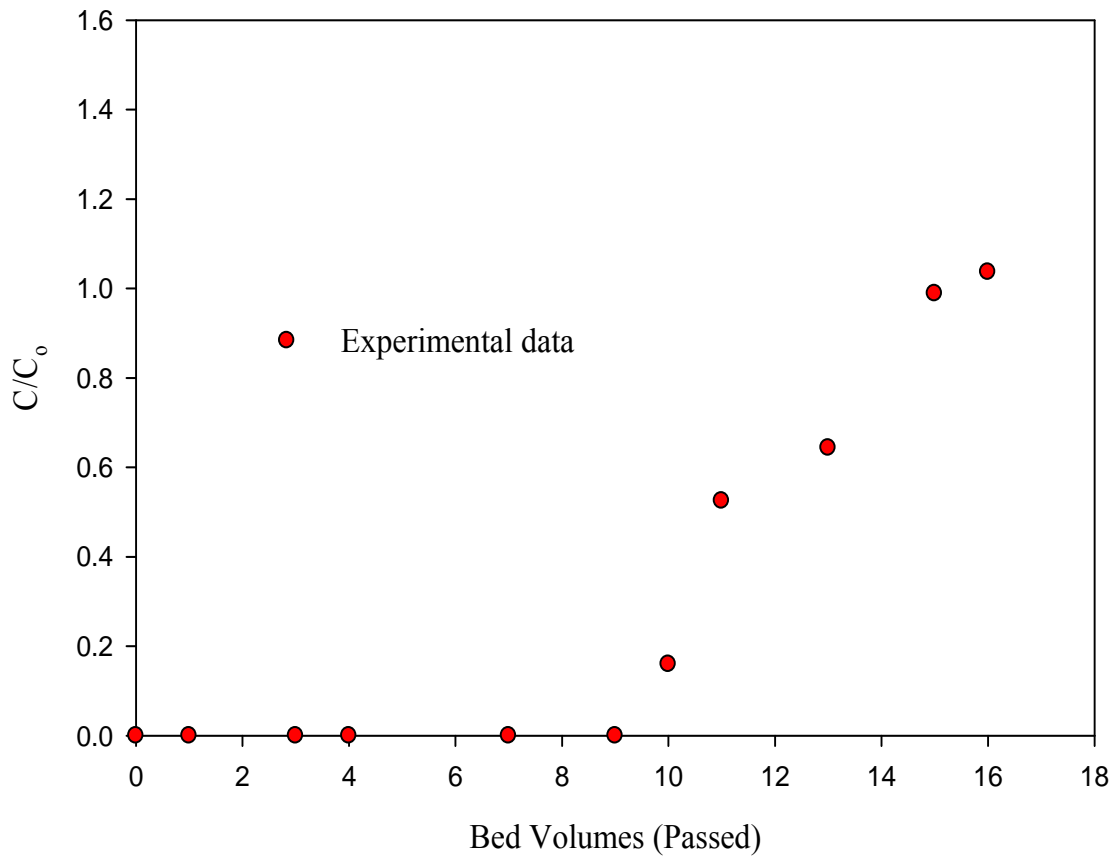
Figure 6.9 Breakthrough curve for arsenate adsorption in R2 column reactor operation with initial As (V) concentration of 500 mg/L and at pH of 6.0 (dose: 81 g, flow rate 3.49 mL/hr)

Other competing ions such as chloride (Cl$^-$), and sulfate (SO$_4^{2-}$) may cause varying degree of reduction in the adsorption efficiency of the AA. Clifford and Ghurye (2002) reported that sulfate concentration of more than 120 mg/L may severely impact the adsorption of As (V) on AA. However, Tripathy and Raichur (2008) reported that varying amount (0 – 100 mg/L) of nitrate, chloride, and sulfate resulted only 3 % decrease in the adsorption of As (V) on to AIAA column fed by an influent As (V) level of 10 mg/L.

The TOC (Total Organic Carbon) concentration in R1 averaged at 3.51± 0.28 mg/L, whereas in R2, the average value of TOC measured at 3.01± 0.46 mg/L (Figure 6.11). The observed TOC data from both R1 and R2 were most likely cell decay products and were also statistically insignificant (p = 0.12) at the 95% confidence level. The data in Figure 6.11 also suggest that there was no removal of TOC by the AA in R2. There is very little information present to suggest the effect of dissolved organic carbon (DOC) on As (V) adsorption by AA. However, a study conducted by Grafe et.al. (2002) showed that As (V) adsorption on ferrihydrite was decreased in the presence of citric acid. In this study, the effect of TOC on As (V) adsorption in R2 may not be significant due to its low levels.

6.5.3 Arsenic Removal Efficiencies

The data in Figure 6.10 show the performance of a one-stage and two-stage reactor systems for the complete removal of arsenic from water under varying arsenic loads. The two-stage reactor was able to maintain a total arsenic removal efficiency of 100% until an arsenic loading of 293.16 mg As. Thereafter, the efficiency of the two-stage process started decreasing with increasing arsenic load and with noticeable

concentrations of As (V) in the effluent of the system (Figure 6.7). This could be due to gradual saturation of the adsorption sites on the AA by As (V) or its strongest competitor PO_4^{3-} ions. The occurrence of complete As (V) breakthrough lead to significant reduction of the removal efficiency of the system, finally rendering it inefficient for further removal of As (III) or As (V) ions.

The one-stage process operated under an influent As (III) concentration of 60 mg/L performed slightly better in maintaining a higher arsenic removal efficiency ($\geq$ 90%) in comparison to the one operated under an influent As (III) of 100 mg/L at the same HRT of 1.0 day. However, the adsorption and desorption patterns were very similar as exhibited by AA in both the cases (Figures 6.3 and 6.5). Initially, with increase in arsenic loads, the total arsenic removal capacity of the one-stage system also increased before reaching peak arsenic removal efficiencies of 90 and 87% respectively (Figure 6.10). This behavior of the AA system could be attributed to the As (V) adsorption rate being higher than the As (III) oxidation rate. Thereafter, the arsenic removal capacity of the one-stage starts decreasing with increasing arsenic loads, suggesting saturation of the adsorption sites on the AA by the As (V) or PO_4^{3-}. The performance of the one-stage systems could be adversely affected by large pH fluctuations (Figures 6.4, 6.6) or strong competition from PO_4^{3-} ions for the same adsorption sites.

The data in Figure 6.10 clearly show that the two-stage system performed better than the one-stage system under the same As load. However, a direct comparison between the one-stage reactor systems and the two-stage reactor process is not feasible due to the difference in operating conditions and the AA materials used in the experiment. However, the pH fluctuation in the two-stage reactor process was better

controlled near the optimum range of 5.5 – 6.0 (Figure 6.8) indicating the probable reason for improved performance compared to the one-stage system.

More studies are needed to ascertain the various specific factors influencing the adsorption of As (V) formed by microbial oxidation of As (III) and gain insight into the biological / physico / chemical processes for total As removal from water.

6.5.4 Adsorption Isotherm

The data in Figure 6.12 showed that As (V) adsorption on AA increased from 58.4% to 95.2% by increasing the AA dosage from 33.3 g/L to 166.7 g/L in the batch adsorption study. This is most likely due to the increase in the available surface for the adsorption of As (V) ions. There was minimal change in the residual As (V) concentration in the solution after the AA reached its maximum adsorption capacity.

6.5.4.1 Langmuir and Freundlich Isotherms

Both Langmuir and Freundlich Adsorption isotherms were used to investigate the extent of adsorption of As (V) by AA under an initial As (V) concentration of 500 mg/L. The equilibrium data fit really well in the Freundlich form compared to Langmuir form as shown in Table 6.1. The correlation coefficient (R^2 = 0.95) obtained in Freundlich form (Figure 6.14) was much better than R^2 value of 0.89 obtained with the Langmuir fit (Figure 6.13). The parameters obtained from both the adsorption isotherms are listed in Table 6.2.

The obtained Langmuir q_m and b values (7.95 mg As (V)/ g of AA; 0.02 L/mg) indicated probable multilayer adsorption of As (V) on AA particles (Chakravarty et al. 2002) instead of monolayer. However, the total uptake capacity of the fixed-bed reactor calculated by integrating the area above the breakthrough curve between the point

corresponding to zero BV and the saturation point was 6.42 mg As (V) /g of AA. The lower estimated value could be due to mass transfer limitation in the fixed-bed reactor because of the extremely closely packed AA beads. In batch adsorption isotherm studies with AA, mass transfer limitation is generally negligible due to the rigorous shaking of the orbital shaker.

The observed low value of the affinity constant (b = 0.02 L/mg) indicated the presence of very weak adsorption bond energy between AA and As (V) ions. This may be because of the strong competition from phosphate ions ($H_2PO_4^-$; HPO_4^{2-}) for the same adsorption sites on AA. The low value can be also due to competition from other ions such as SO_4^{2-} and Cl^- present in the feed of R2.

The dimensionless separation factor or the equilibrium parameter "r" which expresses some of the essential characteristics of the Langmuir adsorption isotherm was estimated to be 0.09. The calculated value was well within the range of 0 - 1 indicating favorable adsorption of As (V) on AA sites (Mckay et al. 1982). However, as mentioned earlier, the adsorption was likely affected by the presence of other competing ions for the same adsorption sites.

The 1/n parameter value (0.48) from Freundlich adsorption isotherm was less than 1 also indicating favorable adsorption of As (V) on AA (Bouguerra et al., 2007; Soon-An et al., 2007).

6.6 Summary and Conclusion

Preliminary results showed that the two-stage column reactor was more efficient in the complete removal of arsenic compared to the one-stage process. The major problem encountered in the operation of the one-stage process was the disintegration of

the AA material only on day 2 of the reactor operation. The maintenance of pH around the optimum range of 5.5-6.0 was also difficult with the observance of wide pH fluctuations. The two-stage reactor performed better with effluent As (V) concentration below the detection limit for at least 9 days into the reactor operation. However, the overall efficiency of the reactor was likely limited by significant pH fluctuations, and the presence of potential competing ions such as PO_4^{3-}, Cl^-, and SO_4^{2-}, respectively. Further investigation is required for the optimal design of a reactor system to achieve complete removal of arsenic for a longer operating time.
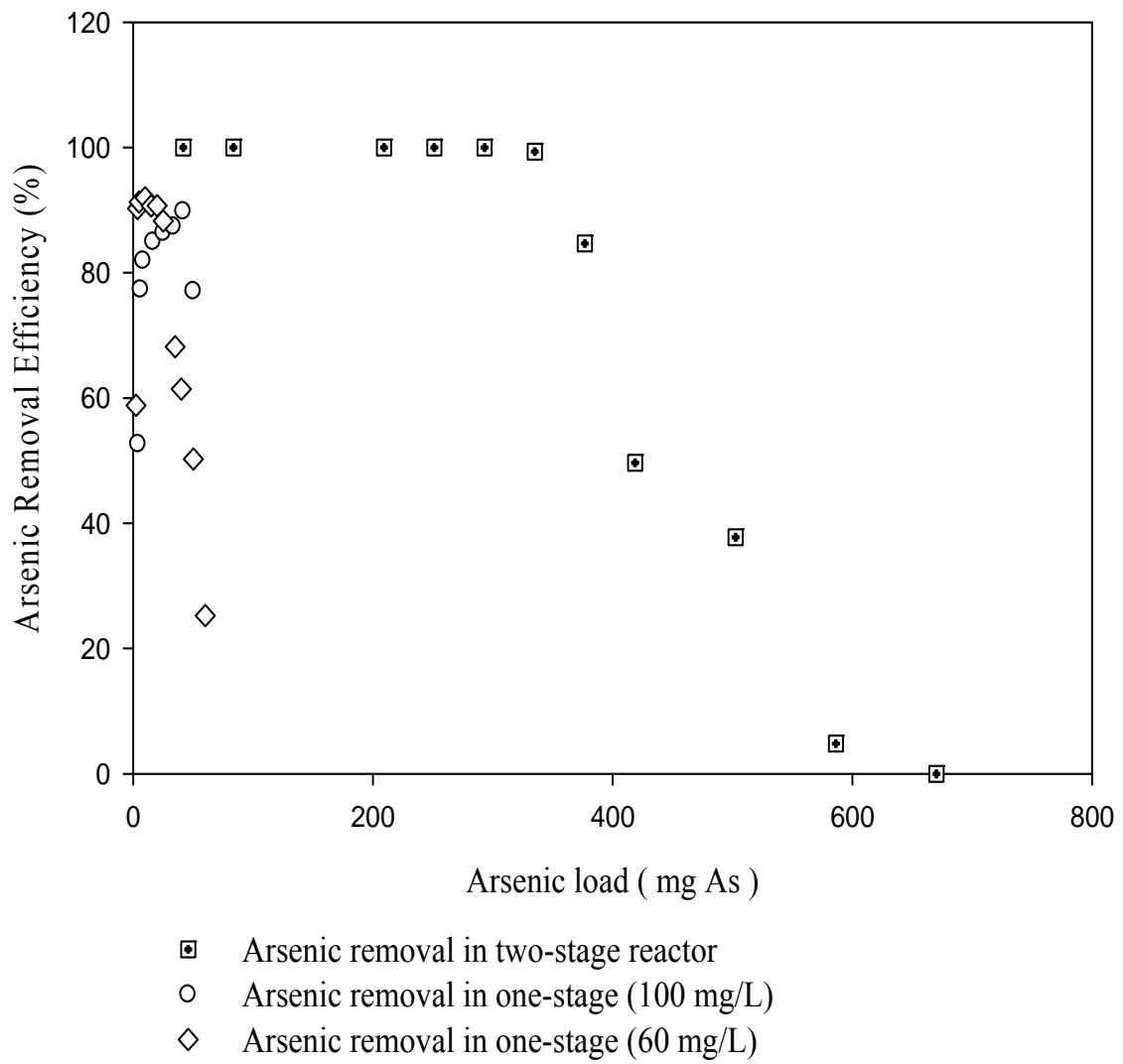
Figure 6.10 Plot of total As removal efficiency of the one-stage and two-stage reactor systems
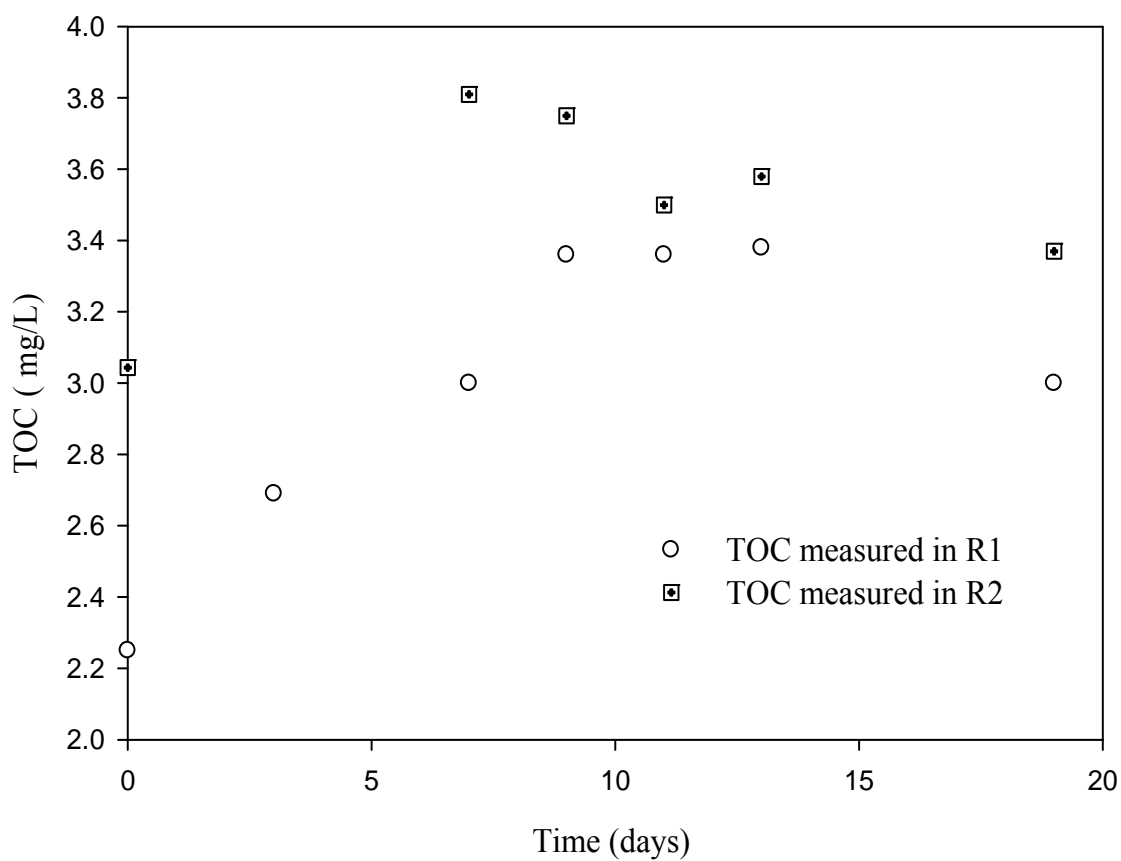
Figure 6.11 TOC concentration measured in R1 and R2 during day 24 – 41 of the

reactors operation (Day 0 indicate the time R2 was attached to R1).
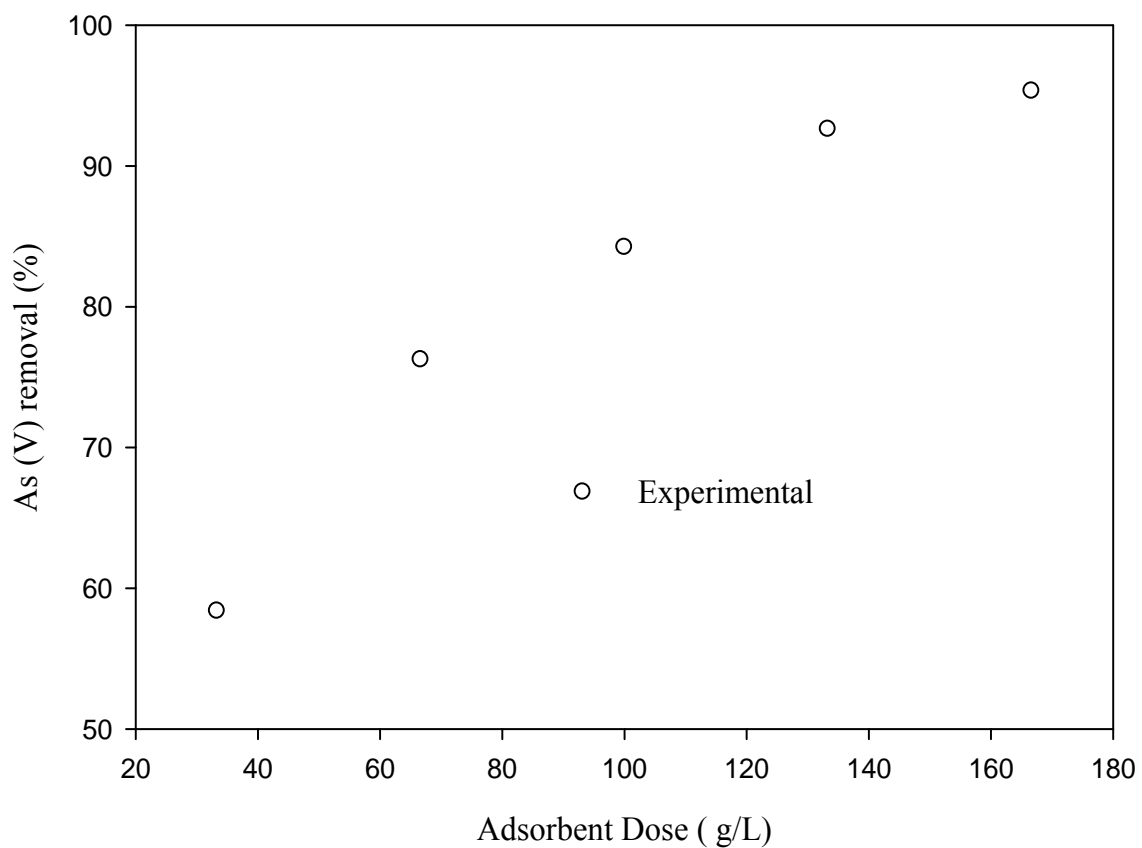
Figure 6.12 Variation of adsorbent doses (g/L) for measuring (%) arsenic removal. Condition: pH 5.7±0.5 (0.1 N HCl), As (V) concentration = 500 mg/L, adsorbent dose varying between 33.33 g/L – 166.67 g/L.

Table 6.2 Langmuir and Freundlich isotherm parameters for As (V) adsorption on AA

Parameter	Value	R^2
Langmuir isotherm		
q_m (mg/g)	7.95	0.89
b (L/mg)	0.02	
Freundlich isotherm		
K (mg/g)	0.58	0.95
1/n	0.48	
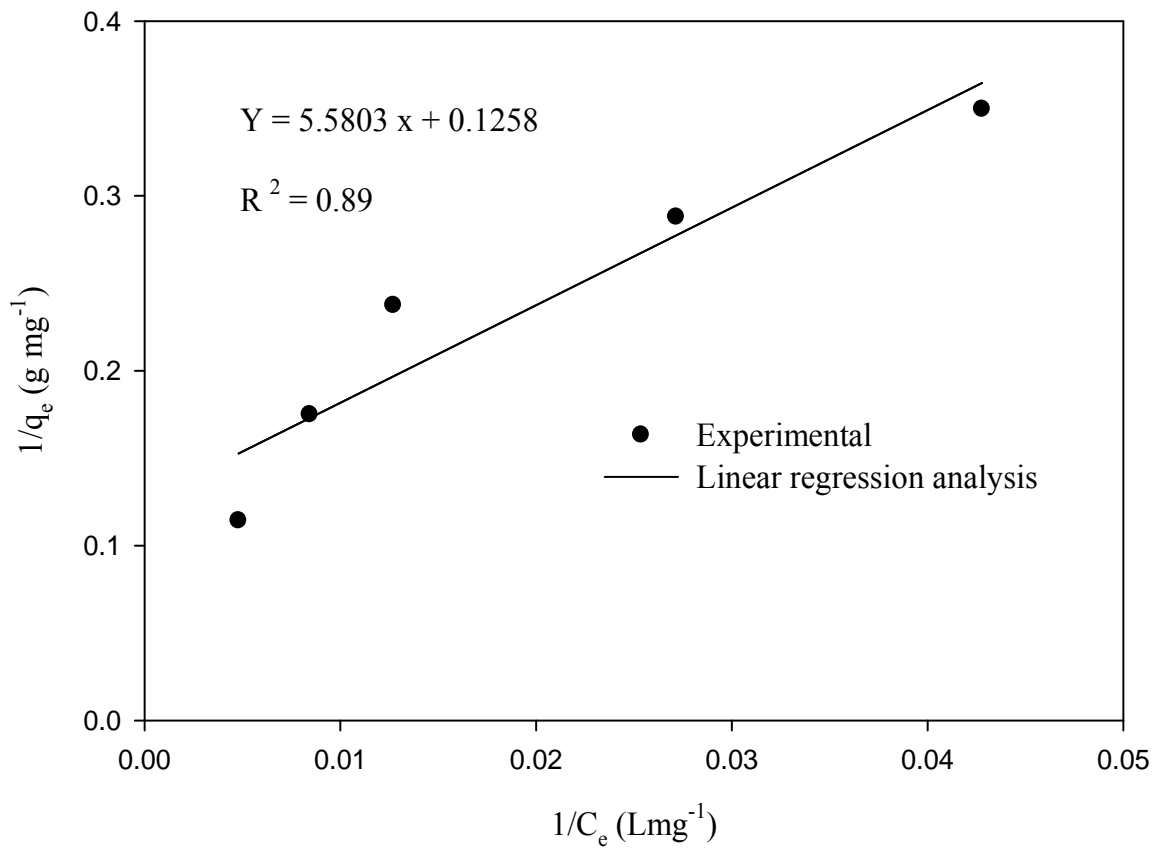
Figure 6.13 Langmuir plot for adsorption of As (V) on Activated Alumina

Y = 0.4873 x - 0.2349

$R^2 = 0.95$
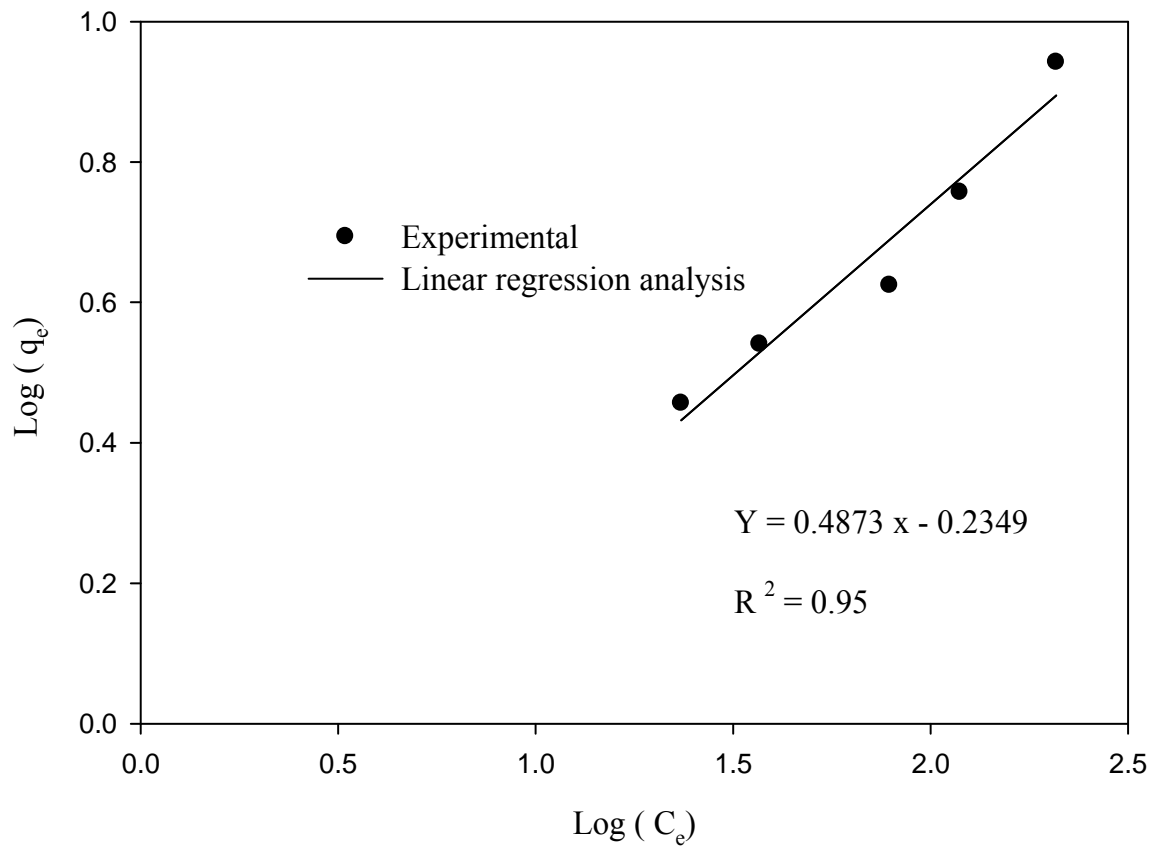
Figure 6.14 Freundlich plot for adsorption of As (V) on Activated Alumina.

Chapter 7: Environmental Implication and Future Research

The pre-oxidation step governing the transformation of As (III) to As (V) is essential for the effective removal of arsenic from water. This step is desirable because As (III) is more toxic and mobile than As (V). Chemical oxidation methods have been used with reasonable success but with the disadvantage of formation of potential harmful by-products. Biological oxidation of As (III) to As (V) using both heterotrophic and chemolithoautotrophic strains only recently has been investigated in bioreactor system technology as an alternative. However, the practical application of this novel chemoautotrophic bacterium *T. arsenivorans* strain b6 in the remediation of arsenic contaminated water would require more specific future research work in the following areas:

1. Batch study may be conducted to investigate whether the *T.arsenivoran*s strain b6 can simultaneously use multiple electron acceptors during As (III) oxidation. In the biofilm study, large difference was reported between the theoretical and actual oxygen uptake by the strain b6 for all the phases of operation. One of the potential reasons for this difference was attributed to the presence of multiple electron acceptors (O_2 and SO_4^{2-}) during the oxidation process. Another probable reason was the use of SO_4^{2-} as an electron acceptor under slightly anaerobic conditions during the biofilm reactor. However, more studies are needed to ascertain the exact cause for this large discrepancy in the measured and theoretical oxygen uptake values.

2. The overall mass balance expressions for arsenic and biomass could be used for the non-linear estimation of the four biokinetic parameters. The transient conditions in the CSTR are very similar to that of the batch study, which would lead to a meaningful

comparison of the obtained parameters from both the studies. Future work could also focus on the effect of an effluent recycle line during As (III) oxidation to As (V) in the CSTR. It would be interesting to investigate if the effluent As (III) level could be lowered below the acceptable drinking water standards. A very important parameter in the operation of the CSTR is the utilization of CO_2 by strain b6 for cell synthesis during the oxidation process. Detailed studies may be performed to evaluate whether CO_2 can be limiting during As (III) oxidation to As (V). Experimental work aided with the development of a mechanistic model can focus on the metabolism pattern of the strain b6 particularly during the operation of the CSTR with long HRTs. The operation of a CSTR with long HRTs causes significant cell lysis prompting a probable shift in the metabolism of the concerned strain.

3. A transient biokinetic model may be developed for simulating the steady-state and transient conditions in the biofilm reactor operation. One of the key features of the transient model would be the inclusion of oxygen utilization along with As (III) oxidation. The attachment of cells on nanomaterials could be also attempted to achieve longer duration of the experimental run and higher As (III) oxidation efficiency.

4. More studies are needed to obtain information regarding the effect of various ions competing for the same adsorption sites on the AA. Phosphate ions are generally known to be the strongest competitor of As (V) and thus removal mechanism may be developed for removing PO_4^{3-} or $H_2PO_4^{-}$ or HPO_4^{2-} prior to the start of the adsorption process. The effect of varying pHs on As (V) adsorption can be further probed to improve the overall efficiency of the arsenic removal process. The by-products as a result of the

biological / chemical process may be also investigated to eliminate any concern of the presence of any harmful contaminants in water.

Chapter 8: Summary and Conclusions

A pre-oxidative step transforming As (III) to As (V) is very effective in the treatment of arsenic contaminated water. The As (III) oxidation ability of the novel chemoautotrophic *Thiomonas arsenivorans* strain b6 was investigated in batch and continuous flow bioreactors. The results of the studies are summarized as follows:

1. The As (III) oxidation capacity of the strain b6 was first investigated in batch reactors under varying As (III) and initial cell concentrations. The strain was able to completely oxidize As (III) levels ranging from 500 to 1,000 mg/L at optimum pH of 6.0 and temperature of 30°C with significant inhibition observed at higher As (III) concentrations ($\geq$ 500 mg/L). The Haldane-substrate inhibition model was used for the determination of the biokinetic parameters using a non-linear least square estimation technique. The model fit well for all the As (III) oxidation curves pertaining to varying initial As (III) concentrations. Sensitivity analysis revealed the model to be most sensitive to Y and K_i whereas, k_d was the least sensitive to model simulations at both high and low As (III) concentrations.

2. The first continuous flow bioreactor to be investigated for As (III) oxidation under varying As (III) loading rates was a completely mixed continuous stirred tank reactor (CSTR). The bioreactor operated under varying As (III) loading rates exhibited excellent As (III) oxidation efficiency exceeding 99% for all the five steady-state conditions in the reactor. The CSTR also demonstrated strong resilience by recovering from an As (III) overloading phase during the bioreactor operation. The intrinsic biokinetic parameters estimated by a linearized technique in this study varied widely from the ones obtained in the batch study. The probable reasons for these variations have

been described in detail in the CSTR study. Very good agreement was observed between the observed data and the transient model simulations. The results of the sensitivity analysis showed that changes in Y and k significantly affected the model outcome compared to the other parameters (K_s and k_d).

3. A fixed-film reactor was the second continuous flow bioreactor to be investigated for As (III) oxidation under varying As (III) loading rates. The As (III) oxidation efficiency of the reactor ranged from 48.2% to 99.3 % for the seven steady-state conditions obtained during the bioreactor operation. Similar to the CSTR, the biofilm reactor also demonstrated strong resilience in recovering from an As (III) overloading phase. The biokinetic parameters determined using the steady-state As (III) flux data and a predictive Monod model were closely related to the ones obtained from the CSTR. The parameter k was found to be very sensitive to model predictions compared to the parameter K_s.

4. The biokinetic parameters obtained in batch and continuous flow studies are summarized in Table 8-1. There could be several potential reasons for the variation in the parameter estimates as mentioned in the chapters 3, 4, and 5. However, these parameters are unique because they are representative of their respective reactors which were operated under different operating conditions. Pure cultures of the same strain may behave very differently in batch, CSTR, and biofilm reactors.

5. The final phase of the research work focused on a preliminary study investigating the potential of a coupling process (biological and chemical) for the complete removal of arsenic from water. The results of the study are summarized below:

The completion of the pre-oxidation step in the batch, CSTR, and biofilm reactors was followed by a preliminary study investigating the potential of a combination of biological and chemical process for the total removal of arsenic from water. The investigation focused on a one-stage and two-stage reactor systems operated under varying influent As (III) concentrations. The fundamental principle of both the processes was based on biological oxidation of As (III) to As (V) and the subsequent adsorption of As (V) on activated alumina (AA) for the complete removal of arsenic. The performance of the one-stage reactor was severely limited by disintegration of the AA material and competition from other ions for the same adsorption sites on AA. The performance was also affected by the failure to maintain the pH around the desired optimum range. In comparison, the two-stage process was successful in keeping the total arsenic level below the detection limits for at least 9 days into the reactor operation. However, high phosphate concentration and the severe difficulties in maintaining the pH around 5.5-6.0 also limited its application in the complete removal of arsenic from water.

Table 8.1 Summary of Obtained Biokinetic Parameters from Bioreactor Studies

Studies	k (mg As (III)/mg cells.hr)	K_s (mg/L)	k_d (hr^{-1})	Y (mg cells/mg As (III))	K_i (mg/L)
Batch Reactor Study	0.85±0.18	33.2±1.87	0.006±0.002	0.088±0.0048	602.4±33.6
CSTR Study	5	20.1	0.008	0.011	-----
Biofilm Study	4.24±0.63	13.2±5.6	------	-----	-----

APPENDICES

APPENDIX A: Quality Assurance and Quality Control

Introduction

Quality Assurance (QA) is characterized by a set of operating principles implemented during sample collection and analysis so as to produce defensible quality data. On the other hand, Quality Control (QC) guidelines are adopted in an experimental procedure to assure credibility of the obtained data (APHA 1995). Both the procedures limit to a great extent the introduction of error into the measured / analytical data.

Arsenic Analyses by Silver Diethyldithiocarbamate (SDDC) Method

As (III), and effluent total As ions were analyzed by the SDDC method. As (V) was analyzed by an Ion Chromatography during the batch study, and by the SDDC method for the remainder course of the study.

Samples were generally analyzed in one batch consisting of no more than seven samples each of As (III), As (V), and total As. A new standard curve for As (III), As (V), and total As was prepared for each analysis with known standards of 0.0, 1.0, 2.0, 5.0, 10.0 and 20.0 µg As. The corresponding absorbance values were measured at 520 nm using a spectrophotometer (Spectronic Instrument, Rochester, NY). Representative standard / calibration curves are shown in Figures C-1, C-2, C-3, and C-4, respectively.

Lab water (deionized distilled water: 18 Ω H_2O) used for the experiment and sample analyses was also tested for the presence of any As (III), or As (V) ions to ensure that the instrument reading (absorbance reading) was below the MDL (Method Detection Limit) level for each analyte in the water. MDL is defined "*constituent concentration, that when processed through the complete method, produces a signal with 99% probability that is different from the blank*" (APHA 1995). If the blank samples showed

any presence of As (III) or As (V) ions, the entire analysis was repeated to ensure that there was no possible source of contamination / interference during the analyses. The RSD (Relative Standard Deviation) of the samples measured using the SDDC method is ± 10% according to APHA (1995). However, laboratory analyses of arsenic samples determined the RSD to be at ± 15%.

As (V) analysis by Ion Chromatography (IC) method

As (V) was analyzed by ion chromatograph (IC) (model IC 25, Dionex Corp., Sunnyvale, CA) equipped with an Ion Pac® As 18 analytical column (4 x 250 mm, Dionex) and Ion Pac® AG 18 guard column (4 x 250 mm, Dionex) according to the EPA method 300.0 (U.S. EPA 1993). The operating conditions have been summarized in Table A-1. The retention time used for the analysis was 8 mins.

The method developed using IC for As (V) analysis was verified using Linear Calibration Range (LCR), Quality Control Sample (QCS), and Method Detection Limit (MDL) in accordance with method 300.0 (EPA 1985). A calibration curve was prepared using standard As (V) concentrations 1, 10, 20, 50, 100, 200 mg/L (Figure C-2). Samples with higher As (V) concentrations were diluted to fit the absorbance reading within the standard linear range. The prepared calibration curve was verified using QCS sample during analysis. The QCS sample consisted of DDW and known calibration verification (CV) of As (V). The CV was basically a freshly prepared solution of 50 mg/L of As (V) in DDW. Both these samples were run against the already established standard As (V) calibration curve. According to the EPA (1985) guidelines, the determined As (V) should be within ± 10% of the stated values. If the determined value was beyond the acceptable range, a new standard calibration curve for As (V) had to be prepared. The QCS was

performed after every 10 analysis (eight samples plus blank and CV). The detection limit of the IC method for As (V) analysis was verified by conducting the MDL procedure. The analysis consisted of very low As (V) concentrations of 0.0, 0.5, and 1.0 mg/L dissolved in DDW. The MDL of the IC method for the detection of As (V) was evaluated to be at 1 mg/L.

 Total Organic Carbon (TOC) analysis

Total Organic Carbon (TOC) of the samples was determined using Total Organic Carbon Analyzer (TOC-5000 ACE, Shimadzu scientific). The TOC of the samples was measured using this following equation:

$$\text{TOC (mg/L)} = \text{TC (Total Carbon)} - \text{IC (Inorganic Carbon)} \qquad \text{(A-1)}$$

As evident from Eq. (A-1), the instrument measured TC and IC of the collected sample and the TOC value was obtained from the difference of the two. The calibration curves for the measurement of TC and IC were already prepared in advance to the analyses. The calibration curves were prepared with concentrations of 1, 2, 5, and 10 mg/L, respectively (Figures C.7, C.8). On the day of the analysis, both the calibration curves were verified by running a known standard (CV: calibration verification) sample against the standard curves. If the measured concentration of the CV sample exceeded ±10%, new standard curves for both TC and IC were established using the same concentrations range to eliminate any bias during measurement. The Quality Control Sample (QCS) included a blank (DDW) and the CV sample and they were both run against the standard curves for TC and IC before and after the completion of the analyses. The MDL of the method for the determination of TOC of samples was 1 mg/L.

Protein Analysis

Protein concentration was determined by a colorimetric method (Micro Test Tube Protocol method) for the total protein quantitation of the collected sample (Bradford 1976). The method has been modified to reduce the non-linear response of the Coomassie Plus Reagent by improving the linearity of a defined range of protein concentration. A protein standard curve was prepared by diluting the contents of one Albumin Standard (BSA) ampule (2mg/mL) into several vials containing the same diluent of different volumes as that of the collected samples. A working range of 1-25 µg/mL was selected for the protein standard curve as shown in Figure C.6. All samples were analyzed in triplicates and the values were reported as average ± SD (standard deviation). The absorbance of the collected samples was measured at 595 nm using a spectrophotometer (Spectronic Instrument, Rochester, NY). The MDL of the Bradford method is 1 µg/mL of protein concentration in collected samples.

The protein standards were verified every time by running a known CV of 2.5 and 5 µg/mL against the already established standard curve prior to each analysis. A new curve was constructed if the determined protein value exceeded ± 10% of the stated values. Samples collected for determining protein concentrations were analyzed immediately after collection.

Viable Cell Count and Biomass Dry Weight

Samples collected for the determination of viable cell count and biomass dry weight were analyzed in triplicates. Replicate analysis of a given same sample showed a maximum RSD of ± 15% in case of both viable cell count and biomass dry weight.

However, a RSD of ± 20% was set as the criteria for sample rejection under both the categories.

Quality of Data

The quality of the obtained data would depend on two important factors: (i) Analytical precision (precision and bias of the analytical method), and (ii) Experimental precision (precision and bias of the experimental method). Precision indicate the similarity or closeness of the values obtained by performing multiple analyses ($n \geq 3$) of a given sample, whereas, bias measures the systematic error. The precision obtained using the SDDC method expressed as the relative standard deviation percentage was ± 15%. This was little higher compared to the ± 10 % reported in the standard methods for the examination of water and wastewater (APHA, 1995). The bias due to the method is not available because of the lack of interlaboratory comparison data (APHA, 1995). However, the laboratory bias determined by subtracting the true value from the laboratory average recovery was 5.34% (100 (true value) – 94.65 (laboratory average)). The other three forms of precision which can be used to denote the accuracy of the experimental data are as follows (Suttigarn 2005):

(i) Precision of the experimental data ($\bar{X} \pm SD$)

(ii) Precision of the estimated mean ($\bar{X} \pm SE$), where $SE = \dfrac{SD}{\sqrt{n}}$ (n = number of samples)

(iii) Confidence interval ($\bar{X} \pm t_{n-1}SE$), where t_{n-1} is the t-test statistics value obtained at the desired confidence level.

Sample Rejection Criteria

The criterion for rejection of samples analyzed by the SDDC method was set at a RSD of ± 15%. However, for protein and TOC analysis, the criteria were little stringent at RSD of ± 10%. Biomass analysis was always subjected to a lot of variations and thus the criterion was set at a higher a limit of RSD ± 20%.

Appendix B: NOMENCLATURE

S = As (III) concentration (ML^{-3})

S_o = Initial As (III) concentration (ML^{-3})

S_i^{obs} = Observed As (III) concentration at the ith sample point (ML^{-3})

S_i^{pred} = Predicted As (III) concentration at the ith sample point (ML^{-3})

t = time $[T]$

k = maximum specific As (III) utilization rate $(MM_x^{-1}T^{-1})$

X = cell concentration (ML^{-3})

X_o = Initial cell concentration (ML^{-3})

K_s = Saturation constant (ML^{-3})

K_s^p = Best fit Saturation constant (ML^{-3})

ΔK_s = variation in the best fit value of the Saturation Constant (ML^{-3})

K_i = inhibition coefficient (ML^{-3})

Y = cell yield coefficient $(M_sM_x^{-1})$

M_s = Mass of the substrate (ML^{-3})

M_x = Dry weight of the cells (ML^{-3})

k_d = endogenous decay coefficient (T^{-1})

σ^2 = Mean Square fitting error

n = number of observed data points

p = number of fitted parameters

S_i = influent As (III) concentration (ML^{-3})

S = As (III) concentration (ML^{-3})

X_i = initial biomass concentration (ML^{-3})

X = biomass concentration (ML^{-3})

μ = specific growth rate of the bacterial strain b6 (T^{-1})

Q = liquid flow rate (L^3T^{-1})

V = volume of the reactor (L^3)

μ_m = maximum specific growth rate of the bacterial strain b6 (h^{-1})

τ = hydraulic retention time (T)

θ_x = mean cell residence time (T)

P_x = biomass productivity ($ML^{-3}T^{-1}$)

P_s = As (V) productivity ($ML^{-3}T^{-1}$)

$q_{As(III)}$ = specific As (III) oxidation rate ($MM_x^{-1}T^{-1}$)

X_f = Biomass density ($M_x L^{-3}$)

L_f = Biofilm thickness (L)

L = Effective mass transfer diffusion layer thickness (L)

S = Bulk substrate concentration (ML^{-3})

S_f = Substrate concentration in the biofilm (ML^{-3})

S_w = Substrate concentration on the attached surface (ML^{-3})

$D_{As(III)}$ = diffusion coefficient of As (III) in water (L^2T^{-1})

T = absolute temperature (K)

R = Universal gas constant (J/mol K)

F = Faraday's constant (C g mol)

λ = Electrolytic conductance (cm^2 ohm c)

$|z|$ = charge on the ion

ε = Porosity

V_v = volume of the void-space in the medium bed (L^3)

V_T = total or bulk volume of the medium bed (L^3)

μ = absolute viscosity of water ($ML^{-1}T^{-1}$)

Re_m = modified Reynolds number

ρ = density of water (ML^{-3})

d_p = diameter of the solid medium (L)

u = superficial velocity (LT^{-1})

A_c = cross sectional area (L^2)

Sc = Schmidt number

D_f = molecular diffusivity of As (III) in biofilm (L^2T^{-1})

a = biofilm specific surface area (L^{-1})

n = number of glass beads

A = surface area of a glass beads (L^2)

V = empty bed volume of the reactor (L^3)

W_w = wet weight of the biofilm (M)

W_d = biofilm dry weight (M)

S_e = effluent As (III) concentration (ML^{-3})

J_{exp} = observed steady-state As (III) flux ($M/L^2.T$)

VL = volumetric As (III) loading rate ($MT^{-1}L^{-3}$)

$J_{As\ (III)}$ = mass of As (III) applied per unit biofilm surface area per unit of time ($ML^{-2}T^{-1}$)

M_s = total mass of glass beads in the reactor (M)

a/m = surface area per unit mass of the glass beads (L^2M^{-1})

v = As (III) oxidation rate ($ML^{-3}T^{-1}$)

Q_r = recycle flow rate (L^3T^{-1})

S_s = As (III) concentration at the biofilm/liquid interface (ML^{-3})

D = diffusion coefficient of As (III) in water (L^2/T)

η = ratio of the actual flux to the flux that would occur in a fully penetrated biofilm

φ = Thiele modulus

$J_{prAs(III)}$ = model predicted As (III) flux in the biofilm ($ML^{-2}T^{-1}$)

b' = overall biofilm loss coefficient (T^{-1})

b = cell decay coefficient (T^{-1})

b_{det} = specific biofilm-detachment rate coefficient (T^{-1}).

K^* = dimensionless variable for measuring mass transfer

S_{min}^* = Growth potential

q_e = mass of As (V) adsorbed per unit weight of AA

q_m = amount of As (V) adsorbed per unit weight of AA

C_e = equilibrium As (V) concentration in the solution (ML^{-3})

b = constant related to the affinity of the binding sites

r = the dimensionless parameter

C_o = initial As (V) concentration (ML^{-3})

K = Freundlich constant

n = Freundlich constant

Abbreviations

As (III) = arsenite

As (V) = arsenate

As = arsenic

MCSM = Modified Cheni selective medium

CFU = Colony Forming Unit

SSE = Residual sum of squares

CV = Calibration Verification

DDW = Deionized Distilled Water

DO = Dissolved Oxygen, ML^{-3}

CSTR = Continuous Stirred Tank Reactor

HRT = Hydraulic Retention Time

LCR = Linear Calibration Range

MDL = Method Detection Limit

VSS = Volatile Suspended Solids

EPS = Extracellular Polymeric Substances

RBC = Rotating Biological Contactor

RSD = Relative Standard Deviation

SDDC = Silver Diethyldithiocarbamate

APHA = American Public Health Association

SD = Standard Deviation

PSS = Protein Synthesizing System

BV = Bed Volumes

EBCT = Empty Bed Contact Time

TOC = Total Organic Carbon

AA = Activated Alumina

$$Y = 0.0337\ X - 7.922$$

$$R^2 = 0.99$$
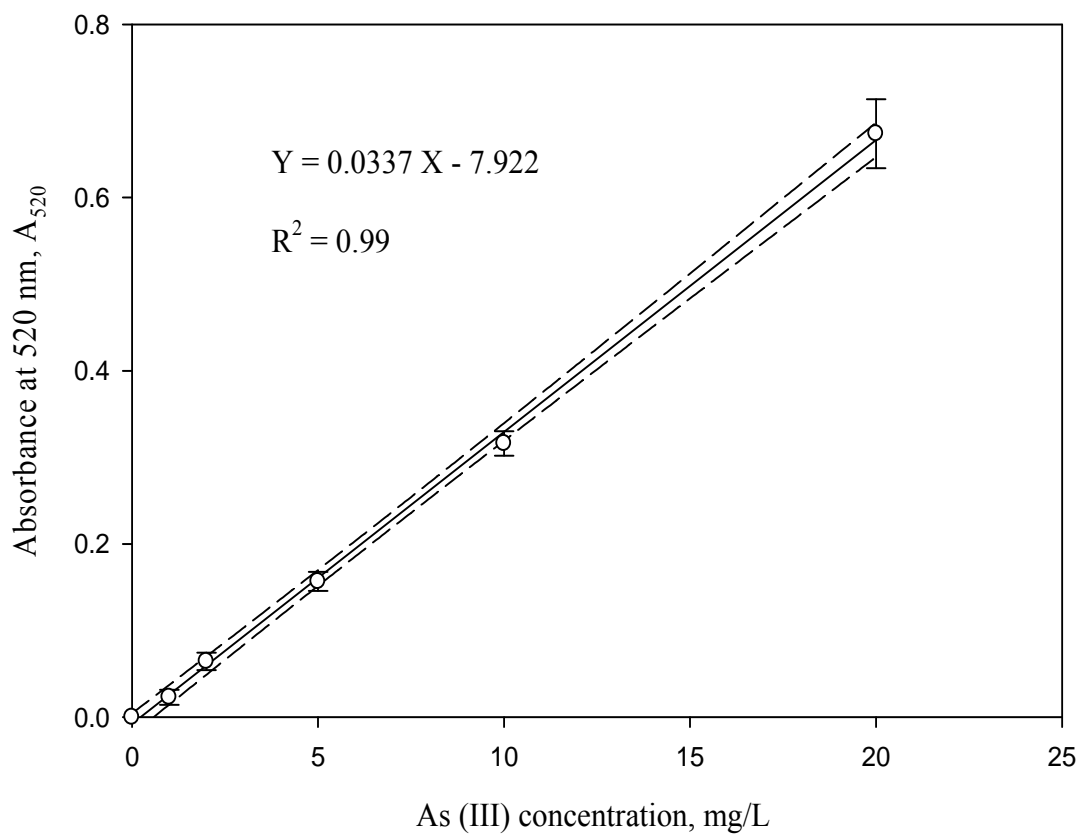
Figure C.1 Example of Standard Curve for As (III) using the SDDC method

$$Y = 0.51128 \, X - 0.7763$$

$$R^2 = 0.9958$$

N = 8 Samples
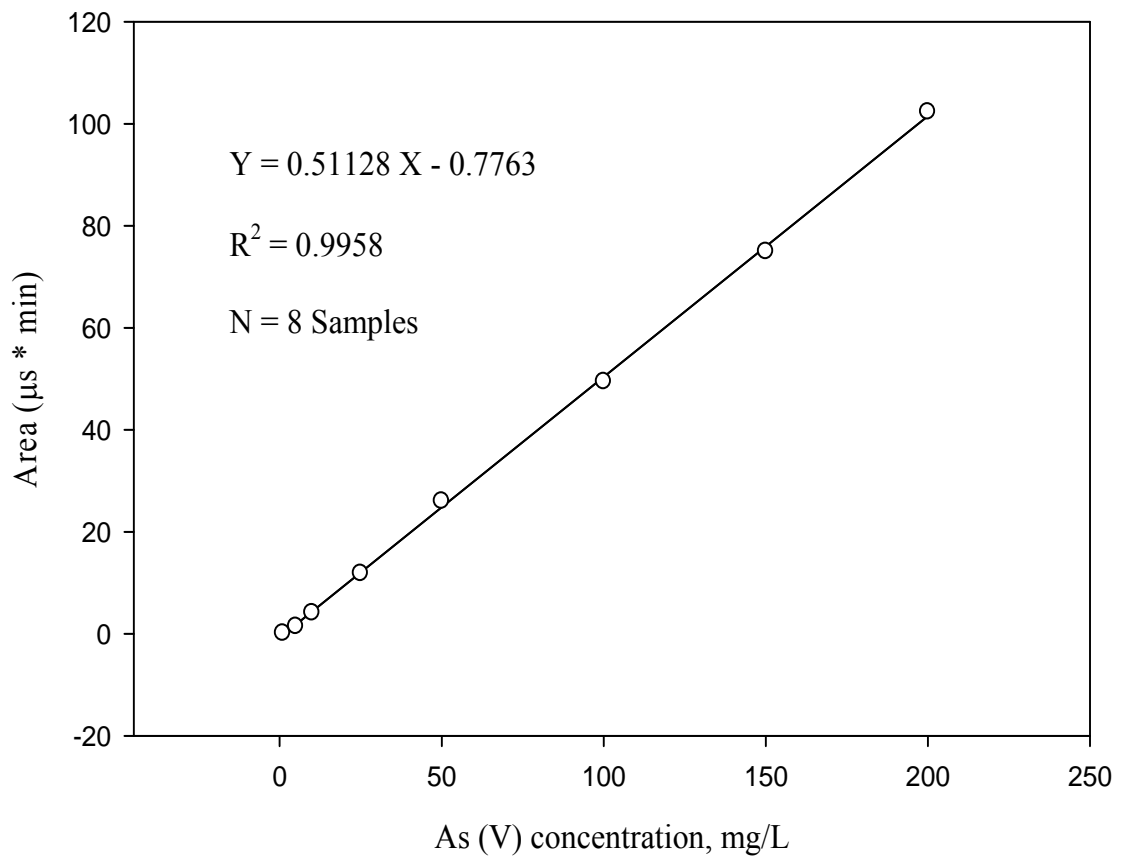
Figure C.2 As (V) linearity in IC method
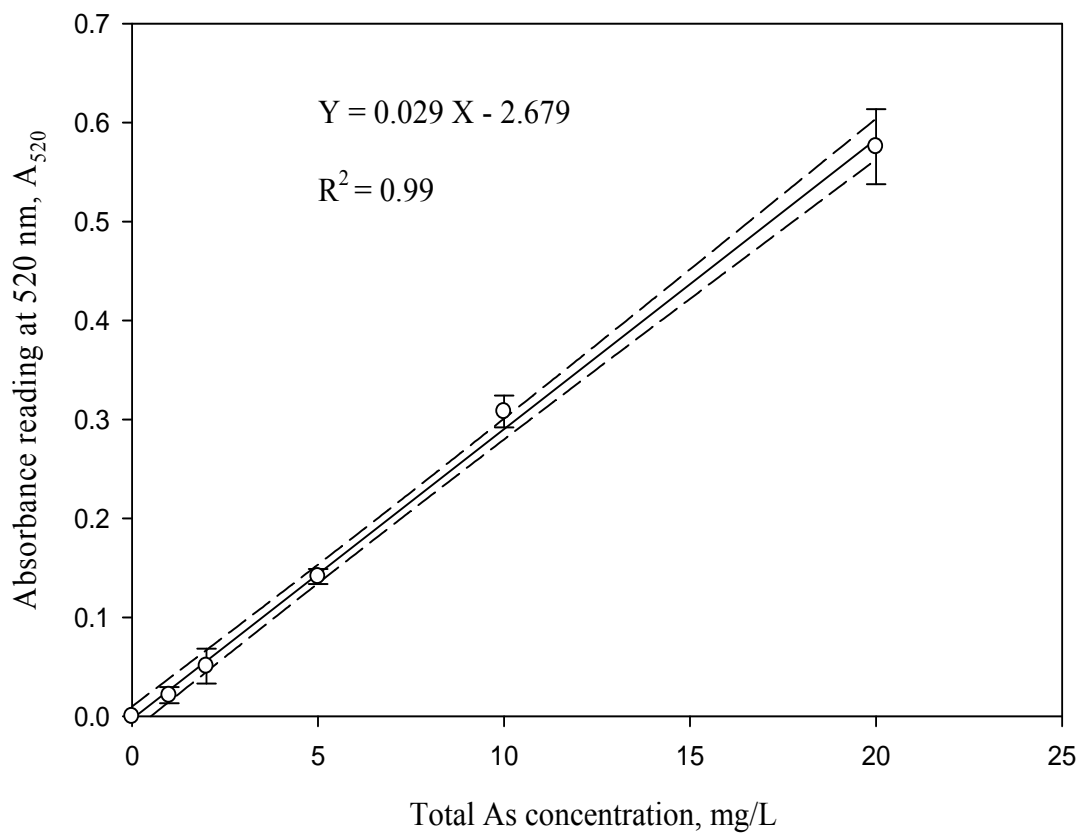
Figure C.3 Example of Standard Curve for total As using the SDDC method

$$Y = 0.0265\ X + 3.371$$

$$R^2 = 0.99$$

Legend:
- □ Experimental
- .... Best fit line
- – – 95% Confidence interval

X-axis: As (V) Concentration, µg/mL

Y-axis: Absorbance at 520 nm, A_{520}
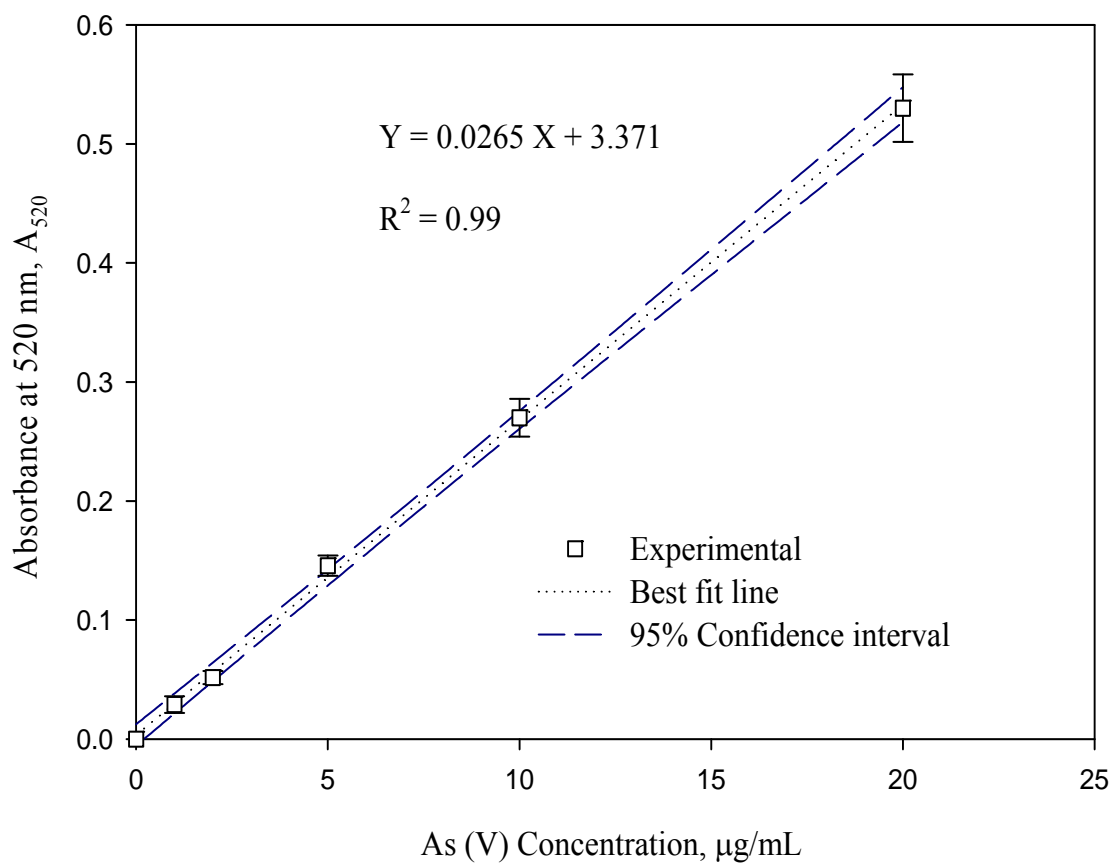
Figure C.4 Example of Standard Curve for As (V) concentration using the SDDC method.

$$y = 6.604x10^{-8} + 7.445$$

$$R^2 = 0.90$$

Experimental
Best fit Line
95 % Confidence Interval
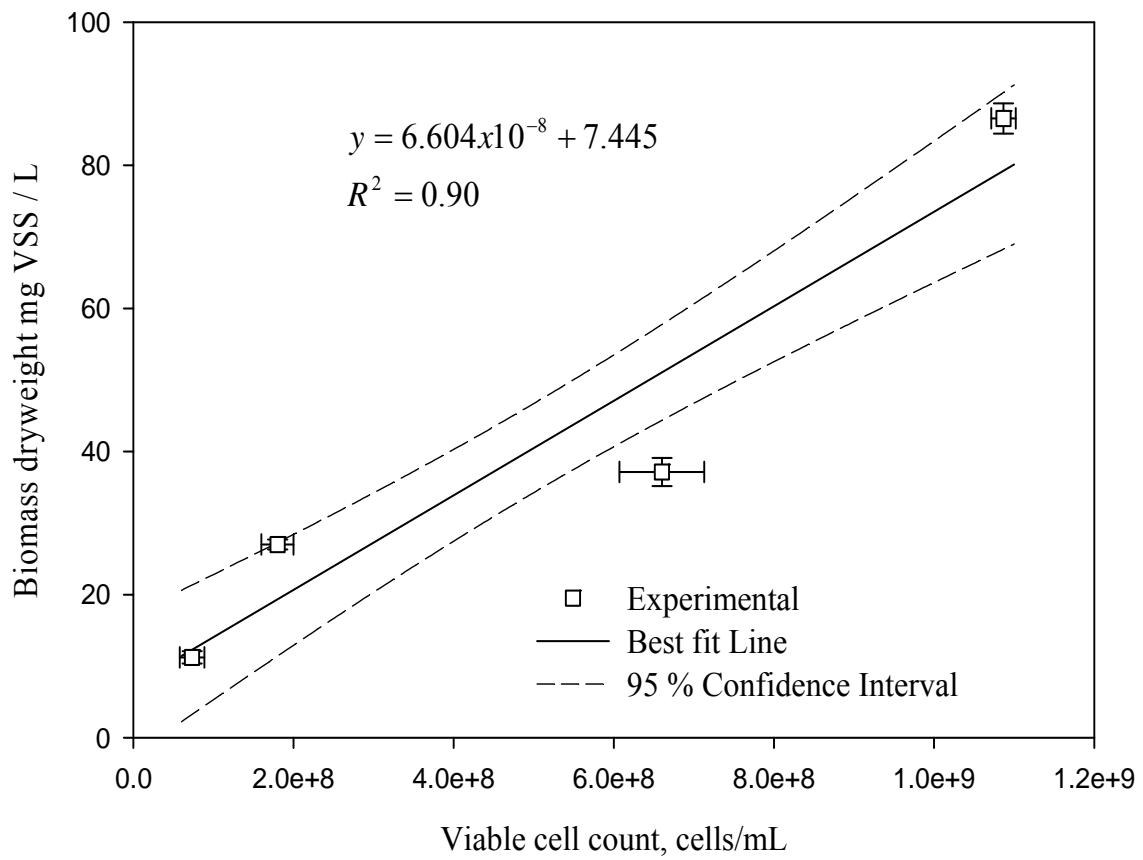
Figure C.5 Calibration curve of viable cell concentration of strain b6 versus biomass dry weight.

$$Y = 0.024\ X + 0.044$$

$$R^2 = 0.98$$
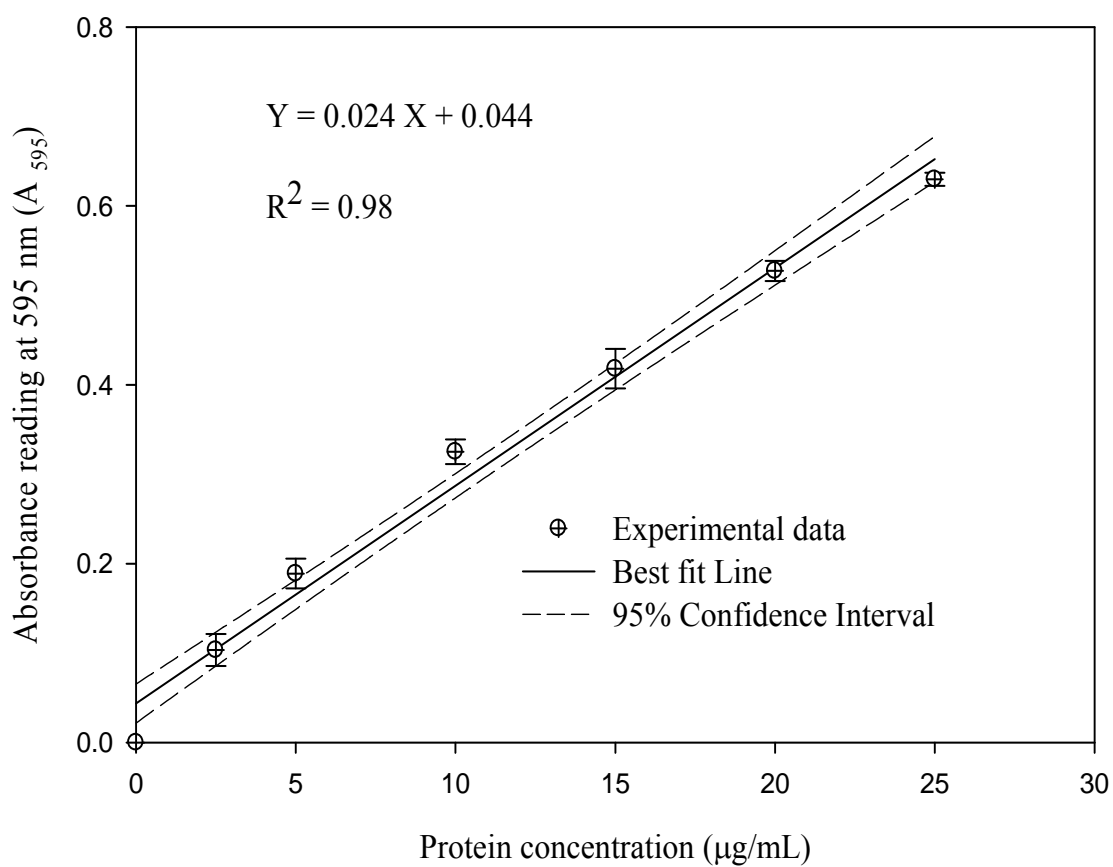
Figure C.6 Calibration curve for the determination of protein concentration using the

Bradford method.

The figure shows a standard calibration curve with Peak Area (µs * min) on the y-axis (ranging from 0 to 60000) and Inorganic Carbon (mg/L) on the x-axis (ranging from 0 to 12). The plot includes:

$$Y = 5158.73 \, x + 1821.19$$

$$R^2 = 0.99$$

Legend:
- ⊕ Experimental
- —— Best fit Line
- – – 95 % CI Interval
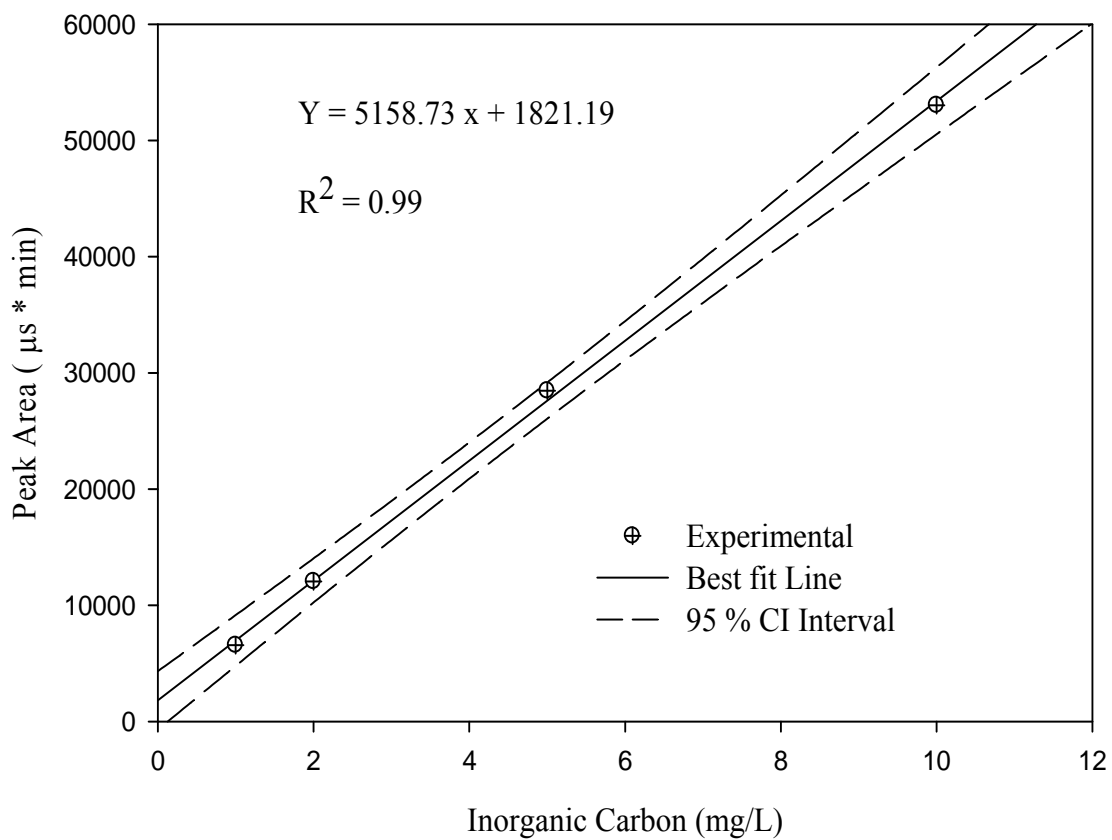
Figure C.7 Standard calibration curve for the determination of Inorganic carbon concentration using a TOC analyzer
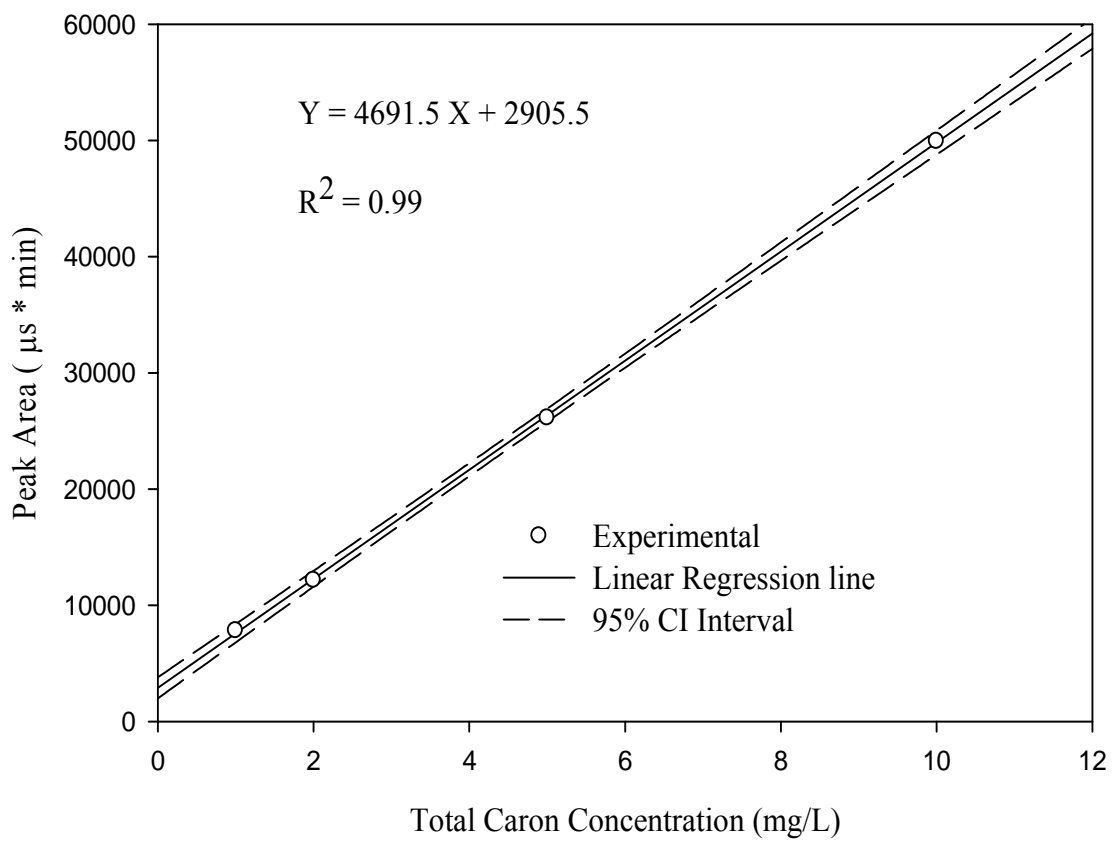
Figure C.8 Standard calibration curve for the determination of Total carbon concentration using the TOC analyzer

Appendix D

Appendix D1: Computation program for the estimation of biokinetic parameters in the study of As (III) oxidation in batch reactors

% This script implements hierarchical iterative least squares fit technique to the solution of an ODE to available data

```
clc;
% the data
t = [48, 96, 120, 144, 168];
S = [480.41, 335.9733, 157.0967, 78.17833, 10.02433];
% set the flags
fine_tuning = 0;
more_fine_tuning = 0;
% the initial guess for the parameters
global Y;
global Kd;
global Ks;
global Ki;
global K;
% Initial estimates
Y = 0.085;
Kd = 0.0058;
Ks = 697;
Ki = 378;
K = 0.85;
% the initial conditions
S0 = 500; % a much better fit is obtained e.g. for S0=1100
X0 = 7.5;
% plot the curve vs. the data
[Tm,SS]=ode113('sys',[0.1:0.1:200],[X0;S0]);
plot(Tm,SS(:,2), 'r');
hold
plot(t,S,'mo');
% set the starting values for "crude" parameters
P0 = [ Kd;  K];
% set the convergence rate control parameter
r = 0.2;
% perform the iterations
for k = 1:15
   odefit;
   Kd = P1(1);
   K = P1(2);
   P0 = P1;
end
% plot the improved curve
```

```matlab
[Tm,SS]=ode113('sys',[0.1:0.1:200],[X0;S0]);
plot(Tm,SS(:,2), 'g');
    % start fine tuning
    fprintf('Start fine tuning...\n');
    fine_tuning = 1;
    % set the initial parameters values
    P0 = [Ks;Ki];
    % reset the rate control
    r = 0.2;
    % perform the iterations
    for k = 1:54
       odefit;

       Ks = P1(1);
       Ki = P1(2);
       P0 = P1;
    end
    % plot the improved curve
    [Tm,SS]=ode113('sys',[0.1:0.1:200],[X0;S0]);
    plot(Tm,SS(:,2), 'b');
    % even more fine tuning
    fprintf('Start more fine tuning...\n');
    fine_tuning = 0;
    more_fine_tuning = 1;
    % set the initial parameter value
P0 = Y;
% reset the rate control
r = 1;
for k = 1:10
   odefit;
   Y = P1;
   P0 = P1;
end
% plot the curve
[Tm,SS]=ode113('sys',[0.1:0.1:200],[X0;S0]);
plot(Tm,SS(:,2), 'k');

% print the report
fprintf('The optimized parameter values:\n');
fprintf('-------------------------------\n');
fprintf('Y = %2.3e\n', Y);
fprintf('Kd = %2.3e\n', Kd);
fprintf('Ks = %2.3e\n', Ks);
fprintf('Ki = %2.3e\n', Ki);
fprintf('K= %2.3e\n', K);
```

```
legend('initial guess', 'crude', 'refined', 'finest');
xlabel('time in sec');
ylabel('S(t) vs. the data');
```
This function file fits an ODE to the given data
```
% This script fits an ode solution to the given data
% generate the reference trajectory
[T,Sref] = ode23('sys',[0.1,t],[X0;S0]);
```
% calculating the numeric derivatives at the reference trajectory
% set the parameter deviations
```
dY = Y/10;
dKs = Ks/10;
dKi = Ki/10;
dK = mu/10;
dKd=Kd/10;
```
% generate the perturbed trajectories
```
if (fine_tuning)
Ks = Ks + dKs;
[T,SdKs] = ode23('sys',[0.1,t],[X0;S0]);
Ks = Ks - dKs;
    Ki = Ki + dKi;
    [T,SdKi] = ode23('sys',[0.1,t],[X0;S0]);
    Ki = Ki - dKi;
    elseif (more_fine_tuning)
    Y = Y + dY;
    [T,SdY] = ode23('sys',[0.1,t],[X0;S0]);
    Y = Y - dY;
  else
  Kd=Kd+dKd;
  [T,SdKd]=ode23('sys',[0,t],[X0;S0]);
  Kd=Kd-dKd;
  K = K + dK;
  [T,SdK] = ode23('sys',[0,t],[X0;S0]);
  K = K - dK;
    end
```
  % build the sensitivity matrix
```
if (fine_tuning)
  A = [(SdKs(:,2)-Sref(:,2))/dKs, (SdKi(:,2)-Sref(:,2))/dKi];
elseif (more_fine_tuning)
  A = (SdY(:,2)-Sref(:,2))/dY;
else
  A = [(SdK(:,2)-Sref(:,2))/dK];
end
A = A(2:end,:);
P1 = P0+r*inv(A'*A)*A'*(S'-Sref(2:end,2));
```

% function files for the previous program and the main program
```
function y = sys(t,x)
global Y;
global Ks;
global Ki;
global K;
global Kd;

y = zeros(2,1);
R = K*x(1)*x(2)/(Ks+x(2)+x(2)^2/Ki);
y(1) = R-Kd*x(1);
y(2) = -R/Y;
```

Appendix D2: Computation program used for model validation using the obtained biokinetic parameters and the Haldane substrate inhibition model

```
clc ;
% Parameter estimates
Y = 0.088;
Kd= 0.006;
Ks= 33.2;
Ki= 602.4;
K =0.85;
% Initial conditions
S0=9.91;
X=7;
    options = [];
    [t y]=ode45('equation',[0.1:0.1:36],[S0;X],options, Y,Ks, Ki,Kd,K,X);
    S=y(:,1); %Value of S stored in the first colum of the returned matrix y
    X=y(:,2);%Value of X stored in the second colum of the returned matrix y
    plot(t,S,'*');
    hold on;
    plot(t,X,'o');
```

Function file used for the computational program file

```
function dydt =equation(t,y,options,Y,Ks, Ki,Kd,K,X)
dydt=[((-(K))*y(1)*y(2))./(Ks+y(1)+((y(1).^2)./Ki));
((K*Y*y(1)*y(2))./(Ks+y(1)+((y(1).^2)./Ki))-Kd*y(2))];
```

Appendix D3: Computational program for steady-state analysis in the CSTR

```
% Example of Steady state modeling for the CSTR
clc;
k=5;
Ks=20.1;
Kd=0.008;
Y=0.011;
S0=4165.62;
D= [0.0133 0.017 0.0208 0.027];
X= [23.2 26.5 30.2 32.4];
S= [19.6 24.1 26.9 31.4];
Sp1= [252.88 448.49 915.55 1801.61 3495.77];
S01= [288.46 493.68 1039.33 2071.60 4130.99];
S0= 288.46:1:4130.99;
Da= 0.0133;
Sa= ((Da+Kd)*Ks)./(k*Y-Da-Kd);
Sp= S0-Sa;
Xp= ((S0-Sa).*(Ks+Sa).*Da)./(k.*Sa);
Yp=Xp. / Sa;
Sf= (Sp./S0)*100;
St= [90 94.88 91.3 92.33];
% plot (S01, Sp1,'o', S0, Sp);
plot (S0, Yp);
```

Appendix D4: Computational program for simulation of transient As (III) and biomass concentrations

```
clc;
% Parameters to be used for transient analysis
global Kd;
global Y;
global k;
global Ks;
% Parameter values to be used for the analysis
k=5.0;
Ks=20.1;
Kd=0.008;
Y=0.011;
tau =74.9;
S0=2071;
X0= 20.2;
P0 = 4.54;
options=[];
[Tm SS]= ode45('trcstr',[993:5:1560],[P0;X0],options,tau,S0,X0);
plot(Tm,SS(:,1));
hold on;
plot(TimeA,sub1,'o');
```

Function file for the above program

```
function y = trcstr1(t,x, options, Y, k, Ks,n,tau,Kd,S0)
y= zeros (2, 1);
y(1)= ((S0-x(1))./(tau))-((k*x(1)*(x(2).^n))./((Ks+(x(1).^n))));
y(2)=(((Y*k*(x(1).^n))./((Ks+(x(1).^n))))-(1./tau)-Kd)*x(2);
```

Appendix D5: Program for analyzing the sensitivity analysis of the parameters k and K_s using the same steady-state predictive flux model

```
clc;
% Parameters to be used for the steady state model
k=101.9;
Ks=0.0132;
XfLf=0.002;
eta = 0.99;
Ss=0:0.001:0.067;
% Simulation of the steady-state flux
J = (eta*XfLf*Ss*k). / (Ks+Ss);
plot (Ss, J,'o');
```

Appendix E1: Initial guess and final convergence values of the parameters k and K_s to establish the uniqueness of the parameter estimates (global minima)

k-start	k-final	Ks-start	Ks-final	Sum of squares
1.8438	101.9021	3.99E-04	0.0132	1.43E-04
0.4688	101.902	2.33E-03	0.0132	1.43E-04
-0.1094	101.9019	-1.44E-04	0.0132	1.43E-04
1.5156	101.9019	1.58E-03	0.0132	1.43E-04
1.2656	101.9019	1.78E-03	0.0132	1.43E-04
0.2656	101.9018	-4.40E-04	0.0132	1.43E-04
1.0625	101.9018	-6.17E-05	0.0132	1.43E-04
0.5938	101.9018	-2.43E-04	0.0132	1.43E-04
1.7188	101.9018	-7.86E-04	0.0132	1.43E-04
1.625	101.9018	-2.59E-04	0.0132	1.43E-04
2.0938	101.9018	-6.87E-04	0.0132	1.43E-04
1.9531	101.9018	-9.18E-04	0.0132	1.43E-04
2.0781	101.9018	3.66E-04	0.0132	1.43E-04
0.125	101.9017	-7.04E-04	0.0132	1.43E-04
1.0156	101.9017	-1.93E-04	0.0132	1.43E-04
1.6406	101.9017	2.37E-03	0.0132	1.43E-04
2.4375	101.9017	2.21E-03	0.0132	1.43E-04
2.5781	101.9017	2.14E-03	0.0132	1.43E-04
1.4531	101.9017	2.44E-03	0.0132	1.43E-04
2.3281	101.9017	-8.19E-04	0.0132	1.43E-04
2.8438	101.9017	-4.90E-04	0.0132	1.43E-04
2.8125	101.9017	2.01E-03	0.0132	1.43E-04
-0.2813	101.9017	2.62E-03	0.0132	1.43E-04
2.9063	101.9017	2.28E-03	0.0132	1.43E-04
1.8125	101.9016	-6.54E-04	0.0132	1.43E-04
2.3906	101.9016	2.08E-03	0.0132	1.43E-04
0.8281	101.9016	-3.74E-04	0.0132	1.43E-04
2.5625	101.9016	-3.58E-04	0.0132	1.43E-04
0.8906	101.9016	2.52E-03	0.0132	1.43E-04
2	101.9016	-5.56E-04	0.0132	1.43E-04
2.625	101.9016	2.41E-03	0.0132	1.43E-04
2.7031	101.9015	-2.26E-04	0.0132	1.43E-04
2.7188	101.9015	1.88E-03	0.0132	1.43E-04
1.3125	101.9015	2.31E-03	0.0132	1.43E-04
2.0156	101.9015	2.47E-03	0.0132	1.43E-04

REFERENCES

Abdrashitova, S. A., Abdullina, G.G., and Ilialetdinov, A.N. (1985). "Glucose consumption and dehydrogenase activity of the cells of the arsenite oxidizing bacterium *Pseudomonas putida*." *Mikrobiologia*., 54(4), 679-681.

Adams, J., and Hansche, P.E. (1973). "POPULATION STUDIES IN MICROORGANISMS I. EVOLUTION OF DIPLOIDY IN *SACCHAROMYCES CEREVISIAE*." *Genetics*., 76, 327-338

Ahn, J., Kim, J., Lim, J., and Hwang, S. (2004). "Biokinetic evaluation and modeling of continuous thiocyanate biodegradation by *Klebsiella sp.*" *Biotechnology Progress*., 20, 1069-1075.

Altschul, S.F., Madden, T.L., Schaffer, A.A., Zhang, J., Zhang, Z., Miller, W., and Lipman, D.J. (1997). "Gapped BLAST and PSI-BLAST: a new generation of protein database search programs." *Nucleic Acids Res*., 25, 3389-3402.

American Public Health Association (APHA). 1995. "Standard Methods for the examination of water and waste water." Washington, DC.

Amy, G. et al. (2000). "Arsenic Treatability Options and Evaluation of Residuals." Management Issues (90771)., AWWARF, Denver.

Anderson, G.L., Williams, J., and Hille, R. (1992). "The purification and characterization of arsenite oxidase from Alcaligenes faecalis, a molybdenum-containing hydroxylase." J. Biol. Chem., 267(33), 23674 – 23682.

Anderson, M.A., Ferguson, J.F., and Gavis J. (1976). "Arsenate Adsorption on Amorphous Aluminum Hydroxide." *Journal of Colloid and Interface Science*., 54(3), 391-399.

Atkinson, B., and I.J. Davies. (1976). "The overall rate of substrate uptake (reaction) by microbial films. Part I. Biological rate equation." *Trans., Inst. Chem.Engr*., 52, 248-259.
Azcue, J.M., and Nriagu, J.O. (1994). "Arsenic: Historical perspectives." In: Nriagu, J.O. (Ed.): Arsenic in the Environment. Part I: Cycling and Characterization, Wiley New York, 1-16.

Badruzzaman, M., Westerhoff, P., and Knappe, D.R.U. (2004). "Intraparticle diffusion and adsorption of arsenate onto granular ferric hydroxide." *Wat.Res*., 38, 4002-4012.
Baes, C.F.J., and Mesmer, R.E. (1976). "The hydrolysis of cations." Wiley Interscience, New York, 369-370.

Basha, C.A., Selvi, S.J., Ramasamy, E., and Chellammal, S. (2008). "Removal of arsenic and sulfate from the copper smelting industrial effluent." *Chem. Eng. J*., 141(1-3), 89 - 98.

Battaglia-Brunet, F., Crouzet, C., Garrido, F., Dictor, M.C., Morin, D., Dekeyser K., Clarens M., and Baranger, P. (2002). "An arsenic (III)-oxidizing bacterial population: selection, characterization, and performance in reactors." *J of App Microbiology*., 93, 656-667.

Battaglia-Brunet, F., Crouzet, C., Garrido, F., Dictor, M.C., Morin, D., Dekeyser K., Clarens M., and Baranger, P. (2002). "An arsenic (III)-oxidizing bacterial population: selection, characterization, and performance in reactors." *J of App Microbiology*., 93, 656-667.

Battaglia-Brunet, F., Joulian, C., Garrido, F., Dictor, M.C., Morin, D., Coupland, K., Johnson, Barrie D., Hallberg, B. K., and Baranger, P. (2006). "Oxidation of arsenite by *Thiomonas* strains and characterization of *Thiomonas arsenivorans* sp.nov." An*tonie van Leeuwenhoek.*, 89(1), 99-108.

Belzile, N., and Tessier, A. (1990). "Interactions between arsenic and iron oxyhydroxides in lacustrine sediments." Geochim. Cosmochim. Acta., 54, 103-109.

Benjamin, M.M., Sletten, R.S., Bailey, R.P., and Bennett, P. (1998). "Sorption of Arsenic by Various Adsorbents." AWWA Inorganic Contaminants Workshop., San Antonio, TX, February 23-24.

Bhumbla, D.K., and Keefer, R.F. (1994). "Arsenic mobilization and bioavailability in soils." In: Niagru, J.O. (Ed): Arsenic in environment. Part1: Cycling and Characterization. Wiley New York, 51-82.

Bhumbla, D.K., and Keefer, R.F. (1994). "Arsenic mobilization and bioavailability in soils." In: Niagru, J.O. (Ed.): Arsenic in environment. Part1: Cycling and Characterization. Wiley New York, 51-82.

Bissen, M., and Frimmel, F.H. (2003). "Arsenic-a review. Part I: Occurrence, Toxicity, Speciation, Mobility." *Acta. Hydrochim. Hydrobiol*., 31(1), 9-18.

Bougerra, W., Marzouk, I., and Hamrouni, B. (2009). "Equilibrium and Kinetic Studies of Adsorption of Boron on Activated Alumina." *Water Environment Research*., 81(12), 2455-2459.

Bouguerra, W., Ben Sik Ali, M., Hamrouni, B., and Dhahbi, M. (2007). "Equilibrium and Kinetic studies of adsorption of silica onto activated alumina." *Desalination*., 206, 141-146.

Bowers, A.R., and Huang, C.P. (1985). "Adsorption characteristics of polyacetic amino acids onto hydrous γ-Al_2O_3." *J. Colloid Interface Sci*., 105, 197-215.

Boyle, R. W., and Jonasson, I.R. (1973). "The geochemistry of As and its use as an indicator element in geochemical prospecting." J. Geochem. Explor., 2, 251-296.

Bradford, M.M. "A rapid and sensitive method for the quantitation of microgram quantities of protein utilizing the principle of protein-dye binding." *Analytical Biochemistry*., 72(1-2), 248-254.

Brock, T.D., and Freeze, H. (1969). "Thermus aquaticus gen.n. and sp. n., a non-sporulation extreme thermophile." *J. Bacteriol*., 98, 289-297.

Bryan, C.G., Marchal, M., Battaglia-Brunet, F., Kugler, V., Lemaitre-Guillier, C., Lievremont, D., Bertin, P.N., and Arsene-Ploetze, F. (2009). "Carbon and arsenic metabolism in Thiomonas strains: differences revealed diverse adaptation processes." *BMC Microbiology*., 9, 127. http://www.biomedcentral.com/147-2180/9/127.

Catherino, H.A. (1967). "The Electrochemical Oxidation of As (III). A consecutive electron transfer reaction." *Journal of Physical Chemistry*., 71(2), 268-274.

Chen, K.Y., and Gupta, S.K. (1978). "Arsenic removal by adsorption." *Journal of Water Pollution Control Federation*, 50 (3), 493-506.

Cheng, R.C., Liang, S., Wang, H.C., and Beuhler, M.D. "Enhanced coagulation for arsenic removal." *Journal of the American Water Works Association*., 86(9), 79-90.

Chirwa, E.M.N., and Wang, Y.T. (1997). "Biological reduction of hexavalent chromium by *Bacillus* sp. in a packed bed bioreactor." *Environ. Sci. Technol*., 31, 1446-1451.

Choi, H., and Silverstein, J. 2007. "Effluent recirculation to improve perchlorate reduction in a fixed film bioreactor". *Biotechnol.Bioeng*., 98(1), 132-140.

Clifford, D. A. (1990). "Ion exchange and Inorganic Adsorption." Water Quality and Treatment, F.W. Pontius, ed., McGraw-Hill, Inc, New York., 613-615.

Clifford, D.A. (1999). Ion exchange and Inorganic Adsorption. In R.D. Letterman, ed. Water Quality and Treatment: A Handbook of Community Water Supplies, 5th ed., New York, NY: McGraw-Hill Inc.

Clifford, D.A., and Ghurye, G., Tripp, A. R. (2003). "Arsenic Removal from Drinking Water Using Ion-Exchange with Spent Brine Recycling." *Journal of the American Water Works Association*., 35, 119-130.

Clifford, D.A., and Lin, C.C. (1995). "Ion-exchange, activated alumina, and the membrane processes for arsenic removal from groundwater." Proceedings of 45th Annual Environmental Engineering Conference, University of Kansas, 1995.

Clifford, D.A., and Wu, M. (2001). "Arsenic treatment technology demonstration: Predicting the effect of water quality on arsenic adsorption by activated alumina." Report to the Montana State University Water Resources Center, 2001.

Clifford, D.A., Ghurye, G.L., Tripp, A.R., and Jian, T. (1997). "Final Report: Phases I and 2, City of Albuquerque Arsenic Study, Field Studies on Arsenic Removal in Albuquerque, NM, Using the University of Houston/USEPA Mobile Drinking Water Treatment Research Facility. Houston, TX: University of Houston, 1997."

Clifford, D.A., Ghurye, G.L., Tripp, A.R., and Jian, T. (1998). "Final Report: Phase 3, City of Albuquerque Arsenic Study, Field Studies on Arsenic Removal in Albuquerque, NM, Using the University of Houston/USEPA Mobile Drinking Water Treatment Research Facility. Houston, TX: University of Houston, 1998."

Commandeur, L.C.M., Eyseren, H.E.V., Opmeer, M.R., Govers, H.A.J., and Parsons, J.R. (1995). "Biodegradation Kinetics of Highly Chlorinated Biphenyls by *Alcaligenes* sp. JB1 in an Aerobic Continuous Culture System." *Environ. Sci. Technol*., 2(12), 3038-3043.

Dastidar, A., and Wang, Y.T. (2009). "Arsenite Oxidation by Batch Cultures of *Thiomonas Arsenivorans* Strain b6." *J. Environ. Eng-ASCE*., 135(8), 708-715.

Dembitsky, V.M., and Levitsky, D.O. (2004). "Arsenolipids." *Progress in Lipd research*., 43, 403-448.

Dixit, S., and Hering, J.G. (2003). "Comparison of Arsenic (V) and Arsenic (III) Sorption onto Iron Oxide Minerals: Implications for Arsenic Mobility." *Environ. Sci.Technol*., 37, 4182-4189.
Dmitriou-Christidis, P., Autenrieth, R.L., Mcdonald, T.J., and Desai, A.M. (2007). "Measurement of biodegradability parameters for single unsubstituted and methylated polycyclic aromatic hydrocarbons in liquid bacterial suspensions." *Biotechnology and Bioengineering*., 97, 922-932.

Dombrowski, P.M., Long, W., Farley, K.J., Mahony, J.D., Capitani, J.F., and Di Toro, D.M. (2005). "Thermodynamic Analysis of Arsenic Methylation." *Environ. Sci. Technol*., 39, 2169-2176.

Donlan, R.M., and Costerton, J.W. (2002). "Biofilms: Survival Mechanisms of Clinically Relevant Microorganisms." *Clinical Microbiology Reviews*., 15(2), 167-193.

Driehaus, W., Jekel, M., and Hildebrandt, U. (1998). "Granular Ferric Hydroxide- A New Adsorbent for the Removal of Arsenic from Natural Water." *J. Water SRT-Aqua.*, 47(1), 30-35.

Driehaus, W., Seith, R., Jekel, M. (1995). "Oxidation of Arsenite (III) with Manganese Oxides in Water Treatment." *Wat.res.*, 29(1), 297-305.

Duquesne, K., Lieutaud, A., Ratouchniak, J., Muller, D., Lett, M.-C., and Bonnefoy, V. (2008). "Arsenite Oxidation by a chemoautotrophic moderately acidophilic *Thiomonas* sp: from the strain isolation to the gene study." *Environmental Microbiology.*, 10(1), 228-237.

Dutta, P.K., Pehkonen, S.O., Sharma, V.K., Ray, A.K. (2005). "Photocatalytic Oxidation of Arsenic (III): Evidence of Hydroxyl Radicals." Environ. Sci. Technol., 39, 1827-1834.

Dutta, P.K., Ray, A.K., Sharma, V.K., Millero, F.J. (2004). "Adsorption of arsenate and arsenite on titanium dioxide suspensions." *Journal of Colloid and Interface Science.*, 278, 270-275.

Eccles, H. (1995). "Removal of heavy metals from effluent streams – why select a biological process." *Intern. Biodeter. Biodegrad.*, 5-16.

Edwards, M. (1994). "Chemistry of Arsenic Removal during Coagulation and Fe-Mn Oxidation." *Journal of the American Water Works Association.*, 86, 64-78.

Eisenthal, R., and Cornish-Bowden, A. 1974. "The direct linear plot: A new graphical procedure for estimating enzyme kinetic parameters." *Biochem.J.*, 139, 715-720.

Eisenthal, R., and Cornish-Bowden, A. 1974. "The direct linear plot: A new graphical procedure for estimating enzyme kinetic parameters." *Biochem.J.*, 139, 715-720.

Ellis, P.J., Conrads, T., Hille, R., and Kuhn, P. (2001). "Crystal structure of the 100 kDa arsenite oxidase from Alcaligenes faecalis in two crystal forms at 1.64 Å and 2.03 Å." *Structure.*, 9, 125-132.

Emett, M.T., Khoe, G.H. (2001). "Photochemical Oxidation of Arsenic by Oxygen and Iron in Acidic Solutions." *Wat.res*. 35(3), 649-656.

Faust, S.D., and Aly, O.M. "Elements of surface chemistry." Adsorption process for water treatment, Faust, S.D., and Aly, O.M, ed., Butterworth Publishers, MA.

Ferguson, J.F., and Gavis, J. (1972). "A review of the arsenic cycle in the natural water." *Wat.res.*, 6, 1259-1574.

Flemming, H.-C., and Wingender, J. (2002). "Extracellular polymeric substances: structure, ecological functions, technical relevance, p. 1223-1231. In G. Bitton (ed.), *Encyclopedia of environmental microbiology.*, vol. 3. Wiley, New York, NY.

Flemming, H.-C., Neu, T.R., and Wozniak, D.J. (2007). "The EPS Matrix: The "house of biofilm cells." *J Bacteriol.*,189(22): 7945–7947

Fogler H.S. (1986). Elements of chemical reaction engineering, 2nd Ed., Prentice-Hall, Upper Saddle River, N.J.

Fogler H.S. (1999). Elements of chemical reaction engineering, 3rd Ed., Prentice-Hall, Upper Saddle River, N.J.

Fornwalt, H.J., and Hutchins, R.A. 1996. "Purifying liquids with activated carbon." *Chem.Engr.*, 73, 179-184.

Frank, P., and Clifford, D.A. (1986). "Arsenic III oxidation and removal from drinking water." U.S. Environmental Protection Agency Report, Cincinnati, OH, 1986.

Frank, P.L., and Clifford, D.A. (1986). "Arsenic (III) Oxidation and Removal from Drinking Water." Summary Report, EPA 600/S2-86/021.

Gallard, H.U., and Von Gunten, U. (2002). "Chlorination of natural organic matter: Kinetics of chlorination and of THM formation." *Wat.res.*, 36, 65.

Gallifuoco, A., Alfani, F., and Cantarella, M. (2002). "Advantages of continuous over batch reactors for the kinetic analysis of enzymes inhibited by an unknown substrate impurity." *Biotechnol.Bioeng.*, 79(6), 641-646

Garcia-Dominguez, E., Mumford, A., Rhine, D.E., and Young, L.Y. (2008). "Novel autotrophic arsenite-oxidizing bacteria isolated from soil and sediments." *FEMS Microbiology Ecology.*, 66 (2), 401-410.

Ghosh, M.M., and Yuan, J.R. (1987). "Adsorption of Inorganic Arsenic and Organoarsenicals on Hydrous Oxides." *Environmental Progress.*, 6, 150-157.

Ghurye, G., and Clifford, D. (2001). "Laboratory study on the oxidation of As (III) to As (V)." EPA/600/R-01/021. March 2001.

Gihring, T.M., and Banfiled J.F. (2001). "Arsenite oxidation and arsenate respiration by a new *Thermus* isolate." *FEMS Microbiology letters.*, 204, 335-340.

Goldberg, S. (2002). "Competitive Adsorption of Arsenate and Arsenite on Oxides and Clay Minerals." *Soil Sci. Soc. Am. J.*, 66, 413-421.

Gooijer de, C.D., Wijffels, R.H., and Tramper, J. (1991). "Growth and Substrate Consumption of *Nitrobacter agilis* cells immobilized in Carrageenan: Part1. Dynamic Modeling." *Biotechnol.Bioeng.*, 38 (3), 224-231.

Grady, C.P.L Jr., Smets, B.F., and Barbeau, D.S. (1996). "Variability in kinetic parameter estimates: A review of possible causes and a proposed terminology." *Wat.res.*, 30, 742-748.

Grafe, M., Eick, M.J., and Grossl, P.R. (2001). "Adsorption of Arsenate and Arsenite on Goethite in the presence and absence of dissolved organic carbon." *Soil Sci. Soc. Am. J.*, 65, 1680-1687.

Green, H.H. (1918). "Description of bacterium which oxidizes arsenite to arsenate, and one which reduces arsenate to arsenite, isolated from a cattle dipping-tank." *S.Afr.J. med. Sci.*, 14, 465-467.

Hanes, C.S. 1932. "Studies on plant amylases: I. The effect of starch concentration upon the velocity of hydrolysis by the amylase of germinated barley." *Biochem.J.*, 26, 1406-1421.

Hanes, C.S. 1932. "Studies on plant amylases: I. The effect of starch concentration upon the velocity of hydrolysis by the amylase of germinated barley." *Biochem.J.*, 26, 1406-1421.

Healy, S.M., Wildfang, E., Zakharyan, R.A., and Aposhian, H.V. (1999). "Diversity of Inorganic Arsenite Biotransformation." *Biological Trace Element Research.*, 68, 249-266.

Heath, M.S., Wirtel, S.A., and Rittmann, B.E. (1992). "Simplified design of biofilm processes using normalized loading curves." *Res.J. Water Pollut.Control Fed.*, 63(2), 185-192.

Hering, J.G., Chen, P.-Y., Wilkie, J.A., and Elimelech, M. (1997). "Arsenic Removal from Drinking Water Coagulation." *J. Environ. Eng-ASCE.*, 8, 800-807.

Hess, R.E., and Blanchar, R.W. (1977). "Dissolution of arsenic from waterlogged and aerated soil." *Soil. Sci. Am. J.*, 41, 861-865.

Hoeft, S.E., Blum, J.S., Stolz, J.F., Tabita, F.R., Witte, B., King, G.M., Santini, J.M., and Oremland, R.S. (2007). "*Alkalilimnicola ehrlichii* sp. nov., a novel, arsenite-oxidizing haloalkaliphilic gammaproteobacterium capable of chemoautotrophic or heterotrophic growth with nitrate or oxygen as the electron acceptor." *Int.J. Syst. Evol. Microbiol.*, **57**, 504-512.

Holmberg, A. (1982). "On the practical identifiability of microbial growth models incorporating Michaelis-Menten type non-linearities." *Math Biosci.*, 62, 23-43.

Hoven, R.N.V., and Santini, J.M. (2004). "Arsenite oxidation by the heterotroph Hydrogenophaga sp.str.NT-14: the arsenite oxidase and its physiological electron acceptor." *Biochimica ET Biophysica ACTA*., 1656(2-3), 148-155.

Hug, S.J., and Leupin, O. (2003). "Iron-Catalyzed Oxidation of Arsenic (III) by Oxygen and Hydrogen Peroxide: pH-Dependant Formation of Oxidants in the Fenton Reaction." *Environ. Sci. Technol*., 37, 2734-2742.

Hung, C., and Pavlostathis, S.G. (1999). "Kinetics and Modelling of Autotrophic Thiocyanate Biodegradation." *Biotechnology and Bioengineering*., 62, 1-11.

Ilialetdinov, A.N., Abdrashitova, S.A. (1981). "Autotrophic oxidation of arsenic by a culture of *Pseudomonas arsenitoxidans*." *Mikrobiologiya*., 50, 197-204.

Ionic conductivity and diffusion at infinite dilution", in CRC Handbook of Chemistry and Physics, 90th Edition (Internet version 2010), David R. Lide, ed., CRC Press/Taylor and Francis, Boca Raton, FL.

Jain, A., and Loeppert, R.H. (2000). "Effect of Competing Anions on the adsorption of Arsenate and Arsenite on Ferrihydrite." *J.Environ. Qual*., 1422-1430.

Jang, M., Min, S.H., Kim, T.H., and Park, J.K. (2006). "Removal of arsenite and arsenate using hydrous ferric oxide incorporated into naturally occurring porous diatomite." *Environ. Sci. Technol*., 40 (5), 1636 - 1643.

Jekel. M.R. (1994). "Removal of Arsenic in Drinking Water Treatment." In J.O.Nriagu, ed, Arsenic in the Environment, Part I: Cycling and Characterization. Vol 26, New York, NY, John Wiley & Sons, Inc, 119-132.

Jennings, P.A. (1975). "A mathematical model for biological activity in expanded bed adsorption columns." Ph.D Thesis, Department of Civil Engineering, University of Illinois, Urbana, IL.

Jensen, J.N. (2001). "Approach to steady state in completely mixed flow reactors." *J. Environ. Eng-ASCE*., 127(1), 13-18.

Jessup, S.M., Geertje, K.V., and Meijer, W.G. (1998). "SOMETHING FROM ALMOST NOTHING: Carbon Dioxide Fixation in Chemoautotrophs." *Annu. Rev. Microbiol*., 52, 191-230.

Johnston, R., and Heijnen, H. (2001). Safe Water Technology for Arsenic Removal. In Technologies for Arsenic Removal from Drinking Water; Ahmed, M.F., Ali, M.A., Adeel, Z., Eds.; The Bangladesh University of Engineering and Technology and the United Nations University: 2001:p1-22.

Katayama Y., Uchino Y., Wood A.P., and Kelly D.P. (2006). "Confirmation of *Thiomonas delicata* (formerly *Thiobacillus delicates*) as a distinct species of the genus *Thiomonas* Moreira and Amils 1997 with comments on some species currently designed to the genus." *International Journal of Systematic and Evolutionary Microbiology*., 56, 2553-2557.

Katsoyiannis, I.A., Zouboulis, A.I., and Jekel, M. (2004). "Kinetics of Bacterial As (III) Oxidation and Subsequent As (V) Removal onto Biogenic Manganese Oxides during Groundwater Treatment." *Ind.Eng.Chem.Res*., 43, 486-493.

Keen, G.A., and Prosser J.L. (1987). "Steady state and transient growth of autotrophic nitrifying bacteria." *Archives of Microbiology*., 147, 73-79.

Klecka G.M. and Maier W.J. (1988). "Kinetics of Microbial Growth on Mixtures of Pentachlorophenol and Chlorinated Aromatic Compounds." *Biotechnology and Bioengineering*., 31(4), 328-335.

Klecka, G.M., and Maier, W.J. (1985). " Kinetics of Microbial Growth on Pentachlorophenol." *Appl.Environ.Microbiol*., 49(1), 46-53.

Knowles, F.C., and Benson, A.A. (1983). "The biochemistry of arsenic." *Trends Biochem Sci*., 8, 178-180.

Kundu, S., Kavalakatt, S.S., Pal, A., Ghosh, S.J., Mandal, M., and Pal, T. (2004). "Removal of arsenic using hardened paste of Portland cement: batch adsorption and column study." *Wat.res*., 38, 3780-3790.

Legault, A.S., Volchek, K., Tremblay, A.Y., and Whittaker, H. (1993). "Removal of Arsenic from Groundwater Using Reagent Binding/Membrane separation." *Environmental Progress*., 12, 157-159.

Legge, J.W., and Turner, A.W. (1954). "Bacterial oxidation of arsenite.III. Cell-free arsenite dehydrogenase." *Aust. J. Biol. Sci*., 7, 496-503.

Letterman, A. (Ed.). (1999). "Water quality and treatment: A handbook of community water supplies." American Water Works Association., McGraw Hill, New York, NY.

Lievremont, D., N'negue, M.-A., Behra, Ph., and Lett, M.-C. (2003). "Biological oxidation of arsenite: batch reactor experiments in presence of kutnahorite and chabazite." *Chemosphere*., 51 (5), 419 - 428.

Lievremont, D., N'negue, M.-A., Behra, Ph., and Lett, M.-C. (2003). "Biological oxidation of arsenite: batch reactor experiments in presence of kutnahorite and chabazite." *Chemosphere*., 51, 419-428.

Lin, T.-F., and WU, J.-K. (2000). "Adsorption of arsenate and arsenite within activated alumina grains: Equilibrium and Kinetics." *Wat. Res*., 35 (8), 2049-2057.

Livingston, A.G., and Chase, H.A. 1989. "Modeling phenol degradation in a fluidized-bed reactor." *AIChE J*., 35, 1980-1992.

Lloyd, J.R. (2003). "Microbial reduction of metals and radionuclides." *FEMS Microbiology Reviews*., 27, 411-425.

Lloyd, J.R., and Oremland R.S. (2006). " Microbial transformations of Arsenic in the Environment from Soda Lakes to Aquifers." *Elements*., 2, 85-90.

Lobry, J.R., and Flandrois, J.P. (1991). "Comparison of estimates of Monod's growth model parameters from the same data set." *Binary*., 3, 20-23.

Longsworth, L.G. (1972). "Diffusion in Liquids." In Gray, D.W. (ed.), American Institute of Physics Handbook, McGraw-Hill Book Company, New York, NY

Lortie, L., Gould, W.D., Rajan, W., McCready, R.G.L. and Cheng, K.-J. (1992). "Reduction of selenate and selenite to elemental selium by *Pseudomonas stutzeri* isolate." *Appl. Environ. Microbiol*., 58, 4042-4044.

Lovley, D.R., and Coates, J.D. (1997). "Bioremediation of metal contamination." *Current Opinion in Biotechnology*., 8, 285-289.

Lovley, D.R., Phillips, E.J.P., Gorby, Y.A., and Landa, E. (1991). "Microbial reduction of uranium." *Nature*., 350, 413-416.

Lovley, D.R., Stolz, J.F., Nord, G.L., and Phillips, E.J.P. (1987). "An aerobic production of magnetite by a dissimilatory iron-reducing microorganism." *Nature*., 330, 252-254.

Lugtu, R.T., Choi, S.C., and YS, O. (2009). "Arsenite oxidation by a facultative chemolithotrophic bacterium SDB1 isolated from mine tailing." *J. Microbiol*., 47 (6), 486-492.

Maier, R.M., Pepper, I.L., and Gerba, C.P. (2009). Environmental Microbiology. Academic Press, Burlington, MA.
Mandal, B.K., and Suzuki, K.T. (2002). "Arsenic round the world: A review." *Talanta*., 58, 201 -235.

Manning, B.A., Fendorf, S.E., Bostick, B., and Suarez, D.L. (2002). "Arsenic (III) oxidation and Arsenic (V) adsorption Reactions on Synthetic Birnessite." *Environ. Sci. technol*., 36, 976-981.

Marquardt, D. (1963). "An Algorithm for Least-Squares Estimation of Nonlinear Parameters". *SIAM Journal on Applied Mathematics*., 11: 431–441.

McEwan, A., Ridge, J.P., McDevitt, C.A., and Hugenholtz, P. (2002). "The DMSO reductase family of microbial molybdenum enzymes: molecular properties and role in the dissimilatory reduction of toxic elements." *Geomicrobiology*., 19, 3-21.

McFadden, B.A., and Shively, J.M. (1991). "Bacterial assimilation of carbon dioxide by the Calvin cycle." In Variations in Autotrophic life, ed. JM Shively, LL Barton, 25-49, London: Academic.

McGeehan, S.L. and Naylor, D.V. (1994). "Sorption and redox transformation of arsenite and arsenate in two flooded soils." *Soil. Sci. Soc. Am. J*., 58, 337-342.

Mckay, G., Blair, H.S., Garden, J.R. (1982). "Adsorption of dyes on chitin, 1. Equilibrium study. *J. Appl. Polym. Sci*., 27(8), 3043-3057.

Molchanov, S., Gendel, Y., Ioslvich, I., Lahav, O. (2007). Improved Experimental and Computational Methodology for Determining the Kinetic Equation and the Extant Kinetic Constants of Fe (II) Oxidation by Acidithiobacillus ferrooxidans." *Appl. Environ. Microbiol*.*,* 73, 1742-1752.

Montgomery, D.C., Peck, E.A., and Vining, G.G. (2001). Introduction to Linear Regression Analysis. John Wiley & Sons, INC, New York.

Moore, J.N., Walker, J.R., Hayes, T.H. (1990). "Reaction Scheme for the Oxidation of As (III) to As (V) by Birnessite." *Clays and Clay Minerals*., 38 (5), 549-555.

Moreira D., and Amils R. (1997). "Phylogeny of Thiobacillus cuprinus and Other Mixotrophic Thiobacilli: Proposal for Thiomonas gen.nov." *International Journal of Systematic Bacteriology*., 47(2), 522-528.

Mukhopadhyay, R., Rosen, B.P., Phung, Le.T., and Silver, S. (2002). "Microbial arsenic: from geocycles to genes and enzymes." *FEMS Microbiology Reviews*., 26, 311-325.

Muller, D., Lievremont, D., Simeonova, D.D., Hubert, J.C., and Lett, M.C. (2003). "Arsenite oxidase aox genes from a metal-resistant beta-proteobacterium." *J. Bacteriol*., 185, 135-141.
Munch, E.V., Lant P., and Keller, J. (1996). "Simultaneous nitrification and de-nitrification in bench-scale sequencing batch reactors." *Wat. Res*., 30(2), 277-284.

Myers, C.R., and Nealson, K.H. (1988). "Bacterial manganese reduction and growth with manganese oxide as the sole electron acceptor." *Science*., 240, 1319-1321.

Nesbitt, H.W., Canning, G.W., Bancroft, G.M. (1998). "XPS study of reductive dissolution of 7Å-birnessite by H_3AsO_3, with constraints on reaction mechanism." Geochimica et Cosmochimica Acta., 62 (12), 2097-2110.

Newman, D.K., Ahmann, D., and Morel, F.M.M. (1998). "A brief review of microbial arsenate respiration." *Geomicrobiol*., 15, 255-268.

Nguyen, V.T., and Shieh, W.K. (1995). "Evaluation of intrinsic and inhibition kinetics in biological fluidized bed reactors." *Wat.res*., 29, 2520-2524.

Nikolaidis, N.P., Dobbs, G.M., and Lackovic, J.A. (2000). "Immobilization of Inorganic Arsenic Species using Iron." United States patent., 6,132,623. Date issued October 17th 2000.

Nordstrom, D.K. (2002). "Worldwide Occurrences of Arsenic in Ground Water." *Science*., 296, 2143-2145.

Nriagu, J.O., and Pacyna, J.M. (1988). "Quantitative assessment of worldwide contamination of air, water, and soils with trace metals." *Nature*., 333, 134-139.

Okereke, A., and Stevens Jr., S.E. (1991). "Kinetics of Iron Oxidation by Thiobacillus ferrooxidans." *Appl Environ Microbiol*., 57(4), 1052-1056.

Onysko, K.A., Budman, H.M., and Robinson, C.W. (2000). "Effect of temperature on the inhibition Kinetics of Phenol Biodegradation by Pseudomonas putida Q5." *Biotechnology and Bioengineering*., 70(3), 291-298.

Oremland, R.S., and Stolz, J.F. (2003). "The Ecology of Arsenic." *Science*., 300 (5621), 939 - 944.

Oremland, R.S., Hoeft, S.E., Santini, J.M., Bano, N., Hollibaugh, R.A., and Hollibaugh, J.T. (2002). "Anaerobic oxidation of arsenite in Mono Lake water, and by a facultative chemoautotroph strain MLHE-1." *Appl. Environmental. Microbiology*., 68, 4795-4802. Osborne, F.H., and Ehrlich, H.L. (1976). "Oxidation of arsenite by a soil isolate of *Alcaligenes*." *J. Appl. Bacteriol*., 41, 295 – 305.

Oscarson, D.W., Huang, P.M., Liaw, W.K. (1983). "Kinetics of Oxidation of Arsenite by various Manganese Oxides." *Soil Science Society of America*., 47, 644-648.

Perker, C.L. (1981). USEPA Contract No. 68-01-5965. The Mitre Corporation, 1-1. Peterson, J.W. (1985). "Industrial wastewater treatment technology." Stoneham, MA, Butterworth Publishers, 53-393.

Philips, S.E., and Taylor, M.L. (1976). "Oxidation of arsenite to arsenate by *Alcaligenes faecalis*." *Appl. Environ. Microbiol*., 32, 392-399.

Rhine, D.E., Onesios, K.M., Serfes, M.E., Reinfelder, J.R., and Young, L.Y. (2008). "Arsenic Transformation and Mobilization from Minerals by the Arsenite Oxidizing Strain WAO." *Environ. Sci. Technol.*, 2008, 42 (5), pp 1423–1429.

Rhine, E.D., Phelps, C.D., and Young, L.Y. (2006). "Anaerobic arsenite oxidation by novel denitrifying isolates." *Environmental Microbiology.*, 8(5), 899-908.

Riefler, G.R., Ahlfeld, D.P., and Smets, B.F. 1998. "Respirometric Assay for Biofilm kinetics Estimation: Parameter Identifiability and Retrievability". *Biotechnol.Bioeng.*, 57 (1), 35-45.

Rittle, K.A., and Drever, J.I., and Colberg, P.J.S. (1995). "Precipitation of arsenic during bacterial sulfate reduction." *Geomicrobiol. J.*, 13, 1-11.

Rittmann, B.E. (1982b). "The effect of shear stress on loss rate." *Biotechnol. Bioeng.*, 24, 501-506.

Rittmann, B.E., and McCarty, P.L. (2001). Environmental Biotechnology: Principles and Application. McGraw-Hill, New York.

Rittmann, B.E., and McCarty, P.L. 1980b. "Evaluation of steady-state biofilm kinetics." *Biotechnol.Bioeng.*, 22, 2359-2373.

Rittmann, B.E., Crawford, L., Tuck, C.K., and Namkung, E. (1986). "In situ determination of kinetic parameters for biofilms: Isolation and characterization of oligotrophic biofilms." *Biotechnol.Bioeng.*, 28, 1753-1760.

Robinson, J.A. 1985. "Determining microbial kinetic parameters using non-linear regression analysis." *Adv. Microb.Ecol.*, 8, 61-114.

Robinson, J.A., and Tiedje, J.M. (1983). "Nonlinear Estimation of Monod growth Kinetic Parameters from a Single Substrate Depletion Curve." *Appl. Environ. Microbiol.*, 1453-1458.

Rosenblum, E., and Clifford, D.A. (1984). "The equilibrium arsenic capacity of activated alumina." U.S.Environmental Protection Agency Report, Cincinnati, OH, 1984.

Rosenblum, E.R., and Clifford, D.A. (1984). "The Equilibrium Arsenic Capacity of Activated Alumina." PB 84/10 527, NTIS, Springfield.

Sadler, R., Olszowy, H., Shaw, G., Biltoft, R., and Connell, D. (1994). "Soil and water contamination by arsenic from a tannery waste." *Water, Air, Soil Pollut.*, 78, 189-198.

Saez, P.B., and Rittmann, B.E. (1992). "Accurate pseudo-analytical solution for steady-state biofilms." *Biotechnol. Bioengineering*. 39, 790-793

Salmassi, T.M., Venkateswaren, K., Satomi, M., Nealson, K.H., Newman, D.K., and Hering, J. G. (2002). "Oxidation of arsenite by Agrobacterium albertimagni, AOL 15, sp.nov., Isolated from Hot Creek, California." *Geomicrobiology Journal*., 19, 53-66.

Santini, J.M., and Hoven Rachel N. (2004). "Molybdenum-Containing Arsenite Oxidase of the Chemolithoautotrophic Arsenite Oxidizer NT-26." *J. of. Bacteriol*., 186(6), 1614-1619.

Santini, J.M., Sly, L.I., Schnagl, R.D., Macy, J.M. (2000). "A new Chemolithoautotrophic Arsenite-Oxidizing bacterium isolated from a Gold mine: Phylogenetic, Physiological, and Preliminary Biochemical studies", *Appl.Environ.Microbiol*., 66(1), 92-97.

Santini, J.M., Sly, L.I., Schnagl, R.D., Macy, J.M. (2000). "A new Chemolithoautotrophic Arsenite-Oxidizing bacterium isolated from a Gold mine: Phylogenetic, Physiological, and Preliminary Biochemical studies", *Appl.Environ.Microbiol*., 66(1), 92-97.

Schnoor, J.L. (1996). "Environmental modeling: Fate and transport of pollutants in water, air and soil." New York: John Wiley & Sons.

Seagren E.A., Kim H., and Smets B.F. (2003). "Identifiability and retrievability of unique parameters describing intrinsic Andrew kinetics." (2003). *App. Microbiol. Biotechnol*., 8, 61, 314-322.

Sehlin H.M., and Lindstorm, E.B. (1992). "Oxidation and reduction of arsenic by *sulfobus acidocaldarius* strain BC." *FEMS Microbiol.Lett*., 93(1), 87-92.

Sengupta, K.K. and Chakladar, J.K. (1989). "Kinetics of the Chromic Acid Oxidation of Arsenic (III)." *Journal of Chemical Society*, Dalton Transaction., 2, 222-225.

Shock, E.L., and Helgeson, H.C. (1988). "Calculation of the thermodynamic and transport properties of aqueous species at high pressures and temperatures: correlation algorithms for ionic species and equation of state predictions to 5 kb and 1000˚C." *Geochimica and Cosmochimica Acta*., 52(8), 2009-2036.

Shock, E.L., and Helgeson, H.C. (1988). "Calculation of the thermodynamic and transport properties of aqueous species at high pressures and temperatures: correlation algorithms for ionic species and equations of state prediction to 5 kb and 1000°C." *Geochimica and Cosmochimica Acta*., 52(8), 2009-2036.

Shooner, F., and Tyagi, R.D. (1996). "Thermophillic microbial leaching of heavy metals from municipal sludge using indigenous sulphur-oxidizing microbiots." *Appl. Microbiol. Biotechnol*., 45, 440-446.

Shuler, M.L., and Kargi, F. (2002). "Bioprocess Engineering basic concepts." Prentice Hall PTR: NJ, 2nd Edition, 70-72, 155-165.

Shuler, M.L., and Kargi, F. (2002). Bioprocess Engineering Basic Concepts. Prentice-Hall, Inc, New Jersey.

Simms, J., and Azizian, F. (1997). "Pilot-plant trials on removal of arsenic from potable water using activated alumina." American Water Works Association Water Quality Technology Conference, Denver, CO, 1997.

Simms, J., Upton, J., and Barnes J. (2000). "Arsenic removal studies and the design of a 20,000 m^3 per day plant in the UK." American Water Works Association Inorganic Contaminants Workshop, Albuquerque, NM, 2000.

Singh, S., Lee, W., DaSilva, N.A., Mulchandani, A., and Chen, W. (2008). "Enhanced arsenic accumulation by engineered yeast cells expressing *Arabidopsis thaliana* phytochelatin synthase." *Biotechnol. Bioeng*., 99 (2), 333 - 340.

Sircar, S., Rao, M.B., and Golden, T.C. (1996). "Drying of gases and liquids by activated alumina." In: Adsorption on new and modified inorganic sorbents. Dabrowski, A., and Tertykh, V.A. (Editors). Studies in Surface Science and catalysis, Vol 99, Elsevier Science, B.V.

Smedley, P.L., and Kinniburgh, D.G. (2002). "A review of the source, behavior and distribution of arsenic in natural waters." *Applied Geochemistry*., 17, 517-568.

Smedley, P.L., Edmunds, W.M., and Pelig-Ba, K.B. In: Appleton, J.D., Fuge, R., McCall, G.J.H (Eds.), *Environmental Geochemistry and Health*., vol 113, Geological Society Special Publication, London, 1996, 153.

Smets, B.F., Riefler, R.G., Lendenmann, U., and Spain, J.C. "Kinetic Analysis of Simultaneous 2, 4-Dinitrotoluene (DNT) and 2, 6-DNT Biodegradation in an Aerobic Fluidized-Bed Biofilm Reactor." *Biotechnol.Bioeng*., 63 (6), 642-653.

Smith, A.H., Hopenhayn-Rich, C., Bates, M.N., Goeden, H.M., Hertz-Picciotto, I., Duggan, H.M., Wood, R., Kosnett, M.J., and Smith, M.T. (1992). "Cancer risks from arsenic in drinking water." *Environ. Health. Persp*., 97, 259 - 267.

Smith, L.H., Kitanidis, P.K., and McCarty, P.L. (1997). "Numerical Modeling and Uncertainties in rate coefficients for methane utilization and TCE Cometabolism by a methane-oxidizing mixed culture." *Biotechnology and Bioengineering*., 53(3), 320-331.

Smith, L.H., McCarty, P.L., and Kitanidis P.K. (1998). "Spreadsheet Method for evaluation of biochemical reaction rate coefficients and their uncertainties by weighted nonlinear least –squares analysis of the integrated Monod equation." *Appl. Environ. Microbiol.*, 64(6), 2044-2050.

Soon-An, O., Chye-Eng, S., and Poh-Eng, L. (2007). "Kinetics of Adsorption of Cu (II) and Cd (II) from Aqueous Solution on Rice Husk and Modified Rice Husk." *Electron.J.Environ.Agric.Food.Chem.*, 6(2), 1764-1774.

Stolz, J.F., Basu, P., Santini, J.M., and Oremland, R.S. (2006). "Arsenic and Selenium in Microbial metabolism." *Annu. Rev. Microbiol.*, 60, 107-130.

Storer, F.F., and Gaudy, Jr, A.F. (1969). "Computational Analysis of Transient Response to Quantitative Shock Loadings of Heterogeneous Populations in Continuous Culture." *Environ. Sci.Technol.*, 3 (2), 143-149.

Strous, M., Heijnen, J.J., Kuenen, J.G., Jetten, M.S.M. (1998). "The sequencing batch reactor as a powerful tool for the study of slowly growing anaerobic ammonium-oxidizing microorganisms."*Appl. Microbiol. Biotechnol.*, 50, 589-596.

Stumm, W., and Morgan, J. (1981). "*Aquatic Chemistry.*" 2nd ed. Wiley New York, USA

Su, C., and Puls, R.W. (2001). "Arsenate and Arsenite Removal by Zero Valent Iron: Effects of Phosphate, Silicate, Carbonate, Borate, Sulfate, Chromate, Molybdate, Nitrate, Relative to Chloride." *Environ. Sci. Technol.*, 35, 4562-4568.

Suttigarn, A., Wang, Y.T. (2005). "Arsenite Oxidation by *Alcaligenes faecalis* Strain O1201." *J. Environ. Eng-ASCE.*, 131**,** 1293-1300.

Tabita, F.R. (1988). "Molecular and cellular regulation of autotrophic carbon dioxide fixation in microorganisms." *Microbiol. Rev.*, 52, 155-189.

Tan, C., Zhang, R., Wen, S., Li, K., Zheng, X., and Zhu, M. (2009). "Adsorption of Hexavalent Chromium from Aqueous Solution on Raw and Modified Activated Carbon." *Water Environment Research.*, 81 (7), 728-734.

Tomei, F.A., Barton, L.L., Lemanski, C.L. and Zocco, T.G. (1992). "Reduction of selenate and selenite to elemental selium by *Wolinella succinogenes.*" *Can. J. Microbiol.*, 38, 1328-1333.

Tripathy, S.S., and Raichur, A.M. (2008). "Enhanced adsorption capacity of activated alumina by impregnation with alum for removal of As (V) from water." *Chemical Engineering Journal.*, 138, 179-186.

United States Environmental Protection Agency (U.S. EPA). (2000). " *Technologies and costs fro removal of arsenic from drinking water.*" *EPA 815-R-00-028*, Cincinnati. (http://www.epa.gov/safewater) (May 5, 2003).

Ure, A., and Berrow, M. (1982). Chapter 3. "The elemental constituents of soils." In: Bowen, H.J.M. (Ed.), Environmental Chemistry. Royal Society of Chemistry, London, 94-203.

USEPA (2001). "National Primary Drinking Water Regulations; Arsenic and Clarifications to Compliance and New Source Contaminants Monitoring; Final Rule." Federal Register 66., 6976-7066.

Van Loosdrecht, M.C.M., Lyklema, J., Norde, W., and Zehnder, A.J.B. 1990. "Influence of interfaces on microbial activity." *Microbiol. Rev*., 54, 75-87.

Van Loosdrecht, M.C.M., Lyklema, J., Norde, W., and Zehnder, A.J.B. (1990). "Influence of interfaces on microbial activity." *Microbiol. Rev*., 54, 75-87.

Volesky, B., and May-Phillips, H.A. (1995). "Biosorption of heavy metals by *Saccharomyces cerevisiae*." *Appl. Microbiol. Biotechnol*., 42, 797-806.

Wackett, L.P., Dodge, A.G., and Ellis, L.B.M. (2004). "Microbial genomics and the periodic table." *Appl. Environ. Microbiol*., 70, 647-655.

Wagman, D.D., Evan, W.H., Parker, V.B., Halow, I., Bailey, S.M., and Schumn, R.H. (1968). "Selected Values of Chemical Thermodynamic Properties, Technical Note." 270-3, NBS, Washington, 95-98.

Wang, S., and Mulligan, C.N. (2006). "Effect of natural organic matter on arsenic release from soils and sediments into groundwater." *Environ. Geochem. Health*., 28, 197-214. Wang, Yi-Tin., and Suttigarn, A. (2007). "Arsenite Oxidation by *Alcaligenes Faecalis* Strain O1201 in a Continuous-Flow Bioreactor." *J. Environ. Eng-ASCE*., 133 (5), 471-476.

Wasay, S.A., Haron, M.J., and Tokunaga, S. (1996). "Adsorption of Fluoride, Phosphate and Arsenate Ions on Lathanum-Impregnated Silica Gel." *Water Environment Research*., 68, 295-300.

Watnick, P.I., and Kolter, R. (1999). "Steps in the development of a Vibrio cholera biofilm." *Mol. Microbiol*., 34, 586-595.

Watnick, P.I., and Kolter, R. (2000). "Biofilm, City of Microbes." *Journal of Bacteriology*., 182 (10), 2675-2679.

Waypa, J.J., Elimelech, M., and Hering, J.G. (1997). "Arsenic Removal by RO and NF Membranes." *Journal of the American Water Works Association*., 89, 102-114.

Webster, J.G. (1999). "The source of arsenic (and other elements) in the Marbel-Matingao River catchment, Mindanao, Philippines." *Geothermics*., 28, 95-111.

Weeger, W., Lievremont, D., Perret, M., Lagarde, F., Hubert, JC., Leroy, M., and Lett, M.C. (1999). "Oxidation of arsenite to arsenate by a bacterium isolated from an aquatic environment." *Biometals*., 12(2), 141-149**.**

Welch, A.H., Westjohn, D.B., Helsel, D.R., and Wanty, R.B. (2000). "Arsenic in groundwater of the United States." Groundwater., 26, 333-337.
WHO (The World Health Organization), 2006.
http://www.who.int/mediacentre/factsheets/fs210/en.

Williamson, K.J., and McCarty, P.L. (1976). "Verification studies of the biofilm model for bacterial substrate utilization." *J. Water Poll: Control Fedr*., 48, 281-289.

Woolard, C.R., and Irvine, R.L. (1995). "Treatment of hypersaline wastewater in the sequencing batch reactor." *Wat. Res*., 29(4), 1159-1168.

Zeng, R.J., Lemaire, R., Yuan, Z., and Keller, J. (2003). "Simultaneous Nitrification, Denitrification, and Phosphorous removal in a lab-scale Sequencing Batch Reactor." *Biotechnology and Bioengineering*., 84 (2), 170-178.

Zhang, S., and Huck, P.M. (1996). "Parameter estimation for biofilm processes in biological water treatment." *Water Res*., 30, 456-464.

Zhang, Y., Yang, M., and Huang, X. (2003). "Arsenic (V) removal with a Ce (IV)-doped iron oxide adsorbent." *Chemosphere*., 51, 945-952.

VITA

Aniruddha Dastidar

Date of Birth: April 24 1978
Place of Birth: Durgapur, West Bengal, India
Degrees Awarded:

May 2005 MCE in Civil Engineering, University of Kentucky, Lexington, Kentucky
June 2002 B.E. in Civil Engineering, J.N.N.C.E, Shimoga, Karnataka, India

Honors:

Student member of American Society of Civil Engineers (ASCE).
Member of the Academic Honor Society: *Delta Epsilon Iota.*
Recipient of the Burt. L Sims Graduate Fellowship for the academic year 2008-2009.

Publications to Date:

A. Dastidar and Y. T. Wang, "Kinetics of Arsenite Oxidation by Chemoautotrophic *Thiomonas arsenivorans* strain b6 in a Continuous Stirred Tank Reactor", *Journal of Environmental Engineering-ASCE.*, 136(10), 1119-1127

A. Dastidar and Y. T. Wang, "Arsenite Oxidation by Batch Cultures of *Thiomonas Arsenivorans* Strain b6", *Journal of Environmental Engineering-ASCE.*, 135(8), 708-715.

Y. T. Wang, A.Suttigarn, and A. Dastidar, "Arsenite Oxidation by Immobilized cells of *Alcaligenes faecalis* Strain O1201 in a Fluidized-Bed Reactor", *Water Environmental Research.*, Vol 81, 2, 173-177.